



Pointing Error Engineering For Telecommunication Missions

Final Report

ESTEC Contract Number 4000123466/18/UK/ND

ESA Technical Officer(s):

Bénédicte Girouart (TEC-SAA), ESTEC, Noordwijk

Nicolas Deslaef (TEC-SAA), ESTEC, Noordwijk

Authors:

Marc Hirth, Astos Solutions GmbH, 70569 Stuttgart, Germany

Thomas Ott, Airbus DS, 88039 Friedrichshafen, Germany

Date: 2022-03-31

Document ref. no. ASTOS-P4COM-FR-001

EUROPEAN SPACE AGENCY
CONTRACT REPORT

The work described in this report was done under ESA contract. Responsibility for the contents resides in the author or organisation that prepared it.



Abstract

The goal of the P4COM was to consolidate and streamline the Pointing Error Engineering Tool (PEET) and extend its applicability to the telecommunication mission sector with growing accuracy demands

The first part of this report covers the activities related to the PEET software. It summarizes needs identified from user and telecommunication mission experts' and provides an overview of the tool update – describing its new features and analyses with the theoretical background.

The second part presents the proposed evolutions for the ESA Pointing Error Engineering Handbook (PEEH) based on lessons learned over the past years and the special needs of telecommunication missions. Another aim of these evolutions is to achieve an alignment with the methods and concepts in PEET (elaborated in precursor studies) which are not yet covered by the current PEEH.

The last part introduces an overview of the setup and analysis of four telecommunication study cases which reflect missions with a high interest to ESA and industry in terms of pointing requirements, challenges and error engineering process. The definition and assessment of these reference cases comparison to heritage approaches was carried out in close co-engineering between study team and consultants from all telecommunication mission primes with the ultimate goal to consolidate PEET and work out its benefits for the application in this field.



Table of Contents

1	Applicable and Reference Documents.....	5
1.1	Applicable Documents	5
1.2	Reference Documents	5
2	Terms, Definitions and Abbreviated Terms	7
2.1	Acronyms	7
2.2	Definitions	8
3	Scope	9
4	Introduction.....	10
5	PEET Software.....	12
5.1	Review of Tool Version V1.0 and Feedback from Users	12
5.2	Tool Overview	14
5.2.1	General Information	14
5.2.2	New Features and Functionality	19
5.2.3	PEET Model Database	36
5.2.4	Remarks on Compatibility.....	63
5.3	Theoretical Background of the Tool Implementation	64
5.3.1	Advanced Statistical Method	64
5.3.2	Correlation and Coherence	74
5.3.3	Generation of error signal data.....	80
5.3.4	Transfer Analysis	93
5.3.5	Error Evaluation	99
5.3.6	Analytical Solutions for Distributions	106
6	Proposed Evolutions to the PEEH	129
6.1	Rationale.....	129
6.2	Summary of Proposed Changes.....	129
6.2.1	Main Chapters	129
6.2.2	Annexes.....	143
7	Study Cases	147
7.1	SmallGEO (OHB).....	147
7.1.1	Motivation	149
7.1.2	Pointing Requirements	149



7.1.3	Heritage Approach.....	150
7.1.4	Pointing Budgets.....	151
7.1.5	Budget Comparison.....	160
7.1.6	Conclusions and Lessons Learnt	166
7.2	E3000 (Airbus DS Toulouse)	166
7.2.1	Motivation	168
7.2.2	Pointing Requirements	169
7.2.3	Heritage Approach.....	171
7.2.4	Pointing Budgets.....	176
7.2.5	Budget Comparison.....	184
7.2.6	Conclusions and Lessons Learnt	188
7.3	Spacebus NEO (Thales Alenia Space).....	189
7.3.1	Motivation	191
7.3.2	Pointing Requirements	191
7.3.3	Heritage approach	192
7.3.4	Pointing Budgets.....	194
7.3.5	Budget Comparison	199
7.3.6	Conclusions and Lessons Learnt	199
7.4	EDRS Global (Airbus DS Ottobrunn).....	200
7.4.1	Motivation	202
7.4.2	Pointing Requirements	202
7.4.3	Heritage Approach.....	212
7.4.4	Pointing Budgets.....	212
7.4.5	Budget Comparison	217
7.4.6	Conclusions and Lessons Learnt	218
7.5	Summary.....	219
7.5.1	Summation Rules	221
7.5.2	Impact of PDF-based LoC evaluation	223
7.5.3	RPE Budgets	226
8	Conclusion and Outlook.....	228



1 Applicable and Reference Documents

1.1 Applicable Documents

- [AD1] ECSS-E-ST-60-10C; Control Performance Standard ECSS-E-ST-60-10C, ESA-ESTEC Requirements & Standards Division, 2008.
- [AD2] ESSB-HB-E-003; ESA Pointing Error Engineering Handbook, Issue 1, 19 July 2011

1.2 Reference Documents

- [RD1] IEEE Standard Specification Format Guide and Test Procedure for Linear Single-Axis, Nongyroscopic Accelerometers; IEEE Std 1253-1998 (R2008); IEEE: New York, NY, USA, 2008
- [RD2] IEEE Standard Specification Format Guide and Test Procedure for Single-Axis Interferometric Fiber Optic Gyros; IEEE Std 952-1997; IEEE: New York, NY, USA, 1998
- [RD3] Control Performance Guidelines, ESSB-E-HB-60-10A; ESA-ESTEC Requirements & Standards Division, 2008
- [RD4] Random Data – Analysis and Measurement Procedures, Bendat J.S., Piersol A.G., 3rd edition, Wiley, 2000
- [RD5] PEET2 - Systems engineering support to the development of the Pointing Error Engineering SW Framework, GNC_F.TCN.779118.ASTR, Iss.1.4, Project Documentation, 2015
- [RD6] Error Budgets for Formation Flying Missions, NPD/5022/TD/TR/001 v1.r1.m0, ESA Documentation, Harwood A., March 2008
- [RD7] Reaction Wheel Microvibration Model, PFF-MEMO-MC-001; Memo, Casasco M., April 2013
- [RD8] Development and Validation of Empirical and Analytical Reaction Wheel Disturbance Models, Masterson R.A., Master Thesis, Massachusetts Institute of Technology, June 1999.P3-EST-TN-7001
- [RD9] Development of Empirical and Analytical Reaction Wheel Disturbance Models, Masterson R.A., Miller D.W., Grogan R.L., AIAA 99-1204, AIAA Structural Dynamics and Materials Conference, St. Louis, USA, 1999.
- [RD10] Star-Tracker Noise Model, Project Documentation, Memo, Casasco M., April 2012
- [RD11] Computational Statistics, Gentle, J.E, Springer, 2009
- [RD12] Dependence in Stochastic Simulation Models, Ghosh S., PhD thesis, Cornell University, 2004
- [RD13] Simulating Dependent Random Variables Using Copulas, Mathworks Online Documentation, <http://de.mathworks.com/help/>, last accessed October 8, 2020
- [RD14] Truncated normal distribution, Wikipedia – The Free Encyclopedia, https://en.wikipedia.org/wiki/Truncated_normal_distribution, last accessed October 8, 2020
- [RD15] PEET V1.0: The State-of-the-Art Pointing and Performance Error Engineering Tool for Space Missions, Hirth M. et al., 10th International ESA Conference on Guidance, Navigation & Control Systems, Salzburg, Austria, 2017



- [RD16] Optical transfer functions, weighting functions, and metrics for images with two-dimensional line-of-sight motion, Pittelkau M.E, McKinley W.G, Opt. Eng. 55(6), 063108 (2016), doi: 10.1117/1.OE.55.6.063108
- [RD17] PEET V1.0: The State-of-the-Art Pointing and Performance Error Engineering Tool for Space Missions, Hirth M. et al., 10th International ESA Conference on Guidance, Navigation & Control Systems, Salzburg, Austria, 2017
- [RD18] Mission Selection: SmallGEO, ASTOS-P4COM-TN-004, Issue 1.2, Technical Note prepared by OHB Systems AG (Bremen), Neumann N., 2021
- [RD19] Mission Selection: Broadcast Mission E3000, ASTOS-P4COM-TN-005, Iss. 1.4, Technical Note prepared by Airbus (Toulouse), Campuzano J., 2021
- [RD20] Mission Selection: SpacebusNEO, ASTOS-P4COM-TN-006 Iss. 1.2, Technical Note prepared by Thales Alenia Space, Guercio N., 2021
- [RD21] Mission Selection: EDRS Global, ASTOS-P4COM-TN-007, Iss.1.3, Technical Note prepared by Airbus (Ottobrunn), Closs M., 2021
- [RD22] EDRS Uncertainty Cone Apportionment Issue 4.0, EDRS.TN.ASTR.00008033, Project documentation
- [RD23] PointingSat Case Study, GNC_F.TCN.788536, Issue 3.0, Airbus Technical Note.



2 Terms, Definitions and Abbreviated Terms

2.1 Acronyms

The following abbreviations are used throughout this document.

Acronyms	
AD	Applicable Document
ASM	Advanced Statistical Method
AST	Analysis Step (in [AD2])
BPE	Beam Pointing Error
BLWN	Band-Limited White Noise
CDF	Cumulative Distribution Function
CRV	(Time-) Constant Random Variable
D	Drift (Signal component)
ECSS	European Cooperation for Space Standardization
ESA	European Space Agency
FRD	Frequency Response Data (MATLAB model type)
GPS	Global Positioning System
GUI	Graphical User Interface
ICDF	Inverse Cumulative Distribution Function
IEEE	Institute of Electrical and Electronics Engineers
I/O	Input/Output
JMI	Java MATLAB Interface
LTI	Linear Time-Invariant
LoS	Line-of-Sight
P	Periodic (Signal component)
PDF	Probability Density Function
PEEH	Pointing Error Engineering Handbook
PEET	Pointing Error Engineering Tool
PEC	Pointing Error Contributor
PES	Pointing Error Source
PSD	Power Spectral Density
RV	(Time-) Random Variable
RP	Random Process
S.I.	Statistical Interpretation
SSM	Simplified Statistical Method



2.2 Definitions

The following definitions are used throughout this document.

Definitions	
Block mask	The input dialog provided by the blocks for parameter input.
Domain	The generic term used to assign error sources to a group according to their time- or ensemble-random properties.
Error Contribution Block	All evaluation blocks where a signal is evaluated w.r.t. a requirement, in general Pointing Error Contribution ("PEC", without the keyword style) block is used interchangeably throughout the document
Signal	The error signal information which is exchanged between adjacent blocks.



3 Scope

This document is the final report for the ESA project P4COM, "Pointing Error Engineering For Telecommunication Missions", ESA contract number 4000123466/18/UK/ND.

The project was led by Astos Solutions GmbH, with Airbus Defence & Space GmbH (Friedrichshafen) as subcontractor. Furthermore, Airbus Defence & Space GmbH (Ottobrunn), Airbus Defence & Space (Toulouse), OHB System AG (Bremen) and Thales Alenia Space (Toulouse/Cannes) contributed as consultant for the telecommunication mission applications and study cases.



4 Introduction

The framework of the ESA Pointing Error Engineering Handbook (PEEH, [AD2]) is specifically intended to guide the compilation of pointing error budgets. A key benefit of the Pointing Error Engineering Tool (PEET) in this respect is its capability to compile the budgets with simplified as well as advanced statistical methods, i.e. probability density estimation, frequency domain characteristics and cross-correlation information of error sources. No known commercial tool is available to compile error budgets with such advanced methods on satellite system level. Moreover, “classical” budget assessments via spreadsheet processing do not and cannot implement such methods sufficiently accurate.

Recently, also missions in the telecommunication sector have to increasingly cope with stringent pointing requirements – e.g. for hosted payload concepts or communication via inter-satellite links. However, the application of the PEEH was mainly focused on Earth Observation and Science missions in the past which was one main reason initiating the P4COM study in the ARTES AT programme.

So far, telecommunication missions mainly apply standardized heritage approaches for performance budgeting based on a classification of budget contributions into different frequency classes (bias, short-term, daily and seasonal errors) and more simplified computation rules within and over the different error classes.

Implementing the PEEH methodology (and realizing its application using PEET) on telecommunication missions requires an initial effort and learning curve as heritage processes for pointing error engineering and budgeting are already in place. However, this is considered as one-time investment. In the long term the benefits of a more efficient design and development process will produce a significant return on invest.

The first part of this report provides an overview of the updated PEET software and its new features. The identification of the actual needs was based on results of a survey conducted among the existing PEET user community at the beginning of the study to ensure the development of an industrial reliable tool in terms of stability, user-friendliness, modelling and reporting functionalities. Further - as the application of the ESA handbook and tool was new in this sector – the tool was complemented with focus on the feedback received from the European telecommunication primes, especially with respect to specific analysis features.

The second part presents the proposed evolutions for the ESA Pointing Error Engineering Handbook based on the lessons learned over the last years and the special needs of telecommunication missions. Another aim of these evolutions is to achieve an alignment with the methods and concepts in PEET (which have been elaborated in recent developments) which are not yet covered by the PEEH – such as the ‘generalized’ domain concept for statistical interpretation (see e.g. [RD17]).

The third part introduces an overview of the setup and analysis of the telecommunication study cases in P4COM, namely SmallGEO (OHB System), E3000 Broadcast Mission (Airbus), SPACEBUS NEO (Thales Alenia Space) and EDRS Global (Airbus). This selection of study cases aims to reflect missions with a high interest to ESA and industry in terms of pointing requirements, pointing challenges and pointing error engineering process as well as to cover the specific interests of all involved primes. The definition, setup and analysis of these reference cases was carried out in close iterative co-engineering between core study team and telecommunication consultants with the ultimate goal to consolidate PEET for the application in this field. Finally, the lessons learned and benefits of applying the ESA handbook methodology and the PEET software to telecommunication



missions are discussed from the perspective of the industry consultants involved in the study.



5 PEET Software

This chapter summarizes all activities performed related to the update of the PEET software. It first describes the results of the review and survey activities which lead to the additional software requirements. Then it provides an overview of the updated PEET V1.1. (working version 1.0.2 during the study) with the new features and functionalities implemented. Finally it recalls and extends the description of the theoretical background of the tool implementation.

5.1 Review of Tool Version V1.0 and Feedback from Users

To identify the needs for the PEET software update, the following tasks were conducted:

- internal review of the tool/algorithms by the study core team (based on experience from earlier development phases, lessons learned and support questions raised by users); this also includes the assessment of all update requests directly related to the statement of work
- survey among all registered tool users
- ESA Pointing Error Engineering Workshop for telecommunication mission at ESTEC
- consultancy of experts from the 3 ESA telecommunication mission primes concerning their specific needs in this domain

Internal review

The internal tool review was based on experience from earlier development phases, lessons learned and support questions raised by users before the study. This task identified about 20 new features/extensions which are of interest for implementation, about 20 streamlining topics for existing functionality, ~15 bugs and a couple of documentation updates.

User survey

An invitation to the online survey was sent to all registered users of PEET V1.0. The survey was made available for roughly 6 weeks. 16 users out of 48 finally participated in the survey. The survey was generally designed to be anonymous, but contact data could be provided.

The following 5 question groups were included:

- general question about the familiarity with PEET and its prototype version, other tools used for performance budgeting, application and use cases, operating systems and MATLAB versions used; this question group had the purpose to help categorizing all specific responses in the detailed question sections
- questions on the PEET graphical user interface to rate both the general satisfaction level and the intuitiveness of specific aspects such as:
 - connecting and parameterizing blocks in the System Editor
 - working with multiple scenarios
 - defining requirement parameters and error source dependencies
 - analysing results and checking compliance with requirements



Comments could be provided in any case to document specific needs or to mentioned encountered issues.

- questions on the quality of the provided documentation in general and the description of specific topics such as:
 - tool installation and start-up
 - tool workflow
 - GUI elements
 - script-based execution
 - hints and guidelines
 - model description
 - troubleshooting
 - missing topics which are not yet covered

Comments could be provided in any case to identify specific improvements.

- questions on functionalities and features concerning:
 - input/output interfaces, model blocks, requirement/ figure of definition or any other auxiliary functionality needs (e.g. PSD estimation form time-series data)
 - any unexpected behaviour (crashes/freezes) or numerical results encountered when using the tool

This question group was the main source for identifying updates and necessary fixes for the tool

- questions on the quality of the provided reporting functionality and result presentation in general and of specific related topics such as:
 - content and configurability of Excel reports
 - plot options and available plot types
 - accessing scenario data/results from the MATLAB workspace

The survey unveiled about 20 further possible extensions and a couple of streamlining topics and bugs which were not already covered by the internal review.

ESA workshop

The ESA Pointing Error Engineering Workshop for telecommunication missions took place on September 17th, 2018 at ESTEC. The purpose of this workshop was to discuss foreseen extensions of PEET and the PEEH during the P4COM activity and to obtain further feedback from the participants (ESA staff, project team, telecommunication consultants and members of the ESA PEE Working group).

All feedback collected from the PEET user survey and inputs were presented and complemented by the results of the project team's internal review. Three additional extension requests were identified concerning the tool.

Feedback from telecommunication mission experts



Initially obtained feedback from the consultants on helpful tool extensions mainly corresponded to the needs which were already identified in the context of above-mentioned tasks, i.e. related to general user-friendliness aspects of the tool.

However, also dedicated support features for the post-processing and conversion of the currently available x/y/z budgets into other telecom specific representations and figures of merit (beam pointing error, antenna coverage) were requested. These analyses are further described in chapter 5.2.2.3.1.

Justification of updates

All collected suggestions for features and extensions were further assessed to decide on their actual their implementation in the tool. The criteria for implementation were:

- specific need for telecom application on the one hand and/or wide applicability for every user on the other
- Ratio between benefit and implementation effort
- “Compliance” with background covered by PEEH and ECSS standard.
- Effect on computation time & load
- Effect on user-friendliness & general usability of the tool
- “Single-source” opinion or feedback received from various sources

This assessment led to about 30 additional or extended mandatory software requirements and about the same number of goal requirements with different priorities. In the end, all (mandatory and goal) requirements could be met.

5.2 Tool Overview

5.2.1 General Information

5.2.1.1 Platforms and Requirements

PEET is mainly designed for Windows platforms but can also be made available for Linux (tested on Ubuntu 20.04). It runs on a standard desktop PC or laptop with 8GB of RAM (16 recommended). The tool is designed as an extension to MATLAB and completely runs inside the MATLAB environment. Apart from a plain 64bit MATLAB installation (>2011b, >2016b recommended), only the Control System Toolbox is required.

5.2.1.2 Architecture and External Interfaces

The static architecture of PEET is shown in Figure 5-1. It mainly consists of two components: a dedicated graphical user interface (GUI) based on Java and the core computational routines implemented as MATLAB classes.

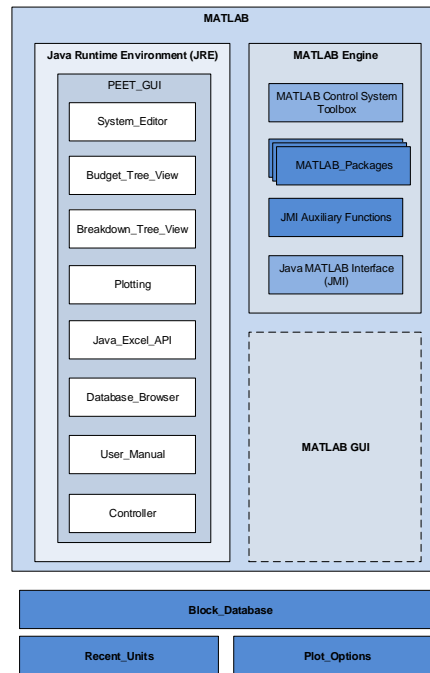


Figure 5-1: PEET static architecture

The GUI is used to define requirement specification parameters, values and identifiers and to set up the pointing system from error sources to the final error using blocks from a database. This can include system transfer models (as in Figure 5-2) or simply comprise a summation of errors on different requirement levels.

Input data can directly be specified in tables or input fields or imported from MS Excel spreadsheets. In addition to numerical inputs, also MATLAB variable names and notation can be used to specify parameters. All relevant scenario data is stored in an XML file which serves as interface for the MATLAB core classes for the initialization and evaluation of the budget.

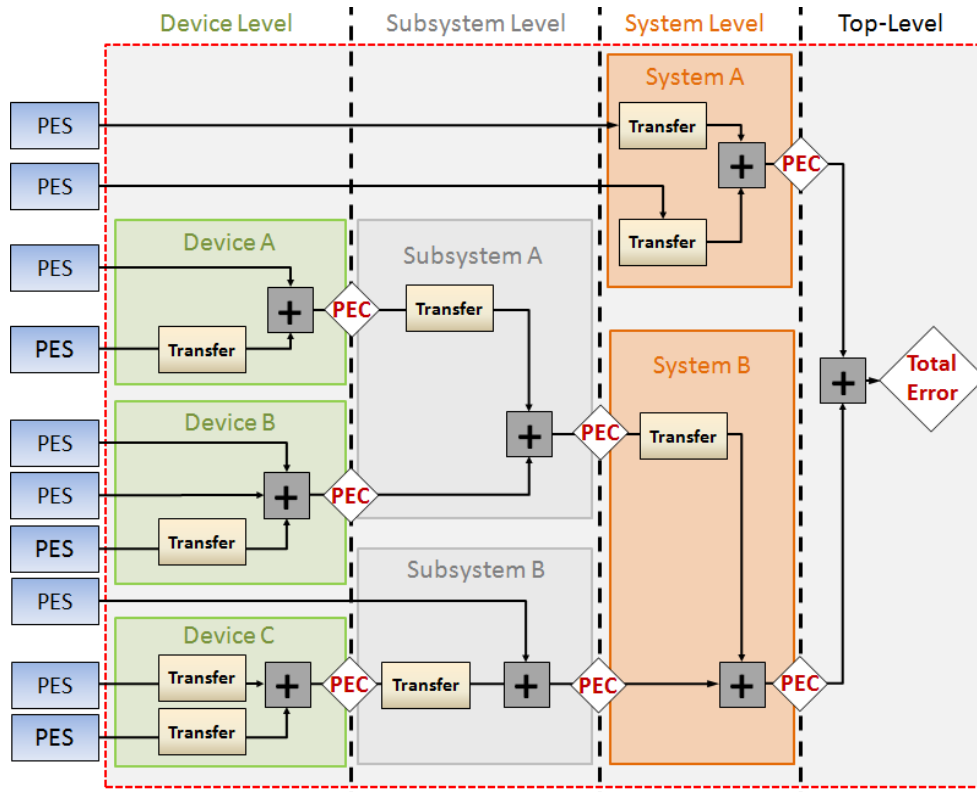


Figure 5-2: Routing from error source to the total error

Once a pointing scenario is created and saved using the GUI, two operational modes are possible. First, the GUI can be used directly to start an evaluation and to inspect the results. The communication between the GUI and the MATLAB classes is realized in this case via the Java MATLAB Interface (JMI). Second, a script-based execution of the tool via user-defined MATLAB scripts is possible. Together with assigning MATLAB workspace variables to system parameters and a large number of user functions, this allows batch-mode operations without further use of the graphical user interface and an integration of PEET in a tool-chain with other analysis modules.

The budget results obtained with PEET can further be exported to MS Excel using a configurable report. Similarly, result plots can be exported manually and automatically in different formats.

5.2.1.3 Graphical User Interface

This section gives a brief introduction to the features of the PEET GUI which consists of several dedicated windows:

System Editor

The editor panel in the System Editor (Figure 5-3) is the main tool to design the architecture of a pointing scenario. It can be populated with a selection of model blocks from the Block Database which then need to be connected to represent the error signal flow. The workflow for moving and connecting blocks is intentionally similar to the workflow with MATLAB Simulink. Different levels (subsystems) are supported for a better overview in complex



systems as well. Double-clicking a block opens a dialog where related parameters including signal & parameter units can be specified (supported by tooltips). The latter can be chosen from a predefined set of SI and non-SI units and also custom units can be created. When connecting blocks, the compliance of units is automatically checked by the tool.

The menus present in the System Editor window serve for file management, requirement definition (multiple requirements sets can be specified in a single scenario), definition of error source dependencies (correlation, coherence and phase relations) and the setup of specific (pre- or user-defined) analyses.

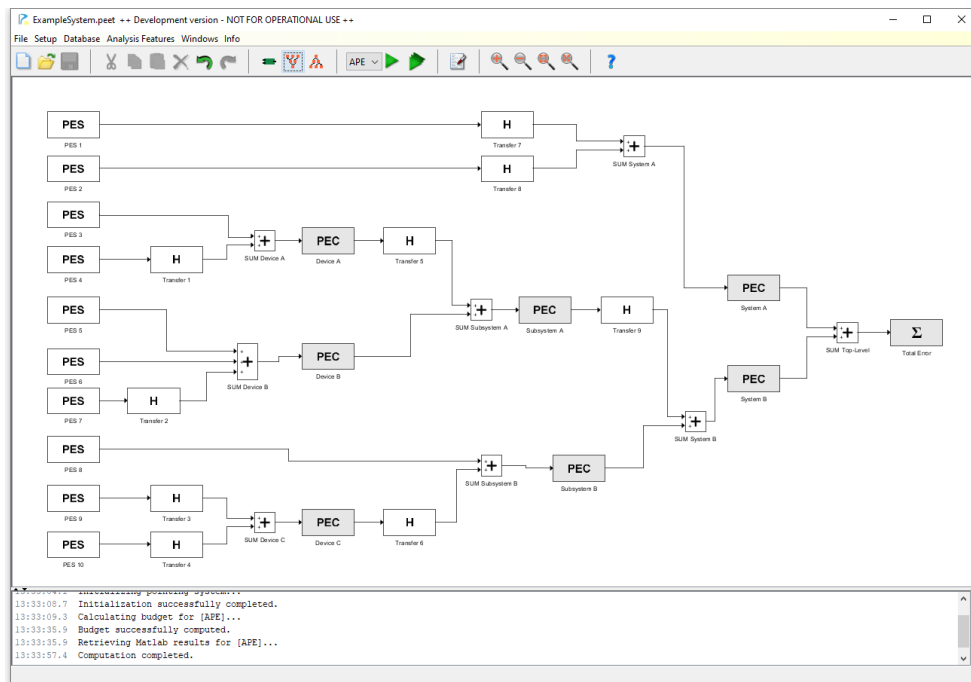


Figure 5-3: The System Editor

An execution log serves as scope to track the evaluation progress and issues occurring meanwhile (e.g. invalid user parameter inputs or ranges).

Block Database

The Block Database (Figure 5-4) - similar to the Library Browser in MATLAB Simulink – contains all building blocks which can be used to populate a pointing scenario. The blocks are categorized in groups (errors sources, static/dynamic systems, etc.).

It contains both generic blocks and parametric models of sensors, actuators and transfer systems which are based on standardized models where available (e.g. [AD1], [RD1], [RD2]). For each model, the block database shows a “quick-view” help with important information about the model (purpose, input/output dimensions) with more detailed background information in the electronic user manual.

Figure 5-4: The Block Database

Budget Tree View

The Budget Tree View (Figure 5-5) serves to analyse error contributions (from different error signal classes) of the entire pointing system. Selecting a block in the tree-like representation of the pointing system shows the related signal content in the information panel on the right. For each signal class, statistical information is provided in terms of mean and standard deviation together with a plot preview of the PDF (or PSD respectively for a random process error signal). In case of spectral requirements, only random process contributions are displayed.

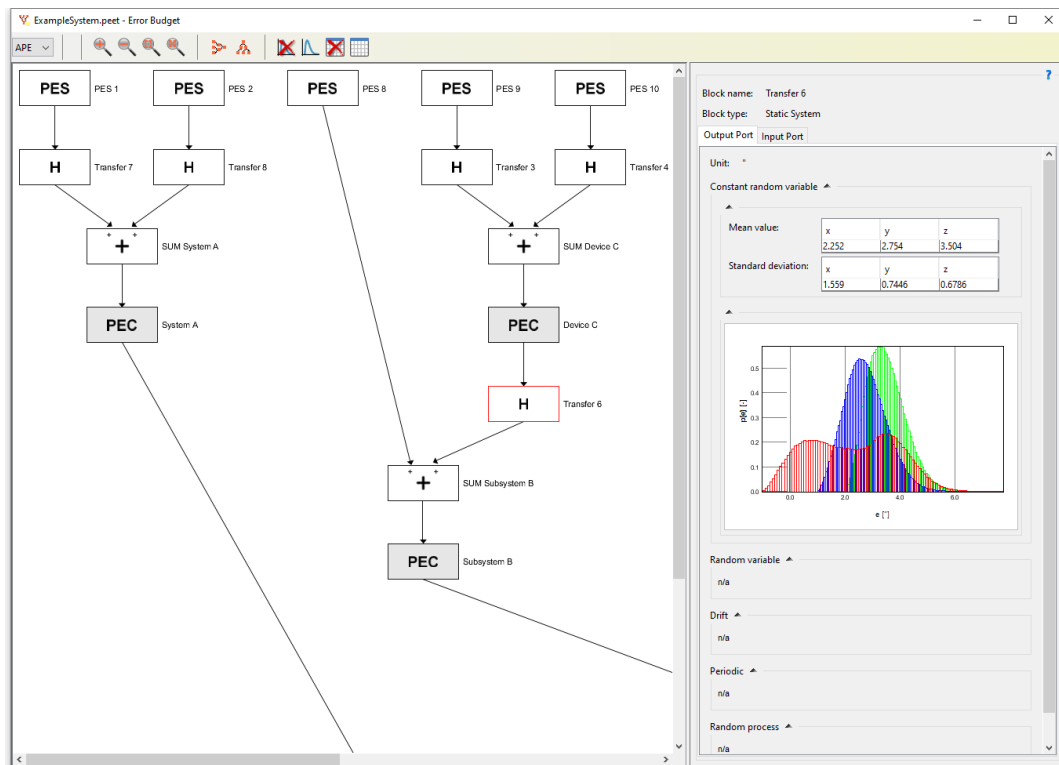


Figure 5-5: The Budget Tree View

Breakdown Tree View

The Breakdown Tree View (Figure 5-6) is used to check the compliance of the budget. It shows only those blocks where requirements have been associated with (by value and optionally an ID). For statistical requirements, the information panel displays a comparison of budget and requirement values for the time-constant, time-random and total error contributions on all axes together with a plot preview of the underlying CDF. In addition, colour-coding is used in the tree view for an easy determination of budget violations or proximity to margins.

For spectral requirements, the budget spectrum is plotted versus the specified requirement function. Further plots and data tables for specific analyses are available additional tabs when enabled.

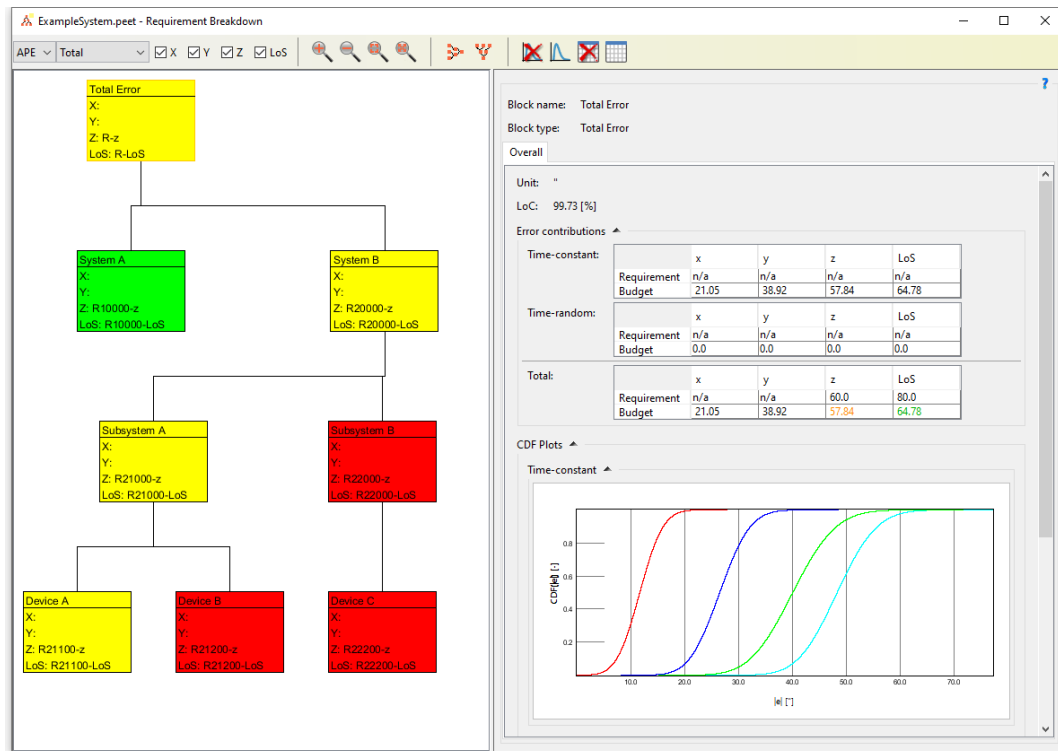


Figure 5-6: The Breakdown Tree View

5.2.2 New Features and Functionality

5.2.2.1 Overview

This chapter provides a brief summary of new functionalities and features in the updated tool version V1.1 compared to the previous version V1.0. Further details about specific features are provided separately in later chapters. Numerous bugs identified in V1.0 were also fixed, but are not explicitly outlined in this report.

General Useability Aspects

- Scenarios created with version V1.0 are automatically converted and backed-up when loaded with PEET V1.1.
- The license management is adapted such that having a C-language compiler configured for MATLAB mex is no longer necessary.
- In tool version V1.0, error messages displayed in the Execution Log were only forwarding lower-level MATLAB error messages which did not allow a user to identify the reason of the error. The error messaging approach in version V1.0 has been significantly improved in that respect. Now all user parameter inputs are carefully checked during the scenario initialization and messages in the Execution Log directly point to the parameter of a block or menu which causes the issue together with information about the cause of an incompatibility (these checks are mainly carried out by the MATLAB algorithms as the GUI has no a-priori information about the content of MATLAB variables).

- An electronic user manual and mathematical background information are accessible from Graphical User Interface. Contextual information can also be received from different block dialogs and menus. Keyword searches, back-and-forth navigation etc. is supported.

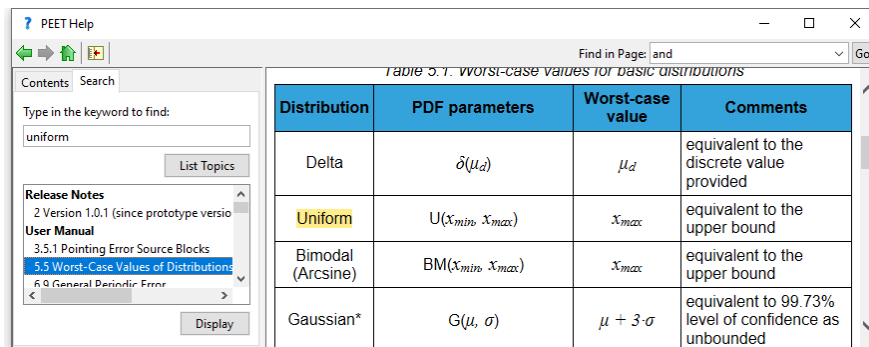


Figure 5-7: Exemplary screenshot of online help

- The functions available to users for script-based execution of the tool and subsequent data access are significantly extended and streamlined. This includes additional function, more user-friendly syntax including optional function arguments and an improved documentation in the user-manual.
- When starting PEET from the MATLAB command window, it is now possible to directly load the last opened or a specified scenario.
- A remarkable fraction of the computation time is spent the generation of histograms. While being essential for the error evaluation at *PEC/Total Error* blocks, generating PDFs for the different signal component at any other blocks has only informative character. Thus, a “fast mode” option is now implemented which skips the generation of auxiliary results for all non-PEC blocks to significantly reduce the computation time. For the same reason, also a “low-resolution mode” is now implemented (which uses less samples for the signal representation) which can be used e.g. for trade-offs or quick assessments where less accurate results are sufficient
- Requirement sets can now be imported from other existing scenarios.
- More keyboard shortcuts for typical operations are implemented.
- A “fit-to-view” option is implemented in the editor and tree views to maximize the displayed window content, e.g. for a more convenient creation of scenario screenshots.
- A color-scheme applied to each scenario simplifies the distinction of windows and taskbar items belonging to different scenarios.
- The import/export of user-defined block groups from/to the local block database has been improved such that sharing scenarios with user-defined database blocks no longer requires manual modifications of the database XML file.
- An undo of deleted blocks/connections in the system editor is now possible.



- An overview spreadsheet summarizing the parameters of all requirement sets defined in a scenario can be automatically generated.
- It is now possible to open multiple block dialogs in parallel to simplify the comparison or copying & pasting of parameter settings
- Recently used and customized units in block dialogs and units are stored and directly made available in drop-down list for quick reuse where compatible.
- The source block of a signal is now explicitly shown on the input port tabs of the Budget Tree View to simplify the tracking.
- The color-coding in the Breakdown Tree View tables is extended such that it also applies to individual entries (per component/axis) to simplify the tracking of requirement compliance.
- It is now possible to quickly show/hide all or individual tables/plots in the Tree Views for a better overview of relevant results.
- The selection of active/disabled PES for certain requirement sets is adapted such that a faster selection and script-based control is possible.
- Additional step-by-step examples are available in the user manual and as example scenario files (for script-based execution and the newly introduced post-processing analyses). Further, the PointingSat case study including its documentation is directly provided with the tool as “complex” example scenario.
- A helper function is provided which allows generation of time-series from PEC data with the corresponding statistical/spectral properties.
- A helper function for a basic PSD estimate from time-series data in a tool-compatible input format is provided.

Plotting and Reporting

- All plot windows now include an unambiguous identifier of the data (including the scenario, requirement set, block and component names) to simplify the distinction.
- Plots can be saved directly from the GUI with the GUI layout or in MATLAB style. Different file formats (.fig, .png, .jpg, .bmp, .png, .pdf) are now also supported,
- PDF plots can now be displayed either as bar plot or as line plots. Correlation plots can be represented as scatter plots or heat-map plots.
- Spreadsheet reports now support both .xls and .xlsx format.
- Generated reports and saved plots are automatically time-stamped to avoid overwriting existing files with the same name (if the respective option is enabled)
- Report sheet names can now be customized with a user-defined prefix or suffix which is especially helpful for script-based executions.
- Axis data to be included in a report can be customized such that irrelevant data does no longer need to be manually removed.



- An automated, customizable plot file generation of all plot types is implemented in the reporting functionality. Links to the plot files are directly made available via links in report spreadsheet.
- All data cells in a report now contain a unique cell reference such that any linking of results in the spreadsheet to other documents is simplified, i.e. no manual update of references is necessary, when the report options are changed or a scenario is extended (as long as block names with linked data remain unchanged).
- A PEC overview report spreadsheet with the results of all requirement sets defined in a scenario can be generated automatically in addition to the already existing full reports “per requirement set”.

Models and Analyses

- Additional metric indices (Windowed Performance/Knowledge Drift, Windowed Performance/Knowledge Reproducibility WPR/WKR) and metric subtypes for Relative Performance/Knowledge Errors (alpha-dependent or windowed variance) are implemented which are in line with the intended ESA PEEH update (see section 6).
- The frequency domain metrics have been revised in general. Improved rational approximations for the filters to be applied to PSD error signals are used for both the previously existing and new metrics. Exact versions of the metrics are now applied to periodic signals to ensure that phase relations between different signal are accurately modelled and maintained.
- New “*General Periodic Error*” models (rectangular, triangular, decaying cosine, exponential decay) are implemented to cover at least a subset of “transient” signals explicitly. These models are based on Fourier series approximations of the actual signals. This frequency domain approach ensures an accurate processing of error metrics and system transfer behaviour.
- Similarly, the existing random variable drift error model is replaced by a frequency domain approach based on a Fourier series approximation. This avoids restrictions in the dynamic system transfer analysis and limitations due to necessary assumptions with the previous approach.
- Analytical PSD error sources now support the distribution of an of ensemble-random parameter similar to the parameter options for random variable error sources.
- The Truncated Gaussian distribution extends the set of temporal distributions of random variable models in *PES (Time-Random)* block.
- The Beta distribution (with scale and shift parameters) extends the set of possible ensemble distributions of parameters in various error source models.
- *Accelerometer Noise* and *Gyro Rate Noise* blocks are no longer restricted to a common parameterization but do support definition a per axis.
- A new *Input PEC* block is implemented which allows inclusion of “processed” PDF/PSD data from external analyses. That means, error source data specified for these blocks are intentionally “fed through” without any statistical interpretation and error metric applied again by the tool.



- A new analysis feature is available to evaluate the contribution (in percent) of each PES and/or PEC block alone to any higher-level PEC block. This simplifies the determination of budget drivers on different levels.
- A new analysis feature is available to perform a weighted evaluation of multiple requirement sets (e.g. for cases where each set is related to an operational mode in which a certain amount of time is spent).
- A new analysis feature is available to express existing x/y/z error contributions directly in terms of azimuth and elevation errors.
- Several new coverage analyses for telecom applications are available (beam pointing error, NS/EW angle conversion, single-spot and multi-spot coverage).
- A generic "post-processing" feature is now implemented. It allows users to define and apply their own analysis algorithm to PEC data using MATLAB code. A specific interface format supports report generation and display (in plots and tables) of the analysis results in the GUI.

5.2.2.2 Script-Based Execution

Once a pointing scenario has been set up and saved as a `.peet` file, it can be controlled, modified and evaluated using MATLAB commands (e.g. executing a MATLAB script file). This is especially useful when parameters in the scenario are defined by MATLAB variable names as related parameters can then be easily modified between computation runs by changing the MATLAB variable itself.

The major purpose of the script-based execution is the modification of parameter values during different computation runs but it also allows automatic evaluation of budgets in a toolchain with other MATLAB tools or scripts. The parameter variation can be realized by the following two means:

- Change the value of a variable in the MATLAB workspace that is linked to a parameter using MATLAB notation in the scenario.
- Change and save values stored in an Excel-file which is linked to the scenario.

Further, a large set of MATLAB functions has been introduced during this study which enable users to modify scenario settings which are usually defined in menus in the GUI. Other functions serve for exporting and inspecting analysis results or for configuring additional analysis features. All functions and their syntax are explicitly described in the software user manual of the tool.

Scenario selection

PEET scenario data can be directly loaded into the MATLAB workspace by calling the main class (`engine.Analysis`) with the scenario path as input argument.

Scenario initialization

Before the actual evaluation can be executed, the scenario needs to be initialized. In addition to a basic initialization routine, specific functions exist to initialize correlation, periodic signal phases and the frequency grid to be used for random process signals.

Inspection/Modification of scenario settings



Once a scenario is initialised, it is possible to inspect the most relevant settings via dedicated helper functions that avoid a manual 'browsing' of the MATLAB scenario object. Available functions for this purpose can be categorized as follows, i.e. to identify:

- block and other general settings (e.g. certain block properties, requirement set parameters or evaluation settings)
- plot settings (e.g. plot formats and display options)
- report settings (e.g. flags for automatic plot generation or information to be included)
- analysis feature settings (dependent on the selected analysis)

In a similar manner, most of the inspectable settings can also be modified directly via function calls.

Evaluation of a scenario

The budget computation can be directly triggered via a specific function after the requirement set to be evaluated has been selected by a setter function. A flag to check for modified values of linked MATLAB variables/Excel tables can be used to ensure that all up-to-date values are used.

Evaluation of analysis features

All specific analysis features described in section 5.2.2.3 can also be triggered using a MATLAB function, once the scenario itself is evaluated.

Inspection of results

Specific functions are implemented to access the same information which is usually provided in the Tree Views of GUI, i.e.

- statistical properties and auxiliary data of each blocks' error signal (by component)
- evaluated budget values of each evaluation block
- plot data (e.g. PDF/CDF/PSD) of the error signals at each block
- results of certain analysis features (table or plot data including descriptions)

Exporting scenario results

Plot information can not only be provided as numeric data (as mentioned above), but plots can be generated and saved in specified formats via function calls. Similarly, the Excel report generation can be triggered.

Support functions

Several support functions are provided with the tool, that are not directly related to the scenario evaluation, but might be useful obtain compatible input data or generate auxiliary output data, i.e. to:

- generate time-series data corresponding to the error signal data at an evaluation block
- compute a 'basic' PSD estimate from time-series data
- check the validity of a correlation matrix and to find a close feasible solution

- compare of the Fourier series approximation used in the tool (e.g. for modelling drift or exponentially decaying signal) to the exact realization

5.2.2.3 Analysis Features

In the context of the study, a menu has been introduced in the GUI which provides different additional analyses to be applied to error contribution block data (PEC and Total Error blocks). These analyses are all “external”, i.e. they do not modify the block output signals which are routed through a scenario itself.

5.2.2.3.1 Post-Processing

In the context of PEET, “post-processing” must be understood as any additional analysis operation applied to nominal budget results at an error contribution block (PEC / Total Error), i.e.

- the PDF of time-constant, time-random and total error contributions in PEC coordinates (x, y, z and/or line-of-sight) for **statistical** requirements
- the power spectral density in PEC coordinates (x, y, z) for **spectral** requirements.

Such operation could be, for instance, a conversion of data to another coordinate representation or applying a specific function or complete algorithm to the axes data input (somewhat similar to the ‘fcn’ or ‘MATLAB Function’ blocks in MATLAB Simulink).

The respective menu provides dedicated analyses with a predefined parameterization but also permits including user-defined algorithms supported by specific templates.

The menu dialog is shown in Figure 5-8. It provides a separated tab for each error contribution block present in the scenario which allows defining or omitting specific analyses individually for each block.

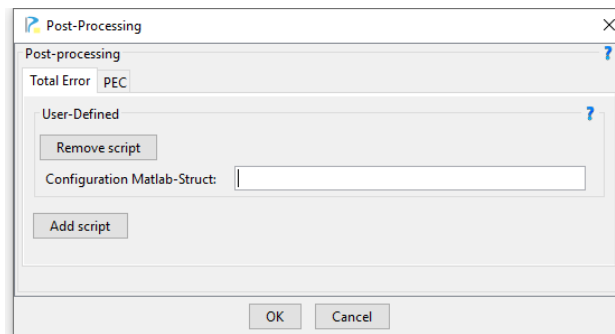


Figure 5-8: Post-Processing menu dialog

Adding a script opens a dialog with a drop-down list for all possible post-processing analyses for the selected block. The options available further depend on the dimension and unit specified for a block (see next subchapters). It is possible to enable multiple analyses for any block (also of the same type, but with different parameter values)

When evaluating a scenario, the analyses are automatically performed and results are presented in the Breakdown Tree View on additional tabs for each defined element. Further, post-processing results can also be automatically included in Excel reports if desired. In this case, one additional sheet is appended in the report for each analysis element specified.

5.2.2.3.1.1 Azimuth/Elevation

This post-processing element converts pointing errors in "Cartesian coordinates" (i.e. around x, y and z-axis) to respective azimuth and elevation errors with respect to a given reference attitude. The analysis is available for all 3D PEC blocks with an [Angle]-compatible unit and is applied to all PEC contributions (time-constant, time-random and total) and all domains for any **statistical** requirement. In addition to the reference angles, both requirement values and associated IDs can optionally be provided.

Analysis results are displayed in the Breakdown Tree View on a separate tab. The information present is equivalent to the one displayed for the standard Cartesian results, i.e.:

- a table holding the budget values for time-constant, time-random and total contributions in comparison to the requirement values and the level of confidence which was used for the evaluation
- a CDF plot of the absolute value (of the azimuth and elevation errors)

The reference azimuth/elevation and selected line-of-sight axis are provided as additional descriptive information.

The algorithm itself applies the following steps:

- Express the reference azimuth φ_{Ref} and elevation θ_{Ref} as components of a unit vector \mathbf{u}_{Ref} in the block frame, i.e. with components (assuming the z-axis as line-of-sight, for any other LoS direction selected in the Evaluation Settings menu, the axes are permuted accordingly, see Figure 5-9):

$$u_{x,\text{Ref}} = \cos(\theta_{\text{Ref}}) \cdot \cos(\varphi_{\text{Ref}})$$

$$u_{y,\text{Ref}} = \cos(\theta_{\text{Ref}}) \cdot \sin(\varphi_{\text{Ref}})$$

$$u_{z,\text{Ref}} = \sin(\theta_{\text{Ref}})$$

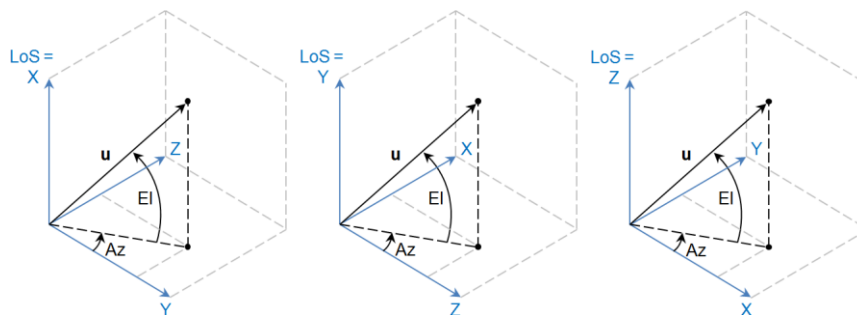


Figure 5-9: Azimuth/elevation definition dependent on selected LoS-axis

- Create a direction cosine matrix $\mathbf{T}(e_x, e_y, e_z)$ for each realization of the error angle input
- Compute the erroneous direction vector \mathbf{u}_e by multiplying \mathbf{T} and \mathbf{u}_{Ref}
- Convert the erroneous direction vector back to azimuth/elevation, i.e. (assuming again the z-axis as line-of-sight, and permutation for other cases):



$$\varphi_e = \tan^{-1}(u_{y,e}, u_{x,e})$$

$$\theta_e = \tan^{-1}(u_{z,e}, \sqrt{u_{x,e}^2 + u_{y,e}^2})$$

- Compute the PDF (and CDF) of the absolute value of the difference between reference azimuth/elevation and the disturbed azimuth/elevation for each realization (i.e. a vector respectively).

$$p(|\Phi_e - \Phi_{\text{Ref}}|)$$

$$p(|\Theta_e - \Theta_{\text{Ref}}|)$$

5.2.2.3.1.2 Coverage (BPE)

This post-processing element represents an analysis feature applicable to geostationary telecommunication missions or any application where a beam pointing error (BPE) with respect to a given reference latitude/longitude on Earth is of interest.

The model assumes a geostationary orbit and a block reference coordinate frame where the x/y/z axes correspond to roll/pitch/yaw respectively. It provides an error budget for the half-cone pointing errors with respect to the direction from the satellite to the provided reference location on Earth and error budgets for an alternative representation of attitude errors in terms of North/South and East/West pointing error angles.

The analysis is available for all 3D PEC blocks with an [Angle]-compatible unit and is applied to all PEC contributions (time-constant, time-random and total) and all domains for any **statistical** requirement. In addition to the position on Earth, the satellite longitude is required as input parameter. Further, requirement values and IDs for the permitted half-cone error can be provided.

Analysis results are displayed in the Breakdown Tree View on a separate tab which consist of:

- A PDF plot of the attitude errors expressed as North/South and East-West angles and a display of the derived yaw coupling coefficients that were used for the conversion
- A tabular overview of the time-constant, time-random and total beam pointing error budget values vs. its requirement value (if specified). Further, the beam pointing error CDF is plotted and the latitude/longitude parameters for the analysis are displayed as additional descriptive information.

The model assumes that x, y and z error signals of the block correspond to roll, pitch and yaw angle errors respectively and that the satellite is in a geostationary orbit. Under these assumptions, first the coupling coefficients of the yaw movement to North/South (K_{NS}) and East/West (K_{EW}) directions can be computed from the analysis parameters:



$$K_{NS} = \sqrt{\frac{(\cos(l) \sin(L_C - L_S))^2}{\left(\frac{R_0}{R_E}\right)^2 + 2(1 - \cos(l) \cos(L_C - L_S)) \left(1 + \left(\frac{R_0}{R_E}\right)\right)}}$$
$$K_{EW} = \sqrt{\frac{\sin^2(l)}{\left(\frac{R_0}{R_E}\right)^2 + 2(1 - \cos(l) \cos(L_C - L_S)) \left(1 + \left(\frac{R_0}{R_E}\right)\right)}}$$

where L_c is the longitude the reference pointing direction sub-point, L_s is the satellite longitude, l is latitude the reference pointing direction sub-point, R_e is the equatorial radius of the Earth (6378.137 km) and R_0 is the distance from the satellite to the sub-satellite point (i.e. 35786 km for a geostationary orbit).

The NS/EW error angles e_{NS} and e_{EW} are computed from the x/y/z error angles e_x , e_y and e_z using these coefficients:

$$e_{NS} = \sqrt{e_x^2 + (K_{NS} \cdot e_z)^2}$$

$$e_{EW} = \sqrt{e_y^2 + (K_{EW} \cdot e_z)^2}$$

The half-cone beam pointing error e_{BPE} is then computed using the NS/EW angles:

$$e_{BPE} = \sqrt{e_{NS}^2 + e_{EW}^2}$$

The PDFs $p(\mathbf{e}_{NS})$, $p(\mathbf{e}_{EW})$ and $p(\mathbf{e}_{BPE})$ of these angles are obtained by evaluating above expressions for each realization of the error angles and computing the respective histograms.

5.2.2.3.1.3 Coverage (Single-Spot)

This post-processing element represents an analysis feature applicable to telecommunication missions or any application where a single-spot antenna pointing performance for a given coverage area is of interest. Both the performance of specific points inside the coverage area as well as the overall spot performance is evaluated.

The analysis is available for all 3D PEC blocks with an [Angle]-compatible unit and is applied to all PEC contributions (time-constant, time-random and total) and all domains for any **statistical** requirement.

The coverage area is defined as a set of azimuth/elevation angles as seen from the satellite, i.e. defined with respect to the line-of-sight axis selected in the Evaluation Settings of the scenario (see Figure 5-9). It can be provided as contour defined by vertex points (see Figure 5-10) or by providing explicit points inside the coverage area which shall be analysed.

In the first case, an [Nx2] matrix of N vertices defined contour of interest and a number M of grid points (per direction) can be configured which defines a linearly spaced grid of additional evaluation points inside this contour. In the second case, the [Nx2] matrix directly

defines the grid points to be considered. Further, requirement values and IDs for the permitted single-spot error can be provided and an optional level of confidence for the PDF evaluation can be specified.

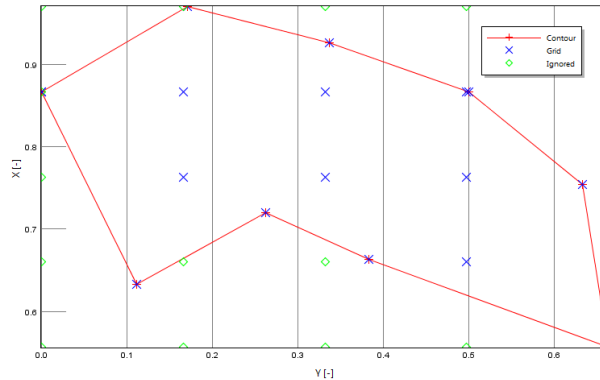


Figure 5-10: Exemplary contour in Az/EI-Map with 5x5 additional grid points

Analysis results are displayed in the Breakdown Tree View on a separate tab which consist of three parts:

- The overall spot performance panel provides the budget values and CDF plots (for the time-constant, time-random and total contributions) in terms of elevation, azimuth and half-cone error. For the latter, also a comparison to the requirement values is provided (if specified).
- The grid performance overview panel provides a plot of the budget values (in terms of azimuth, elevation and half-cone error) individually for each grid point. The applied level of confidence and the selected line-of-sight axis is available as additional descriptive information.
- The azimuth-elevation map panel provides a plot visualizing the coverage contour and the used grid points (as shown in the figure above).

The grid definition via contour vertices first requires the detection of grid points inside the area encircled by the coverage contour and on the contour boundaries. For this purpose, only standard MATLAB functions (e.g. 'inpolygon', 'polyarea') are used.

The procedure to determine the azimuth and elevation errors is identical to the one already described in section 5.2.2.3.1.1, but repeatedly executed for each grid point. The half-cone errors are computed for each grid point using the dot-product between the reference unit direction vector \mathbf{u}_{Ref} and the unit direction vector \mathbf{u}_e with the attitude error vector applied, i.e.

$$e_{\text{half-cone}} = \cos^{-1} \left(\mathbf{u}_e^T \mathbf{u}_{\text{Ref}} \right)$$

Further, above operations are executed for each realization of the x/y/z attitude angle vector which leads to vectors of attitude errors in terms of azimuth, elevation and half-cone errors for each grid point. Then, the error PDFs are evaluated separately for each grid point and each of the three vectors.



The overall spot performance is computed by appending the half-cone error vectors (azimuth and elevation vectors respectively) errors of each spot into single large error vector. Then, the PDF of this large vector is computed.

This algorithm implies the computation of a large number of histograms (3 per grid point and domain) and computing a histogram from a large dataset (for the overall spot performance) which can have a significant impact on memory consumption and computation time (in the range of several minutes).

Thus, it is recommended to reduce the grid point number as far as possible (< 100 as rule of thumb). To avoid memory conflicts, the samples used to construct the overall spot PDF from the data of each spot is internally restricted. If the length of the overall spot PDF vector would exceed a length of to 10^8 , only a subset of the error data from of each spot is used for the combination to ensure that this limit is not exceeded.

5.2.2.3.1.4 Coverage (Multi-Spot)

This post-processing element represents an analysis feature applicable to telecommunication missions or any application where a multi-spot antenna pointing performance is of interest.

The analysis is available for all 3D PEC blocks with an [Angle]-compatible unit and is applied to all PEC contributions (time-constant, time-random and total) and all domains for any **statistical** requirement.

The orientation of each spot in the antenna array is defined as azimuth/elevation pair as seen from the satellite, i.e. defined with respect to the selected line-of-sight axis. The worst-case thermo-elastic deformation of the antenna array can be taken into account in the model.

As for the single-spot case analysis described in the previous section, the main parameter input is an [Nx2] matrix defining the orientation of each of the N spots. Further optional parameters are requirement values and IDs for the reference spot and the worst-case spot.

Concerning the (simple) thermo-elastic deformation model, the maximum daily amplitude (defined for the spot with the largest nominal radial distance from the reference spot) needs to be provided. Two options exist for that purpose:

- the maximum daily thermo-elastic amplitude is directly applied to “farthest” spot from the reference spot, i.e. such that their angular distance increases in elevation by the specified maximum daily amplitude value. For all other spots, the thermo-elastic amplitude value is scaled with the ratio of each spots’ radial distance from the reference spot and the radial distance of the farthest spot
- dimensionless scale factors in the range [-1,1] are explicitly provided as [N x 1] vector and each entry in the vector is used to scale the maximum daily amplitude value. The result is then applied individually to each of the N spots such that their radial distance from the reference spot is increased or decreased accordingly.

Analysis results are displayed in the Breakdown Tree View on a separate tab which consist of five parts:

- The reference spot performance panel provides the reference spot budget values and CDF plots (for the time-constant, time-random and total contributions) in terms of elevation, azimuth and half-cone error. For the latter, also a comparison to the requirement values is provided (if specified).



- The worst-case spot performance panel provides the budget values (for the time-constant, time-random and total contributions) for the worst-case spot in terms of elevation, azimuth, thermo-elastic error and half-cone error. For the latter, also a comparison to the requirement values is provided (if specified).
- The spot performance overview panel provides a plot of the budget values (in terms of azimuth, elevation and half-cone error) individually for each spot. The applied level of confidence and the selected line-of-sight axis is available as additional descriptive information.
- The thermo-elastic error contribution overview panel provides a plot of the thermo-elastic error contributions in terms of elevation individually for each spot.
- The azimuth-elevation map panel provides a plot visualizing the nominal spot locations

The procedure to determine the azimuth, elevation and half-cone errors for each spot is similar to the one described for the single-spot case described in section 5.2.2.3.1.3 (with each 'spot' in this model equivalent to a 'grid point' of the single spot case).

The only difference is that not only the $x/y/z$ attitude error input, but also the thermo-elastic errors affect the de-pointed unit direction vector \mathbf{u}_c . Thus, first the elevation errors due to the thermo-elastic deformation are applied to the nominal spot direction unit vectors before further applying the rotation due to the $x/y/z$ error angles. As the thermo-elastic effect is implemented in a worst-case sense, i.e. using the maximum daily amplitude, its contribution is constant (but different for each spot). Consequently, the de-pointed unit direction vectors applied to each spot are determined once already during the scenario initialization and passed as a parameter to the core function to avoid unnecessary repetition of computation steps during the scenario evaluation.

5.2.2.3.1.5 User-Defined Analysis

Different to the previously described analyses, this option can be chosen for all PEC blocks, no matter what their signal dimension or output unit is.

It uses a generic interface which can be used to include any kind of user-defined algorithm which shall be applied to the error signal available at a PEC block (similar to a 'MATLAB Function' block in MATLAB Simulink) in the evaluation routine of a scenario. Further, results can be automatically displayed in the GUI and/or included in Excel reports in tabular format or as plot.

If selected, only one parameter needs to be provided which is the variable name of a MATLAB structure which must be available in the MATLAB workspace when initializing a scenario. Further, a MATLAB function m-file is required which contains the user-defined algorithm.

Their main content and purpose are described in the following paragraphs. An application example is provided with the tool and described in detail in the software user manual.

Post-Processing Configuration Structure

The configuration structure can have any variable name supported by MATLAB contains the most essential parameters for the execution of a user-defined post-processing analysis. The mandatory and optional fieldnames of the structure are explained in detail in the user manual. Further, a template file is provided with the tool which contains brief explanations and which can be used as starting point.

Mandatory fields of the structure are:



- An arbitrary name string for the post-processing analysis which is used for internal identification of the element, but also defines the name of the tab (or sheet) where the results get displayed in the GUI (or Excel report).
- The absolute path of the associated post-processing function m-file which contains the user-defined algorithm (see next subchapter).
- A string indicating to which type of requirement (spectral or statistical) the function applies. As the input data and format is different for these two cases, a distinction is necessary.

All remaining structure fields are optional. They can be used to access external user-parameters in the main function, to further describe the analysis in reports or GUI or the further restrict the application of the analysis (e.g. certain components or ensemble domains).

Post-Processing Function m-File

Any user-defined function to be used for a post-processing analysis must have the following form with 3 input arguments and one output argument:

```
y = postProcFunctionName(u, uUnit, extParam)
```

`postProcFunctionName` is a placeholder and any MATLAB compatible function name can be used. The function m-file must have the same name and correspond to the one defined in the configuration structure (see previous paragraph). Further sub-functions can be used in the m-file without restriction.

The function is called for every domain and every component specified in the configuration structure – but only if the input for this domain/component is not empty. Thus, there is no need to account for empty inputs in the function body.

Further, there is no explicit restriction on the function body implemented by a user (obviously excluding syntax errors).

During the scenario initialization, the function is executed and fed by dummy inputs of proper dimension for the block and requirement type. This checks the consistency of the function itself, but is also necessary to retrieve information about the output size, type and additional optional settings which can be used to refine the output data (described further below).

Function Inputs

It is ensured that the three input arguments `u`, `uUnit` and `extParam` are always available.

The first input `u` depends on the requirement type assigned in the configuration structure and is always provided in the unit associated to the block. For a statistical requirement, it is a numerical matrix holding the samples for each axis and the line-of-sight component. For a spectral requirement, `u` is a structure with two fields containing the frequency vector and numerical matrix of the PSD data in [unit/Hz].

The second input `uUnit` contains information about the block unit including its SI conversion factor and the unit name and symbol.

This last input `extParam` represents a MATLAB structure containing any parameters that shall be made accessible in the function. It corresponds to the variable linked in the respective field of the configuration structure. In addition to any user-defined parameters in the structure, the currently evaluated domain and component identifiers are always made



available in the parameter structure by the tool. This provides the possibility to apply any component- or domain- specific operations in the algorithm.

Function Output

The generic interface supports only a single output argument y . However, y needs to be provided as cell array, such that a configurable number of outputs can effectively be realized.

The content of each cell element is generally arbitrary and can be accessed from the scenario object in the workspace after the evaluation.

If the results shall be displayed automatically in the GUI or included in a report, the content of a cell elements needs to be defined as structure with reserved field names for the following 'data types' (detailed description in the user manual and in a dedicated template file provided with the tool):

- Numerical tabular data (field name `tableData`): in addition to the actual data matrix, table title, row and column headers can be specified, units, requirement values and IDs can be assigned, and a description text can be provided.
- Plot data (field name `plotData`): in addition to mandatory abscissa and ordinate data to be plotted, also a title, arbitrary description text, requirement values and IDs can be assigned. Further, typical layout options (legend, axis labels, units, axis/line styles and markers) can be configured
- Sample data with PDF/CDF information (field name `pdfData`): in this case, any input data is evaluated as nominally for the data available at a PEC block, i.e. for each assigned sample set a PDF/CDF plot and a tabular overview of the budget values for a given level of confidence and a comparison to requirement values (if specified) is automatically generated. Level of confidence values to be applied can be chosen per element of the sample set.

An arbitrary number of different output types can be used within one post-processing analysis (but only one per cell element/output) as indicated with the code snippet below.

```
y{1}.plotData.[paramFields] = ...  
y{2}.plotData.[paramFields] = ...  
y{3}.pdfData.[paramFields] = ...  
y{4}.tableData.[paramFields] = ...  
y{5}. ...
```

The sequence of the outputs also defines the sequence in which the results are displayed in the GUI.

5.2.2.3.2 Weighted Evaluation

This analysis feature allows a weighted evaluation of the results from multiple requirement sets, i.e. a combination of the form:

$$\text{Error}_{\text{Weighted}} = \frac{\sum_i \text{Error}_{\text{Req},i} \cdot \text{Weight}_i}{\sum_i \text{Weight}_i}$$

As a potential application example of this feature, assume that the requirement sets present in a scenario correspond to different operational modes of a system and the fraction of time spent in each mode differs over the considered period. In this case, the overall performance

over the entire lifetime could be represented by applying (in above 'equation') a weight to the result of each requirement set according to the fraction of time spent in each mode.

The analysis can be applied either to spectral or statistical requirement sets. This distinction is necessary as these two types cover entirely different data which cannot not be combined.

Depending on the selected type, only compatible requirement sets can be selected from a list in the respective menu (see Figure 5-11) and a corresponding weight can be assigned to each.

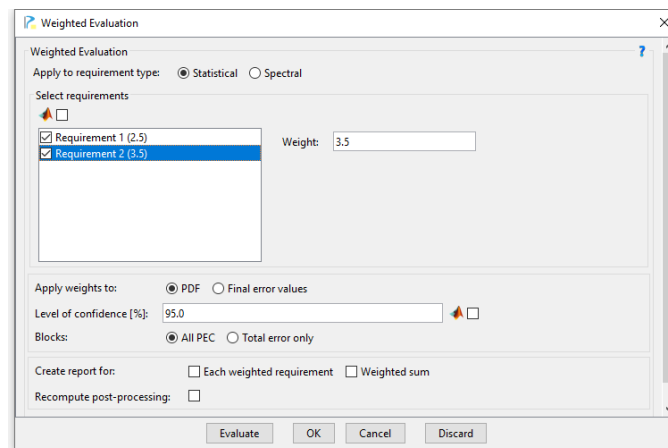


Figure 5-11: Weighted Evaluation menu

In the statistical case, it is possible to further define how the weights w_i shall be applied to obtain the error $e_{weighted}$:

- To the scalar final error values of each requirement set $e_{LoC,i}$, i.e. **after** each requirement set is nominally evaluated (with the levels of confidence LoC_i as specified for the requirement set), i.e.:

$$e_{weighted} = \frac{\sum e_{LoC,i} \cdot w_i}{\sum w_i}, \quad LoC_i / 100 = \int_0^{e_{LoC,i}} p(|e_i|) de_i$$

- Alternatively, the weights can also be applied to the samples, i.e. on the individual errors e_i of each requirement set **before** summing the results and evaluating the combined error with a given common level of confidence $LoC_{weighted}$ i.e.

$$LoC_{weighted} / 100 = \int_0^{e_{weighted}} p\left(\frac{\sum |e_i \cdot w_i|}{\sum w_i}\right) de$$

In the case of spectral requirements, the weights w_i are applied to the power spectral densities $G_i(f)$ resulting from each requirement set as:

$$G(f)_{weighted} = \frac{\sum G_i(f) \cdot w_i^2}{\sum w_i^2}$$



In both cases, the analysis feature can be applied to all PEC blocks in a scenario or to the final Total Error block only. Analysis results are not displayed in the GUI, but exported to a specific spreadsheet report. The information provided with the report can be further customized via menu options. It is also possible to recompute any compatible post-processing analyses (see previous chapters) using the weighted results and to include the results in the report.

5.2.2.3.3 PES-/PEC-to-PEC Percentages

The PES-to-PEC analysis can be used to assess the impact of each error source block alone on all error contribution blocks (PEC and Total Error blocks) present in a scenario. It returns the ratio of a block's contribution and the overall contribution in percent individually for the time-constant, time-random and total error components for a statistical requirement set. The PEC-to-PEC options performs a similar analysis between all error contribution blocks respectively.

After evaluation, the analysis results are presented in tabular form in the Budget Tree View on specific tabs for each error source/contribution block. Further, a result overview is documented in the report spreadsheet (see figure below).

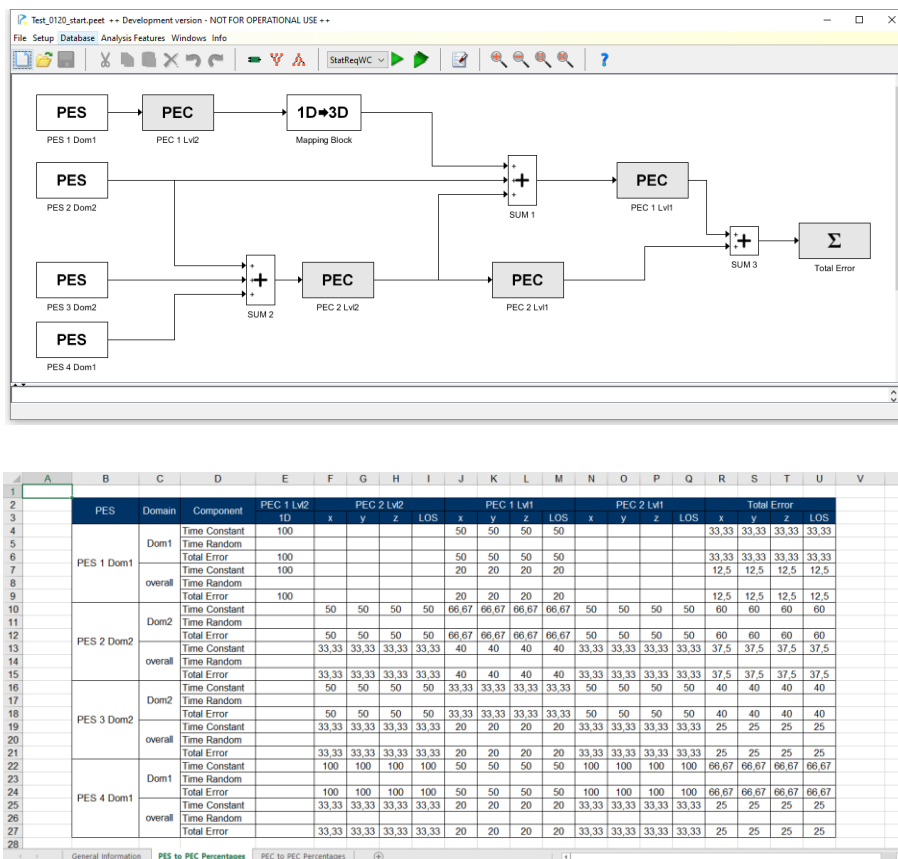


Figure 5-12: Exemplary scenario (top) and PES-to-PEC analysis results (bottom)



5.2.3 PEET Model Database

This chapter describes the various building blocks present in the PEET model database.

5.2.3.1 Common Block Settings

Several panels and configuration settings are common to most of the database blocks. In general, the signal and system dimension can be switched between 1D and 3D.

Generic blocks (e.g. *PES*, *Static System*, *Dynamic System* blocks) allow a free definition of the output unit from various SI and non-SI units. Other blocks are restricted to a certain class of units (e.g. time), however an output unit can still be chosen within the respective class (e.g. [min], [s] or [h]). The same is true for most of the model parameters itself where at least the unit within a certain unit group can be customized. Internally, all signal and parameter data are automatically converted to SI unit for the computation routines and converted back the user-specified unit for display purposes in the GUI or a report.

Certain blocks manipulate the incoming signal, but do not necessarily change the signals' unit (e.g. a *Coordinate Transformation* blocks). In such case, by default, the output unit is inherited from the input signal. If this is not desired, the respective selection can be unchecked and an output unit can be selected from of a compatible unit of the same unit group.

In addition, all blocks provide the possibility to add an arbitrary user-defined description of the block. This feature might be used to document modelling assumptions or information to be directly included in a report and which can be directly accessed as tooltip in the GUI when sharing scenarios with other users. Tooltips with a brief description of specific settings are also available and further provide a direct link to the respective detailed description in the software user manual.

5.2.3.2 Block Overview

Table 5-1: Block overview with supported I/O unit (groups)

Block	Category	Dimensions	Input unit	Output unit
Accelerometer Noise	PES	1D and 3D	-	[Length/Time ²]
Camera Range Noise	PES	3D	-	[Length]
Container	Basic	-	-	-
Coordinate Transformation	Static	3D	Any	Input unit
Dynamic System	Dynamic	1D or 3D	Any	Any
Feedback System	Basic	-	-	-
Flexible Plant	Dynamic	3D	[Force · Length]	[Angle]
General Periodic Error	PES	1D or 3D	-	Any
GPS	PES	3D	-	[Length] or [Length/Time]



Gyro Rate Noise	PES	1D or 3D	-	[Angle]
Gyro-Stellar Estimator	Dynamic	3D	[Angle] and [Angle/Time]	Input units
Input PEC	PES	1D or 3D	Any	Any
Input Port	Basic	Inherited	-	Inherited
Mapping	Basic	1D → 3D	-	Any
Output Port	Basic	Inherited	Inherited	-
PEC	Evaluation	1D or 3D	Inherited	Input unit
PES (Time-Constant)	PES	1D or 3D	-	Any
PES (Time-Random)	PES	1D or 3D	-	Any
PID Controller	Dynamic	1D or 3D	Any	Any
Reaction Wheel (Force)	PES	3D	-	[Force]
Reaction Wheel (Torque)	PES	3D	-	[Force · Length]
Rigid Plant	Dynamic	3D	[Force · Length]	[Angle]
Star Tracker Noise	PES	3D	-	[Angle]
Static System	Static	1D or 3D	Any	Any
Summation	Basic	Inherited	Inherited	Input unit
Total Error	Evaluation	1D or 3D	Any	(Input unit)
Total Error (Position)	Evaluation	3D	[Length] and [Angle]	[Length]

5.2.3.3 Block Descriptions

Blocks which have a modified functionality (with respect to the previous tool version V1.0) or have been newly introduced in this study are marked with an asterisk. For all “heritage” blocks, a brief description is provided as well.

5.2.3.3.1 Accelerometer Noise*

The output of this block represents the noise spectrum of a linear accelerometer. The acceleration noise model is based on [RD1] with a more specific mapping of the parameters derived from [RD2].

The following noise contributions are included in the model (defined by a respective coefficient and illustrated in Figure 5-13):

- Velocity random walk (N)
- Acceleration random walk (K)

- Bias instability (B)
- Quantization noise (Q)

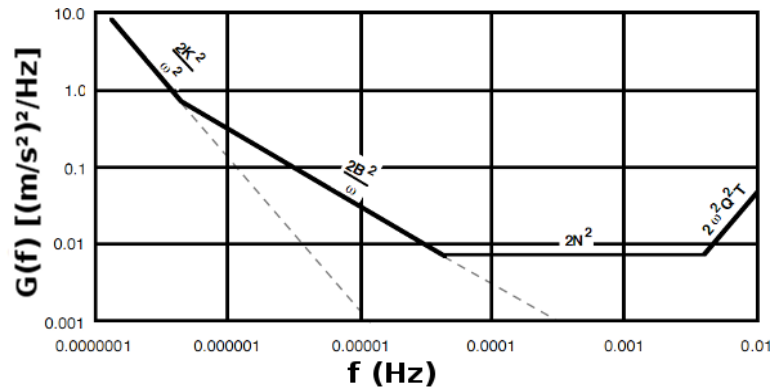


Figure 5-13: Acceleration noise PSD derived from [RD1] and [RD2]

While in tool version V1.0, the same spectrum was applied to all axes, it is now possible to define coefficients for each axis separately (e.g. to account for the typical presence of a less sensitive direction).

5.2.3.3.2 Camera Range Noise

The output of this block represents 3D bias and band-limited white noise contributions to the range measurement using a camera type sensor. Both bias and noise scale with the overall range to the target. The flat noise spectrum is realized such that the given standard deviation is ideally realized within the bandwidth determined by the given sampling time.

5.2.3.3.3 Container (with Input Port & Output Port)

Container blocks are a special block type. They can be used to abstract a complex block structure into a single block symbol similar to a “Subsystem” in Simulink. A *Container* has no block mask, but a double-click open a new system editor window which can be populated with other blocks as on the main system editor level. The link to a higher level of the system editor is realized by the *Input Port* and *Output Port* blocks (their number within a *Container* is not restricted).

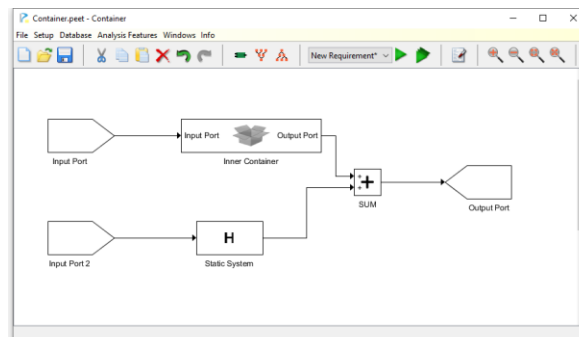


Figure 5-14: Exemplary content of a container block with two input ports and one output port

Figure 5-14 shows an example of a *Container* block with two inputs and one output. Nesting is also possible, i.e. further *Container* can be placed inside a *Container* to represent lower system levels or to “tidy up” the System Editor.

5.2.3.3.4 Coordinate Transformation

The output of this block represents the input signal expressed in a different coordinate frame following a user-defined conversion. The parameters for the block are a set of 3 rotation angles and a corresponding rotation sequence. Possible options cover both classical Euler sequences (e.g. 1-2-1, 1-3-1, etc.) as well as Tait-Bryan sequences (1-2-3, 3-2-1, etc.)

5.2.3.3.5 Dynamic System

The output of this block represents the response of an LTI dynamic system to the given input signal. It supports LTI model types with a parameterization similar to the one required for the corresponding models in MATLABs' Control System Toolbox:

- Zero-Pole-Gain model with vectors containing the zero/pole locations of a transfer function and a scalar gain
- Transfer Function model either defined by the nominator/denominator coefficients of a rational transfer function or by string expression for the rational function (e.g. $1 / (s^2 + 3*s)$)
- State-Space model of the dynamic system defined by the typical A, B, C and D matrices

In addition, a fourth option “MATLAB LTI-Model” exists as shortcut which allows linking to a single variable in the MATLAB workspace which represents the entire system in one of the above-mentioned formats.

5.2.3.3.6 Feedback System

Feedback System blocks are a special block type. They can be used to realize any kind of (feedback) loop structure. Similar to a *Container*, a *Feedback System* has no block mask, but a double-click opens a new System Editor (sub-)window which can be populated with other blocks as on the main editor level.

Nesting is also possible, i.e. further *Feedback System* blocks can be placed inside a *Feedback System* to represent implicitly inner loops.

The entire content of the (topmost) feedback system is internally converted to one single closed-loop transfer function from all inputs to all outputs to maintain the tree-like structure of the entire pointing system. Due to this conversion, it is not possible to access or display intermediate results of building blocks within the feedback system, but only the error signal at the inputs and outputs.

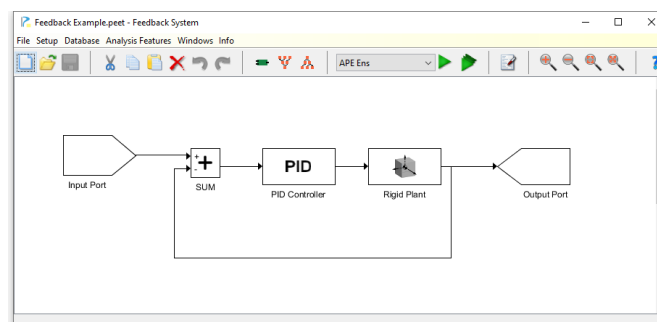


Figure 5-15: Exemplary loop realized in a feedback system block with one input port and one output port

5.2.3.3.7 Flexible Plant

The output of this block represents the 3D attitude response of a flexible body to a torque input. The flexible body dynamics takes into account n flexible modes defined by the user to extend the rigid body dynamics. The underlying model is given by the following set of differential equations (note that the coupling between the flexure and the spacecraft linear acceleration/force is neglected):

$$\Theta \dot{\omega} - \delta \ddot{a} = N$$

$$\ddot{a} + 2\zeta \Omega \dot{a} + \Omega^2 a = \delta^T \dot{\Omega}$$

with:

- Θ spacecraft inertia matrix (3x3)
- ω vector of spacecraft angular rates (3x1); integration of this quantity gives the block output
- δ matrix of coupling coefficients (3xn)
- N vector of torques acting on the spacecraft body (3x1), i.e. the block input
- a vector containing the amplitudes of n flexible modes (nx1)
- ζ diagonal matrix containing the damping ratio of the flexible modes (nxn)
- Ω diagonal matrix containing the cantilever frequencies of the flexible modes (nxn)

Internally, the model is realized in an equivalent state-space representation, which is given by:

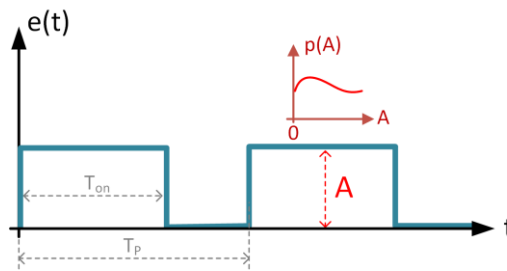
$$\begin{bmatrix} \Theta & -\delta & \mathbf{0} \\ \delta^T & -\mathbf{I} & \mathbf{0} \\ \mathbf{0} & \mathbf{0} & \mathbf{I} \end{bmatrix} \dot{\mathbf{x}} = \begin{bmatrix} \mathbf{0} & \mathbf{0} & \mathbf{0} \\ \mathbf{0} & 2\zeta \Omega & \Omega^2 \\ \mathbf{0} & \mathbf{I} & \mathbf{0} \end{bmatrix} \mathbf{x} + \begin{bmatrix} N \\ \mathbf{0} \\ \mathbf{0} \end{bmatrix}$$

with state vector $\mathbf{x} = [\omega, \dot{a}, a]^T$ and \mathbf{I} and $\mathbf{0}$ unity and zero-matrices of proper size. Furthermore, above system model is extended such that the attitude (rather than the rates) is used as output.

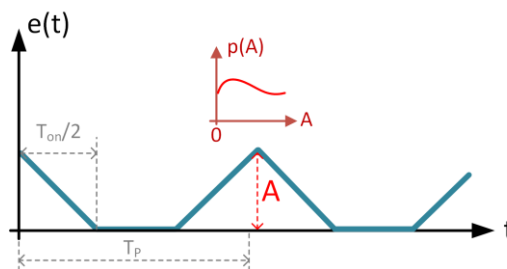
5.2.3.3.8 General Periodic Error*

The output of this block represents a temporal periodic (but non-sinusoidal) error source dependent on the selected signal type. It can also be used as a workaround to model certain “transient” signals under the assumption that they (re)occur periodically. The following signal types are available:

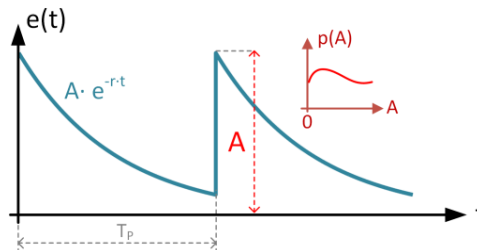
- A rectangular step signal defined by its fundamental period T_p , its amplitude A and the on-off ratio (T_{on}/T_p) in [%].



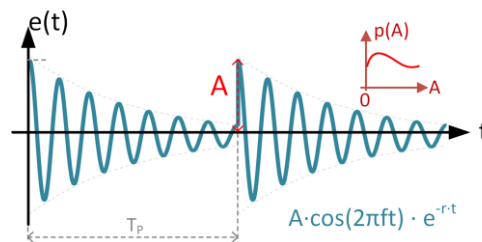
- A rectangular signal defined by its fundamental period T_p , its amplitude A and the on-off ratio (T_{on}/T_p) in [%].



- An exponentially decaying signal from amplitude A towards zero with the dimensionless decay rate r :



- A cosine signal with frequency f and initial amplitude A which exponentially decays towards zero with the dimensionless decay rate r :



All above models are internally parameterized as a Fourier series approximation with a specific coefficient set for each signal type (see chapter 5.3.4.6 for the precise model coefficients). The error signal is then realized as standard sinusoidal signal with components at different frequencies (according to the Fourier frequencies of the series approximation and amplitudes corresponding to the series coefficients). The tool also

provides a helper function to assess the impact of the approximation (w.r.t. the real signal) and guidelines for the parameter ranges which lead to a good approximation quality.

The (ensemble) distribution of the amplitude can be set to follow any of the supported distributions present in the tool (i.e. discrete, uniform, arcsine, (Truncated) Gaussian, Rayleigh, Beta or user-defined, see also chapter 5.2.3.3.15).

5.2.3.3.9 GPS

The output of this block represents a 3D bias and a simplified noise spectrum of a GPS sensor either on position or velocity level. For the simplified noise spectra, the random walk contributions basically need to be integrated over time. This is internally realized by feeding a white noise through an integrator which essentially gives a $1/f$ contribution to the spectrum which is added to the flat (“white”) background of the spectrum. Parameters for the noise bandwidth and the standard deviations determine the magnitudes of the spectra for the white and random walk contributions.

5.2.3.3.10 Gyro Rate Noise

The output of this block represents the noise spectrum of a gyroscopic sensor with a rate noise model based on [RD2]. The following noise contributions are included in the model (defined by a respective coefficient and illustrated in Figure 5-16):

- Angle random walk (N)
- Rate random walk (K)
- Bias instability (B)
- Quantization noise (Q)

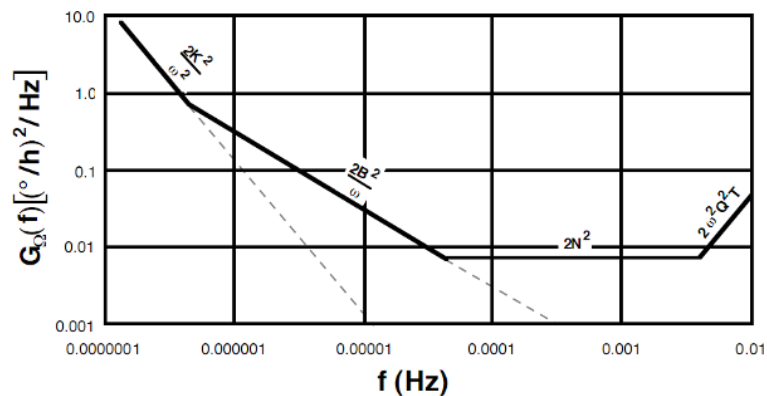


Figure 5-16: Gyro rate noise PSD derived from [RD2]

While in tool version V1.0, the same spectrum was applied to all axes, it is now possible to define coefficients for each axis separately.

5.2.3.3.11 Gyro-Stellar Estimator

The outputs of this block represent the 3D attitude estimation errors (1st output) and rate estimation errors (2nd output) after filtering the measurement inputs with a fixed-gain Kalman filter. Both attitude measurement errors (1st input) and rate measurement errors (2nd input) can contain time-constant and time-random contributions.



The gyro-stellar estimator is a model-replacement Kalman filter used to fuse data from gyro and star-tracker to get an estimate of the spacecraft attitude and of the gyro bias. The measurement update is then performed using star-tracker data.

The following fixed-gain model is realized independently for each axis based on the derivation given in [RD5] (implementation #3):

$$\begin{bmatrix} \hat{e}_\phi \\ \hat{e}_\omega \end{bmatrix} = \frac{1}{s^2 + K_p s + K_d} \begin{bmatrix} sK_p + K_d & s \\ sK_d & s^2 + sK_p \end{bmatrix} \begin{bmatrix} n_\phi \\ n_\omega \end{bmatrix}$$

with

- \hat{e}_ϕ attitude estimation error (first output signal)
- \hat{e}_ω (gyro) rate bias estimation error (second output signal)
- K_p, K_d Kalman gains > 0 (user parameters)
- n_ϕ (star tracker) attitude measurement errors (first input signal)
- n_ω (gyro) rate measurement error (second input signal)
- s Laplace domain frequency variable ($s = i\omega = 2\pi if$)

Note that K_d is equivalent to $-k_2$ in [RD5] to allow both gains to be specified as positive numbers.

5.2.3.3.12 Input PEC*

The output of this block represents an 'evaluated' error signal, i.e. a signal where both the respective error index (metric) and the statistical interpretation are assumed to be already applied.

It can be used, for instance, to include results from external analyses which have already covered above-mentioned steps. Consequently, the output can also be individually specified for each requirement set defined in a scenario, as the metrics and statistical interpretation usually differ for each requirement set. By default, no contribution is set for each requirement set. This ensures that the block can also be used in cases where no externally analysed data is available for all requirement sets. For all other cases, the following models can be used:

- A numerically defined time-constant PDF which represents the effective contribution of a time-constant error source
- A numerically defined time-random PDF which represents the effective contribution of a time-random error source
- Magnitude data of the effective power spectral density of a time-random error for which (optionally) also a cross-power spectrum can be defined.

For PDF inputs, the block internally generates samples according to the input PDF and maps these to either the constant random variable (time-constant PDF input) or the random variable component (time-random PDF input). Different to any standard random variable input, no further modification is applied to the samples (i.e. concerning error metrics and statistical interpretation).

For PSD inputs, no frequency domain metric related to the requirement set is applied. In case of spectral requirements, the input thus directly reflects the contribution of the source. For statistical requirements, the statistical interpretation is applied as for any other PSD contribution, just skipping the step of previously applying the frequency domain metric.

5.2.3.3.13 Mapping Block

The output of this block represents a 3D spatial distribution of a one-dimensional signal, e.g. for mapping the force along the thrust axis of one thruster (or several thrusters) to a force or torque noise in the reference frame of the pointing error.

The *Mapping* block internally duplicates the 1D input signal N times (according to the number of “devices” to be mapped), extends this copy for each device to a 3D signal scaled with the conversion factors in the mapping matrix and sums the contributions from all devices. For both random variable type inputs and noise spectra, this approach implicitly assumes mutual correlation (or coherence) between the contributions of different devices.

This block only serves as a quick-helper to realize multiple devices with the same properties. In case no correlation or coherence between different devices needs to be realized, the different devices can alternatively be modelled by copying the 1D source blocks and feeding their outputs to “single device” mapping blocks each (or by directly setting them up as 3D components).

5.2.3.3.14 PEC

The PEC block has no effect on the input signal itself and just routes the input signal to the output. It is only used to evaluate the current error signal with respect to the given requirement and to compare the result to specified requirement value(s) if provided for the requirement set.

5.2.3.3.15 PES (Time-Constant)*

The output of this generic block represents the contribution of a time-constant error source. The time-constant error can either be represented by a discrete value or as an ensemble-random quantity defined by a statistical distribution, i.e. a PDF p_E (see Figure 5-17).

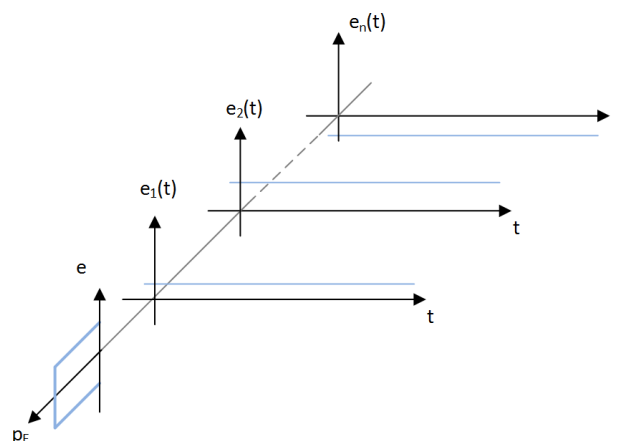
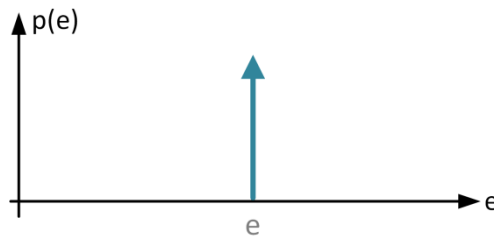


Figure 5-17: PES (Time-Constant): Temporal and ensemble behaviour of the error e for different realizations

The following distribution types are available:

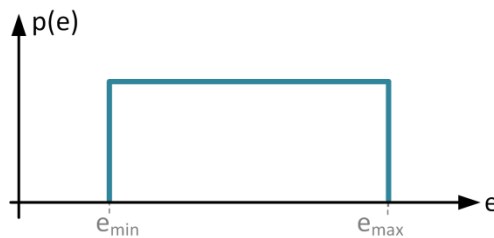


- A constant bias for each axis fully determined by a deterministic value μ . The PDF of such an error is given by (δ denotes the Dirac-Delta function):



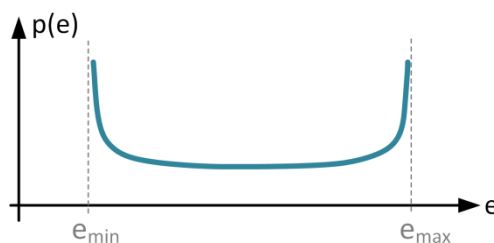
$$p_E(e) = \delta(e - \mu)$$

- A uniformly distributed error between a minimum value e_{\min} and a maximum value e_{\max} for each axis. The PDF of such an error is given by:



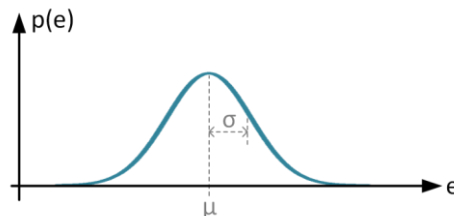
$$p_E(e) = \frac{1}{e_{\max} - e_{\min}}$$

- A “bimodal”, i.e. arcsine distributed error between a minimum value e_{\min} and a maximum value e_{\max} for each axis. The PDF of such an error is given by:



$$p_E(e) = \frac{\pi^{-1}}{\sqrt{(e_{\max} - e)(e - e_{\min})}}$$

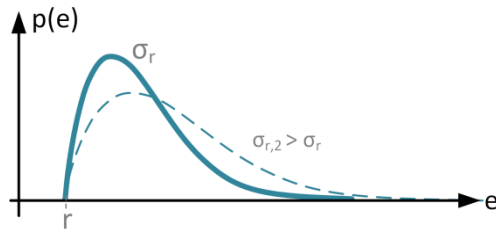
- A normal (Gaussian) distributed error individually for each axis by specifying its mean value μ and its standard deviation $\sigma > 0$. The PDF of such an error is given by:



$$p_E(e) = \frac{1}{\sigma\sqrt{2\pi}} \exp\left[-\frac{1}{2}\left(\frac{e - \mu}{\sigma}\right)^2\right]$$

- A Rayleigh distributed error individually for each axis by its scale parameter $\sigma_r > 0$. Furthermore, an additional shift parameter r is introduced which removes the restriction

of a zero minimum value ($r=0$ represents the “standard” Rayleigh distribution). The PDF of such an error is given by:



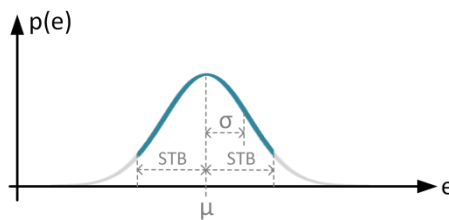
$$p_E(e) = \frac{e-r}{\sigma_r^2} \exp\left[-\frac{(e-r)^2}{2\sigma_r^2}\right]$$

(for $e \geq r$, zero else)

- An error which follows a normal distribution which is truncated at one or two given bounds dependent on the selected truncation type. In all cases, the mean value μ and the standard deviation $\sigma > 0$ need to be specified which refer to the “original” unbounded Gaussian distribution (i.e. mean and standard deviation of the truncated PDF are thus different).

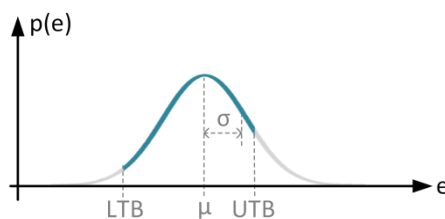
The truncation type can be one of the following (with resulting PDFs as shown below):

- The Gaussian distribution is truncated at a given (non-negative) symmetric bound (STB) relative to the provided mean value.



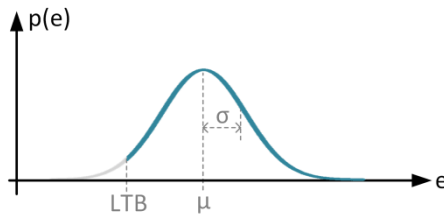
$$p_E(e) = \frac{\frac{1}{\sigma\sqrt{2\pi}} \exp\left[-\frac{1}{2}\left(\frac{e-\mu}{\sigma}\right)^2\right]}{CDF_G(\mu + STB) - CDF_G(\mu - STB)}$$

- The Gaussian distribution is truncated at an arbitrary lower bound (LTB) and upper bound (UTB), i.e. not with respect to the mean.



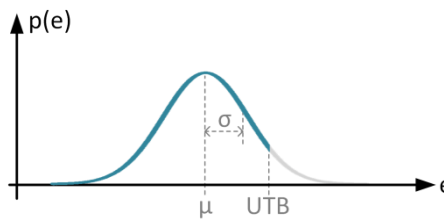
$$p_E(e) = \frac{\frac{1}{\sigma\sqrt{2\pi}} \exp\left[-\frac{1}{2}\left(\frac{e-\mu}{\sigma}\right)^2\right]}{CDF_G(UTB) - CDF_G(LTB)}$$

- The Gaussian distribution is truncated at an arbitrary lower bound (LTB).



$$p_E(e) = \frac{\frac{1}{\sigma\sqrt{2\pi}} \exp\left[-\frac{1}{2}\left(\frac{e-\mu}{\sigma}\right)^2\right]}{1 - CDF_G(LTB)}$$

- The Gaussian distribution is truncated at an arbitrary upper bound (UTB).



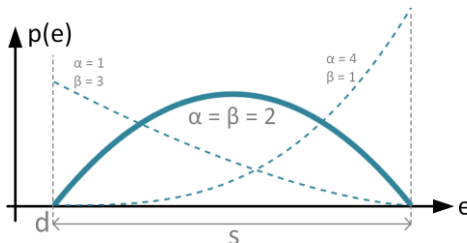
$$p_E(e) = \frac{\frac{1}{\sigma\sqrt{2\pi}} \exp\left[-\frac{1}{2}\left(\frac{e-\mu}{\sigma}\right)^2\right]}{CDF_G(UTB)}$$

In all cases above, CDF_G denotes the cumulative distribution function (CDF) of a Gaussian distribution:

$$CDF_G(e) = \frac{1}{2} \left[1 + \operatorname{erf}\left(\frac{x-\mu}{\sigma\sqrt{2}}\right) \right]$$

where erf denotes the error function. The correction with the CDF is necessary to “normalize” the PDF after truncation.

- A Beta distributed error individually for each axis by the shape parameters $\alpha \geq 0$ and $\beta \geq 0$. Further, an additional scale parameter $s \geq 0$ and an additional offset parameter d have been introduced to extend the domain of definition from $[0, 1]$ to $[d, s+d]$. The PDF of such an error is given by:



$$p_E(e) = \frac{\left(\frac{e-d}{s}\right)^{\alpha-1} \left(1 - \frac{e-d}{s}\right)^{\beta-1}}{|s| \operatorname{Beta} \alpha, \beta}$$

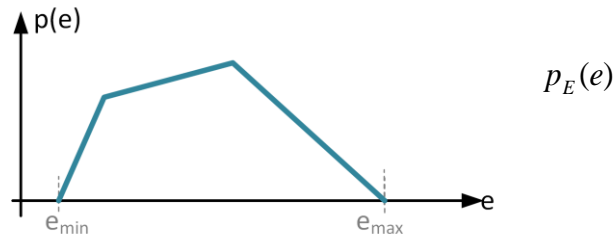
(for $d \leq e \leq d+s$, zero else)

where the standard Beta distribution itself is defined by the Gamma function Γ :

$$\operatorname{Beta} \alpha, \beta = \frac{\Gamma(\alpha)\Gamma(\beta)}{\Gamma(\alpha + \beta)}$$

- An arbitrary (but bounded) user-defined PDF individually for each axis by specifying the error value and a related “density” point by point in tabular form. If the specified data does not represent a valid PDF (i.e. no unity area in the given range, it is automatically converted into a valid PDF by proper normalization.

The first and last point provided represent the explicit bounds of the distribution.



5.2.3.3.16 PES (Time-Random)*

The output of this generic block represents the contribution of a time-random error source. According to AST-1 in [AD2], time-random errors can either be described as (time-) random variable or as random process in case sufficient information on the frequency spectrum of the error source is available.

Random Variable Models

Generally, a time-random error can be described by statistical distributions (see Figure 5-18). The PDF $p_T(e, \beta_{1...k})$ describes the temporal behaviour of the error source, where $\beta_{1...k}$ denotes the parameters of this distribution (e.g. mean value and standard deviation in case of a Gaussian). Furthermore - and completely optional - in most cases it is also possible to define a statistical distribution $p_E(\beta_i)$ for one of the parameters of the temporal behaviour. This should be understood as an ensemble-randomness, i.e. the parameter is considered as constant over time, but can vary over different “conditions” (e.g. observations, satellites, etc.).

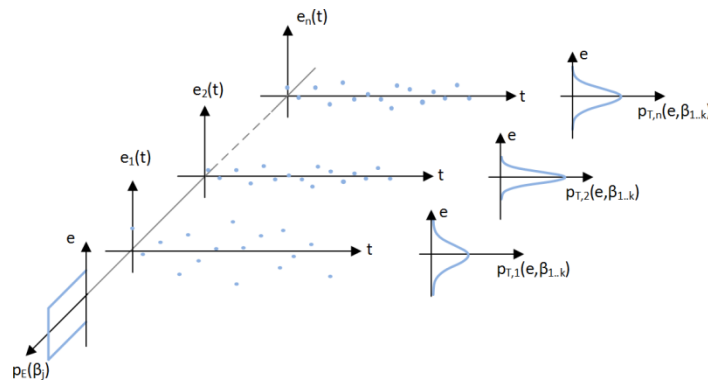
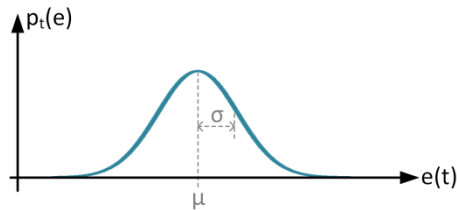


Figure 5-18: PES (Time-Random): General temporal behaviour of the error e with ensemble-random parameter (optional)

The tool provides three different signal classes (Gaussian, uniform and drift) for random variables in accordance with [AD2].

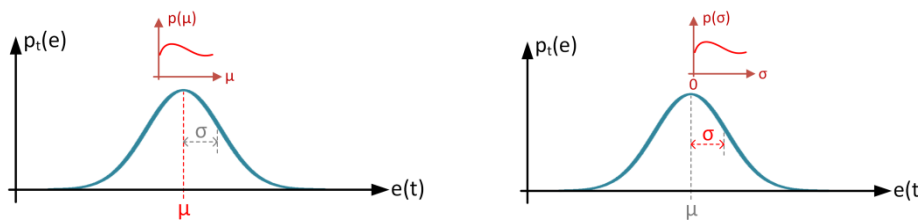
Gaussian Random Variable

The Gaussian signal class models a normal distributed temporal error individually for each axis defined by its mean value μ and its standard deviation $\sigma > 0$, i.e. a PDF $p_T(e, \mu, \sigma)$ in terms of Figure 5-18.



$$p_T(e) = \frac{1}{\sigma\sqrt{2\pi}} \exp\left[-\frac{1}{2}\left(\frac{e-\mu}{\sigma}\right)^2\right]$$

Optionally, as illustrated below, one of these parameters can be chosen as distributed. In terms of Figure 5-18, this is equivalent to specifying the ensemble PDF $p_E(\beta_j)$ with either $\beta_j = \mu$ or $\beta_j = \sigma$.



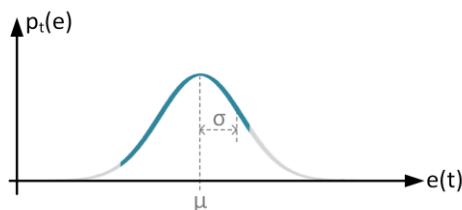
Available options for the parameter distribution are equivalent to those for the PES (Time-Constant) block described in chapter 5.2.3.3.15.

Truncated Gaussian Random Variable

The truncated Gaussian signal class models a normal distributed temporal error similar to the one described in the previous paragraph, but explicit bounds can be specified for the error values dependent on the selected truncation type.

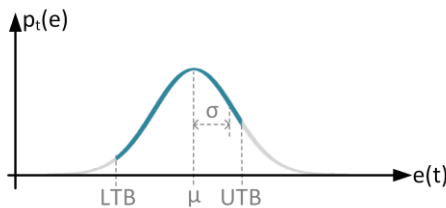
As for the PES (Time-Constant) block described in chapter 5.2.3.3.15, the following truncation options are implemented:

- Symmetric truncation



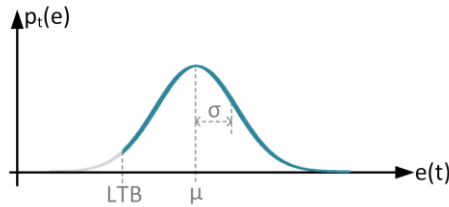
$$p_T(e) = \frac{\frac{1}{\sigma\sqrt{2\pi}} \exp\left[-\frac{1}{2}\left(\frac{e-\mu}{\sigma}\right)^2\right]}{CDF_G(\mu + STB) - CDF_G(\mu - STB)}$$

- Two-sided truncation



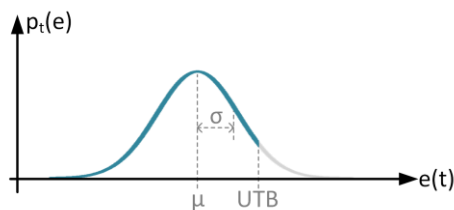
$$p_T(e) = \frac{\frac{1}{\sigma\sqrt{2\pi}} \exp\left[-\frac{1}{2}\left(\frac{e-\mu}{\sigma}\right)^2\right]}{CDF_G(UTB) - CDF_G(LTB)}$$

- Lower bound truncation



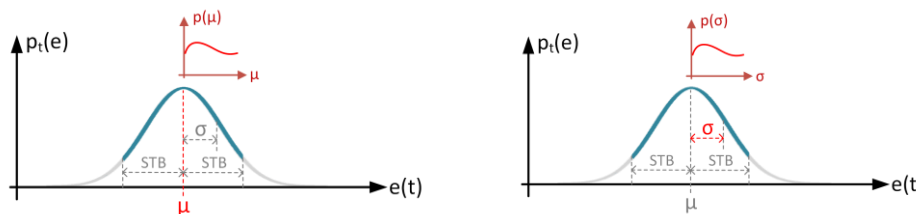
$$p_T(e) = \frac{1}{\sigma\sqrt{2\pi}} \exp\left[-\frac{1}{2}\left(\frac{e-\mu}{\sigma}\right)^2\right] \frac{1}{1 - CDF_G(LTB)}$$

■ Upper bound truncation



$$p_T(e) = \frac{1}{\sigma\sqrt{2\pi}} \exp\left[-\frac{1}{2}\left(\frac{e-\mu}{\sigma}\right)^2\right] \frac{1}{CDF_G(UTB)}$$

Optionally, as for the non-truncated Gaussian case, the mean value or standard deviation can be chosen as distributed parameter over an ensemble (with all distribution options as for the PES (Time-Constant) block). In terms of Figure 5-18, this is equivalent to specifying the ensemble PDF $p_E(\beta_j)$ with either $\beta_j = \mu$ or $\beta_j = \sigma$.



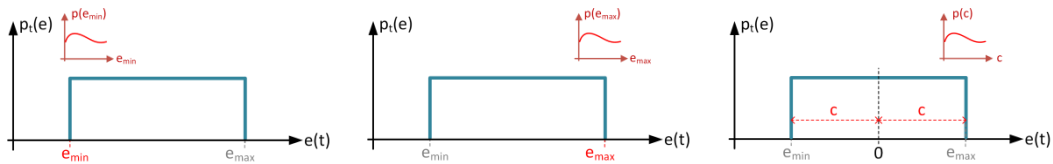
Uniform Random Variable

The Uniform Signal class models an equally distributed temporal error individually for each axis by specifying its lower bound e_{min} and its upper bound e_{max} in the respective panels, i.e. a PDF $p_T(e, e_{min}, e_{max})$ in terms of Figure 5-18.



$$p_T(e) = \frac{1}{e_{max} - e_{min}}$$

Optionally, as illustrated below, one of these temporal distribution bounds can also be chosen as distributed parameter and also a distributed range > 0 of a zero-mean uniform distribution can be specified.



In terms of Figure 5-18, this equivalent to specifying the PDF $p_E(\beta_j)$ with either $\beta_j = e_{\min}$, $\beta_j = e_{\max}$ or $\beta_j = c$.

Available options for the parameter distribution are equivalent to those for the PES (Time-Constant) block described in chapter 5.2.3.3.15.

Drift signal

The drift Signal class models a special kind of error source. It realizes a linear drift in time (with individual drift rate D for each axis) which is repeatedly corrected to zero after a certain reset time Δt_D (common to all axes). Although the temporal PDF $p_T(e, D, \Delta t_D)$ is always uniform with lower bound zero and upper bound $D \cdot \Delta t_D$, this signal is in fact not random, but deterministic.

Optionally, as indicated in Figure 5-19, an ensemble distribution can be assigned for the drift rate. Available options for the parameter distribution are again equivalent to those for the PES (Time-Constant) block described in chapter 5.2.3.3.15.

Internally, always full cycles (i.e. an integer “sawtooth” number) are assumed, to be compliant with the statistics given in [RD3].

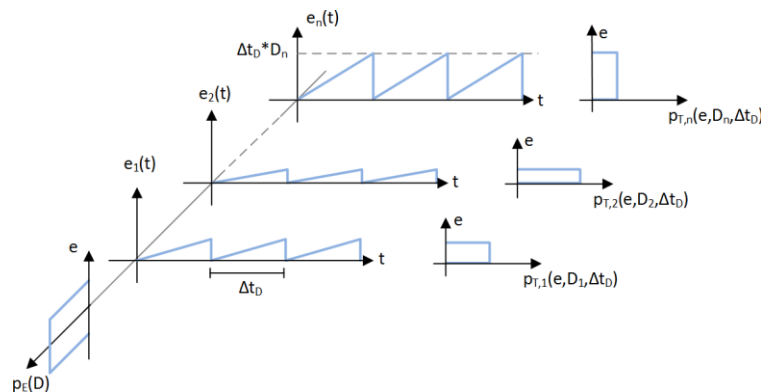


Figure 5-19: PES (Time-Random) - Drift: Temporal behaviour of the error e with ensemble-random drift rate (optional)

Different to previous PEET versions (V1.0.1 and earlier), a frequency domain approach (Fourier series approximation) is implemented to represent the temporal drift error signal as for the – basically equivalent – General Periodic Error block models described in chapter 5.2.3.3.8.

This enables a routing of drift signal through any dynamic system block model, taking into account resets in the time-windowed analysis and temporal "correlation" of drift signals with different reset times and other periodic signals (at the cost of a slightly less accurate representation of the temporal PDF itself).

Random Process Models

If – different to the random variable description – also information about the frequency spectrum of an error source is available, it can be modelled as a random process. This approach has two major advantages:

- The error after the transfer analysis (AST-2 in [AD2]) can exactly be predicted, also in the case that signals are fed through dynamic system blocks.
- Metric filters can exactly be applied to the random process signals for the pointing error index contribution (AST-3 in [AD2]) and no approximations are necessary as partially applied in the Tables in [AD1].

PEET provides three different types of random processes (Periodic, PSD and BLWN) in accordance with [AD2], where the last option is a derived simplified setup for a PSD.

Periodic Signal

The periodic random process is a special kind of random process. It realizes a zero-mean sinusoidal signal in time which is defined by an amplitude $A > 0$.

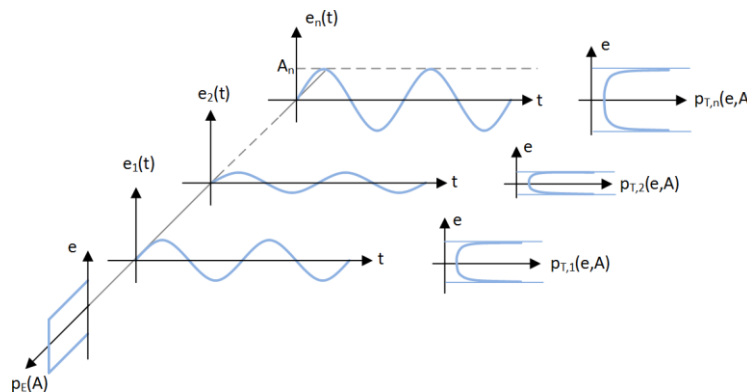


Figure 5-20: PES (Time-Random) - Periodic: Temporal behaviour of the error e with ensemble-random amplitude (optional)

Frequency and corresponding amplitude values are jointly specified in a table (matrix) in the GUI. It is also possible to account for multiple frequencies (e.g. to model harmonics) and related amplitudes in one error source by adding additional rows to the table for additional frequencies.

With the advanced statistical method, also the phases between periodic signals have an effect on the resulting PDF. By default, all periodic signals have zero-phase difference, but phases can be individually specified in a respective menu.

Optionally, as indicated in Figure 5-20, an ensemble distribution can be assigned for the drift rate. Available options for the parameter distribution are again equivalent to those for the PES (Time-Constant) block described in chapter 5.2.3.3.15. As the amplitude is restricted to be positive, any amplitude distribution with a lower bound < 0 is automatically truncated at 0.

Although the temporal PDF $p_T(e,A)$ of a periodic signal is always a bimodal (arcsine) distribution with bounds $[-A, A]$, this signal is in fact not random, but deterministic. However, its power spectral density can explicitly be expressed as:

$$G(f) = \frac{A^2}{2} \delta(f - f_p)$$

where δ denotes the Dirac-Delta function and f_p is the frequency of the sinusoid. Internally, always full cycles (i.e. integer number of periods) are assumed, to be compliant with the statistics given in [AD1] and [AD2].

Power Spectral Density (PSD)

The PSD type models a zero-mean stationary, ergodic Gaussian random process represented by an arbitrary user-defined power spectral density $G(f)$. The spectrum can also be limited to a certain bandwidth as indicated in Figure 5-21:

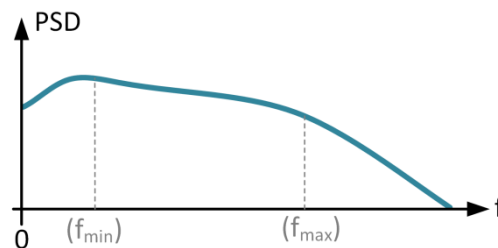


Figure 5-21: PES (Time-Random) - PSD: Spectrum of the error e with (optionally) limited bandwidth

All spectral density models are defined as single-sided amplitude spectra (i.e. $P(f) = \sqrt{G(f)}$ on unit/ $\sqrt{\text{Hz}}$ level). The conversion to a power spectral density is carried out internally.

The following options are available for the PSD representation:

- **Analytical:**
The amplitude spectra are defined by an analytical function of frequency, e.g. $1 / (f.^{2+5*f})$
- In the 1D case, this is one single function and in the 3D case at least 3 functions for the autospectra (xx/yy/zz components). Dependent on the selected option for the cross-spectrum definition, also functions for the latter (i.e. xy/xz/xz components) are required.

In addition, the PSD functions can contain a common 1D parameter which can be used to describe a varying shape of any PSD component in each realization of an ensemble. The available options are equivalent to those for the PES (Time-Constant) block described in chapter 5.2.3.3.15.
- **Numerical:**
The amplitude spectra are defined by a vector of frequencies and vectors of corresponding magnitudes of the spectrum which are jointly specified in a table (matrix). where each frequency is represented by a row.
- **LTI-Model**
This option represents another auxiliary way to realize the magnitude of a spectrum. It is introduced as often noise shaping filters are used to create noise time series with a predefined spectrum in time-domain simulations. With this option, typical



representations of these filters can directly be reused. The following options for the model options are available:

- Transfer Function (by coefficients or rational function)
- State Space
- Zero-Pole-Gain
- Matlab LTI Model
- Frequency Response Data

The parameters and settings for the first four options are basically identical to the ones for the *Dynamic System* block (see chapter 5.2.3.3.5) and are not repeated here.

The transfer function type defined as rational function is the LTI-equivalent for the analytical PSD representation. Thus, it equivalently provides the option to define a 1D ensemble parameter with a given distribution to be used in any I/O of the entire transfer function.

Frequency Response Data is the LTI-equivalent for the numerical PSD representation. It is defined by a vector of frequencies and corresponding (complex) frequency responses.

The following options are implemented for the definition of the cross-spectra:

- By coherence, i.e. the cross-power spectra are automatically determined from a user-defined coherence factor, i.e. a constant coherence over all frequencies is realized. The definition of the coherence factors is managed globally for all error sources in a specific menu. By default, no coherence is assumed.
- Explicit, the data for the cross-power spectra is explicitly in the same format as the auto-spectra.

Further, two options are available to define the valid bandwidth for analytical PSD models: either globally (i.e. the defined spectrum is considered valid over the entire frequency range specified for the scenario) or with explicit user-defined bounds (i.e. zero power is assumed outside these bounds). For numerically defined PSD models, the bandwidth is directly given by the provided frequency vector.

As already mentioned, all PSD type models represent a zero-mean stationary, ergodic random process, i.e. its statistical properties do neither vary over time, nor over the ensemble of realizations. Furthermore, the underlying PDF is assumed to be Gaussian. Thus, the error source PDF is fully characterized through the knowledge of the PSD $G(f)$, since it alone determines the variance (or standard deviation) of the signal [RD4], at least when the process is zero-mean. For a single-sided spectrum, the relation between variance and PSD is then given by:

$$\sigma_e^2 = \int_0^{\infty} G(f) df$$

In case the spectrum has a limited bandwidth (as indicated in Figure 5-21), the bounds for the integration change to f_{\min} and f_{\max} respectively.

Another important property of this setup is that if a Gaussian process undergoes a linear transformation (e.g. a transfer through a linear time-invariant dynamic system in AST-2 of [AD2]), the output is still a Gaussian, i.e. the output properties can exactly be determined.

The LTI model implementation of the spectra first realizes a dynamic system model $H(s)$ (with $s = 2\pi if$). The respective magnitude of the amplitude spectrum is then computed by taking its absolute value, i.e.

$$P(f) = \sqrt{G(f)} = |H(2\pi if)|$$

Band-Limited White Noise (BLWN)

The BLWN type models a special case of a power spectral density $G(f)=const$, i.e. it realizes a flat (“white”) spectrum with zero magnitude outside a certain bandwidth (see Figure 5-22). It is fully defined by this bandwidth and the desired standard deviation of the process.

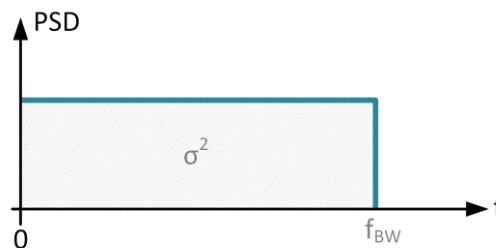


Figure 5-22: PES (Time-Random) – BLWN: Power spectral density of the error e

The magnitude of the realized power and amplitude spectral density within the given bandwidth is given by:

$$G(f) = \frac{\sigma^2}{f_{BW}}$$

in [unit²/Hz] or

$$P(f) = \sigma / \sqrt{f_{BW}}$$

in [unit/ $\sqrt{\text{Hz}}$] respectively.

5.2.3.3.17 PID Controller

The output of this block represents the control signal of an ideal Proportional-Integral-Derivative (PID) controller. The ideal controller is realized as a single-input single-output transfer function of the following form for each axis:

$$K(s) = K_p + \frac{K_I}{s} + K_D s$$

with:

- K total controller transfer function
- K_p proportional gain of the controller
- K_I integral gain of the controller
- K_D differential gain of the controller



- s Laplace domain frequency variable ($s = i\omega = 2\pi if$)

5.2.3.3.18 Reaction Wheel

PEET provides two special pointing error source blocks for setting up disturbance forces and torques on the spacecraft interface which are generated by a single reaction wheel. The 3D output disturbance is always provided with respect to the wheel frame (defined by the wheel spin around the z-axis). The orientation of the wheel with respect to the spacecraft/reference frame can be realized with the *Coordinate Transformation* block, multiple wheels by repeated use of these blocks. The models cover periodic (harmonic) error contributions as well as noise contributions dependent on the user input. They are based on [RD7] (which are itself further based on [RD8] and [RD9]) and briefly explained in the following paragraphs.

Reaction Wheel (Force)

The disturbance force model includes models for the radial and axial translation mode of the wheel and covers different kinds of parameter sets for the excitation force inputs. The definition of axial force parameters is optional.

Radial force model:

The radial (wheel x-y plane) disturbance forces acting on the spacecraft interface are modelled using the set of equations described below:

$$\begin{bmatrix} m & 0 \\ 0 & m \end{bmatrix} \begin{bmatrix} \ddot{x} \\ \ddot{y} \end{bmatrix} + \begin{bmatrix} c_r & 0 \\ 0 & c_r \end{bmatrix} \begin{bmatrix} \dot{x} \\ \dot{y} \end{bmatrix} + \begin{bmatrix} k_r & 0 \\ 0 & k_r \end{bmatrix} \begin{bmatrix} x \\ y \end{bmatrix} = \mathbf{F}_r$$

$$c_r = 4\pi\xi_r f_r m$$

$$k_r = m(2\pi f_r)^2$$

$$\mathbf{F}_{r,SC} = \begin{bmatrix} k_r & 0 \\ 0 & k_r \end{bmatrix} \begin{bmatrix} x \\ y \end{bmatrix}$$

with:

- m flywheel mass
- \mathbf{F}_r the (x,y) excitation forces for the radial translation mode
- ξ_r damping coefficient of the radial translation mode
- f_r frequency of the radial translation mode
- $\mathbf{F}_{r,SC}$ resulting (x,y) disturbance forces at the spacecraft interface



Axial force model:

The axial (wheel z-axis) disturbance forces acting on the spacecraft interface are modelled using the set of equations described below:

$$m\ddot{z} + c_a\dot{z} + k_a z = F_a$$

$$c_a = 4\pi\xi_a f_a m$$

$$k_a = m(2\pi f_a)^2$$

$$F_{a,SC} = k_a z$$

with:

- m flywheel mass
- F_a the excitation forces for the axial translation mode
- ξ_a damping coefficient of the axial translation mode
- f_a frequency of the axial translation mode
- $F_{a,SC}$ resulting (z) disturbance force at the spacecraft interface

Excitation force model:

The overall excitation force comprises both (broadband) noise and tonal disturbances:

$$\mathbf{F} = \begin{bmatrix} \mathbf{F}_r \\ F_a \end{bmatrix} = \begin{bmatrix} F_r \\ F_r \\ F_a \end{bmatrix} = \begin{bmatrix} F_{r,tonal} + F_{r,noise} \\ F_{r,tonal} + F_{r,noise} \\ F_{a,tonal} + F_{a,noise} \end{bmatrix}$$

Tonal disturbance model:

The tonal force contributions to both the axial and translational force are realized as periodic 3D signal with amplitudes at frequencies of the corresponding harmonics. The amplitude A_k of the k-th harmonic ($k=1\dots N$, index for radial and axial mode omitted) and the corresponding frequency f_k are obtained from:

$$A_k = C_k \Omega^2$$

$$f_k = h_k \Omega$$

where Ω is the spin speed of the wheel, C_k is the amplitude coefficient of the k-th harmonic and h_k the harmonic number (i.e. the ratio of frequency of k-th harmonic to spin frequency of the wheel).



Alternatively, the radial disturbance can also be defined by the static imbalance coefficient U_s (i.e. considering only the first harmonic) resulting in an amplitude/frequency set:

$$A_1 = U_s \Omega^2$$

$$f_1 = \Omega$$

Different to the model realized in the PEET prototype, with the advanced statistical method also the phase shift between periodic signals plays a role and needs to be accounted for.

The phases of all periodic signals are entirely set up in a specific menu. As in particular for this model the phase shift between the radial axes x and y is exactly 90° , the phase for the y -axis cannot be set individually as it is uniquely determined by the phase of the x -axis signal. The arbitrary phase angle between different harmonics however, can be specified by the user.

Reaction Wheel (Torque)

The disturbance torque model includes a model for the rocking mode (in the x - y plane) only as axial disturbance are negligible according to [RD7].

Rocking mode model:

The disturbance torques due to the rocking mode (wheel x - y plane) which act on the spacecraft interface are modelled using the set of equations described below [RD7]:

$$\begin{bmatrix} I_{rr} & 0 \\ 0 & I_{rr} \end{bmatrix} \begin{bmatrix} \ddot{\phi} \\ \ddot{\theta} \end{bmatrix} + \begin{bmatrix} c_{rock} & \Omega I_{zz} \\ -\Omega I_{zz} & c_{rock} \end{bmatrix} \begin{bmatrix} \dot{\phi} \\ \dot{\theta} \end{bmatrix} + \begin{bmatrix} k_{rock} & 0 \\ 0 & k_{rock} \end{bmatrix} \begin{bmatrix} \phi \\ \theta \end{bmatrix} = \mathbf{T}_{rock}$$

$$c_{rock} = 4\pi \xi_{rock} f_{rock} I_{rr}$$

$$k_{rock} = I_{rr} (2\pi f_{rock})^2$$

$$\mathbf{T}_{rock,SC} = \begin{bmatrix} k_{rock} & 0 \\ 0 & k_{rock} \end{bmatrix} \begin{bmatrix} \phi \\ \theta \end{bmatrix}$$

with:

- I_{rr} flywheel inertia perpendicular to spin axis
- I_{zz} flywheel inertia about spin axis
- \mathbf{T}_{rock} (x,y) excitation torques for the rocking mode
- ξ_{rock} damping coefficient of the rocking translation mode
- f_{rock} frequency of the rocking mode



- $\mathbf{T}_{rock,SC}$ resulting (x,y) disturbance torques at the spacecraft interface

Excitation torque model:

According to [RD7], the overall excitation torque comprises (broadband) noise and tonal disturbances for the rocking mode and negligible disturbance torques around the z-axis.

$$\mathbf{T} = \begin{bmatrix} \mathbf{T}_{rock} \\ 0 \end{bmatrix} = \begin{bmatrix} \mathbf{T}_{rock} \\ \mathbf{T}_{rock} \\ 0 \end{bmatrix} = \begin{bmatrix} \mathbf{T}_{rock,tonal} + \mathbf{T}_{rock,noise} \\ \mathbf{T}_{rock,tonal} + \mathbf{T}_{rock,noise} \\ 0 \end{bmatrix}$$

Tonal disturbance:

The tonal torque contribution from the rocking mode is realized as a periodic 3D signal with amplitudes at frequencies of the corresponding harmonics. The amplitude A_k of the k-th harmonic ($k=1\dots N$, index for rocking mode omitted) and the corresponding frequency f_k are obtained from:

$$A_k = C_k \Omega^2$$

$$f_k = h_k \Omega$$

where Ω is the spin speed of the wheel, C_k is the amplitude coefficient of the k-th harmonic and h_k the harmonic number (i.e. the ratio of frequency of k-th harmonic to spin frequency of the wheel).

Alternatively, the rocking mode can also be defined by the dynamic imbalance coefficient U_d (i.e. considering only the first harmonic) resulting in an amplitude/frequency set:

$$A_1 = U_d \Omega^2$$

$$f_1 = \Omega$$

As for the force model, the periodic component phase shift between the radial axes x and y is exactly 90° and the phase for the y-axis cannot be set individually, but the phase angle between different harmonics.

5.2.3.4 Rigid Plant

The output of this block represents the 3D attitude response of a rigid body to a torque input. The block realizes an ideal plant model following the equation

$$\Theta \dot{\omega} = \mathbf{N}$$

with:

- Θ body inertia matrix (3x3)



- ω vector of body angular rates (3x1), integration of this quantity gives the block output
- N vector of torques acting on the body (3x1) as block input

5.2.3.5 Star Tracker Noise

The output of this block represents the bias-free 3D noise spectrum of a star tracker considering field of view and pixel noise contributions. The z-axis is considered as boresight axis, x- and y-axes correspond the cross-axes with equal noise contributions.

The underlying model is based on [RD10]. The PSD of the field of view noise spectrum with standard deviation n_{FOV} is represented by the following first order transfer function:

$$P_{FOV} = \frac{\sqrt{T_{FOV}}}{1 + s \frac{T_{FOV}}{2}} n_{FOV}$$

The correlation time T_{FOV} is assumed to be proportional to the inverse of the velocity v_{star} (pixels/sec) with which the star image moves on the sensor pixel matrix with N pixels:

$$T_{FOV} = \frac{N}{v_{star} \sqrt{N_{stars}}}$$

The star velocity itself can be linked to the average spacecraft angular velocity ω_{SC} :

$$v_{star} = \omega_{SC} \frac{N}{FOV} \sin \beta \cos \alpha$$

where FOV is the sensor field of view, β is the angle between the sensor boresight and the spacecraft rotation axis and α is the angle between the star image direction of motion on the detector matrix and the detector reference axis. The PSD of the pixel noise with standard deviation n_{pixel} is modelled using a 2nd-order filter as (again, the additional factor of $\sqrt{2}$ compared to [RD10] is necessary to realize for conversion to a one-sided spectrum):

$$P_{pixel} = \frac{\omega_0^2 \sqrt{T_{pixel}}}{s^2 + 2\xi\omega_0 s + \omega_0^2} n_{pixel}$$

where ξ is the filter damping coefficient and the characteristic frequency ω_0 is given by:

$$\omega_0 = \frac{4\xi}{T_{pixel}}$$



The correlation time T_{pixel} is again assumed to be proportional to the inverse of the velocity v_{star} :

$$T_{pixel} = \frac{N_{pixels}}{v_{star}}$$

where N_{pixels} is the size of the centroiding window in pixels.

The overall noise spectrum is then obtained by summation of the two contributions. This implies a summation on the level of power spectra, i.e. both expressions are squared before the summation (* denotes the complex conjugate transpose):

$$G_{STR} = G_{FOV} + G_{pixel} = (P_{FOV}P_{FOV}^*) + (P_{pixel}P_{pixel}^*)$$

5.2.3.6 Static System

The output of this block represents the input signal multiplied with a constant system matrix. By default, the units of the input/output are inherited from the input signal, but also any unit compatible to the input signal and an arbitrary output unit can be specified. The unit of the system matrix is derived from the selected units, i.e. if the input unit is [A] and the output unit is [B], it is assumed that the system model parameters are provided in a unit [B/A].

The system matrix is used to pre-multiply the input signal, i.e. Output = Matrix · Input and can be used to scale the input signal or to introduce a coupling between axes of the input.

5.2.3.7 Summation

The output of this block represents the sum or difference of the input signals dependent on the selected convention. All input signals must have a compatible unit (i.e. have the same unit group) and input signal dimensions. As for the Sum block in Simulink, a string sequence defines the sign applied to each output and the number of outputs itself (e.g. “+-+” translates to “subtract input 2 from the sum of inputs 1 and 3”).

For all error signal parts which are represented by samples (i.e. all but PSD), the summation/subtraction is directly applied to the samples. For PSD contributions, also the cross-spectra are taken into account.

5.2.3.8 Total Error

The *Total Error* block no output port and serves as “endpoint” of the budget tree, i.e. its highest level. Thus, only a single block of that type is allowed in a PEET scenario (to evaluate signals on lower level than the final error, an arbitrary number of *PEC* blocks can be used at any stage of a budget tree).

Requirement values which shall be associated with this block are completely defined via a respective the menu. The *Total Error* block has no effect on the input signal itself. It is only used to evaluate the input error signal with respect to the given requirement (and compare it to the specified requirement value(s) if provided).

The content of the different parts of the input error signal (CRV, RV, drift, periodic signal and random process part) is summed according to AST-4 of [AD2]. In case a random



process error contribution is present, first its variance is computed within the user-defined evaluation bandwidth.

The overall error is computed per axis (x,y,z) and with respect to the user defined LoS axis. Note that the latter is the only special feature that links the block really to pointing. Disregarding the LoS error, this block (and PEET) could be used to compute any kind of 3-axis budget (i.e. PEET could generally be understood as "Performance Error Engineering Tool" rather than a "Pointing Error Engineering Tool" only.

5.2.3.9 Total Error (Position)

The *Total Error (Position)* block supports only 3D input signals. It has one position error and at least one attitude error input while the number of further attitude error inputs depends on the block settings.

As the standard *Total Error* block, this block serves an "endpoint" of the budget tree (i.e. its highest level). Different to the latter, it allows the computation of a position/displacement error budget which is the result of "pure" 3-axis position errors and 3-axis attitude errors which couple into equivalent position errors due to dedicated "lever arms" (e.g. as it is the case for formation flying missions).

The implemented model in the PEET prototype for an "exact" position budget was based on Eq.5 in [RD6]:

$$\begin{aligned}\mu_{\text{tot},x} &= \mu_{\text{pos},x} - \sum_{i=1}^{N_{\text{att}}} (y_i \mu_{\text{att},z,i} - z_i \mu_{\text{att},y,i}) & \sigma_{\text{tot},x}^2 &= \sigma_{\text{pos},x}^2 + \sum_{i=1}^{N_{\text{att}}} (y_i^2 \sigma_{\text{att},z,i}^2 + z_i^2 \sigma_{\text{att},y,i}^2) \\ \mu_{\text{tot},y} &= \mu_{\text{pos},y} - \sum_{i=1}^{N_{\text{att}}} (z_i \mu_{\text{att},x,i} - x_i \mu_{\text{att},z,i}) & \sigma_{\text{tot},y}^2 &= \sigma_{\text{pos},y}^2 + \sum_{i=1}^{N_{\text{att}}} (z_i^2 \sigma_{\text{att},x,i}^2 + x_i^2 \sigma_{\text{att},z,i}^2) \\ \mu_{\text{tot},z} &= \mu_{\text{pos},z} - \sum_{i=1}^{N_{\text{att}}} (x_i \mu_{\text{att},y,i} - y_i \mu_{\text{att},x,i}) & \sigma_{\text{tot},z}^2 &= \sigma_{\text{pos},z}^2 + \sum_{i=1}^{N_{\text{att}}} (x_i^2 \sigma_{\text{att},y,i}^2 + y_i^2 \sigma_{\text{att},x,i}^2)\end{aligned}$$

with (axis index omitted):

- μ_{tot} total mean of resulting displacement error
- σ_{tot} total standard deviation of resulting displacement error
- μ_{pos} overall mean of "pure" position error contributors
- σ_{pos} overall standard deviation of "pure" position error contributors
- N_{att} number of attitude error couplings to position
- $\mu_{\text{att},i}$ mean of i-th attitude error
- $\sigma_{\text{att},i}$ standard deviation of i-th attitude error
- X_i, Y_i, Z_i components of coupling vector of i-th attitude error

Different to Eq. 5 in [RD6], there is no summation over different position error contributors. The summation of these contributors has to be realized using standard *Summation* blocks in the PEET scenario.



As the direction of individual contributors (sign relations) are not exactly known using means and (always positive) standard deviations only, the PEET prototype alternatively offered of a more conservative approach using a “worst case” option. Here, the total mean is computed using absolute values according to the following equation:

$$\begin{aligned}\mu_{tot,x} &= \left| \mu_{pos,x} \right| + \left| \sum_{i=1}^{N_{att}} (y_i \mu_{att,z,i} - z_i \mu_{att,y,i}) \right| \\ \mu_{tot,y} &= \left| \mu_{pos,y} \right| + \left| \sum_{i=1}^{N_{att}} (z_i \mu_{att,x,i} - x_i \mu_{att,z,i}) \right| \\ \mu_{tot,z} &= \left| \mu_{pos,z} \right| + \left| \sum_{i=1}^{N_{att}} (x_i \mu_{att,y,i} - y_i \mu_{att,x,i}) \right|\end{aligned}$$

Above equations rely on the simplified statistical method. With the introduction of the advanced statistical method, the decomposition in mean and variance values is no longer necessary and the position error can directly be expressed precisely without the need for a further distinction (“Exact” or “Worst case”):

$$\begin{aligned}e_{tot,x} &= e_{pos,x} - \sum_{i=1}^{N_{att}} (y_i e_{att,z,i} - z_i e_{att,y,i}) \\ e_{tot,y} &= e_{pos,y} - \sum_{i=1}^{N_{att}} (z_i e_{att,x,i} - x_i e_{att,z,i}) \\ e_{tot,z} &= e_{pos,z} - \sum_{i=1}^{N_{att}} (x_i e_{att,y,i} - y_i e_{att,x,i})\end{aligned}$$

5.2.4 Remarks on Compatibility

The new PEET release (V1.1) is compatible with all current MATLAB versions starting from 2011b (as the previous releases) up to the latest version used for the test campaign (2020b). No immediate issues with newer MATLAB versions are expected in the near future, but for any future PEET releases, it might no longer be possible to maintain compatibility over such large range of MATLAB version.

First, applied MATLAB functions have become obsolete or have changed their behaviour meanwhile which caused additional effort to maintain the functionality in a version-dependent way. Second, PEET uses the MATLAB class concept in its core algorithms. The way class property definitions are handled have changed over the versions as well and a parallel set of algorithms had to be established (for MATLAB >2019b) to avoid warnings or even potential errors in latest MATLAB versions. In a similar way, PEET’s JAVA GUI communicates with MATLAB via the rather undocumented JAVA-MATLAB-Interface (JMI) which has been present in MATLAB basically ever since. Starting from MATLAB 2016b a dedicated JAVA API was introduced and there is no way to predict up to which point both interfaces will be maintained in parallel.

Summarizing, while the PEET software is basically considered complete in terms of its core features and functionality, special attention must be taken to maintain compatibility with future MATLAB releases.



5.3 Theoretical Background of the Tool Implementation

This section describes the mathematical aspects and considerations mandatory for the specific tool implementation of the advanced statistical method, the treatment of correlation, the use of ensemble domains, the realization of the transfer system analysis (AST-2 in [AD2]) and the Fourier series approximations used for drift and 'transient' (i.e. general periodic) error signals.

5.3.1 Advanced Statistical Method

The PEET prototype was based on the **simplified statistical method** (SSM) as described in [AD2]. This method assumes applicability of the central limit theorem at the final error level, i.e. that its PDF has a (nearly) Gaussian shape. Consequently, all error sources can be entirely described only via their basic statistical moments (mean and variance) neglecting their real underlying PDF. These moments are exact statistical quantities, even after summation of different error sources with arbitrary PDF during the systems transfer (AST-2 in [AD2]).

The PDF-based **advanced statistical method** (ASM) maintains and propagates the information of the underlying PDF from each error source (and their combination during the system transfer) in the signal for the final error contribution. The realization in the tool does however not follow a typical Monte-Carlo simulation approach in the time-domain, but a frequency domain approach which allows also accurately taking into account random process contribution and their transfer analysis by "analytical" propagation.

5.3.1.1 Wrap-up of PDF Properties and Rules

5.3.1.1.1 Error Source PDFs

A representation of the error source PDF first requires the derivation of analytical descriptions for all PDFs that contain the respective distribution parameters available to the user for the setup of random variable error sources. This is straightforward for the basic distributions $p(e)$ provided in [AD1] and [AD2] and analytical solutions for these PDFs are provided in a later section of this document (together with other related properties).

For a time-random error source e which can additionally have an ensemble random parameter k (see Tables in Appendix B of [AD1]), their joint distribution is required for the mixed statistical interpretation (the subscripts T and E in the equation below indicate that the distributions describes a quantity random over time and ensemble):

$$\text{Prob}(e(k,t) \in D) = \int_D p_{E,T}(e,k) de dk$$

with:

- p probability density function
- e error signal
- k ensemble random variable
- t temporal variable
- D integration domain
- E,T PDF subscripts to describe both temporal and ensemble quantities



This joint distribution is often not explicitly known, but the distribution of the ensemble parameter k itself and the distribution of the temporal behaviour for a given value of the parameter. According to Bayes' rule, the "unknown" joint density can then be expressed as:

$$p_{E,T}(e,k) = p_T(e|k) p_E(k)$$

with:

- p probability density function
- e error signal
- k ensemble random variable
- $_{E,T}$ PDF subscripts to describe both temporal and /or ensemble quantities
- $p(e/k)$ conditional probability of the error signal given a value of the ensemble variable

The required PDF according to [AD1] is the marginal density of a single variable alone ("time"). Generally, a marginal distribution can be derived from a joint density by integrating over all but the desired variable x_i :

$$p(x_i) = \int p(x_1, \dots, x_n) dx_1 \dots dx_{i-1} dx_{i+1} \dots dx_n$$

with:

- $p(x_i)$ marginal PDF of variable the i -th random variable
- $p(x_i, \dots)$ joint PDF of all random variables
- x_i specific random variable i

Especially for the required mixed statistical interpretation cases, this yields the expression given in the tables in Appendix B of [AD1] and chapter 8 of [AD2]:

$$p_T(e) = \int p(e,k) dk = \int p_T(e|k) p_E(k) dk$$

with:

- p probability density function
- e error signal
- k ensemble random variable
- $_{E,T}$ PDF subscripts to describe temporal and /or ensemble quantities
- $p(e/k)$ conditional probability of a the error signal given a value of the ensemble variable



Such PDFs are present for Gaussian and uniform random errors ([AD1]). Analytical solutions are provided in a later subsection of this document as well, however closed form solutions do not always exist – even for the restricted set of distributions provided in the reference.

Sidenote: In PEET V1.0, similar expressions were also used for the representation of drift signals (according to Table B-7 in [RD3]). As their temporal distribution also follows a uniform distribution, these PDFs were however just a subset of those derived for uniform temporal random errors. The current implementation uses a frequency domain approach for drift signals (see chapter 5.3.3.5.2).

5.3.1.1.2 Correlated Error Sources

In terms of the simplified statistical method, error contributions are either summed assuming full or no correlation using dedicated summation rules for these two cases. PEET shall treat correlation in a more generalized way by allowing the specification of an arbitrary correlation between different axes of a single error source and between different error sources.

In terms of PDF, this again requires the knowledge of joint probability densities, e.g.

$$p(x_1, y_1, z_1)$$

with:

- p probability density function
- $x/y/z$ axis identifiers
- 1 indexer for error source #1

to describe the correlation between three axes of an error source or

$$p(x_1, x_2, x_3, \dots)$$

with:

- p probability density function
- x x-axis identifier
- 1,2,3 indexers for error sources #1, #2, #3

to describe the correlation the between x-axes of all error sources. Thus, generally one joint PDF for the entire set of n error sources and their axis is required:

$$p(x_1, \dots, x_n, y_1, \dots, y_n, z_1, \dots, z_n)$$

with:

- p probability density function
- $x/y/z$ axis identifiers
- 1, ..., n error sources identifiers

5.3.1.1.3 Summation of Errors

For the simplified statistical method, the summation of error contributions follows dedicated rules on how to combine means and variances dependent on the given correlation and source type (time-constant and time-random).



The summation of error contributions for the advanced statistical method needs to be realized using a convolution of the involved PDFs. In the correlated case, this requires again the joint density of the two error sources, e.g. for the sum of two errors X_1 and X_2 :

$$p_{X_1+X_2}(x) = \int_{-\infty}^{\infty} p_{X_1, X_2}(x_1, x-x_1) dx_1 = \int_{-\infty}^{\infty} p_{X_1, X_2}(x-x_2, x_2) dx_2$$

In case the errors are independent (i.e. uncorrelated), this collapses to a convolution of marginal PDFs:

$$p_{X_1+X_2}(x) = \int_{-\infty}^{\infty} p_{X_1}(x_1) p_{X_2}(x-x_1) dx_1 = \int_{-\infty}^{\infty} p_{X_1}(x-x_2) p_{X_2}(x_2) dx_2$$

5.3.1.1.4 Error Evaluation

For the simplified statistical method, the evaluation of the error $e_{tot,LoC}$ which is not exceeded with a given level of confidence basically reduces simple expression which contains the multiplication of the total error variance with a confidence factor n_p :

$$e_{tot,LoC} = |\mu_{tot}| + n_p \cdot \sigma_{tot}$$

with:

- $e_{tot,LoC}$ total error for a given level of confidence
- μ_{tot} total mean value
- n_p confidence factor
- σ_{tot} total standard deviation

A confidence factor $n_p=1$ (2,3,...) corresponds to a confidence level of 68.3% (95.5%, 99.7%,...) for Gaussian distribution. The absolute value of the mean value is used as the worst case of the error needs to be considered.

For the advanced statistical method, the assumption of a Gaussian distribution (i.e. applicability of the central limit theorem) is not necessary and the total error $e_{tot,LoC}$ for a given level of confidence LoC in [%] can be determined from:

$$LoC/100 = \int_0^{e_{tot,LoC}} p(|e|) de$$

with:

- LoC level of confidence in [%]
- $e_{tot,LoC}$ total error for a given level of confidence
- e error signal
- p probability density function



The PDF of the absolute value for the total error is used again, as the direction (sign) of the error is usually not of interest, but its magnitude. If an explicit requirement value e_r is assigned for the total error in addition, then also the following questions can be covered:

- “Does the error value $e_{tot,LoC}$ fulfil the requirement?”, i.e. $|e_{tot,LoC}| < e_r$
- “What is the probability that the required error is not exceeded?”, i.e. what is $\text{Prob}[e_r]$

5.3.1.2 Implementation Baseline

Different approaches were assessed in the predecessor study on how the PDF information of error signals can be represented, propagated and evaluated.

A completely analytical approach following the rules and equations presented in the previous chapters is generally the most accurate way, but it turned out to be infeasible for several reasons. First, from a pragmatic point of view, this would require a toolbox capable of dealing with symbolic variables expressions. Here, the MATLAB Symbolic Toolbox was a suitable candidate, but in compliance with the software requirement on the restricted use of MATLAB toolboxes (to ensure a wide applicability of the PEET tool due to expected license issues for most of the potential users).

But even without that restriction, closed-form solutions for all required PDFs are not guaranteed. This already holds for the set of initial error source representations with a fixed set of parameters for the mixed statistical interpretation (see section 5.3.6.2) and becomes even more critical for the signal summation where products of arbitrary PDFs have to be integrated.

A numerical representation of the PDFs solves this problem without a significant loss of accuracy as long as the resolution is sufficiently fine. The summation of error signals then turns into a numerical convolution of vectors describing the PDF and the final error evaluation to a numerical integration of PDFs.

The fundamental remaining problem with this approach is again pragmatic. As soon as any of the sources (or one of its parameters) is correlated with another source (or parameter), joint PDFs are required. This information is expected to be not available to a user in basically all cases as usually only correlation coefficients and the marginal densities for all error sources, axes or parameters are known or can be estimated.

Alternatively, vectors of random samples can be used to represent numerically a PDF, i.e. when computing a histogram of these samples with proper normalization, the PDF can be “recovered” from a set of samples. The resolution of the PDF basically only depends on the length of the sample vectors.

This approach basically has several advantages. Methods exist to “inject” arbitrary correlation between multivariate samples based on correlation coefficients and to “shape” the samples to follow an arbitrary PDF (see chapter 5.3.1.4). The signal summation collapses to a simple vector addition in this case. As MATLAB is highly efficient and suitable for numerical matrix and vector operations also for large dimensions, this approach was chosen as baseline.

Obviously, a certain numerical error is introduced in the evaluation when deriving the PDF from the histogram of random samples. For a sufficiently large sample size (around $1e6$ samples), this error is expected to be in the order of 1% with respect to an exact analytical solution. Compared to the gain in accuracy by using the advanced statistical method itself



(i.e. removing the systematic error of the simplified method for non-Gaussian total error contributions), this error is considered negligible and completely tolerable.

Example: Uniform distribution $p(e) = U(-1,1)$ and a 99.7% level of confidence

- Analytical result with ASM:

$$0.997 = \int_0^{e_{tot,LoC}} |U(-1,1)| de = \int_0^{e_{tot,LoC}} U(0,1) de = \int_0^{e_{tot,LoC}} \frac{1}{1-0} de = e_{tot,LoC}$$

with:

- $e_{tot,LoC}$ total error for a given level of confidence
- $U(a,b)$ uniform distribution with bounds a and b

- Simplified method:

$$e_{tot,n_p} = |\mu_{tot}| + n_p \cdot \sigma_{tot} = \left| \frac{1+(-1)}{2} \right| + 3 \cdot \sqrt{\frac{(1-(-1))^2}{12}} = 1.7321$$

with:

- e_{tot,n_p} total error for a given confidence factor
- μ_{tot} total mean value
- n_p confidence factor
- σ_{tot} total standard deviation

i.e. analytical result + 73.73% systematic error

5.3.1.3 Concept of Statistical Domains

The concept of statistical domains first arose in the predecessor study during the assessment of physically and probabilistic meaningful correlation options between different types of error sources (see chapter 5.3.2) and a more flexible definition and evaluation of pointing error requirements (chapters 5.3.1.3.1 and 5.3.1.3.2).

[AD2] clearly distinguishes between time-constant and time-random error sources and according to the summation rules in AST-4. This implicitly splits the contributions to the total error already in two domains "Time" and "Ensemble" which are separately evaluated. Between these domains, also no correlation can be specified as they have physically nothing in common (e.g. the distribution of a misalignment and the distribution of the temporal noise of a sensor).

The temporal domain is common ("global") for the error evaluation, however different ensemble domains could exist. For instance, ensemble random contributions could be assigned to domains such as "Manufacturing" (misalignments, displacements, multiple satellites, etc.) or "Observations" (error contributions that do not vary in time over a single observation, but due to varying conditions between different observations).

These domains are independent by definition, and consequently also no correlation is meaningful between them. Furthermore, a tailored treatment for these domains is possible

in terms of requirement specification which is – most importantly - still compliant with the rules and methods in [AD1] and [AD2].

5.3.1.3.1 Statistical Domains and Statistical Interpretation

According to [AD1] and [AD2], one of the key requirement specification parameters is the statistical interpretation of the error contributions. The three interpretation types are related to the following budgeting tasks (see also Figure 5-23).

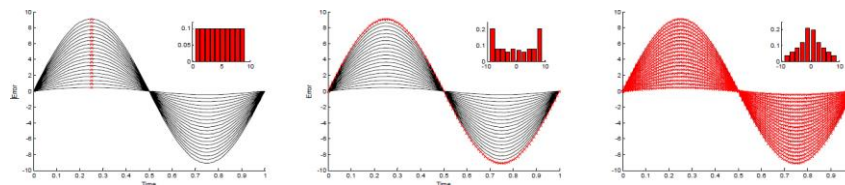


Figure 5-23: Illustration of ensemble (left). Temporal (center) and mixed (right) statistical interpretation [AD1]

- Ensemble interpretation: “What is the distribution of the temporal worst-case error values in all single realizations?”
- Temporal interpretation: “What is the temporal distribution of the temporal worst-case realization?”
- Mixed Interpretation: “What is the distribution of the entire error values over both time and ensemble?”

In all three cases, the temporal domain and an ensemble domain is involved and a “treatment” can be assigned to each of these domains.

- With the “ensemble” interpretation, the ensemble domain is treated statistically and the temporal domain as worst case.
- With the “temporal” interpretation, the temporal domain is treated statistically and the ensemble domain as worst case.
- With the “mixed” interpretation, both temporal and ensemble domain are treated statistically.

Thus, each interpretation can be mapped to a “pair” of domain treatments as shown in Table 5-2. The fourth pair has no direct equivalence in [AD1] and [AD2] and leads to very conservative results as it only considers a discrete overall worst case value over both time and ensemble.

Table 5-2: Mapping between “domain treatment” concept in PEET and “statistical interpretation” (SI) in [AD1] and [AD2]

Ensemble domain Temporal domain	Statistical	Worst Case
Statistical	Mixed SI	Temporal SI
Worst Case	Ensemble SI	-*



* This combination is not explicitly covered in [AD1] and [AD2] and leads to a very conservative result for the deterministic overall worst-case value.

The main advantage of this generalized equivalent for the statistical interpretation is that it allows an individual choice on how different ensemble domains are evaluated and thus a more flexible definition of requirements.

Example:

“The pointing error shall be smaller than X over all times for the worst-case satellites and for 99.7% of all observations.”

This means that the temporal domain and the “Observations” ensemble domain are treated statistically while the ensemble domain “Manufacturing” is treated as worst-case.

5.3.1.3.2 Statistical Domains and Level of Confidence Evaluation

Following the considerations above, a separate treatment for each ensemble domain can be chosen and generally also a level of confidence could be assigned individually to the contributions from different domains.

This generally results in two different evaluation methods for the final error: a common evaluation or an individual evaluation of the domain contributions.

For the common evaluation, the error contributions e_i from N_D different domains i are summed first and then one total error $e_{tot,LoC}$ for the common level of confidence LoC in [%] is determined:

$$LoC/100 = \int_0^{e_{tot,LoC}} p(e) de \quad \text{with} \quad p(e) = \left(\sum_{i=1}^{N_D} e_i \right)$$

- LoC level of confidence in [%]
- $e_{tot,LoC}$ total error for a given level of confidence
- e error signal
- p probability density function
- N_D number of domains
- i domain index

In this case, only the statistical treatment can be different for each domain, but the evaluation itself is identical to the case of one single ensemble domain.

Example:

“The pointing error shall be smaller than X over all times for 99.7% of all satellites and observations.”

For the individual evaluation, the errors $e_{LoC,i}$ for the levels of confidence LoC_i defined for each of the N_D different domains are evaluated. Then these contributions are linearly summed to form the total error $e_{tot,LoC}$:

$$e_{tot,LoC} = \sum_{i=1}^{N_D} e_{LoC,i} \quad \text{with} \quad LoC_i/100 = \int_0^{e_{LoC,i}} p(|e_i|) de_i$$

where

- LoC_i level of confidence in [%] for domain i



- $e_{tot,LoC}$ total error for the given level(s) of confidence
- $e_{LoC,i}$ error in domain i for the given level of confidence of domain i
- e_i error signal in domain i
- p probability density function
- N_D number of domains
- i domain index

Example:

“The worst-case pointing error in time shall be smaller than X for 99.7% of all satellites and 68% of all observations.”

Both approaches are generally valid and possible. The individual evaluation is the more conservative one, as it sums the “worst-case” contributions from the various domains which do not necessarily occur at the same instant or realization. The common evaluation accounts for the statistics of the summed (independent) contributions.

5.3.1.4 Random Sample Generation

The numerical approach for random variable error sources and distributed parameters requires the generation of random samples that represent both the random variable with the desired PDF and the desired correlation between the axes and error sources.

Several methods exist to create samples of correlated standard normal distributed random variables. The method used in PEET is based on [RD11]. It first requires the covariance matrix Σ of size $m \times m$ for the m error signals to be realized. As standard normals are used (i.e. having unity variance), the covariance matrix is equal to the matrix of correlation coefficients. Then a Cholesky decomposition is applied to the matrix to obtain an upper triangular matrix \mathbf{A} :

$$\Sigma = \mathbf{A}^T \mathbf{A}$$

where

- Σ covariance matrix ($m \times m$)
- \mathbf{A} upper triangular matrix obtained from Cholesky decomposition

In a next step, a vector \mathbf{n} of length n_s is drawn from of standard normal distribution. Both operations are easily feasible using standard MATLAB functions. Then a matrix \mathbf{N} of size $n_s \times m$ is computed:

$$\mathbf{N} = [\mathbf{n}_1 \quad \dots \quad \mathbf{n}_m] = \mathbf{A} \mathbf{n}$$

where

- \mathbf{N} $n_s \times m$ matrix
- \mathbf{n} standard normal sample vector of length n_s
- \mathbf{A} upper triangular matrix obtained from Cholesky decomposition
- \mathbf{n}_i correlated sample vector of length n_s

This matrix contains m vectors of standard normal samples with the desired correlation between each vector. The next step is to transform these to the desired target distribution. This is realized using the so called NORTA (NORmal To Anything) algorithm [RD12].



In an intermediate step, the CDF of the normal distribution (hard-coded in the tool) is applied to each column in the matrix \mathbf{N} .

$$\mathbf{U} = [\mathbf{u}_1 \quad \dots \quad \mathbf{u}_m], \quad \mathbf{u}_i = \Phi(\mathbf{n}_i)$$

where

- \mathbf{U} $n_s \times m$ matrix
- \mathbf{n}_i correlated sample vector of length n_s
- Φ cumulative distribution function of the normal distribution
- \mathbf{u}_i vector of correlated uniform samples of length n_s

For this specific case, results in a set of vector \mathbf{u}_i whose samples represent a uniform distribution between 0 and 1. Then, similarly the ICDF of the target distribution is applied to each value of the vectors \mathbf{u}_i .

$$\mathbf{X} = \mathbf{x}_1 \quad \dots \quad \mathbf{x}_m, \quad \mathbf{x}_i = ICDF_{\text{target}}(\mathbf{u}_i)$$

where

- \mathbf{X} $n_s \times m$ matrix
- \mathbf{u}_i vector of correlated uniform samples of length n_s
- $ICDF$ inverse cumulative distribution function
- \mathbf{x}_i vector of correlated samples of length n_s with desired distribution

This finally gives vectors of random samples \mathbf{x}_i for each error signal which describe random variables with the desired PDF. And, more important, the transformation method preserves the correlation.

Preserving the correlation under any monotonic transformation is only valid assuming rank correlation (i.e. Spearman coefficients), but not for linear correlation as e.g. represented by Pearson product-moment coefficients [RD12],[RD13]. As the matrix Σ itself requires Pearson product-moment coefficients ρ_p for the setup, first a conversion from Spearman (ρ_s) to Pearson (ρ_p) coefficients is internally realized [RD13]:

$$\rho_p = 2 \sin\left(\rho_s \frac{\pi}{6}\right)$$

where

- ρ_s Spearman correlation coefficient
- ρ_p Pearson product-moment coefficient

The ICDFs of the target distributions are also represented numerically and each \mathbf{x}_i is interpolated for the current \mathbf{u}_i value. The reason for this numerical approach (although the ICDFs related to the required basic target distributions are available) is computational speed, as the evaluation of certain special functions (e.g. the inverse of the complementary error function) turned out to be significantly slower and the numerical error introduced by the interpolation is basically negligible.



The sample generation procedure described above is separately applied to generate all temporal random variable samples and all ensemble random variable samples (per ensemble domain) based on the respective temporal and ensemble covariance matrices.

5.3.2 Correlation and Coherence

5.3.2.1 Correlation

According to [AD1] and [AD2], for the simplified statistical method, theoretically any kind of correlation could be realized between error contributors. Being just expressed by variances, covariances could artificially be created for any PEC combination (or the respective summation rule could be applied). The definition is fully up to the "user" and there is no explicit guideline except for a separated treatment of time-constant and time-random quantities in [AD2].

With the system transfer analysis included, a definition at PEC level would however be uncomfortable for a user, as the correlation needs to be specified at each summation block separately and with respect to the currently present situation (i.e. taking into any previously transfer steps applied to the error signals to be summed). For that reason, correlation is entirely defined at PES level and the software accounts for a correct propagation.

With the sample-based approach realized for the advanced statistical method, any "feasible" (see chapter 5.3.2.3.3) correlation could be "imprinted" directly to the samples of the entire pointing system using the correlation matrix Σ as described in the previous chapter.

However, feasible correlation is not equivalent to physically meaningful correlation. Two factors play a role for this decision as further discussed in the next subchapters:

- The statistical domain associated to an error source (which is also one of the reasons to introduce the domain concept described in chapter 4.4).
- The classification of the error source according to [AD2], i.e. its type (time-constant random variable, time-random variable, random process, periodic errors and drift errors).

5.3.2.2 Correlation and Domains

Consider a time-constant random variable error source PES 1 which describes the distribution of a sensor misalignment and a time-random PES 2 (without ensemble distributed parameters for simplicity) that describes the temporal noise of this sensor. In this case, the domains "manufacturing" and "time" are present which are totally independent and have physically nothing in common.

Similarly, assume two time-constant random variables error sources, PES 1 as described above and PES 3 which describes the distribution of a sensor bias dependent on an inertial orientation in space. Both sources describe an ensemble randomness, but the underlying ensemble domains "manufacturing" and "orientation in orbit" have no influence on each other thus specifying correlation between them has no physical meaning.

Thus, error sources which are described in different domains are independent from each other per definition and no option to define a correlation between different domains is present in the tool, i.e.:

- No correlation can be defined between time-constant and time-random properties of an error source e.g. PES 1 ("manufacturing") and PES 2 ("time").



- No correlation can be defined between ensemble properties from different domains, e.g. “manufacturing” and “orientation in orbit” above.
- However, correlation can be defined between a time-constant error source and the ensemble properties of a time-random error source, provided that they are described in the same signal domain. Assume for instance, PES 4 describes a Gaussian time-random error and its standard deviation is an ensemble-random parameter which depends also on the “orientation in orbit” (as PES 3), i.e. both “ensemble” parameters are given in the same domain).

The distinction between the general domains “time” and “ensemble” can be evaluated automatically by the tool as the assignment is known from the definition of the error sources. A further distinction between different “ensemble” domains is however up to the user and a manual assignment of parameters to an ensemble domain cannot be avoided.

Furthermore, this distinction implies that the global correlation matrix Σ is basically composed of several subsets, i.e. one part for the temporal domain and one for each ensemble domain present in a pointing scenario. Consequently, the sample generation for these subsets can be independently generated with the only constraint that there is no correlation between the different subsets.

5.3.2.3 Correlation and Error Source Type

PEET distinguishes between different types of error signal data according to the classification of error sources in [AD2]:

- Time-constant random variables (CRV)
- Time-random random variables (RV)
- Random processes defined by power spectral densities (RP)
- Periodic sinusoidal errors (P)
- Drift errors (D)
- Transient errors:

While a generic transient cannot be covered by the tool, an implementation for specific periodically occurring ‘transients’ is available. With the Fourier series approximation for used for that purpose, this class is treated equivalently to (a set of) ‘standard’ sinusoidal periodic signals (P).

This classification is necessary as it defines fundamental error source types present in the software and as different rules need to be applied respectively in the transfer analysis (see chapter 5.3.4).

Furthermore, these types also differ in the temporal behaviour and in the availability of ensemble random parameters and thus impact where correlation can be specified. As mentioned in the previous chapter, first there is a distinction between correlation in a temporal or ensemble sense.

5.3.2.3.1 Ensemble Correlation

The possibility to specify ensemble correlation between error sources is completely determined by the presence of their ensemble parameters in a common domain. Thus, there is no intrinsic restriction between different signals types (CRV, RV, etc.) per se.



The only restriction that could occur is that one of the ensemble parameters is discrete, i.e. it effectively has no distribution. In this case, specifying a correlation with respect to another distributed parameter is meaningless.

In general, RP errors sources in the tool are set up as "discrete", i.e. they are not defined in a statistical sense, but represented by a single PSD which has no distributed parameters. Only for specific PSD definitions (analytical or transfer function defined as rational function) where the spectrum is defined with an explicit functional expression (i.e. as string), it is possible to introduce an arbitrary parameter p which can be subject to an ensemble distribution (e.g. $1/(f+p)$ for the analytical magnitude case or $1/(p*(p+s))$ for the Laplace domain definition of a transfer function). This 1D parameter has been introduced to allow an implicit approximate model for non-stationarity, i.e. assuming that such case can be expressed with a variation of the PSD magnitude over an ensemble of realizations, where each realization still represents a stationary solution.

Consequently, the following correlation options are provided to the user via the GUI, if non-discrete parameters are present:

Table 5-3: Possible ensemble correlation settings dependent on error source type

Type	CRV	RV	RP	P	D
CRV	x	x	(x)	x	x
RV	x	x	(x)	x	x
RP	(x)	(x)	(x)	(x)	(x)
P	x	x	(x)	x	x
D	x	x	(x)	x	x

5.3.2.3.2 Temporal Correlation

The restrictions on the temporal correlation options can be derived from the inherent physical properties of the different error source types.

Time-constant random variables

CRVs can never be temporarily correlated as they are not described in the domain "time" by definition or, alternatively expressed, they have a discrete value in time. Consequently, specifying a temporal correlation is impossible or meaningless.

Time-random variables

In contrary, being fully described in a statistical way, a time-random variable can always be correlated with other time-random variables. No further distinction is necessary between different distributions of time-random variables (uniformly or Gaussian in the tool).

Random process

Random process type error sources are not described in the time-domain, but described by their PSD as function of frequency and their corresponding measure of dependence is coherence. This is incompatible with other PES types (RV, P, D) and requires a separate description (see chapter 5.3.2.4).



Periodic signals

Periodic signals are deterministic in time which means that there is basically no “degree of freedom” to specify the temporal correlation with respect to other temporal sources, but it is inherently defined. This even holds for the temporal correlation of periodic signals at different frequencies which always results in a zero correlation.

The only exception are periodic signals at the same frequency, where a one-by-one relation between the phase difference $\Delta\varphi$ of the signals and the resulting correlation coefficient ρ exists:

$$\rho = \cos(\Delta\varphi)$$

where

- ρ correlation coefficient
- $\Delta\varphi$ phase difference between two periodic signals at same frequency

As in this case the correlation is more an “coincidental” property and the phase difference between the periodic signals is the physically important quantity, phase relations are expected as user inputs and not correlation coefficients. This also allows specifying relations between periodic signals at different frequencies which impacts the PDF of the summed temporal signal (but could not be specified by a correlation coefficient alone - which would always be zero in this case).

Drift errors

Drift signals are also deterministic in time, i.e. they have no randomness which could be described by correlation with respect to any other PES type. Within the drift signal class, the "correlation" is fully defined by the signal parameters already.

Summary

Consequently, the following correlation options are provided to the user via the GUI for specifying temporal correlation:

Type	CRV	RV	RP	P	D
CRV					
RV		x			
RP			x*		
P				x**	
D					

* by coherence, * implicitly by phase relations for signals at same frequency

5.3.2.3.3 Feasibility of Correlation Matrix

The temporal and ensemble correlation between different PES and their axes is specified by providing correlation coefficients between -1 and 1 for the matrix Σ . However, the defined matrix of correlation coefficients is not necessarily a valid correlation matrix. The premise is that Σ is at least positive semidefinite.



This condition is checked in the tool by computing the eigenvalues of the correlation matrix. If all are positive, no further action is required and the correlated random samples can be generated according to the method described in chapter 5.3.1.4.

In one or more eigenvalues are negative, the specified correlation cannot be realized. In this case, the user is informed about the mismatch and can manually modify the settings. In addition (and especially not to interrupt batch-mode computations), an alternative feasible realization is computed which is “close” to the originally specified correlation matrix.

The method for this alternative realization is based on a heuristic method called eigenvalue correction method in [RD12]. First the orthogonal matrix \mathbf{U} of the eigenvectors and the diagonal matrix \mathbf{D} of the eigenvalues are computed, i.e. the infeasible matrix Σ_{inf} is factorized as \mathbf{UDU}^T . The all negative eigenvalues (diagonal elements of \mathbf{D}) are replaced by 0. The resulting matrix \mathbf{D}_0 is used to compute an intermediate matrix \mathbf{M} :

$$\mathbf{M} = \mathbf{UD}_0\mathbf{U}^T$$

with

- \mathbf{M} intermediate positive semi-definite matrix
- \mathbf{U} orthogonal matrix with eigenvectors of correlation coefficients matrix
- \mathbf{D} diagonal matrix of eigenvalues of correlation coefficients matrix
- \mathbf{D}_0 diagonal matrix of eigenvalues with all negative values in \mathbf{D} replaced by 0

This operation ensures a positive semidefinite matrix, but no unity entries on the main diagonals as required. The latter is achieved by scaling the matrix \mathbf{M} using a diagonal matrix \mathbf{S} with the square root of the inverse of the diagonal elements of \mathbf{M} , i.e.

$$\Sigma_{feas} = \mathbf{SMS}$$

where

- Σ_{feas} feasible correlation matrix ‘close’ to specified infeasible matrix
- \mathbf{M} intermediate matrix from equation above
- \mathbf{S} diagonal matrix square root of the inverse of the diagonal elements of \mathbf{M}

5.3.2.3.4 Correlation and Pointing Error Indices

The temporal and ensemble correlation properties at PES level are expected to be available or estimated for the “original” error source properties, i.e. before any kind of filtering (due to the pointing error index) or statistical interpretation is applied.

Concerning the ensemble correlation, this is straight-forward in all cases, as even when the ensemble domain is treated worst-case, the initial correlation between the “uninterpreted” samples can be realized. Furthermore, the pointing error index analysis only has an effect on the temporal distribution of a source.

However, this is different for the temporal correlation of time-random variable error sources. The pointing error index analysis has to be applied based on the reference tables for the different contribution in [AD1], and thus the resulting temporal PDFs of the sources directly represent the “filtered” signals. As no real time- or frequency domain filtering can be applied for this error source type, the conversion of the correlation between the unfiltered signals



to the correlation of the filtered signals cannot be predicted or computed. This implies that the temporal correlation effectively can only be realized between these filtered samples.

5.3.2.4 Coherence

Coherence can be used as measure to describe the relation (“dependence”) of two random process error sources over frequency similarly as correlation can be used to describe the relation of random variable error sources over time or an ensemble.

Usually, coherence is expressed as a real valued function $\gamma(f)$ that relates the auto-power spectra ($G_{1,1}(f)$, $G_{2,2}(f)$), and the cross-power spectrum ($G_{1,2}(f)$) of two random processes in the following way:

$$\gamma(f) = \frac{|G_{i,j}(f)|}{\sqrt{G_{i,i}(f)G_{j,j}(f)}}$$

where

- $\gamma(f)$ coherence function dependent on frequency f
- $G_{i,i}(f)$ auto-power spectral density for component i (j respectively)
- $G_{i,j}(f)$ cross-power spectral density between component i and j

The general indices i,j can represent the different sources (e.g. 1 or 2 as mentioned above) or the axes (x,y,z) of one or both sources. The function $\gamma(f)$ takes values between 0 (no coherence) and 1 (fully coherent) for each frequency point which means that it also needs to be defined for the entire frequency range covered by the random processes. To cope easily with the possible numerical spectrum definition in the tool and related issues with non-overlapping frequency ranges of different PSDs), a coherence factor (also in the range [0,1]) is used instead, i.e. a constant coherence function over frequency. This is not considered as a real restriction, as the knowledge of entire coherence functions is expected to be unavailable/unknown in most of the cases and if, the cross-spectrum itself can still be explicitly defined in PEET.

The coherence factor is then used to determine the magnitude of the cross-spectrum using the auto-spectra information provided by the user:

$$|G_{i,j}(f)| = \gamma \sqrt{G_{i,i}(f)G_{j,j}(f)}$$

with definition as above, but $\gamma(f)$ being a constant over frequency f .

Different to the approach for the random variables (where correlation information is directly “imprinted” in the samples, the coherence (or cross-spectrum) information between different random process error sources needs to be propagated through the pointing system to be properly available at any stage of the system where random process signals are summed.

A prerequisite for this approach is that the “history” of the signal through the pointing system can be tracked. For that reason, a dedicated data structure for the coherence handling and its propagation is realised which was already used in the prototype of PEET (V0.7). The method behind is illustrated in Figure 5-24 for the covariance propagation used in the

prototype for two pointing error sources PES 1 and PES 2 and an arbitrary transfer system H (2D signals are used for simplicity).

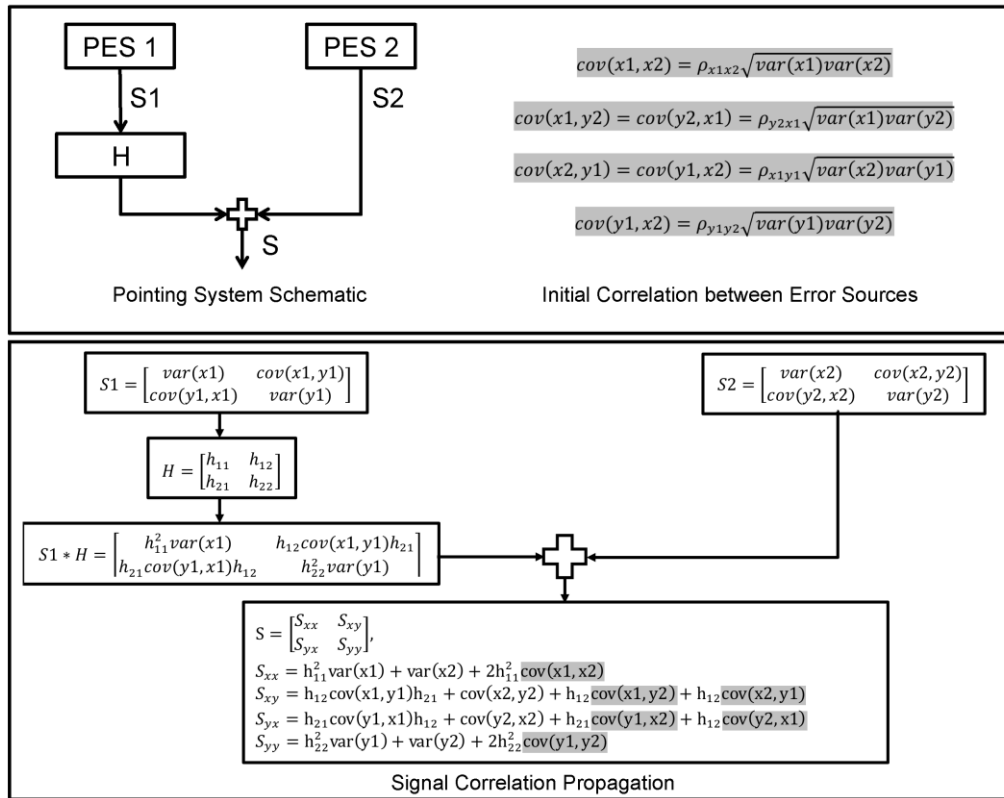


Figure 5-24: Propagation of correlation between two random variable PES in the PEET prototype

The lower part of the figure shows the components of the covariance matrix for each signal. Considering the summed signal S, the resulting covariance can be fully determined by the covariance matrices of S1 and S2 and the contribution from initially defined correlation coefficients between the signals (highlighted in grey) as long as the "path" of the signals is known. This generally also holds for 3D signals, complex pointing systems and also for power spectral density matrices (instead of covariance matrices) and coherence factors (instead of correlation coefficients).

5.3.3 Generation of error signal data

PEET distinguishes between different types of error signal data according to the classification of error sources in [AD2]. Apart from a pure classification purpose, this distinction is mainly required for the software as dedicated signal structures have to be realized for each type to account for different rules concerning the evaluation (chapter 5.3.5), summation and transfer (chapter 5.3.4) of error sources.

5.3.3.1 Time-Constant Random Variables

The error signal contribution of a time-constant random variable e_{CRV} is represented by a vector of samples s_{CRV} , for each axis (the axis index is omitted in the notation). The samples



are generated according the method described in chapter 5.3.1.4 and taking into account the specified ensemble correlation. The “target” PDF used for this method is derived from the corresponding table for bias errors in [AD1] which is shown again below for completeness. The equivalent mean and standard deviation values are no longer explicitly needed for the model (but can obviously be retrieved numerically from the sample vectors).

Table 5-4: Budget contributions for bias errors [AD1]

Index	S.I.	Distribution			Index
		P(e)	$\mu(e)$	$\sigma(e)$	
APE	E	P(B)	μ_B	σ_B	For P(B), μ_B and σ_B see B.6
	T	$\delta(B_{wc})$	B_{wc}	0	B_{wc} =worst-case bias.
	M	P(B)	μ_B	σ_B	For P(B), μ_B and σ_B see B.6
MPE	All	As for APE			MPE
RPE	All	$\delta(0)$	0	0	No contribution by definition
PDE	All	$\delta(0)$	0	0	No contribution by definition
PRE	E	P(ΔB)	0	$2^{1/2} \sigma_B$	Only if bias can vary between observations, otherwise zero contribution.
	T	$\delta(B_{max}-B_{min})$	$B_{max}-B_{min}$	0	
	M	P(ΔB)	0	$2^{1/2} \sigma_B$	

Different to the table, the PRE contribution with PEET is always zero and a warning is thrown to indicate that deviation from the reference. The reason is that the required PDF that describes the bias change PDF(ΔB) between two observations cannot be automatically determined or derived from the distribution PDF(B) as it represents an independent source.

Generating the samples at PES level following above table basically implies that the pointing error index contribution and “statistical interpretation” (i.e. part of AST-3 in [AD2]) are actually applied before the transfer analysis step (AST-2). The first part cannot be avoided, as the analytical “rules” for the index contributions are only available for the specific error source types provided in the tables of [AD1] and no real index dependent “filtering” can be applied to arbitrary PDFs (this is not an issue directly related to the time-constant random variables, but to the time-random ones which have more complex index dependent contributions).

5.3.3.2 Time-Random Variables

The error signal contribution of a time-random variable e_{RV} is – as for the time-constant one - represented by vector of samples s_{RV} for each axis (the axis index is omitted in the notation). The generation of the vectors is however different for two reasons:

- Any temporal mean value of the distribution first has to be removed and “shifted” to an additional time-constant distribution (see next paragraph).
- In case one of the temporal distribution parameters is distributed itself over an ensemble, first the samples for this parameter have to be generated with the specified ensemble correlation (w.r.t. other parameters of the same domain).

5.3.3.2.1 Mean Splitting

While [AD2] clearly follows a separated treatment of time-constant and time-random errors sources, [AD1] and [RD3] do not explicitly account for such strict separation, i.e. Gaussian temporal errors (Tables B-2 in these references) are required to be zero-mean while uniform random errors (Tables B-4) range from 0 to an upper bound C. The latter cases consequently have a non-zero mean (C/2 for each realization) which basically can be interpreted as a time-constant contribution.

For a direct evaluation of these errors, apart from the underlying "physical" difference, this distinction plays no role. It does however when the system transfer step is taken into account as demonstrated in the subsequent example.

Example

Assume a temporal uniform random error which has large bias in compared to the "width" of the bounds of the distribution, e.g. $U(99,101)$. This error is transferred through a simple high-pass H with a high frequency gain of 10. The expected output (assuming a sufficiently high "frequency" of the errors signal) is as follows:

Due to the high-pass behaviour, the time-constant part of the error signal is filtered out while the time-random (high-f) part is amplified according the system gain, which is also the result one would obtain from a time-domain simulation (see Figure 5-26).

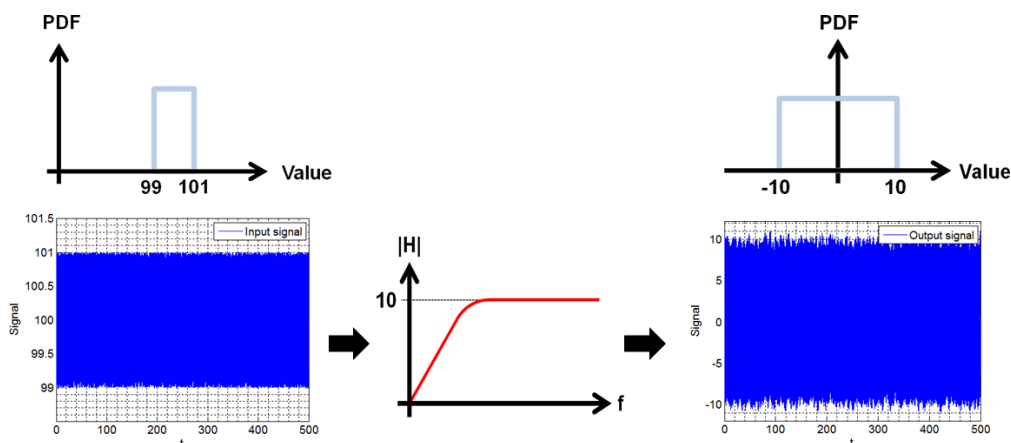


Figure 5-25: Expected behaviour in system transfer and simulation results

As different transfer rules are applied to time-constant and time-random errors in PEET (see chapter 5.3.4), a strict separation of these contributions is necessary to provide the correct result. The result of such "splitting" is shown in Figure 5-26 (top), where the signal is decomposed into a discrete time-constant error $\delta(100)$ and a uniform temporal error $U(-1,1)$. The result in this case corresponds to the expected behaviour.

Without splitting (bottom of Figure 5-26), the transfer rule applies the system worst-case gain to the whole initial uniform distribution, which results in a much larger - and essentially wrong - overall contribution.

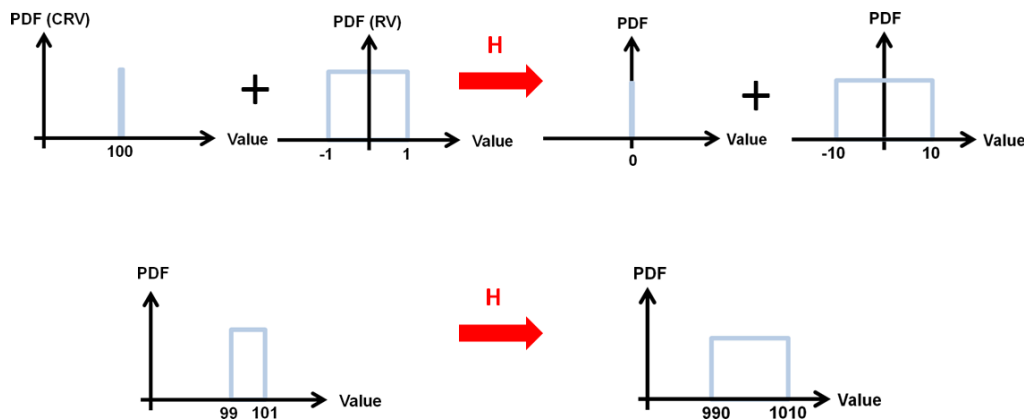


Figure 5-26: Difference between "split" (top) and "combined" transfer (bottom)

[AD1] provides rules for the contribution of uniform and Gaussian time-random random variable errors (Tables B-3 and B-4). Thus, for these source types, the tables have to be properly adapted to account for the mean shift. As the tool also provides additional options for the parameter distribution (distributed mean value for the Gaussian errors, generalized lower, upper and symmetric distributed bounds for the uniform distribution), the rules had to be additionally extended for these setup options.

Table 5-5 and Table 5-6 show the result after mean splitting for the Gaussian and uniform errors dependent on the pointing error index and the statistical interpretation.

Table 5-5: Contributions of Gaussian time-random errors after mean splitting

Index	S.I	$G(p(\mu), \sigma)$		$G(\mu, p(\sigma))$	
		$p_E(e)$ of CRV	$p_T(e)$ of RV	$p_E(e)$ of CRV	$p_T(e)$ of RV
APE	E	$p(\mu)$	$\delta(3\sigma)$	$\delta(\mu)$	$p(3\sigma)$
	T	$\delta(\mu_{WC})$	$G(0, \sigma)$	$\delta(\mu)$	$G(0, \sigma_{WC})$
	M	$p(\mu)$	$G(0, \sigma)$	$\delta(\mu)$	$\int G(0, \sigma) p(\sigma) d\sigma$
MPE	E	$p(\mu)$	$\delta(0)$	$\delta(\mu)$	$\delta(0)$
	T	$\delta(\mu_{WC})$	$\delta(0)$	$\delta(\mu)$	$\delta(0)$
	M	$p(\mu)$	$\delta(0)$	$\delta(\mu)$	$\delta(0)$
RPE	E	$\delta(0)$	$\delta(3\sigma)$	$\delta(0)$	$p(3\sigma)$
	T	$\delta(0)$	$G(0, \sigma)$	$\delta(0)$	$G(0, \sigma_{WC})$
	M	$\delta(0)$	$G(0, \sigma)$	$\delta(0)$	$\int G(0, \sigma) p(\sigma) d\sigma$
WPD	All	No contribution			
WPR	All	As for RPE (i.e. upper bound)			



where

- p probability density function
- μ mean value
- σ standard deviation
- w_c index denoting the worst –case value of a parameter
- E,T PDF index indicating a temporal or ensemble distribution
- δ Dirac-delta (i.e. discrete) PDF
- G Gaussian PDF

Table 5-6: Contributions of uniform time-random errors after mean splitting

Index	S.I.	$U(a, p(b))^*$		$U(-p(c), p(c))$	
		$p_E(e)$ of CRV	$p_T(e)$ of RV	$p_E(e)$ of CRV	$p_T(e)$ of RV
APE	E	$\frac{a + p(b)}{2}$	$\frac{p(b) - a}{2}$	$\delta(0)$	$p(c)$
	T	$\frac{a + \delta(b_{wc})}{2}$	$U\left(-\frac{b_{wc} - a}{2}, \frac{b_{wc} - a}{2}\right)$	$\delta(0)$	$U(-c_{wc}, c_{wc})$
	M	$\frac{a + p(b)}{2}$	$\int U(-x, x) p(x) dx$ $x = \frac{b - a}{2}$	$\delta(0)$	$\int U(-c, c) p(c) dc$
MPE	E	$\frac{a + p(b)}{2}$	$\delta(0)$	$\delta(0)$	$\delta(0)$
	T	$\frac{a + \delta(b_{wc})}{2}$	$\delta(0)$	$\delta(0)$	$\delta(0)$
	M	$\frac{a + p(b)}{2}$	$\delta(0)$	$\delta(0)$	$\delta(0)$
RPE	E	$\delta(0)$	$\frac{p(b) - a}{2}$	$\delta(0)$	$p(c)$
	T	$\delta(0)$	$U\left(-\frac{b_{wc} - a}{2}, \frac{b_{wc} - a}{2}\right)$	$\delta(0)$	$U(-c_{wc}, c_{wc})$
	M	$\delta(0)$	$\int U(-x, x) p(x) dx$ $x = \frac{b - a}{2}$	$\delta(0)$	$\int U(-c, c) p(c) dc$
WPD	All	No contribution			



WPR	All	As for RPE (i.e upper bound)
-----	-----	------------------------------

* analogous for $U(p(a), b)$

where

- p probability density function
- a lower bound of a uniform distribution
- b upper bound of a uniform distribution
- w_C index denoting the worst –case value of a parameter
- E,T PDF index indicating a temporal or ensemble distribution
- δ Dirac-delta (i.e. discrete) PDF
- U Uniform PDF

5.3.3.2.2 Sample Generation

Generating the samples at PES level following above tables basically implies that the pointing error index contribution and “statistical interpretation” (i.e. part of AST-3 in [AD2]) are actually applied before the transfer analysis step (AST-2). The first part cannot be avoided, as the analytical “rules” for the index contributions are only available for the specific error source types provided in the tables of [AD1] and no real index dependent “filtering” can be applied to arbitrary PDFs.

As samples are required for both for temporal and ensemble domains, first the samples for the ensemble parameters are generated as described in chapter 5.3.1.4 (i.e. accounting for possible correlation with other parameters in the same domain).

Then the samples for the temporal domain are generated for a “normalized” PDF (uniform or Gaussian respectively) with the same method (i.e. including correlation with other temporal sources) and then scaled with the previously generated ensemble parameter samples and appended in one large vector (per axis). This step-by-step method also avoids the need of having analytical expressions for the conditional integrals in the “mixed interpretation” cases in the sample generation, as the “desired statistics” are achieved automatically.

Furthermore, as the time-constant and time-random part after mean splitting represent one single physical source, they are fully correlated in an ensemble sense by definition. This is achieved by using the same samples for the distributed parameter in the generation of both the time-constant and time-random part of the variables.

5.3.3.3 Random Process

Random process spectra inputs in PEET are entirely defined on amplitude level as $P(f)=\sqrt{G(f)}$ (i.e. in terms of [unit/ $\sqrt{\text{Hz}}$]). Internally, these spectra (auto-spectra and cross-spectra in the 3D case) are directly converted to power level $G(f)$ as required for the later system transfer (see chapter 5.3.4.4):

$$\mathbf{G}(f) = \begin{bmatrix} G_{xx}(f) & G_{xy}(f) & G_{xz}(f) \\ G_{xy}(f) & G_{yy}(f) & G_{yz}(f) \\ G_{xz}(f) & G_{yz}(f) & G_{zz}(f) \end{bmatrix}$$

where

- $\mathbf{G}(f)$ 3D power spectral density matrix



- $G_{i,j}(f)$ auto-power spectral densities ($i = j$) and cross-power spectral densities ($i \neq j$) for all axes

All diagonal elements (i,i) and all sources where explicitly provided cross-spectra (i,j) are converted to power spectra by (* denotes the complex conjugate transpose):

$$G_{i,j}(f) = P_{i,j}(f)P_{i,j}^*(f)$$

where

- $G_{i,j}(f)$ cross-power spectral density between axis i and axis j
- $P_{i,j}(f)$ cross-amplitude spectral density between axis i and axis j

The entire cross-spectral density is internally stored in MATLAB numerically as a frequency response object (frd). The number of frequency points used for the frd is determined by default from user inputs concerning a global minimum and maximum frequency and a given resolution per frequency decade. In case of a discrete definition of the spectra by the user, all provided points are appended to the frequency grid and a zero response is used for all ranges of the global grid which are not covered by the discrete definition.

Furthermore, it is possible to refine the frequency grid by taking into account the frequencies of zeros and poles of dynamic system models used in the pointing system. Around these points of interest, a 10 times more dense grid (compared to the global resolution) is generated to account for any kind of features (e.g. peaks) in their close range that might be important for the system transfer.

For numerically defined spectra, the frequency grid of the provided data does not necessarily match with the global grid created by the tool. In this case, the numerical data is linearly interpolated on the global grid on PSD level. This ensures that first, the computed variance with the does not differ from the variance obtained with the 'raw' input grid (as a trapezoidal integration is used) and second, that all spectra can be properly summed by providing data at identical frequency grid points. Using the grid refinement option, further all 'raw' grid points are included in the global grid.

Different to the random variables, no domain treatment (statistical interpretation) and error index contributions needs to be considered at PES level as the latter can be exactly determined by applying frequency-domain metric filters at any stage of the pointing system (see chapter 5.3.5).

5.3.3.4 Periodic Signals

Periodic signals can be defined as composed of multiple frequency components (N_f components). Each frequency "layer" consists of an amplitude and an initial phase φ for each axis. The amplitude itself can be an ensemble-distributed parameter, thus is it represented by a sample vector \mathbf{s}_A of length N_A for each axis.

The provided amplitude information is combined with the phase information by expressing both quantities as a vector of phasors, i.e. complex amplitude vectors:

$$\bar{\mathbf{s}}_A = \mathbf{s}_A \cdot \cos(\varphi) + i \sin(\varphi)$$

where

- $\bar{\mathbf{s}}_A$ complex-valued amplitude phasor of length N_A



- s_A real-valued amplitude samples of length N_A
- φ periodic signal phase

These vectors are setup for each of the N_f frequency sets and for each axis. Each frequency set is saved on a separate layer.

As for the random descriptions with PSDs, no domain treatment (statistical interpretation) and error index contributions needs to be considered at PES level as the latter can be exactly determined by applying frequency-domain metric filters at any stage of the pointing system (see chapter 5.3.5).

5.3.3.5 Drift Errors

5.3.3.5.1 Implementation in previous PEET version (V1.0)

The error signal contribution of a drift error e_D was represented by vector of samples s_D for each axis (the axis index is omitted in the notation).

The signal structure of drift signals was similar to the structure of random variable signals. Samples were drawn for each axis according to the PDFs provided in the corresponding ECSS table (see Table 5-7) using the given parameters for the reset times T_D and the (optionally distributed) drift rate D . The samples then represent an already interpreted signal with applied pointing metric similarly as for the random variable error sources.

However, there was no need for splitting of the temporal mean in this case (although existent), as no transfer of drift signals through dynamic systems was allowed in the tool (since a straight-forward frequency-domain based prediction of the temporal behaviour of the output signal is not trivial).



Table 5-7: Contributions from drift errors (Table B-7 in [RD3]) under the assumption of no resets within an observation

Index	S.I.	Distribution			Notes
		$P(\epsilon)$	$\mu(\epsilon)$	$\sigma(\epsilon)$	
APE	E	$P(T_D D) = \frac{1}{T_D} P(D)$	$T_D \mu_D$	$T_D \sigma_D$	T _D is the worst case drift before resetting occurs, for a given value of D. D _{wc} is the worst case D. For P(D), μ _D and σ _D see B.5.9.
	T	$U(0, T_D D_{wc})$	$\frac{1}{2} T_D D_{wc}$	$\frac{1}{\sqrt{12}} T_D D_{wc}$	
	M	$\int P(\epsilon D) P(D) dD$	$\frac{1}{2} T_D \mu_D$	$\frac{1}{\sqrt{12}} T_D \sigma_D$	
MPE	E	$P((T_D - \frac{\Delta T}{2}) D) = \frac{1}{T_D - \frac{\Delta T}{2}} P(D)$	$(T_D - \frac{\Delta T}{2}) \mu_D$	$(T_D - \frac{\Delta T}{2}) \sigma_D$	Note that T _D ≥ ΔT, so that max MPE for given D is $(T_D - \frac{\Delta T}{2}) D$
	T	$U(\frac{\Delta T}{2} D_{wc}, (T_D - \frac{\Delta T}{2}) D_{wc})$	$\frac{1}{2} T_D D_{wc}$	$\frac{T_D - \Delta T}{\sqrt{12}} D_{wc}$	
	M	$\int P(\bar{\epsilon} D) P(D) dD$	$\frac{1}{2} T_D \mu_D$	$\frac{T_D - \Delta T}{\sqrt{12}} \sigma_D$	
RPE	E	$P(\frac{\Delta T}{2} D) = \frac{2}{\Delta T} P(D)$	$\frac{1}{2} \Delta T \mu_D$	$\frac{1}{2} \Delta T \sigma_D$	For given value of D, RPE range is $\pm \frac{1}{2} D \Delta T$
	T	$U(-\frac{\Delta T}{2} D_{wc}, \frac{\Delta T}{2} D_{wc})$	0	$\frac{\Delta T}{\sqrt{12}} D_{wc}$	
	M	$\int P(\delta \epsilon D) P(D) dD$	0	$\frac{\Delta T}{\sqrt{12}} \sigma_D$	
PDE	E/M	$P(T_{PRE} D) = \frac{1}{T_{PRE}} P(D)$	$T_{PRE} \mu_D$	$T_{PRE} \sigma_D$	Note that T _D > T _{PRE} >> ΔT
	T	Temporal interpretation does not apply			
PRE	all	0	0	0	No contribution by definition

According to [RD3], temporal interpretation does not apply for a PDE error. However, a "physical" interpretation of such signal gives no clear reason for this non-applicability. Figure 5-27 illustrates the temporal behaviour of a drift error for different (ensemble) realizations of a (uniformly distributed) drift rate. The reset time (T_D) of the drift is chosen to be larger than the stability time (T_{PDE}) for the PDE - which is again larger than the PDE window time (ΔT). This setup corresponds to the assumptions provided in Table 5-7, i.e. "**T_D > T_{PRE} >> ΔT**".

Temporal interpretation takes into account the temporal behaviour of the worst-case ensemble, i.e. the one with the maximum drift rate (D_{max}) in this case. From Figure 5-27, one can identify that the PDE contribution in this case is always constantly D_{max} · T_{PDE}, i.e. it can be represented by a discrete mean value with zero variance.

The only assumption that has to be made is that a drift reset during an "observation" is not present (as otherwise the correct contribution might be difficult to describe analytically). As this premise is already mandatory for other contributions (otherwise also the RPE contribution would be non-applicable), the mentioned description for the PDE error was implemented in the software.

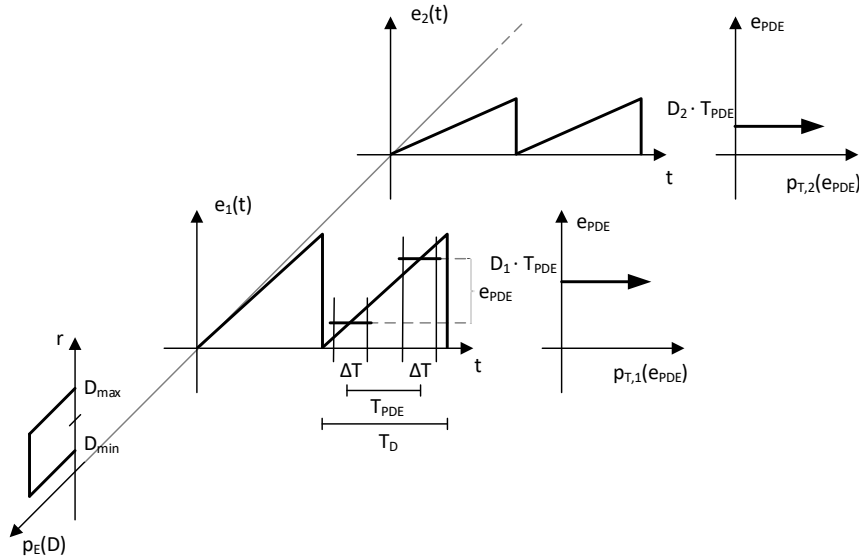


Figure 5-27: Illustration of PDE for a drift contribution with a distributed rate ([RD5], notation modified to match Table 5-7)

5.3.3.5.2 Current Implementation in PETT V1.1

The random variable description for drift signal as described in the previous section has several significant disadvantages.

First, per definition, it does not carry any frequency information of the signal. While for zero-mean time-random variables (describing a 'noise behaviour') approximate assumptions for the dynamic system transfer can be made (i.e. worst-case assumption of scaling the noise magnitude with the H-Infinity gain of the dynamic system while preserving the distribution of the samples, see section 5.3.4.2.3), this is clearly not possible for a deterministic drift signal where the system output is very unlikely to preserve the uniformly distributed temporal signal shape.

Second, the approximate evaluation rules in Table 5-7 on how drift contributions contribute to a certain metric require further assumptions, i.e. they neglect the possibility of a reset during an observation or during a considered time window in general.

Finally, having only temporal samples of the temporal distribution of multiple drift signals with different reset times available, it is not possible to sum them correctly, i.e. to correctly account for the actual fixed temporal relation between the signals.

These drawbacks are avoided by using a frequency domain approach for the signal, e.g. by using a Fourier series approximation in one of the following forms:

$$x(t) = \sum_{k=-n}^n a_k \cdot e^{jk\omega_0 t} = a_0 + 2 \sum_{k=1}^n A_k \cdot \cos(k\omega_0 t + \varphi_k) = a_0 + 2 \sum_{k=1}^n [B_k \cdot \cos(k\omega_0 t) - C_k \cdot \sin(k\omega_0 t)]$$

where

- $x(t)$ the temporal signal at time t
- n the order of the series approximation



- a_k a complex series coefficient
- ω_0 the fundamental frequency of the signal ($= 2\pi/T_D$, with drift reset time T_D)
- a_0 the real valued DC coefficient
- A_k a real-valued amplitude coefficient
- φ_k a real-valued phase
- B_k, C_k real-valued coefficients for the cosine/sine form

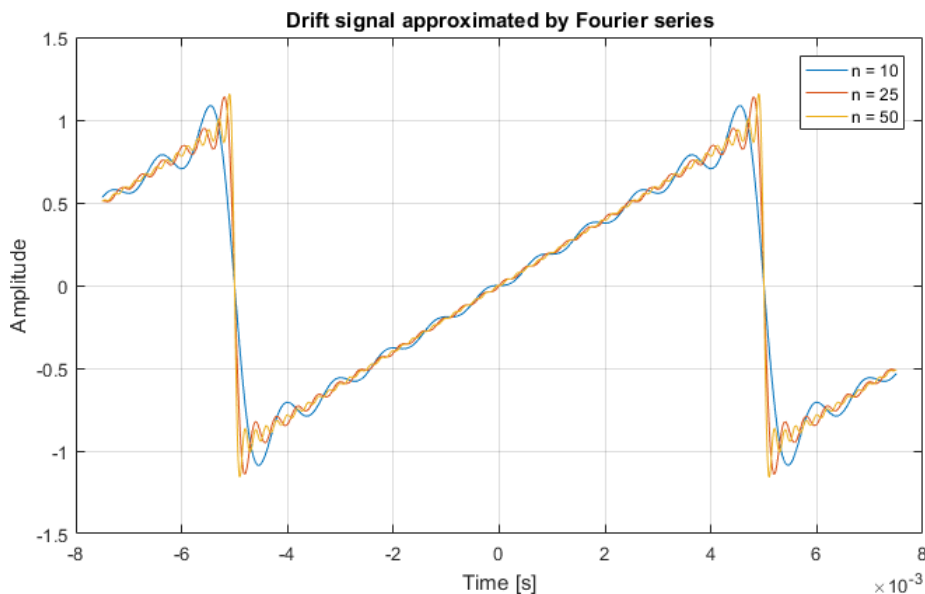
In particular, the parameters below are used for modelling a drift signal ranging from 0 to a maximum value $T_D \cdot D$ before a reset:

$$a_0 = \frac{T_D \cdot D}{2} , \quad A_k = \frac{T_D \cdot D}{2\pi k} , \quad \omega_0 = \frac{2\pi}{T_D} , \quad \varphi_k = \frac{\pi}{2}$$

where

- T_D the reset time of the drift (i.e. its period)
- D the drift rate

An exemplary time-series resulting from such approximation for three different series orders is shown in the figure below (the DC coefficient a_0 is not included).



It has to be noted that this model suffers from one drawback: an overshoot at the reset time occurs that exceeds the nominal signal amplitude (2 in the example above) of up to 18% (peak-peak) of the 'jump size'. This effect – also called the Gibb's phenomenon – is always present for partial sums of a Fourier transform when jumps/discontinuities are present and can also not be mitigated by simply increasing the series approximation order. However, this drawback is considered of minor importance compared to the advantages present for the dynamic system transfer and the consideration of resets in the signal when applying the metric filters.

For the implementation in PEET, a series order of $n=25$ is considered sufficient to represent the temporal signal behaviour.

The drift signal implementation is then entirely equivalent to the periodic signal implementation presented in section 5.3.3.4, i.e.

$$\bar{s}_{D,k} = s_{D,k} \cdot \cos(\varphi_k) + i \sin(\varphi_k)$$

where

- $\bar{s}_{D,k}$ complex-valued amplitude phasor of (ensemble) length N_D
- $s_{D,k}$ real-valued amplitude samples of (ensemble) length N_D
- φ_k periodic signal phase

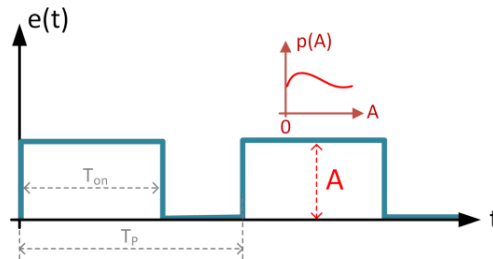
with one such phasor vector \bar{s}_D for each order of the Fourier series approximation. The DC coefficient a_0 is not considered in this drift signal, but realized as a separate time-constant random variable (as for any mean of a time-random variable, see section 5.3.3.2.1)

5.3.3.6 Transient Errors

While a generic transient error of arbitrary form cannot be explicitly covered by the tool with its statistical approach, an implementation for specific periodically occurring ‘transients’ is implemented. For such case, a Fourier series approximation can be used similarly as for the drift signals described in the previous chapter. These approximations in turn can then again be represented as a ‘standard’ periodic signal.

The following model types are available with their approximation parameters as provided below (note that M is used in the equations to represent the amplitude A in the figures to avoid confusion with the coefficients A_k):

Rectangular error

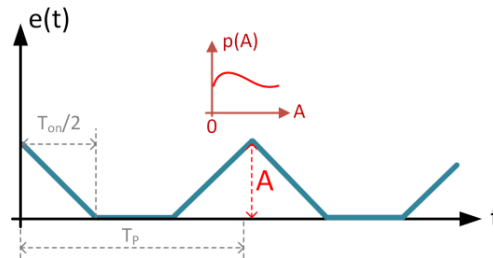


$$a_0 = M \frac{T_{on}}{T_p}, \quad A_k = M \frac{T_{on}}{T_p} \cdot \text{sinc}\left(k\omega_0 \frac{T_{on}}{2}\right), \quad \omega_0 = \frac{2\pi}{T_p}, \quad \varphi_k = 0$$

where

- M the magnitude (‘amplitude’) of the rectangular signal
- T_p the fundamental period of the signal
- T_{on} the time ($<T_p$) during which the signal is non-zero

Triangular error

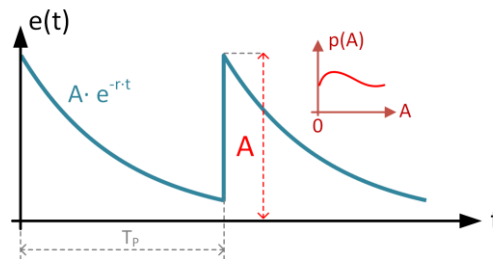


$$a_0 = M \frac{T_{on}/2}{T_p} , \quad A_k = M \frac{T_{on}/2}{T_p} \cdot \text{sinc}^2 \left(k\omega_0 \frac{T_{on}/2}{2} \right) , \quad \omega_0 = \frac{2\pi}{T_p} , \quad \varphi_k = 0$$

where

- M the magnitude ('amplitude') of the triangular signal
- T_p the fundamental period of the signal
- T_{on} the time ($<T_p$) during which the signal is non-zero

Exponential decay



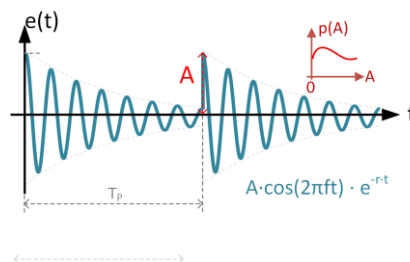
$$a_0 = \frac{M}{T_p \cdot r} , \quad a_k = \frac{M}{T_p \cdot (r + jk\omega_0)} , \quad \omega_0 = \frac{2\pi}{T_p}$$

$$\Rightarrow A_k = 2 \text{Re } a_k , \quad \varphi_k = \arg a_k$$

where

- M the initial magnitude ('amplitude') of the signal
- T_p the fundamental period of the signal
- r the decay rate of the signal

Decaying cosine





$$a_0 = \frac{M \cdot r}{T_p \cdot r^2 + \omega_c^2}, \quad a_k = \frac{M \cdot (r + jk\omega_0)}{T_p \cdot [(r + jk\omega_0)^2 + \omega_c^2]}, \quad \omega_0 = \frac{2\pi}{T_p}$$
$$\Rightarrow A_k = 2 \operatorname{Re} a_k, \quad \varphi_k = \arg a_k$$

where

- M the initial amplitude of the cosine signal
- T_p the fundamental period of the signal
- ω_c the frequency of the cosine signal
- r the exponential decay rate of the signal

5.3.4 Transfer Analysis

Dependent on the type or nature of an error contribution, different rules need to be applied to compute or approximate the output error contribution after the transfer analysis. This is also the reason why PEET distinguishes between time-constant random variables (CRV), time-random variables (RV), random processes (RP), periodic processes/signals (P) and drift errors (D).

The rules applied to these signal types in the transfer analysis are introduced in the following subchapters.

5.3.4.1 Time-Constant Random Variables

5.3.4.1.1 Summation/Subtraction

Being completely defined by numerical sample vectors, the summation of CRV contributions is simply a sum of vectors $\mathbf{s}_{CRV,i}$ for each axis. Similarly, the subtraction is a simple vector difference for each axis. No covariance information needs to be processed explicitly as the entire correlation information is imprinted in the samples.

For two signals, the resulting components are given by:

$$\mathbf{s}_{CRV, \text{sum/diff}} = \mathbf{s}_{CRV,1} \pm \mathbf{s}_{CRV,2}$$

- $\mathbf{s}_{CRV, \text{sum}}$ vector of summed CRV samples
- $\mathbf{s}_{CRV, \text{diff}}$ vector of subtracted CRV samples
- $\mathbf{s}_{CRV,i}$ CRV sample vector of an axis of two signals $i = 1, 2$

5.3.4.1.2 Static System Transfer

A static system is simply a constant 3x3 matrix \mathbf{H} in the 3D case or a scalar scale factor H in the 1D case. The components $s_{CRV,ax,out}$ of the output sample vectors $\mathbf{s}_{CRV,ax,out}$ for each axis after the system transfer of input sample vectors $\mathbf{s}_{CRV,ax,in}$ (with components $s_{CRV,ax,in}$) are given by:

$$\begin{bmatrix} s_{CRV,x,out} \\ s_{CRV,y,out} \\ s_{CRV,z,out} \end{bmatrix} = \begin{bmatrix} H_{xx} & H_{xy} & H_{xz} \\ H_{yx} & H_{yy} & H_{yz} \\ H_{zx} & H_{zy} & H_{zz} \end{bmatrix} \begin{bmatrix} s_{CRV,x,in} \\ s_{CRV,y,in} \\ s_{CRV,z,in} \end{bmatrix}$$



where

- $\mathbf{s}_{CRV,ax,out}$ vector component transferred CRV samples for axis ax
- $\mathbf{s}_{CRV,ax,in}$ vector component of input CRV samples for axis ax
- H_{ij} axis components of $i,j (= x,y,z)$ of static gain matrix \mathbf{H}

for the 3D case, i.e. by a matrix multiplication with corresponding axes components, “element-wise” for each entry in the sample vectors.

5.3.4.1.3 Dynamic System Transfer

A dynamic system is simply a 3x3 LTI-model $\mathbf{H}(f)$ in the 3D case or a 1x1 LTI-model $H(f)$ in the 1D case.

As the CRV input signal is time-constant per definition, the response of the system to the input signal is determined using its DC gain, i.e. the response $\mathbf{H}(f=0)$.

The components $s_{CRV,ax,out}$ of the output sample vectors $\mathbf{s}_{CRV,ax,out}$ for each axis after the system transfer of input sample vectors $\mathbf{s}_{CRV,ax,in}$ (with components $s_{CRV,ax,in}$) are given by:

$$\begin{bmatrix} s_{CRV,x,out} \\ s_{CRV,y,out} \\ s_{CRV,z,out} \end{bmatrix} = \begin{bmatrix} H_{xx}(0) & H_{xy}(0) & H_{xz}(0) \\ H_{yx}(0) & H_{yy}(0) & H_{yz}(0) \\ H_{zx}(0) & H_{zy}(0) & H_{zz}(0) \end{bmatrix} \begin{bmatrix} s_{CRV,x,in} \\ s_{CRV,y,in} \\ s_{CRV,z,in} \end{bmatrix}$$

where

- $\mathbf{s}_{CRV,ax,out}$ vector component transferred CRV samples for axis ax
- $\mathbf{s}_{CRV,ax,in}$ vector component of input CRV samples for axis ax
- $H_{ij}(0)$ axis components of $i,j (= x,y,z)$ of DC gain matrix of dynamic system \mathbf{H}

for the 3D case, i.e. by a matrix multiplication with corresponding axes components, “element-wise” for each entry in the sample vectors.

5.3.4.2 Time-Random Variables

5.3.4.2.1 Summation/Subtraction

Having the same representation as CRVs, the summation of RV contributions $\mathbf{e}_{RV,i}$ is also simply a sum of two vectors $\mathbf{s}_{RV,i}$ and the subtraction a simple vector difference for each axis. Again, no covariance information needs to be processed explicitly as the entire correlation information is imprinted in the samples.

$$\mathbf{s}_{RV,sum/diff} = \mathbf{s}_{RV,1} \pm \mathbf{s}_{RV,2}$$

where

- $\mathbf{s}_{RV,sum}$ vector of summed RV samples
- $\mathbf{s}_{RV,diff}$ vector of subtracted RV samples
- $\mathbf{s}_{RV,i}$ RV sample vector of an axis of two signals $i = 1,2$

5.3.4.2.2 Static System Transfer

A static system is simply a constant 3x3 matrix \mathbf{H} in the 3D case or a scalar scale factor H in the 1D case.

The components $s_{RV,ax,out}$ of the output sample vectors $\mathbf{s}_{RV,ax,out}$ for each axis after the system transfer of input sample vectors $\mathbf{s}_{RV,ax,in}$ (with components $s_{RV,ax,in}$) are given by:

$$\begin{bmatrix} s_{RV,x,out} \\ s_{RV,y,out} \\ s_{RV,z,out} \end{bmatrix} = \begin{bmatrix} H_{xx} & H_{xy} & H_{xz} \\ H_{yx} & H_{yy} & H_{yz} \\ H_{zx} & H_{zy} & H_{zz} \end{bmatrix} \begin{bmatrix} s_{RV,x,in} \\ s_{RV,y,in} \\ s_{RV,z,in} \end{bmatrix}$$

where

- $\mathbf{s}_{RV,ax,out}$ vector component transferred RV samples for axis ax
- $\mathbf{s}_{RV,ax,in}$ vector component of input RV samples for axis ax
- H_{ij} axis components of $i,j (= x,y,z)$ of static gain matrix \mathbf{H}

for the 3D case, i.e. by a matrix multiplication with corresponding axes components, “element-wise” for each entry in the sample vectors.

5.3.4.2.3 Dynamic System Transfer

A dynamic system is a 3x3 LTI-model $\mathbf{H}(f)$ in the 3D case or a 1x1 LTI-model $H(f)$ in the 1D case.

Different to the CRV, an RV input signal is random in time. However, “per definition”, no information about the frequency spectrum is available, i.e. a direct link to a certain response or range of $\mathbf{H}(f)$ is not feasible. Furthermore, the LTI response to a non-Gaussian input signal cannot even be simply be predicted for a general case.

For these reasons, the following **assumption** has been agreed:

- The signal is transferred by multiplying it with the worst-case gain of the system (i.e. its infinity norm), i.e. the output PDF is a conservatively scaled version of the input PDF.

As the dynamic system transfer of an RV is based on this (conservative) assumptions, it is recommended to model error sources always as random processes as soon as any information about the frequency spectrum is available.

The components $s_{RV,ax,out}$ of the output sample vectors $\mathbf{s}_{RV,ax,out}$ for each axis after the system transfer of input sample vectors $\mathbf{s}_{RV,ax,in}$ (with components $s_{RV,ax,in}$) are then given by:

$$\mathbf{s}_{RV,ax,out} = \|\mathbf{H}(f)\|_{\infty} \mathbf{s}_{RV,ax,in}$$

where

- $\mathbf{s}_{RV,ax,out}$ vector component transferred RV samples for axis ax
- $\mathbf{s}_{RV,ax,in}$ vector component of input RV samples for axis ax
- $\|\mathbf{H}(f)\|_{\infty}$ H-infinity gain of dynamic system \mathbf{H}



5.3.4.3 Periodic Signal

5.3.4.3.1 Summation/Subtraction

When summing periodic signals, the summation depends on whether the signals have common frequency components or not. For all N_f non-common frequency components, the layers are simply appended to the output signal (i.e. the number of sets increases) without any real operation on the signal components.

For common frequency components, the phasor vectors of the signals are linearly added or subtracted for each axis, i.e. for two signals (omitting the axes index):

$$\bar{\mathbf{s}}_{A,sum} = \bar{\mathbf{s}}_{A,1} \pm \bar{\mathbf{s}}_{A,2}$$

where

- $\bar{\mathbf{s}}_{A,sum}$ complex-valued amplitude phasors of length N_A
- $\bar{\mathbf{s}}_{A,i}$ complex-valued amplitude phasors of the signals $i = 1,2$ to be summed

5.3.4.3.2 Static System Transfer

A static system is simply a constant 3x3 matrix \mathbf{H} in the 3D case or a scalar scale factor H in the 1D case.

The transfer does not change any of the frequencies of the periodic signal. Even more, if the static system is diagonal, also the phases of the signals remain unchanged and the output phasors of each axis are only scaled by the corresponding main diagonal element $H_{ax,ax}$ of the system.

In the general case, when \mathbf{H} has non-zero off-diagonal entries, also the phasors of the cross-axes contribute to the output phasors for each axis:

$$\begin{aligned}\bar{\mathbf{s}}_{A,x,out} &= H_{xx}\bar{\mathbf{s}}_{A,x} + H_{xy}\bar{\mathbf{s}}_{A,y} + H_{xz}\bar{\mathbf{s}}_{A,z} \\ \bar{\mathbf{s}}_{A,y,out} &= H_{yx}\bar{\mathbf{s}}_{A,x} + H_{yy}\bar{\mathbf{s}}_{A,y} + H_{yz}\bar{\mathbf{s}}_{A,z} \\ \bar{\mathbf{s}}_{A,z,out} &= H_{zx}\bar{\mathbf{s}}_{A,x} + H_{zy}\bar{\mathbf{s}}_{A,y} + H_{zz}\bar{\mathbf{s}}_{A,z}\end{aligned}$$

where

- $\bar{\mathbf{s}}_{A,ax,out}$ complex-valued amplitude phasors of length N_A after transfer
- $\bar{\mathbf{s}}_{A,i}$ complex-valued input amplitude phasors
- H_{ij} axis components of $i,j (= x,y,z)$ of static gain matrix \mathbf{H}

This operation is applied to the data in each frequency layer of the signal.

5.3.4.3.3 Dynamic System Transfer

A dynamic system is a 3x3 LTI-model $\mathbf{H}(f)$ in the 3D case or a 1x1 LTI-model $H(f)$ in the 1D case.

As with the static systems, the transfer does not change any of the frequencies of the periodic signals. If the dynamic system is diagonal, the output phasors of each axis in a layer are scaled by the corresponding (complex) response $H_{ax,ax}(f=f_p)$ at the frequency f_p associated to the layer. This accounts both for the scaling and the phase shift introduced by the dynamic system.

In the general case, when $\mathbf{H}(f)$ has non-zero off-diagonal elements, again, also the phasors of the cross-axes contribute to the output phasors for each axis:

$$\begin{aligned}\bar{\mathbf{s}}_{A,x,out} &= H_{xx}(f_p)\bar{\mathbf{s}}_{A,x} + H_{xy}(f_p)\bar{\mathbf{s}}_{A,y} + H_{xz}(f_p)\bar{\mathbf{s}}_{A,z} \\ \bar{\mathbf{s}}_{A,y,out} &= H_{yx}(f_p)\bar{\mathbf{s}}_{A,x} + H_{yy}(f_p)\bar{\mathbf{s}}_{A,y} + H_{yz}(f_p)\bar{\mathbf{s}}_{A,z} \\ \bar{\mathbf{s}}_{A,z,out} &= H_{zx}(f_p)\bar{\mathbf{s}}_{A,x} + H_{zy}(f_p)\bar{\mathbf{s}}_{A,y} + H_{zz}(f_p)\bar{\mathbf{s}}_{A,z}\end{aligned}$$

where

- $\bar{\mathbf{s}}_{A,ax,out}$ complex-valued amplitude phasors of length N_A after transfer
- $\bar{\mathbf{s}}_{A,i}$ complex-valued input amplitude phasors
- $H(f_p)$ complex-values system response for 'axes' i,j ($= x,y,z$) of dynamic system \mathbf{H} evaluated frequency f_p associated to the phasor

This operation is applied to the data in each frequency layer of the signal.

5.3.4.4 Random process

5.3.4.4.1 Dynamic System Transfer

A dynamic system is a 3x3 LTI-model $\mathbf{H}(f)$ in the 3D case or a 1x1 LTI-model $H(f)$ in the 1D case. Then according to [RD4], the output spectral density matrix $\mathbf{G}_{out}(f)$ after system transfer is given by:

$$\mathbf{G}_{out}(f) = \mathbf{H}(f) \mathbf{G}_{in}(f) \mathbf{H}^*(f)$$

where

- $\mathbf{G}_{out}(f)$ output power-spectral density matrix after system transfer
- $\mathbf{G}_{in}(f)$ input power-spectral density matrix
- $\mathbf{H}(f)$ 3x3 dynamic system LTI model

and (*) denotes the complex conjugate transpose.

5.3.4.4.2 Static System Transfer

A static system is simply a constant 3x3 matrix \mathbf{H} in the 3D case or a scalar scale factor H in the 1D case. It can somehow be understood as a special case of a dynamic system, with a constant gain over all frequencies. Thus, the same rule applies also in this case:

$$\mathbf{G}_{out}(f) = \mathbf{H} \mathbf{G}_{in}(f) \mathbf{H}^*$$

where

- $\mathbf{G}_{out}(f)$ output power-spectral density matrix after system transfer
- $\mathbf{G}_{in}(f)$ input power-spectral density matrix
- \mathbf{H} 3x3 static system gain matrix

As \mathbf{H} is a real matrix, the complex conjugate transpose is a "simple" transpose in this case.



5.3.4.4.3 Summation/Subtraction

The components of the power spectral density matrix $\mathbf{G}_{out}(f)$ of a summation or subtraction of signals with power spectral matrices $\mathbf{G}_1(f)$ and $\mathbf{G}_2(f)$ can be derived from:

$$G_{out,(i,j)}(f) = G_{i1,j1}(f) + G_{i2,j2}(f) \pm G_{i2,j1}(f) \pm G_{i1,j2}(f)$$

where

- $G_{out,(i,j)}(f)$ output power-spectral density of axis combination i,j
- $G_{in}(f)$ input power-spectral density matrix
- $i = x,y,z$ indexer for the first axis
- $j = x,y,z$ indexer for the second axis
- 1,2 indexer for the first/second summand

The power spectrum on x of the sum is then given for instance ($i=j=x$) by:

$$G_{out,(x,x)}(f) = G_{x1,x1}(f) + G_{x2,x2}(f) + G_{x2,x1}(f) + G_{x1,x2}(f)$$

The first two summands are the spectra for the x-axis of the two signals, the last two summands are cross-spectrum components between the x-axis of the two signals.

Note that the similarity to the expression for the variance of a sum or difference of two random variables x and y :

$$Var(x + y) = Var(x) + Var(y) \pm 2Cov(x, y)$$

- Var the variance
- Cov the covariance
- x,y random variables

Similarly, the y-z cross-power spectrum of the differential signal is given by ($i=y,j=z$):

$$G_{out,(y,z)}(f) = G_{y1,z1}(f) + G_{y2,z2}(f) - G_{y2,z1}(f) - G_{y1,z2}(f)$$

In this case the first two summands are the cross-spectra for the yz-axes of each individual input signal and the last two summands are the cross-spectra for the yz-axes between the two input signals.

In both cases above, the first two summands are directly provided in the spectral density matrices $\mathbf{G}_1(f)$ and $\mathbf{G}_2(f)$.

The last two summands are computed using the coherence information provided by the user at PES level. If any system transfer has been applied to the signals to be summed/subtracted in advance, a similar system transfer propagation is automatically applied for these cross-axis components.

5.3.4.5 Drift Errors

Being modelled as Fourier series approximation, all operations (summation/subtraction, static/dynamic system transfer) are entirely equivalent to the procedure for 'standard' periodic signals (see chapter 5.3.4.3). The separate transfer routines for drift signals are only kept for 'heritage' reasons. For dynamic systems, this new approach has its largest



benefit as a proper determination of the output signal was not possible with the previous random variable description for drift signals.

5.3.4.6 Transient Errors

As 'transient' error signals are implemented as a special case of periodically occurring signals and modelled as Fourier series approximation similar to drift signals, their summation, static and dynamic transfer is also fully equivalent to the evaluation of 'standard' periodic signals (see chapter 5.3.4.3).

5.3.5 Error Evaluation

This chapter describes how the error signal content of the different error source types is treated in the evaluation (AST-3 and AST-4 in [AD2]) of the final error or similarly at any other evaluation level defined by a PEC block in the tool.

5.3.5.1 Error Index Contribution and Statistical Treatment

5.3.5.1.1 Random Variables

For the sample-based time-constant & time-random variable error contributions, both pointing error index contribution and statistical treatment are already applied when generating the samples of a distribution according to the tables in chapter 5.3.3. Consequently, no further operation on the samples needs to be applied. Only the PDF information needs to be derived numerically from the samples as described later in chapter 5.3.5.2.1 from the sample vectors $s_{CRV,i}$ and $s_{RV,i}$ for each axis.

5.3.5.1.2 Random Process

Random process contributions are represented as PSDs and no error index contribution or statistical treatment needs to be taken into account before the error evaluation.

For the error index contribution, [AD2] provides dedicated pointing error metrics for all pointing error indices. These metrics can be represented by frequency domain filters with transfer function $F_{index}(f)$ which can be applied to each element $G(f)$ of the power spectral density matrix $\mathbf{G}(f)$:

$$G_{index}(f) = |F_{index}(f)| G(f) |F_{index}(f)|$$

where

- $G_{index}(f)$ 'metric-filtered' power-spectral density
- $G(f)$ unfiltered power-spectral density
- $F_{index}(f)$ frequency domain filter representation of a metric

Then $G_{index}(f)$ is an exact representation of the power spectrum of the filtered signal. However, in case of statistical requirement, not the power spectrum but the PDF of the time-domain signal of the random process is of interest.

As Gaussian stationary random processes are represented, the temporal PDF is known to be Gaussian with zero mean. The standard deviation of the random process can be obtained by integration of the power spectrum [RD4] over a given frequency range:

$$\sigma_{index}^2 = \int_{f_{min}}^{f_{max}} G_{index}(f) df$$



where

- $G_{index}(f)$ 'metric-filtered' power-spectral density
- σ_{index} variance of random process for given metric
- $f_{min/max}$ bounds of evaluation frequency bandwidth

This integration is executed numerically for the auto-spectra of each axis. Then, the PDF $G(\theta, \sigma_{index})$ of the random process contribution is fully defined.

Having a Gaussian temporal distribution, the statistical interpretation is essentially identical to the one for zero-mean Gaussian errors following Table B-2 in [AD1] (for APE, as the index contribution has already be accounted for by other means).

Then for the resulting distribution, sets of samples $s_{RP,i}$ for each axis are generated (for the evaluation purpose only) which are considered uncorrelated w.r.t. to all other error source types.

5.3.5.1.3 Periodic Signals

Periodic signals are represented by n layers of complex phasor vectors $\bar{s}_{A,i}$ of length N_A for each axis which contain the amplitude and phase information of the signal and a frequency associated to this layer.

For the pointing error index contribution, the signal frequency domain filters $F_{index}(f)$ are used ([AD2]). The filters are similar to the ones used as for the random processes, but they include phase information and are only evaluated at the N_f frequencies j present in the periodic signal.

Then, for each frequency layer the metric filter magnitude is applied to the phasor vector for each axis i to obtain the filtered amplitudes:

$$\bar{s}_{A,i,index,j} = F_{s,index}(f_j) \bar{s}_{A,i}$$

where

- $\bar{s}_{A,i,index,j}$ complex-valued phasors of 'metric-filtered' amplitudes for axis i and frequency j
- $\bar{s}_{A,i,j}$ complex-valued input amplitude phasors for axis i and frequency j
- $F_{s,index}$ signal domain metric including phase information
- f_j j -th frequency in periodic signal

From these phasors, the real amplitudes and phases can be recovered using the relations (axis and frequency indices omitted):

$$A = |\bar{s}_A|, \quad \varphi = \tan^{-1} \left(\frac{\text{Im}(\bar{s}_A)}{\text{Re}(\bar{s}_A)} \right)$$

where

- \bar{s}_A complex-valued amplitude phasor of length N_A
- φ periodic signal phase vector



- **A** real-valued amplitude vector

Concerning the statistical treatment, the evaluation of periodic signal is the most complex of all error sources types even though (or just because) the temporal behaviour is deterministic.

First, the temporal periodic signals are generated for each realization k of the distributed amplitudes over all N_f frequencies according to the analytical expression:

$$\mathbf{s}_{temp,k} = \sum_{j=1}^{N_f} A_{j,k} \cos(2\pi f_j t + \varphi_{j,k})$$

where

- $s_{temp,k}$ real-valued temporal signal for frequency j and ensemble realization k
- $\varphi_{j,k}$ periodic signal phase for frequency j and ensemble realization k
- $A_{j,k}$ real-valued amplitude for frequency j and ensemble realization k
- f_j j -th frequency in periodic signal
- t time vector

This results in N_A temporal realizations of the signals for each single axis. Then the statistical treatment can directly be applied to the set of temporal realizations:

- Temporal domain: worst-case
Ensemble domain: statistical
The required PDF is described by N_A samples of the worst-case value in each $s_{temp,k}$.
- Temporal domain: statistical
Ensemble domain: worst-case
The required PDF is described by the samples of $s_{temp,k}$ which contains the overall worst-case value of all vectors s_{temp} .
- Temporal domain: statistical
Ensemble domain: statistical
The required PDF is described by all samples in all $N_A s_{temp,k}$.
- Temporal domain: worst-case
Ensemble domain: worst-case
The required quantity is not a PDF, but just the discrete overall worst-case value of all vectors s_{temp} .

The results from one of the cases above then form the required sample vectors $s_{P,i}$ for each axis.

Determination of the evaluation vector for the temporal samples

The determination of the evaluation (“time”) vector t used for the generation of the periodic signals is also critical. First, the “sampling” needs to fast enough to properly account for the highest frequency component in the signal. Second, the overall time span covered needs to be such that integer multiples of the lowest frequency signal period (ideally of all signals) are covered. Otherwise, due to the part of the “incomplete” cycle, the result does no longer match the result expected from [AD1], e.g. zero-mean and a standard deviation of Amplitude/ $\sqrt{2}$.

If more than one signal is involved, finding a common multiple of all periods and a sufficiently large resolution at the same time result in a more and more increasing length of the time vector (which could even exceed the available memory. For that reason, the following approach is implemented:

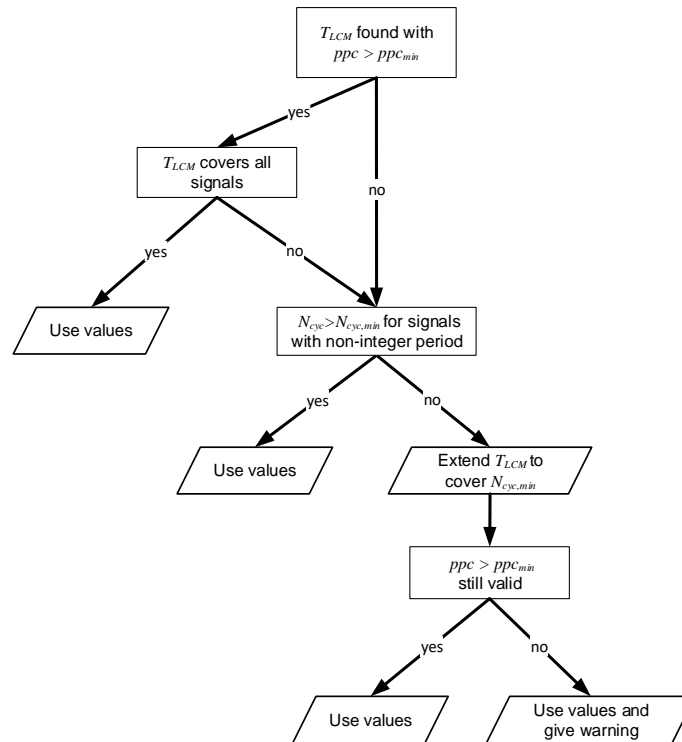


Figure 5-28: Logic for periodic signal sample vector generation

First, all involved signal periods which are integer multiples of a larger present period are removed (as accounting for the largest period ensures integer cycles also for the remaining ones). Then all remaining signal components whose amplitudes fall below a certain ratio w.r.t. to the largest signal amplitude are neglected in the determination of the evaluation vector, as these components have negligible influence on the resulting PDF.

The least common multiple (LCM) of all signal periods T_{LCM} is determined starting from the period of the “slowest” signal. If the resulting number is too large (e.g. two irrational periods), only the largest feasible value is used. Then, with this feasible number as “simulation time”, the resolution ppc (points per cycle) for the fastest signal component is compared to a threshold ppc_{min} .

Furthermore, the systematic error made due to non-integer periods decreases significantly with the overall number of periods N_{cyc} realized, such that non-integer periods can be accepted if they are above a certain threshold $N_{cyc,min}$.

This logic is only required to produce matching results with respect to those in the tables in [AD1]. If the evaluation period (which is a requirement specification parameter in [AD2]) is explicitly taken into account, above logic would not be necessary and only a sufficient resolution needed to be checked.



5.3.5.1.4 Drift Errors

Different to the implementation in PEET V1.0, drift signals are no longer represented by a random variable description, but by a Fourier series approximation. Thus, they are basically represented as a periodic signal and are also evaluated as such (see chapter 5.3.5.1.3). For that purpose, the drift signal component is added to the 'standard' periodic signal first as described in chapter 5.3.4.3.1.

5.3.5.1.5 Transient Errors

As 'transient' error signals are implemented as a special case of periodically occurring signals and modelled as Fourier series approximation similar to drift signals, their evaluation is also fully equivalent to the evaluation of 'standard' periodic signals (see chapter 5.3.5.1.3).

5.3.5.1.6 Worst-Case Values

Dependent on the user-defined statistical treatment, worst-case values of different PDFs have to be determined.

For all PDFs related to ensemble parameters, (time-constant and time-random) random variables and drift errors, these worst-case values are already required at PES level as they define the PDF properties to be realized (see tables in chapter 5.3.3) and can be computed analytically as only the fundamental PDFs in chapter 5.3.6.1 are involved. Table 5-8 below shows these worst-case values.

Table 5-8: Worst-case values for the basic distribution

Distribution	PDF parameters	Worst-case value	Comments	
Delta	$\delta(\mu_D)$	μ_D	equivalent to the discrete value provided	
Uniform	$U(x_{min}, x_{max})$	x_{max}	equivalent to the upper bound	
Bimodal (Arcsine)	$BM(x_{min}, x_{max})$	x_{max}	equivalent to the upper bound	
Gaussian*	$G(\mu, \sigma)$	$\mu + 3\sigma$	equivalent to 99.73% level of confidence as unbounded	
Rayleigh	$R(r, \sigma_r)$	$r + 3.4393 \sigma_r$	equivalent to 99.73% level of confidence as unbounded	
Truncated Gaussian	Both bounds	$G_T(\mu, \sigma, LTB, UTB)$	UTB	equivalent to the upper bound
	Symmetric	$G_S(\mu, \sigma, STB)$	$\mu + STB$	equivalent to the upper bound
	Upper bound	$G_U(\mu, \sigma, UTB)$	UTB	equivalent to the upper bound
	Lower bound	$G_L(\mu, \sigma, LTB)$	$\mu + 3\sigma$	equivalent to 99.73% level of confidence as unbounded



Beta	$\text{Beta}(\alpha, \beta, d, s)$	$d+s$	equivalent to the upper bound
User-Defined	-	$\max(e)$	numerical definition, WC is directly largest value provided

*The definition of the worst-case value of a Gaussian distribution is a convention selected to be in line with the Table B-4 of [AD1]. If any other bound different from “3 σ ” needs to be applied, then a Truncated Gaussian with a symmetric bound can be used instead.

As the signs of initial worst-case values (at PES level) can be inverted during the transfer analysis steps, they do not necessarily lead to the worst-case for the final error. For that reason, the following convention is introduced:

“Worst-case values always take into account the “most positive” value of a distribution, not the largest absolute value. This means that positive errors are always assumed to worsen a budget in the initial setup.”

This convention gives the user a clear indication on how error sources need to be set up and a control on how they are treated in the evaluation.

Example:

For a uniform distribution U(-3, -1) the worst-case value is -1. To obtain a worst-case value of -3, the error source needs to be defined as U(1,3) and a static system with a gain of -1 needs to be used in the system transfer. If all other sources are positive as well, this indeed gives the overall worst-case.

5.3.5.2 Evaluation of Statistical Requirements

5.3.5.2.1 PDF and CDF Generation from Samples

The basis for the determination of each PDF is always a sample vector \mathbf{s} (i.e. \mathbf{s}_{CRV} , \mathbf{s}_{RV} , \mathbf{s}_{RP} , \mathbf{s}_P , and \mathbf{s}_D) of sufficient length N_s to represent the current distribution. First, a histogram of the samples is generated by counting the samples that fall in one of N_{bin} different bins. The ratio between sample number and bin number is chosen such that sufficient resolution (bin number itself) and accuracy (sufficient samples per bin) is realized. In a next step, the vector of samples per bin needs to be normalized, i.e. divided by the “area” below the histogram to represent a valid PDF with unity area. The CDF is then obtained by numerical integration of the PDF vector using a trapezoidal method.

Separate PDFs are generated for each error type to display these contributions in the budget for the input and output of each block in the Budget Tree View of PEET. The CDFs are only used for the further evaluation of the total error and displayed in the Breakdown Tree View.

5.3.5.2.2 Total Error Contribution

According to AST-4 in [AD2], it has to be distinguished between time-constant, time-random and total pointing error contributions for each axis. Furthermore, also a line-of-sight error needs to be provided (in case of 3D budget) which can also be broken down into these sub-contributions.

Axis Budgets

The time-constant error contribution of each axis i is simply the contribution of the time-constant random variable error sources represented by the sample vector $\mathbf{s}_{CRV,i}$:



$$\mathbf{e}_{TC,i} = \mathbf{s}_{CRV,i}$$

The time-random contribution is represented by the samples of the remaining contributions:

$$\mathbf{e}_{TR,i} = \mathbf{s}_{RV,i} + \mathbf{s}_{RP,i} + \mathbf{s}_{P,i} + \mathbf{s}_{D,i}$$

Finally, the total error is the sum of all sample vectors:

$$\mathbf{e}_{tot,i} = \mathbf{e}_{TC,i} + \mathbf{e}_{TR,i}$$

Line-Of-Sight Budget

The line-of-sight budget is computed from the error contributions of the axis perpendicular to the selected line-of-sight axis [AD2]. Exemplary for a line-of-sight direction along the x-axis, this gives (element-wise for each component of the sample vectors above):

$$e_{TC,LoS} = \sqrt{e_{TC,y}^2 + e_{TC,z}^2}$$

$$e_{TR,LoS} = \sqrt{e_{TR,y}^2 + e_{TR,z}^2}$$

$$e_{tot,LoS} = \sqrt{e_{tot,y}^2 + e_{tot,z}^2}$$

For a line-of-sight direction along the y- or z-axis, the axis indices have to be permuted respectively.

Level confidence evaluation

For this evaluation, the PDF of the absolute value of each error contribution above needs to be integrated from 0 until the specified level of confidence value is reached, i.e.:

$$LoC/100 = \int_0^{e_{tot,LoC}} p(|e|) de$$

Internally, this is realized by interpolation of the numerical CDF to find the value $e_{tot,LoC}$ for the given level of confidence value.

In case multiple user-defined ensemble domains are specified which are intended to be evaluated individually, all above steps are also carried out individually for the results of each domain.

5.3.5.3 Evaluation of Spectral Requirements

The evaluation of spectral requirements is comparably trivial. Only random process type error sources contribute to this requirement and all other sources are neglected. The only operation which is necessary is to apply the metric filters to the power spectral densities as described in section 5.3.5.1.2. The filtered result is then simply plotted versus the associated requirement function to detect violations.



5.3.5.4 Simplified Statistical Method

In parallel to the advanced statistical method, also the simplified statistical method can still be used in PEET. By “definition”, the only real difference between the two methods is the amount of information required or applied for the evaluation of an error contribution. Consequently, all methodological updates mentioned in the previous sections (domain treatment, definition and restrictions of correlation between signal classes, treatment of periodic signals) are also valid for the simplified method.

In terms of implementation, the software thus uses the same error source setup and system transfer approach based on samples even for the simplified method. At *PEC* or *Total Error* blocks however, only the statistical moments (mean and standard deviation) of the current contribution are taken into account (according to the evaluation rules of the simplified method of [AD2] repeated in chapter 5.3.1.1.4) while the PDF information available from the samples is ignored and only confidence factors ($n_p = 1,2,3$) can be specified.

With this approach, a budget evaluation with the simplified method leads to the same result as in the prototype presuming:

- Only full or no correlation has been specified between axes of all individual error sources
- No “infeasible” correlation between different sources (i.e. between temporal and ensemble properties, between different error signal classes) has been defined in the prototype scenario or manual budget and the correlation is either “full or “none”
- No periodic sources at different frequencies have been specified (as both the ECSS table for periodic signals and the prototype implementation do not account for the impact of different frequencies in the summation of periodic signals)

5.3.6 Analytical Solutions for Distributions

The analytical solutions (where available) for the following quantities are presented for the distributions present in PEET:

PDF
<p>The PDF $p(x)$ is a function that describes the relative likelihood for the random variable x to take on a given value. It has the following property</p> $\int_{-\infty}^{\infty} p(x)dx = 1$ <p>If no further information on the support of x is provided, the valid range is $[-\infty, \infty]$.</p>
Mean Value
<p>The mean value of a random variable is its first moment, i.e. its expected value. In terms of the PDF, this can be expressed as:</p> $\mu_x = \int_x x p(x)dx$



Root Mean Square
<p>The RMS value of a random variable is the square root of its second moment. In terms of the PDF, this can be expressed as:</p> $RMS_x^2 = \int_x x^2 p(x) dx$
Standard Deviation
<p>The variance of a random variable is its second central moment, i.e. the expected value of the squared deviation from the mean. In terms of the PDF, this can be expressed as:</p> $\sigma_x^2 = \int_x (x - \mu_x)^2 p(x) dx$ <p>The standard deviation σ is simply the square root of this quantity.</p>
CDF
<p>The cumulative distribution function describes the probability that the value of a random variable with a given distribution is found to have a value less than or equal to x.</p> $CDF(x) = \int_{-\infty}^x p(\bar{x}) d\bar{x}$ <p>The function output ranges always between 0 and 1. If no further information on the support of x is provided, the valid range is $[-\infty, \infty]$.</p>
ICDF
<p><i>ICDF</i>(x) is the inverse function of the CDF (range [0,1]). It only exists if the CDF is strictly monotonic increasing and maps a given probability to a certain function value of the PDF.</p>

For the description of the various quantities, the following special functions are required:

- $erf(x)$, $erf^{-1}(x)$: The error function and its inverse
- $erfc(x)$, $erfc^{-1}(x)$: The complementary error function $1-erf(x)$ and its inverse
- $\Gamma(s,x)$: The incomplete Gamma function
- $Ei(x)$: The exponential integral
- $I_x(x, \alpha, \beta)$: The regularized incomplete beta function
- $I_x^{-1}(x, \alpha, \beta)$: The inverse regularized incomplete beta function

5.3.6.1 Basic Distributions

These distributions are required for time-constant random variables and the distributions of parameters (amplitudes of periodic signals, bounds of uniform temporal RVs, distributed



mean and standard deviation of Gaussian temporal RVs). Their PDFs below are required first in analytical form in the software to create a numerical representation of the CDF, PDF, and ICDFs. The analytical results for the different properties were further used for the verification of the numerical results.

All results have been computed with Mathematica. In some cases, the expressions have been further simplified by hand (indicated by '*' in the tables below).

5.3.6.1.1 Delta Distribution

PDF
$p(x) = \delta(x - \mu_D)$
Mean Value
$\mu_x = \mu_D$
Root Mean Square
$RMS_x^2 = \mu_D^2$
Standard Deviation
$\sigma_x^2 = 0$
CDF
$CDF(x) = \begin{cases} 1 & \text{for } x \geq \mu_D \\ 0 & \text{for } x < \mu_D \end{cases}$
ICDF
$ICDF(x) = \mu_D$
(special case by definition, as the CDF is not strictly monotonic for the discrete case)

5.3.6.1.2 Uniform Distribution

PDF
$p(x) = \frac{1}{x_{\max} - x_{\min}}$ for $x_{\min} < x < x_{\max}$, 0 else
Mean Value
$\mu_x = \frac{x_{\max} + x_{\min}}{2}$
Root Mean Square



$RMS_x^2 = \frac{1}{3} x_{\max}^2 + x_{\min} x_{\max} + x_{\min}^2$
Standard Deviation
$\sigma_x^2 = \frac{(x_{\max} - x_{\min})^2}{12}$
CDF
$CDF(x) = \begin{cases} 0 & \text{for } x \leq x_{\min} \\ \frac{x - x_{\min}}{x_{\max} - x_{\min}} & \text{for } x_{\min} < x < x_{\max} \\ 1 & \text{for } x \geq x_{\max} \end{cases}$
ICDF
$ICDF(x) = x_{\min} (1 - x) + x_{\max} x$

5.3.6.1.3 Bimodal (Arcsine) Distribution

PDF
$p(x) = \frac{\pi^{-1}}{\sqrt{(x_{\max} - x)(x - x_{\min})}}$ for $x_{\min} < x < x_{\max}$, 0 else
Mean Value
$\mu_x = \frac{x_{\max} + x_{\min}}{2}$
Root Mean Square
$RMS_x^2 = \frac{1}{8} 3x_{\max}^2 + 2x_{\min} x_{\max} + 3x_{\min}^2$
Standard Deviation
$\sigma_x^2 = \frac{(x_{\max} - x_{\min})^2}{8}$
CDF



$$CDF(x) = \begin{cases} 0 & \text{for } x \leq x_{\min} \\ \frac{2}{\pi} \sin^{-1} \left(\sqrt{\frac{x - x_{\min}}{x_{\max} - x_{\min}}} \right) & \text{for } x_{\min} < x < x_{\max} \\ 1 & \text{for } x \geq x_{\max} \end{cases}$$

ICDF

$$ICDF(x) = x_{\min} + (x_{\max} - x_{\min}) \sin \left(\frac{\pi}{2} x \right)^2$$

5.3.6.1.4 Gaussian Distribution**PDF**

$$p(x) = \frac{1}{\sigma\sqrt{2\pi}} \exp \left[-\frac{1}{2} \left(\frac{x - \mu}{\sigma} \right)^2 \right]$$

Mean Value

$$\mu_x = \mu$$

Root Mean Square

$$RMS_x^2 = \mu^2 + \sigma^2$$

Standard Deviation

$$\sigma_x^2 = \sigma^2$$

CDF

$$CDF(x) = \frac{1}{2} \operatorname{erfc} \left(\frac{\mu - x}{\sqrt{2}\sigma} \right)$$

ICDF

$$ICDF(x) = \mu - \sqrt{2}\sigma \operatorname{erfc}^{-1}(2x)$$

5.3.6.1.5 Rayleigh Distribution

The parameter r has been introduced to allow a shift of the distribution along the abscissa (i.e. not restricted to minimum value of zero). This is required to use this distribution also as parameter distribution, e.g. as upper bound of a temporal uniform PDF.

PDF*

$$p(x) = \frac{x - r}{\sigma_r^2} \exp \left[-\frac{(x - r)^2}{2\sigma_r^2} \right] \quad \text{for } x \geq r, \quad 0 \text{ else}$$

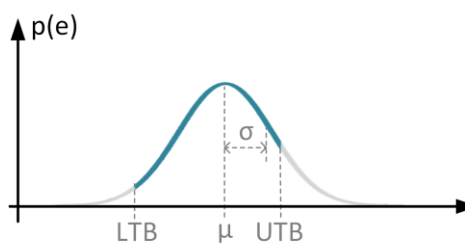


Mean Value*
$\mu_x = r + \sigma_r \sqrt{\frac{\pi}{2}}$
Root Mean Square*
$RMS_x^2 = \frac{4 - \pi}{2} \sigma_r^2 + \left(r + \sigma_r \sqrt{\frac{\pi}{2}} \right)^2$
Standard Deviation*
$\sigma_x^2 = \frac{4 - \pi}{2} \sigma_r^2$
CDF*
$CDF(x) = 1 - \exp\left[-\frac{(x-r)^2}{2\sigma_r^2}\right] \quad \text{for } x \geq r$
ICDF*
$ICDF(x) = r + \sigma_r \sqrt{-\ln[(1-x)^2]}$

5.3.6.1.6 Truncated Gaussian

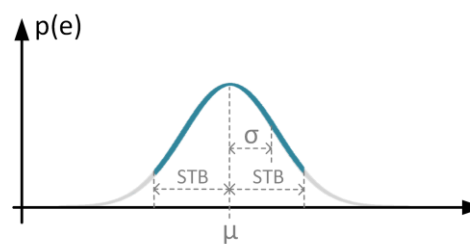
Only the results for the truncation at two different finite bounds are provided. The finite upper/lower bound (UTB > LTB) and symmetric truncation at a bound around the mean (STB > 0) can be derived as subsets:

Two-Sided Truncation



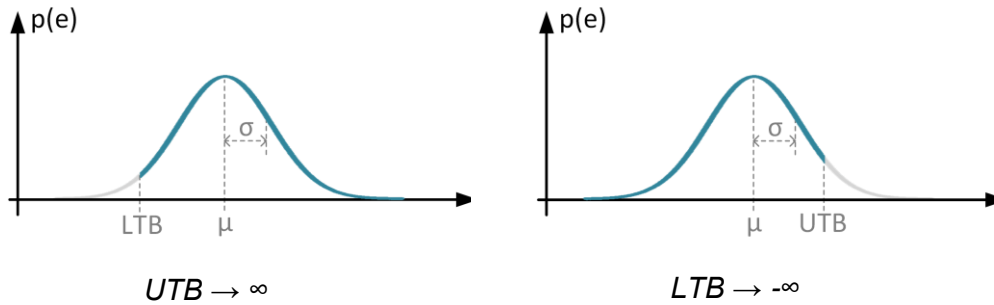
Truncation at lower bound

Symmetric Truncation



$$UTB = \mu + STB, \quad LTB = \mu - STB$$

Truncation at upper bound



Furthermore, the following auxiliary quantities are used to express the remaining properties in a compact way [RD14]:

$$\alpha = \left(\frac{LTB - \mu}{\sigma} \right), \quad \beta = \left(\frac{UTB - \mu}{\sigma} \right),$$

$$\xi = \left(\frac{x - \mu}{\sigma} \right)$$

$$Z = \Phi(\beta) - \Phi(\alpha)$$

where $\phi(\Phi)$ is the PDF (CDF) of a standard normal distribution ($\mu=0, \sigma=1$). CDF_G denotes the CDF of the non-normalized distribution (with μ and σ).

PDF
$p(x) = \frac{\frac{1}{\sigma\sqrt{2\pi}} \exp\left[-\frac{1}{2}\left(\frac{x-\mu}{\sigma}\right)^2\right]}{CDF_G(UTB) - CDF_G(LTB)} = \frac{\phi(\xi)}{\sigma Z} \quad \text{for } LTB \leq x \leq UTB, \quad 0 \text{ else}$
Mean Value
$\mu_x = \mu + \frac{\phi(\alpha) - \phi(\beta)}{Z} \sigma$
Root Mean Square
$RMS_x^2 = \left(\mu + \frac{\phi(\alpha) - \phi(\beta)}{Z} \sigma \right)^2 + \sigma^2 \left[1 + \frac{\alpha\phi(\alpha) - \beta\phi(\beta)}{Z} - \left(\frac{\phi(\alpha) - \phi(\beta)}{Z} \right)^2 \right]$
Standard Deviation
$\sigma_x^2 = \sigma^2 \left[1 + \frac{\alpha\phi(\alpha) - \beta\phi(\beta)}{Z} - \left(\frac{\phi(\alpha) - \phi(\beta)}{Z} \right)^2 \right]$
CDF



$CDF(x) = \frac{\Phi(\xi) - \Phi(\alpha)}{Z}$
ICDF*
$ICDF(x) = \mu - \sqrt{2}\sigma \operatorname{erfc}^{-1}\left[2(CDF_G(LTB) + x(CDF_G(UTB) - CDF_G(LTB)))\right]$

5.3.6.1.7 Beta Distribution

The parameters d and $s \geq 0$ have been introduced to allow a shift and a scaling of the distribution along the abscissa (i.e. to extend the domain $[0,1]$ of a standard Beta distribution to $[d, d+s]$). This is required to apply this distribution also as parameter distribution, e.g. as upper bound of a temporal uniform PDF.

PDF
$p(x) = \frac{\left(\frac{x-d}{s}\right)^{\alpha-1} \left(1 - \frac{x-d}{s}\right)^{\beta-1}}{ s \operatorname{Beta}(\alpha, \beta)} \text{ for } d \leq x \leq d+s, \text{ zero else}$ <p style="text-align: center;">with</p> $\operatorname{Beta}(\alpha, \beta) = \frac{\Gamma(\alpha)\Gamma(\beta)}{\Gamma(\alpha + \beta)}$
Mean Value
$\mu_x = \frac{d + \frac{\alpha + \beta + s\alpha}{\alpha + \beta}}$
Root Mean Square
$RMS_x^2 = \frac{\frac{s^2\alpha\beta}{1 + \alpha + \beta} + s\alpha + d}{\alpha + \beta}^2$
Standard Deviation
$\sigma_x^2 = \frac{s^2\alpha\beta}{\alpha + \beta} \frac{1}{1 + \alpha + \beta}$
CDF
$CDF(x) = I_x\left(\frac{x-d}{s}, \alpha, \beta\right)$
ICDF



$$ICDF(x) = d + s \cdot I_x^{-1} x, \alpha, \beta$$

5.3.6.2 Composed Distributions

These distributions would be basically required for time-random variables where one the distribution parameters is distributed itself in an ensemble sense and the domain treatment of both temporal and ensemble domain are statistical ("mixed interpretation" in [AD1]). They result from integration of the temporal PDF p_T conditioned on the parameter η (e.g. amplitude, drift rate or bound) of the ensemble PDF p_E , i.e.:

$$p(x) = \int_{-\infty}^{\infty} p_T(x | \eta) p_E(\eta) d\eta$$

With the numerical approach for the basic, the resulting properties in the table are not required in analytical form in the software itself. They are only used as additional verification approach for the numerical results, although, in many case, closed-form solutions or explicit compact expressions could not be identified.

5.3.6.2.1 Gaussian RV

In this case, the temporal PDF p_T is the Gaussian PDF given in 5.3.6.1.4.

5.3.6.2.1.1 Distributed mean value

The parameter $\eta = \mu$ of p_T has a distribution p_E , which is any of the distribution described in 5.3.6.1.

Uniformly distributed mean value U(a,b) with b>a

PDF
$p(x) = \frac{\operatorname{erf}\left[\frac{a-x}{\sqrt{2}\sigma}\right] - \operatorname{erf}\left[\frac{b-x}{\sqrt{2}\sigma}\right]}{2(a-b)}$
Mean Value
$\mu_x = \frac{1}{2}(b+a)$
Root Mean Square
$RMS_x^2 = \frac{1}{4}(b+a)^2 + \frac{1}{12}(\sigma^2 + b^2 - 2ab + a^2)$
Standard Deviation
$\sigma_x^2 = \frac{1}{12}(12\sigma^2 + b^2 - 2ab + a^2)$
CDF*



$CDF(x) = \frac{a - b - \exp\left[-\frac{(a-x)^2}{2\sigma^2}\right] \sqrt{\frac{2}{\pi}}\sigma + \exp\left[-\frac{(b-x)^2}{2\sigma^2}\right] \sqrt{\frac{2}{\pi}}\sigma + (x-a) \operatorname{erf}\left[\frac{a-z}{\sqrt{2}\sigma}\right] + (b-x) \operatorname{erf}\left[\frac{b-z}{\sqrt{2}\sigma}\right]}{2(a-b)}$
ICDF
No explicit or compact solution found

Bimodal (arcsine) distributed mean value BM(a,b) with b>a

PDF
No explicit or compact solution found
Mean Value
$\mu_x = \frac{1}{2}(b + a)$
Root Mean Square
$RMS_x^2 = \frac{1}{4}(b + a)^2 + \frac{1}{8}(8\sigma^2 + b^2 - 2ab + a^2)$
Standard Deviation
$\sigma_x^2 = \frac{1}{8}(8\sigma^2 + b^2 - 2ab + a^2)$
CDF
No explicit or compact solution found
ICDF
No explicit or compact solution found

Gaussian distributed mean value G(μ_E,σ_E)

PDF
$p(x) = \frac{1}{\sqrt{2\pi}\sqrt{\sigma^2 + \sigma_E^2}} \exp\left[-\frac{(x - \mu_E)^2}{2(\sigma^2 + \sigma_E^2)}\right]$
Mean Value
$\mu_x = \mu_E$
Root Mean Square
$RMS_x^2 = \mu_E^2 + \sigma^2 + \sigma_E^2$
Standard Deviation



$\sigma_x^2 = \sigma^2 + \sigma_E^2$
CDF
$CDF(x) = \frac{1}{2} \operatorname{erfc} \left[\frac{\mu_E - x}{\sqrt{2} \sqrt{\sigma^2 + \sigma_E^2}} \right]$
ICDF
$ICDF(x) = \mu_E - \sqrt{2} \operatorname{erfc}^{-1}[2x] \sqrt{\sigma^2 + \sigma_E^2}$

Rayleigh distributed mean value $R(r, \sigma_r)$

PDF
$p(x) = \frac{\exp \left[-\frac{x-r^2}{2\sigma^2} \right] \left(\exp \left[\frac{x-r^2 \sigma_r^2}{2\sigma^2 \sigma^2 + \sigma_r^2} \right] \sqrt{\pi} \left(1 + \operatorname{erf} \left[\frac{x-r \sigma_r}{\sqrt{2\sigma} \sqrt{\sigma^2 + \sigma_r^2}} \right] \right) (x-r)\sigma_r + \sqrt{2\sigma} \sqrt{\sigma^2 + \sigma_r^2} \right)}{2\sqrt{\pi} \sigma^2 + \sigma_r^2^{3/2}}$
Mean Value
$\mu_x = r + \sqrt{\frac{\pi}{2}} \sigma_r$
Root Mean Square
$RMS_x^2 = \left(r + \sqrt{\frac{\pi}{2}} \sigma_r \right)^2 + \frac{1}{2} (2\sigma^2 + (4 - \pi) \sigma_r^2)$
Standard Deviation
$\sigma_x^2 = \frac{1}{2} (2\sigma^2 + (4 - \pi) \sigma_r^2)$
CDF
$CDF(x) = \frac{\exp \left[-\frac{x-r^2}{2\sigma^2 + \sigma_r^2} \right] \left(- \left(1 + \operatorname{erf} \left[\frac{x-r \sigma_r}{\sqrt{2\sigma} \sqrt{\sigma^2 + \sigma_r^2}} \right] \right) \sigma_r + \exp \left[\frac{x-r^2}{2\sigma^2 + \sigma_r^2} \right] \left(1 + \operatorname{erf} \left[\frac{x-r}{\sqrt{2\sigma}} \right] \right) \sqrt{\sigma^2 + \sigma_r^2} \right)}{2\sqrt{\sigma^2 + \sigma_r^2}}$
ICDF
No explicit or compact solution found

5.3.6.2.1.2 Distributed standard deviation

The parameter $\eta = \sigma$ of p_T has a distribution p_E , which is any of the distribution described in 5.3.6.1.



As the standard deviation needs to be larger than zero, the ensemble distributions are automatically truncated at zero (e.g. if the specified lower bound of a uniform distribution is smaller than zero or a Gaussian ensemble distribution is specified).

Uniformly distributed standard deviation U(a,b) with b>a

PDF*
$p(x) = \frac{\Gamma\left[0, \frac{(x-\mu)^2}{2a^2}\right] - \Gamma\left[0, \frac{(x-\mu)^2}{2b^2}\right]}{2(a-b)\sqrt{2\pi}}$
Mean Value
$\mu_x = \mu$
Root Mean Square
$RMS_x^2 = \mu^2 + \frac{1}{3}(b^2 + ab + a^2)$
Standard Deviation
$\sigma_x^2 = \frac{1}{3}(b^2 + ab + a^2)$
CDF
$CDF(x) = \frac{1}{2} + \frac{-2a\sqrt{\pi}\operatorname{erf}\left[\frac{x-\mu}{\sqrt{2a}}\right] + 2b\sqrt{\pi}\operatorname{erf}\left[\frac{x-\mu}{\sqrt{2b}}\right] + \sqrt{2}(x-\mu)\left(Ei\left[-\frac{(x-\mu)^2}{2a^2}\right] - Ei\left[-\frac{(x-\mu)^2}{2b^2}\right]\right)}{4(b-a)\sqrt{\pi}}$
ICDF
No explicit or compact solution found

Bimodal (arcsine) distributed standard deviation BM(a,b) with b>a

PDF
No explicit or compact solution found
Mean Value
$\mu_x = \mu$
Root Mean Square
$RMS_x^2 = \mu^2 + \frac{1}{8}(3b^2 + 2ab + 3a^2)$
Standard Deviation



$\sigma_x^2 = \frac{1}{8}(3b^2 + 2ab + 3a^2)$
CDF
No explicit or compact solution found
ICDF
No explicit or compact solution found

Gaussian distributed standard deviation G(μ_E, σ_E)

PDF
No explicit or compact solution found
Mean Value
$\mu_x = \mu$
Root Mean Square
$RMS_x^2 = \mu^2 + \mu_E^2 + \sigma_E^2$
Standard Deviation
$\sigma_x^2 = \mu_E^2 + \sigma_E^2$
CDF
No explicit or compact solution found
ICDF
No explicit or compact solution found

Rayleigh distributed standard deviation value R(r, σ_r)

PDF
$p(x) = \frac{\exp\left[-\frac{ x-\mu }{\sigma_r}\right]}{2\sigma_r} \text{ for } r = 0$ No explicit or compact solution found for $r \neq 0$.
Mean Value
$\mu_x = \mu$
Root Mean Square
$RMS_x^2 = \mu^2 + 2\sigma_r^2 + \sqrt{2\pi}r\sigma_r$



Standard Deviation
$\sigma_x^2 = 2\sigma_r^2 + \sqrt{2\pi}r\sigma_r$
CDF
$CDF(x) = \begin{cases} 1 - \frac{1}{2} \exp\left[-\frac{x-\mu}{\sigma_r}\right] & \text{for } x \geq \mu \\ \frac{1}{2} \exp\left[-\frac{\mu-x}{\sigma_r}\right] & \text{for } x < \mu \end{cases} \quad \text{and } r = 0$ <p style="text-align: center;">No explicit or compact solution found for $r \neq 0$.</p>
ICDF
$ICDF(x) = \begin{cases} \mu + \ln(2x)\sigma_r & \text{for } 0 < x \leq 1/2 \\ \mu - \ln(2(1-x))\sigma_r & \text{for } 1/2 < x < 1 \end{cases} \quad \text{and } r = 0$ <p style="text-align: center;">No explicit or compact solution found for $r \neq 0$.</p>

5.3.6.2.2 Uniform RV

In this case, the temporal PDF p_T is the uniform PDF given in 5.3.6.1.2.

5.3.6.2.2.1 Distributed upper bound

The parameter $\eta = x_{max}$ of p_T has a distribution p_E , which is any of the distribution described in 5.3.6.1.

As the smallest value of the distributed upper bound needs to be larger than the lower bound, the ensemble distributions are automatically truncated at this bound (e.g. if the specified upper bound of a bimodal ensemble distribution is larger than x_{max} or a Gaussian ensemble distribution is specified).

Note, that the uniform random variable description in Table B-4 of [AD1] is a special case of this distribution with $x_{min}=0$ and $x_{max}=c$.

Uniformly distributed upper bound U(a,b) with $b > a$

PDF
$p(x) = \begin{cases} \frac{1}{a-b} \ln \left[\frac{x_{min} - a}{x_{min} - b} \right] & \text{for } x_{min} \leq x \leq a \\ \frac{1}{a-b} \ln \left[\frac{x_{min} - x}{x_{min} - b} \right] & \text{for } a < x \leq b \end{cases}$
Mean Value
$\mu_x = \frac{1}{4}(2x_{min} + b + a)$
Root Mean Square



$RMS_x^2 = \frac{1}{16} 2x_{\min} + b + a^2 + \frac{1}{144} (7a^2 - 2ab + 7b^2 - 12ax_{\min} - 12bx_{\min} + 12x_{\min}^2)$
Standard Deviation
$\sigma_x^2 = \frac{1}{144} (7a^2 - 2ab + 7b^2 - 12ax_{\min} - 12bx_{\min} + 12x_{\min}^2)$
CDF*
$CDF(x) = \begin{cases} \frac{(x - x_{\min}) \ln \left[\frac{x_{\min} - a}{x_{\min} - b} \right]}{a - b} & \text{for } x_{\min} \leq x \leq a \\ \frac{a - x + x_{\min} \ln \left[\frac{x_{\min} - a}{x_{\min} - x} \right] + x \ln \left[\frac{x_{\min} - x}{x_{\min} - b} \right] - x_{\min} \ln \left[\frac{x_{\min} - a}{x_{\min} - b} \right]}{a - b} & \text{for } a < x \leq b \end{cases}$
ICDF
No explicit or compact solution found

Bimodal distributed upper bound BM(a,b) with b>a

PDF
$p(x) = \begin{cases} \frac{1}{\sqrt{(x_{\min} - a)(x_{\min} - b)}} & \text{for } x_{\min} \leq x \leq a \\ \frac{1}{\pi} \left(\pi - 2 \tan^{-1} \left[\frac{\sqrt{(a - x)(x_{\min} - b)}}{\sqrt{(x_{\min} - a)(x - b)}} \right] \right) \frac{1}{\sqrt{(x_{\min} - a)(x_{\min} - b)}} & \text{for } a < x \leq b \end{cases}$
Mean Value
$\mu_x = \frac{1}{4} (2x_{\min} + b + a)$
Root Mean Square
$RMS_x^2 = \frac{1}{16} 2x_{\min} + b + a^2 + \frac{1}{48} (3a^2 - 2ab + 3b^2 - 4ax_{\min} - 4bx_{\min} + 4x_{\min}^2)$
Standard Deviation
$\sigma_x^2 = \frac{1}{48} (3a^2 - 2ab + 3b^2 - 4ax_{\min} - 4bx_{\min} + 4x_{\min}^2)$
CDF*



$CDF(x) = \begin{cases} \frac{2}{\pi} \left(\tan^{-1} \left[\sqrt{\frac{(a-x)}{(x-b)}} \right] - \tan^{-1} \left[\sqrt{\frac{(a-x)(x_{\min}-b)}{(x_{\min}-a)(x-b)}} \sqrt{\frac{x_{\min}-a}{x_{\min}-b}} \right] + \dots \right) & \text{for } x_{\min} \leq x \leq a \\ \frac{1}{\sqrt{(x_{\min}-a)(x_{\min}-b)}} + \frac{\left(\pi - 2 \tan^{-1} \left[\sqrt{\frac{(a-x)(x_{\min}-b)}{(x_{\min}-a)(x-b)}} \right] \right) (x-a)}{\pi \sqrt{(x_{\min}-a)(x_{\min}-b)}} & \text{for } a < x \leq b \end{cases}$
ICDF
No explicit or compact solution found

Gaussian distributed upper bound G(μ_E,σ_E)

PDF
No explicit or compact solution found
Mean Value
$\mu_x = \frac{x_{\min} + \mu_E}{2}$
Root Mean Square
$RMS_x^2 = \frac{x_{\min} + \mu_E}{4}^2 + \frac{1}{12} x_{\min}^2 - 2x_{\min}\mu_E + \mu_E^2 + 4\sigma_E^2$
Standard Deviation
$\sigma_x^2 = \frac{1}{12} (x_{\min}^2 - 2x_{\min}\mu_E + \mu_E^2 + 4\sigma_E^2)$
CDF
No explicit or compact solution found
ICDF
No explicit or compact solution found

Rayleigh distributed upper bound R(r,σ_r)

PDF
No explicit or compact solution found
Mean Value



$\mu_x = \frac{2r + 2x_{\min} + \sqrt{2\pi}\sigma_r}{4}$
Root Mean Square
$RMS_x^2 = \frac{2r + 2x_{\min} + \sqrt{2\pi}\sigma_r}{16} + \frac{1}{24} (2r^2 - 4rx_{\min} + 2x_{\min}^2 + 2\sqrt{2\pi}\sigma_r (r - x_{\min}) + 16\sigma_r^2 - 3\pi\sigma_r^2)$
Standard Deviation
$\sigma_x^2 = \frac{1}{24} (2r^2 - 4rx_{\min} + 2x_{\min}^2 + 2\sqrt{2\pi}\sigma_r (r - x_{\min}) + 16\sigma_r^2 - 3\pi\sigma_r^2)$
CDF
No explicit or compact solution found
ICDF
No explicit or compact solution found

5.3.6.2.2.2 Distributed lower bound

The parameter $\eta=x_{\min}$ of p_T has a distribution p_E , which is any of the distribution described in 5.3.6.1.

As the largest value of the distributed lower bound needs to be smaller than the upper bound, the ensemble distributions are automatically truncated at this bound (e.g. if the specified lower bound of a bimodal ensemble distribution is smaller than x_{\min} or a Gaussian ensemble distribution is specified).

Uniformly distributed lower bound U(a,b) with b>a

PDF
$p(x) = \begin{cases} \frac{1}{b-a} \ln \left[\frac{x_{\max} - a}{x_{\max} - x} \right] & \text{for } a \leq x \leq b \\ \frac{1}{b-a} \ln \left[\frac{x_{\max} - a}{x_{\max} - b} \right] & \text{for } b < x \leq x_{\max} \end{cases}$
Mean Value
$\mu_x = \frac{1}{4} (2x_{\max} + b + a)$
Root Mean Square
$RMS_x^2 = \frac{1}{16} (2x_{\max} + b + a)^2 + \frac{1}{144} (12x_{\max}^2 - 12bx_{\max} + 7b^2 - 12ax_{\max} - 2ab + 7a^2)$
Standard Deviation



$\sigma_x^2 = \frac{1}{144} (12x_{\max}^2 - 12bx_{\max} + 7b^2 - 12ax_{\max} - 2ab + 7a^2)$
CDF
$CDF(x) = \begin{cases} \frac{a - x + (x_{\max} - x) \ln \left[\frac{x_{\max} - a}{x_{\max} - x} \right]}{a - b} & \text{for } a \leq x \leq b \\ \frac{(x - b) \ln \left[\frac{x_{\max} - a}{x_{\max} - b} \right] + b - a - (x_{\min} - b) \ln \left[\frac{x_{\min} - a}{x_{\min} - b} \right]}{b - a} & \text{for } b < x \leq x_{\max} \end{cases}$
ICDF
No explicit or compact solution found

Bimodal distributed lower bound BM(a,b) with b>a

PDF
$p(x) = \begin{cases} \frac{2 \tan^{-1} \left[\sqrt{\frac{(a-x)(x_{\max} - b)}{(x_{\max} - a)(x - b)}} \right]}{\pi \sqrt{(x_{\max} - a)(x_{\max} - b)}} & \text{for } a \leq x \leq b \\ \frac{1}{\sqrt{(x_{\max} - b)(x_{\max} - a)}} & \text{for } b < x \leq x_{\max} \end{cases}$
Mean Value
$\mu_x = \frac{1}{4} (2x_{\max} + b + a)$
Root Mean Square
$RMS_x^2 = \frac{1}{16} (2x_{\max} + b + a)^2 + \frac{1}{48} (4x_{\max}^2 - 4bx_{\max} + 3b^2 - 4ax_{\max} - 2ab + 3a^2)$
Standard Deviation
$\sigma_x^2 = \frac{1}{48} (4x_{\max}^2 - 4bx_{\max} + 3b^2 - 4ax_{\max} - 2ab + 3a^2)$
CDF



$CDF(x) = \begin{cases} \frac{\left(2 \tan^{-1} \left[\sqrt{\frac{(a-x)(x_{\max}-b)}{(x_{\max}-a)(x-b)}} \right] (x-x_{\max}) + \left(\tan^{-1} \left[\sqrt{\frac{a-x}{x-b}} \right] \sqrt{(x_{\max}-a)(x_{\max}-b)} \right) \right)}{\pi \sqrt{(x_{\max}-a)(x_{\max}-b)}} & \text{for } a \leq x \leq b \\ \frac{x-x_{\max} + \sqrt{(x_{\max}-a)(x_{\max}-b)}}{\sqrt{(x_{\max}-a)(x_{\max}-b)}} & \text{for } b < x \leq x_{\max} \end{cases}$
ICDF
No explicit or compact solution found

Gaussian distributed lower bound G(μ_E,σ_E)

PDF
No explicit or compact solution found
Mean Value
$\mu_x = \frac{x_{\max} + \mu_E}{2}$
Root Mean Square
$RMS_x^2 = \frac{x_{\max} + \mu_E}{4} + \frac{1}{12} (x_{\max}^2 - 2x_{\max}\mu_E + \mu_E^2 + 4\sigma_E^2)$
Standard Deviation
$\sigma_x^2 = \frac{1}{12} (x_{\max}^2 - 2x_{\max}\mu_E + \mu_E^2 + 4\sigma_E^2)$
CDF
No explicit or compact solution found
ICDF
No explicit or compact solution found

Rayleigh distributed lower bound R(r,σ_r)

PDF
No explicit or compact solution found
Mean Value



$\mu_x = \frac{2r + 2x_{\max} + \sqrt{2\pi}\sigma_r}{4}$
Root Mean Square
$RMS_x^2 = \frac{2r + 2x_{\max} + \sqrt{2\pi}\sigma_r}{16} + \frac{1}{24} (2r^2 - 4rx_{\max} + 2x_{\max}^2 + 2\sqrt{2\pi}\sigma_r r - x_{\max} + 16\sigma_r^2 - 3\pi\sigma_r^2)$
Standard Deviation
$\sigma_x^2 = \frac{1}{24} (2r^2 - 4rx_{\max} + 2x_{\max}^2 + 2\sqrt{2\pi}\sigma_r (r - x_{\max}) + 16\sigma_r^2 - 3\pi\sigma_r^2)$
CDF
No explicit or compact solution found
ICDF
No explicit or compact solution found

A.1.1.1 Distributed range of symmetric zero-mean uniform distribution

The parameter $\eta = x_{\max} = -x_{\min}$ of p_T has a distribution p_E , which is any of the distribution described in 5.3.6.1.

As the symmetric bound needs to be larger than zero, the ensemble distributions are automatically truncated at zero (e.g. if the specified upper bound of a bimodal ensemble distribution is smaller than zero or a Gaussian ensemble distribution is specified).

Uniformly distributed symmetric bound U(a,b) with b>a>0

PDF
$p(x) = \begin{cases} \frac{1}{2(b-a)} \ln \left[\frac{-b}{x} \right] & \text{for } -b \leq x \leq -a \\ \frac{1}{2(b-a)} \ln \left[\frac{b}{a} \right] & \text{for } -a < x < a \\ \frac{1}{2(b-a)} \ln \left[\frac{b}{x} \right] & \text{for } a \leq x \leq b \end{cases}$
Mean Value
$\mu_x = 0$
Root Mean Square
$RMS_x^2 = \frac{1}{9} (b^2 + ab + a^2)$
Standard Deviation



$\sigma_x^2 = \frac{1}{9}(b^2 + ab + a^2)$	
CDF	
$CDF(x) = \left\{ \begin{array}{l} \frac{b+x+x \ln \left[\frac{b}{-x} \right]}{2(b-a)} \end{array} \right.$	for $-b \leq x \leq -a$
$\frac{b-a+x \ln \left[\frac{b}{a} \right]}{2(b-a)}$	for $-a < x < a$
$\frac{b-2a+x+x \ln \left[\frac{b}{x} \right]}{2(b-a)}$	for $a \leq x \leq b$
ICDF	
No explicit or compact solution found	

Bimodal distributed symmetric bound BM(a,b) with $b>a>0$

PDF*	
$p(x) = \left\{ \begin{array}{l} \frac{1}{\pi\sqrt{ab}} \tan^{-1} \left[\frac{\sqrt{a}}{\sqrt{b}} \sqrt{\frac{b+x}{a+x}} \right] \end{array} \right.$	for $-b \leq x < -a$
$\frac{1}{2\sqrt{ab}}$	for $-a \leq x \leq a$
$\frac{1}{\pi\sqrt{ab}} \tan^{-1} \left[\frac{\sqrt{a}}{\sqrt{b}} \sqrt{\frac{b-x}{x-a}} \right]$	for $a < x \leq b$
Mean Value	
$\mu_x = 0$	
Root Mean Square	
$RMS_x^2 = \frac{1}{24} (3b^2 + 2ab + 3a^2)$	
Standard Deviation	
$\sigma_x^2 = \frac{1}{24} (3b^2 + 2ab + 3a^2)$	



CDF	
$CDF(x) = \begin{cases} \frac{4x \tan^{-1} \left[\sqrt{\frac{a(b+x)}{b(a+x)}} \right] + \sqrt{ab} \left(\pi + 2 \tan^{-1} \left[\frac{a+b+2x}{2\sqrt{-(a+x)(b+x)}} \right] \right)}{4\pi\sqrt{ab}} & \text{for } -b \leq x < -a \\ \frac{1}{2} \left(1 + \frac{x}{\sqrt{ab}} \right) & \text{for } -a \leq x \leq a \\ \frac{3}{4} - \frac{1}{2\pi} \left(\tan^{-1} \left[\frac{a+b-2x}{2\sqrt{(x-a)(b-x)}} \right] \right) - \frac{2x}{\sqrt{ab}} \tan^{-1} \left[\sqrt{\frac{a(x-b)}{b(a-x)}} \right] & \text{for } a < x \leq b \end{cases}$	
ICDF	
No explicit or compact solution found	

Gaussian distributed symmetric bound $G(\mu_E, \sigma_E)$

PDF
No explicit or compact solution found
Mean Value
$\mu_x = 0$
Root Mean Square
$RMS_x^2 = \frac{1}{3} \mu_E^2 + \sigma_E^2$
Standard Deviation
$\sigma_x^2 = \frac{1}{3} (\mu_E^2 + \sigma_E^2)$
CDF
No explicit or compact solution found
ICDF
No explicit or compact solution found

Rayleigh distributed symmetric bound $R(r, \sigma_r)$ with $r > 0$

PDF
No explicit or compact solution found



Mean Value	
$\mu_x = 0$	
Root Mean Square	
$RMS_x^2 = \frac{1}{3} r^2 + \sqrt{2\pi} r \sigma_r + 2\sigma_r^2$	
Standard Deviation	
$\sigma_x^2 = \frac{1}{3} \left(r^2 + \sqrt{2\pi} r \sigma_r + 2\sigma_r^2 \right)$	
CDF	
$CDF(x) = \begin{cases} \frac{1}{4\sigma_r} \left(2\sigma_r \exp \left[-\frac{r+x}{2\sigma_r} \right] + \sqrt{2\pi} r + x \left(1 + \operatorname{erf} \left[\frac{r+x}{\sqrt{2}\sigma_r} \right] \right) \right) & \text{for } x < -r \\ \frac{1}{2\sigma_r} \left(\sigma_r + \sqrt{\frac{\pi}{2}} r + x \right) & \text{for } -r \leq x \leq r \\ \frac{1}{4\sigma_r} \left(-2\sigma_r \exp \left[-\frac{r-x}{2\sigma_r} \right] + 4\sigma_r + \sqrt{2\pi} r + x + \sqrt{2\pi} x - r \operatorname{erf} \left[\frac{r-x}{\sqrt{2}\sigma_r} \right] \right) & \text{for } r < x \end{cases}$	
ICDF	
No explicit or compact solution found	



6 Proposed Evolutions to the PEEH

6.1 Rationale

The release of the ESA Pointing Error Engineering Handbook [AD2] in its current version took place in 2011. In the last decade, it has been used in several ESA space mission studies and projects in the last years and became a well-known and broadly accepted reference in the European space community. Since then, also several studies were initiated by ESA to develop and improve PEET as a supporting tool in applying the handbook methodology.

These studies developed concepts and implemented refined methods in the PEET software (e.g. the generalized statistical interpretation concept or the PDF-based advance statistical method, [RD15]) which are not yet (or not in detail) reflected in the PEEH. Further, during the P4COM study,

- additional and revised metrics were introduced which are also proposed for implementation in the PEEH (see sections 6.2.1.1 or 6.2.1.8)
- the existing frequency domain metrics (on power level) were complemented by signal domain metrics which consider also phase information (e.g. for processing periodic signals, see section 6.2.1.8)
- frequency domain models for a set of certain typical (periodically reoccurring) transients were introduced (see 6.2.1.6) which allow a more accurate evaluation using the handbook methodology.

The main purpose of this task was to align the information in the PEEH and the functionalities available in the tool and to complement the draft with comments and extensions for a better understanding.

It has to be noted that the handbook draft proposed by the study team is not – and cannot – be considered as ready for publication of a new release. It is intended to serve as one of possibly many inputs for further iterations and consolidation in ESA working groups outside the scope of this study.

6.2 Summary of Proposed Changes

The following subchapters briefly and qualitatively describe the proposed changes and update for the PEEH. All chapter numbers mentioned refer to unmodified “baseline” document.

6.2.1 Main Chapters

6.2.1.1 Chapter 4 “Pointing error: from sources to system performance”

This chapter was generalized and renamed to “Spacecraft pointing”. An additional subchapter “Definition of pointing” was introduced which provides all necessary mathematical notations and conventions for the definition of pointing errors (e.g. angles, line-of-sight, knowledge vs performance). The subchapter on time-windowed pointing error indices was complemented by figures illustrating the various performance and knowledge indices defined in the ECSS standard and includes the suggested additional metrics as a refinement of the relative pointing errors, namely:

- **Windowed Performance Drift/Windowed Knowledge Drift (WPD/WKD):**
This metric describes a linear trend ('smear') within a given time window of width Δt (see Figure 6-2).
- **Windowed Performance Residual/Windowed Knowledge Residual (WPR/WKR):**
This metric describes the remaining (zero-mean) jitter in a time-window of width Δt after any linear trend has been removed (see Figure 6-2).
- **Location-dependent RPE/RKE within a time window of width Δt :**
This Windowed Relative Stability (WRS) metric describes the instantaneous deviation at time t from the mean in a time window. The location with respect to the window centre t_c is defined by $\gamma \in [-\Delta t/2, \Delta t/2]$ as illustrated in Figure 6-3.
The former Windowed Variance (WV) metric related to the RPE is renamed to Windowed Expected Distribution (WED) and describes the expected distribution of the deviation from the mean in the time window
- **Location-dependent WPR/WKR within a time window of width Δt :**
Similar as above, this Windowed Relative Jitter (WRJ) metric describes the instantaneous error with respect to mean value within a time window for a reference location $-\Delta t/2 \leq \gamma \leq \Delta t/2$, but after any linear trend was removed from the time window. As equivalent to the WED metric for the RPE, also a Windowed Expected Jitter (WEJ) metric is introduced to describe the respective expected distribution in that sense.

These metrics are partially based on publications from Pittelkau ([RD16] - where predecessor publication have already been the basis for the frequency domain metrics in the current PEEH) – and partially on inputs provided by ESA based on return of experience from other projects. A respective publication of the derived frequency domain metrics is intended after the end of the study.

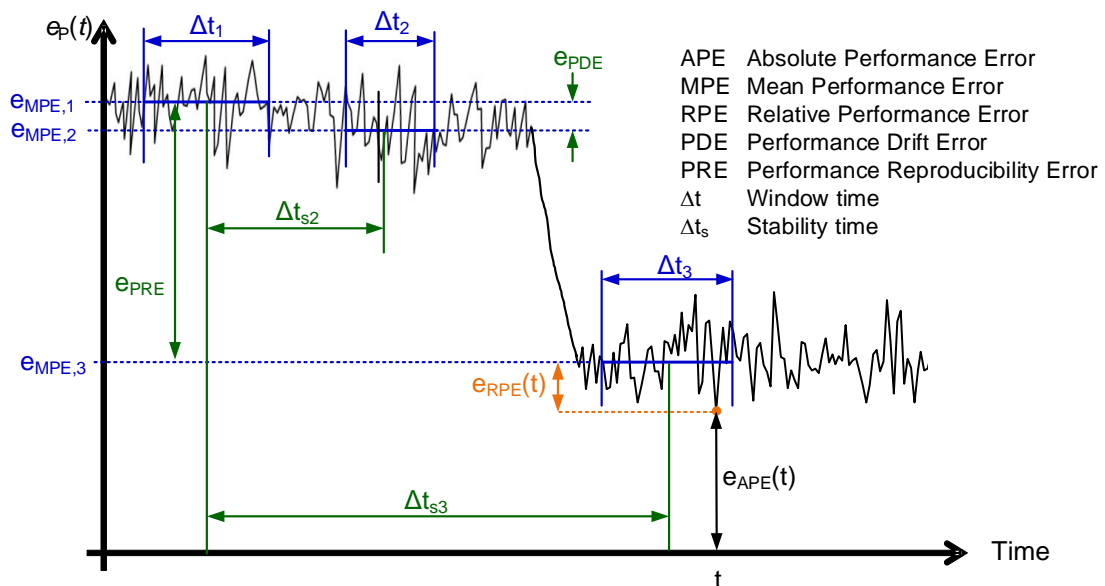


Figure 6-1: Illustration of ECSS instantaneous time pointing performance error indices

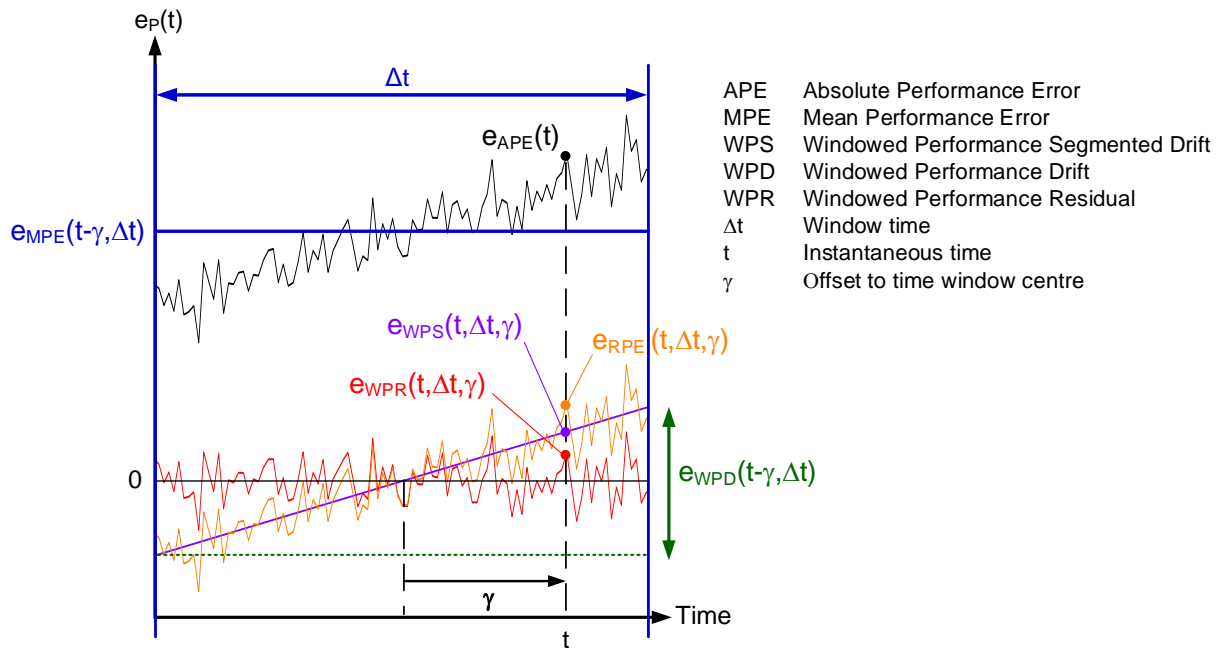


Figure 6-2: Illustration of extended instantaneous error indices with separation of RPE into linear drift and residual

Table 6-1: Complemented list of instantaneous pointing error indices

Pointing Error Indices			
<i>index</i>		<i>instantaneous</i>	
$e_{APE}(t)$		$= e_p(t)$	
$e_{AKE}(t)$		$= e_K(t)$	
$e_{MPE}(t - \gamma, \Delta t)$		$= \bar{e}_p(t - \gamma, \Delta t)$	
$e_{RPE}(t, \gamma, \Delta t)$		$= e_p(t) - \bar{e}_p(t - \gamma, \Delta t)$	
$e_{WPS}(t, \gamma, \Delta t)$		$= \gamma r_{WPD}(t - \gamma, \Delta t)$	
$e_{WPD}(t - \gamma, \Delta t)$		$= \Delta t r_{WPD}(t - \gamma, \Delta t)$	
$e_{WPR}(t, \gamma, \Delta t)$		$= e_p(t) - (e_{MPE}(t - \gamma, \Delta t) + e_{WPS}(t, \gamma, \Delta t))$	
$e_{PDE}(t - \gamma, \Delta t_1, \Delta t_2, \Delta t_s)$		$= \bar{e}_p(t - \gamma, \Delta t_1) - \bar{e}_p(t - \gamma + \Delta t_s, \Delta t_2)$	
$e_{PRE}(t - \gamma, \Delta t_1, \Delta t_2, \Delta t_s)$			
$\Delta t, \Delta t_1, \Delta t_2$	window time	e_{index}	instantaneous error
Δt_s	stability time	$e_K(t)$	knowledge error signal
		$e_p(t)$	performance error signal

time average:	$\bar{e}(t - \gamma, \Delta t) = \langle e(t - \gamma) \rangle_{\Delta t} = \frac{1}{\Delta t} \int_{t-\gamma-\Delta t/2}^{t-\gamma+\Delta t/2} e(\tau) d\tau$
linear drift rate:	$r_{\text{WPD}}(t - \gamma, \Delta t) = \frac{12}{\Delta t^3} \int_{-\Delta t/2}^{\Delta t/2} \alpha e(t - \gamma + \alpha) d\alpha$

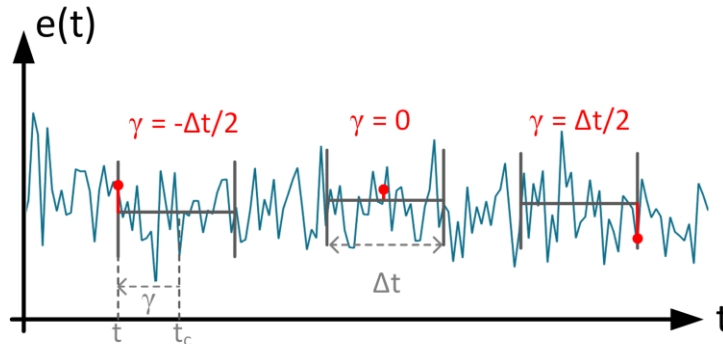


Figure 6-3: Instantaneous relative error dependent on reference location γ

6.2.1.2 Chapter “Objectives and scope of the handbook”

This new chapter was introduced to provide a general overview on the objective of pointing error engineering and the intended use of the handbook in this respect. It outlines different analyses methods (experiment, numerical simulation, compiled budgets) and sets the focus of the handbook framework on the budget compilation which shall enable a design and development process which tailorable, responsive and integrated – being understood as an interface to results obtained by more complex or detailed analyses.

6.2.1.3 Chapter 5 “Pointing error engineering framework”

Proposed changes in this chapter were mainly related to an extension of the “Framework elements” subchapter. In particular:

- Figures were added to illustrate the difference between ensemble-random and time-random behaviour of random variables and a combination of both. Similarly, subscripts were introduced in the PDF notation to clearly distinguish the statistical properties a PDF describes (i.e. ensemble, temporal or both).
- The subchapter on conditional probability was replaced by a more top-level chapter on “Joint, Conditional and Marginal Probability density”. It provides the respective definitions and shows the derivation of the integral PDF expression which is the baseline for all approximate budget tables of the different error contributors in the ECSS standard ([AD1], tables in Annex B) – consequently allowing readers to obtain the rationale for these expressions.
- A subchapter “Level of confidence” was introduced to show and illustrate the difference between one-sided and two-sided probability distributions and why the one-sided CDF is usually applied for pointing requirements.
- The overview table in section “Summary of Statistical Properties with Respective PDF” was extended to account for additional typical PDFs (such as Beta and Truncated



Gaussian) which also aligns the set of distributions available in PEET. Further, the “bimodal” distribution is formally renamed to “arcsine” distribution, as “bimodal” describes an entire class of distributions while the specific PDF provided relates to the PDF of a sinusoidal signal.

- The section was further extended by general rules for the summation of random variables (in terms of mean value, standard deviations for fully correlated/uncorrelated cases and PDF) and their multiplication with a scalar value.
- The chapter “Statistical interpretation in context of framework” now also introduces the concept of generalized ensemble domains and the respective mapping to the statistical interpretation concept of the ECSS standard (see Table 6-2).
- This concept was elaborated in the precursor study PEET2 (e.g. [RD17]) with the aim of providing a more flexible and ultimately less conservative way of specifying requirements (e.g. by considering only a subset of contributors of an ensemble as worst-case while others are still evaluated statistically).

Table 6-2: Mapping between generalized concept and statistical interpretation in [AD1]

		Temporal domain	
		domain treatment	
		statistical	worst-case
Ensemble domain	statistical	mixed interpretation	ensemble interpretation
	worst-case	temporal interpretation	-

 Generalized Concept  ECSS-E-ST-60-10C

Further, a note was added on the determination of worst-case values or time-series in case (Monte Carlo) simulation results are available and temporal interpretation applies.



In this case, the worst-case may actually depend on the level of confidence associated to a requirement, i.e. the time-series realized with the worst-case ensemble parameter of a given temporal distribution does not necessarily correspond to the time-series containing the worst-case value for every given level of confidence (graphically, the CDFs of different realizations are crossing). This can however not be considered using a simplified approach using mean values and standard deviations where the individual worst-case values need to be determined from the given distribution for each error source a priori.

- A chapter “Rotational Coordinate Transformations” was added to introduce the relations between rotation matrices and pointing error angles represented as vectors.
- A chapter “Deterministic Signal” was added to introduce general periodic signals and transients and their description by Fourier transforms and amplitude/power/energy spectra and to prepare the basics for their evaluation in the frequency domain
- A new chapter “Linear Time-Invariant Systems” provides the main definitions and references for LTI system theory basics which are required for the dynamic system transfer expressions in later chapters (e.g. for AST-2).
- The “Random Process” chapter was complemented by a figure and additional notes on strongly and weakly stationary process conditions.
- A chapter “Dependency of error signals” was added that introduces the definition of the covariance matrix and the relation to the correlation coefficient for random variables. Similarly, the cross-spectral density matrix and the coherence function is introduced for random processes highlighting the analogy between these two descriptions (i.e. between the expressions of full/non-correlated random variables and full/non-coherent power spectral densities).

6.2.1.4 Chapter 6 “Pointing error requirement formulation”

No significant changes were proposed for the initial “Overview” and “Specification parameters” subchapter apart from some minor rephrasing and fixing of typos. For the subchapter “Notes on requirement specification parameters” the following changes were made:

- Suggestions are made to include in the chapter “Pointing error indices” additional guidelines on modified error indices for some special cases and about possible zero contribution for certain error indices when evaluating budgets using the ECSS tables
- The “Statistical interpretation” chapter was modified such that it also accounts for the generalized ensemble domain concept (see 6.2.1.3)
- The “Evaluation period” chapter was updated such that it becomes clear that this parameter has a driving impact on how error sources must be classified such that the desired statistics are accounted for in a budget as illustrated with the following example:

Assume a geostationary satellite with a requirement on the performance of (an ensemble of short-term) imaging observations. Further assume that a periodic disturbance is present with a period of one orbit (e.g. a thermo-elastic distortion). Although the nature of the disturbance itself is periodic, it does not appear as periodic within the relevant evaluation period which is equivalent to the much shorter duration of a single observation (cf. Figure 6-4).

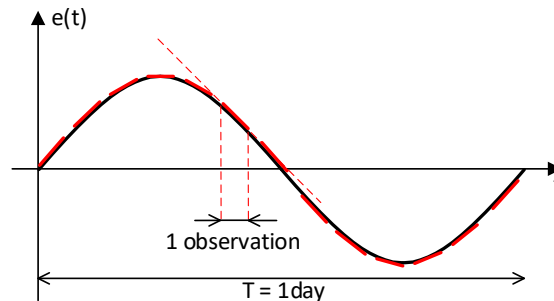


Figure 6-4 Long-term disturbance and short-term evaluation period

Thus, describing the temporal behaviour of the disturbance within one observation as periodic would ultimately link the wrong statistical properties for the time frame of interest. Indeed, a more suitable model would be the combination of a time-constant distribution and a drift contribution with an arcsine distributed value and drift rate. If the observation duration is significantly smaller, even a time-constant bias with an arcsine-distributed ensemble value only would be appropriate.

Above statement does not only apply the systematic approach in the framework of the PEEH, but also to time-domain simulations in general. While performing a simulation over an entire period of the disturbance and decomposing the time-series afterwards into the single observations for analysis would be compatible with a periodic model, simulations of an ensemble of single observations would not without special measures. In this case, the phase of the periodic signal needs to be shifted accordingly between different runs to account for all possible conditions which is effectively equivalent to the above-mentioned decomposition into bias (and drift). Consequently, also physically time-varying error sources may need to be mapped to a different time-random or even time-constant representation based on the evaluation period of interest to be properly represented in the statistical analysis.

- A note was added to the “Level of confidence” which highlights the difference between the level of confidence as requirement parameter and the level of confidence related to the identification of error source properties itself.

6.2.1.5 Chapter 7 “Pointing error analysis methodology”

The analysis methodology structure schemes have been updated such that they match to the different evaluation method of the generalized domain concept and the less conservative summation rules for AST-4 when combining time-constant and time-random contribution (see 6.2.1.9)

6.2.1.6 Chapter 8 “Characterization of pointing error source: AST-1”

The subchapter “PES error data classification” was updated to account for the complemented PES signal classes (e.g. truncated Gaussian, transients). Further, the difference between random process and random variable description (w.r.t. conditions, application, benefits/drawbacks) has been detailed.



The subchapters “Time-constant PES description” and “Time-random PES description” were complemented by notes on a necessary domain assignment when applying the generalized domain concepts and figures illustrating the time- and ensemble behaviour of these sources. In all tables related to statistical interpretation, it is made clear whether the resulting PDF describes temporal or ensemble properties via respective subscripting.

Further, the following changes were proposed for the subchapters of “Random variable PES description”:

- A new section “Gaussian and truncated Gaussian random” was introduced to describe the related distributions, their statistical properties and possible ensemble variations of their parameters.
The implicitly imposed 3-Sigma bound for practical application of the generally unbounded Gaussian distribution in the ECSS tables is highlighted and that a truncation can be used to restrict the worst-case values to a more/less stringent range. Finally, a note has been added that any temporal mean value of a Gaussian generally needs to be mapped to a time-constant PES
- A new section “Periodic” was introduced to recall the distribution and statistical properties of a sinusoidal error source modelled as random variable. Drawbacks and restrictions (e.g. assuming full periods, no phase information for summation) of this model compared to a frequency domain model are highlighted their statistical properties and possible ensemble variations of their parameters.
- The section “Uniform random” was complemented with possible ensemble variations of the distribution parameters. A specific note was added that any non-zero mean temporal contribution needs to be modelled as time-constant PES for a proper evaluation.
- The “Drift” section was complemented with a link to the assumptions that are made and necessary for the simplified random variable description.

In the corresponding “Random process PES description”, the following updates were proposed:

- The note in “Gaussian Random” on the first approximation of a PSD with a given variance only was adapted to mention the (known or approximate) noise bandwidth rather than the Nyquist frequency.
- The term “bimodal” for the sinusoidal distribution in the “Periodic” section was renamed to “arcsine” to relate to the actual explicit distribution used..
- A subchapter “Drift” was added to introduce the frequency domain model for the drift signal based on a Fourier series approximation (including the series coefficients related to drift rate and reset time parameters) discussing the advantages compared to the random variable model, but also the drawbacks (e.g. overshoot due to Gibb’s phenomenon).
- The “Transient” chapter was extended such that it provides explicit Fourier series coefficients for at least selected periodically reoccurring transient signals including as shown in Table 6-3.

Finally, a chapter “Guidelines for PES description” is introduced that summarizes general topics for the PES definition and classification as well as specification of cross-correlation between different PES.



Table 6-3: Fourier-series coefficients for selected (periodically occurring) errors

Fourier series coefficients ($\omega_0 = 2\pi/T_p$ each)		
a_0	a_k	Signal type
$M \frac{T_{on}}{T_p}$	$M \frac{T_{on}}{T_p} \cdot \text{sinc} \left(k\omega_0 \frac{T_{on}}{2} \right)$	<p style="text-align: center;">Rectangular</p>
$M \frac{T_{on}/2}{T_p}$	$M \frac{T_{on}/2}{T_p} \cdot \text{sinc}^2 \left(k\omega_0 \frac{T_{on}}{2} \right)$	<p style="text-align: center;">Triangular</p>
$\frac{M}{T_p \cdot r}$	$\frac{M}{T_p \cdot (r + jk\omega_0)}$	<p style="text-align: center;">Exponential decay</p>
$\frac{M \cdot r}{T_p \cdot r^2 + \omega_c^2}$	$\frac{M \cdot (r + jk\omega_0)}{T_p \cdot [(r + jk\omega_0)^2 + \omega_c^2]}$	<p style="text-align: center;">Exponentially decaying cosine</p>
Real-valued coefficients: $A_k = 2 \text{Re } a_k$, $\varphi_k = \arg a_k$		



6.2.1.7 Chapter 9 “Transfer analysis: AST-2”

The “Frequency-domain” chapter has been divided in two further subchapters “Dynamic System Transfer” and “Static System Transfer”. These subchapters recall the transfer rules for random process PES (MIMO transfer of PSDs), periodic PES (transfer of complex amplitudes containing magnitude and phase information) and random variables (mean values for both static and dynamic systems and standard deviations for static systems). A note on missing information for a dynamic system transfer using a random variable model is provided. Further, the static transfer rules are illustrated by a coordinate transformation as a typical use case example.

The “Time-domain” chapter has been complemented with some clarification and a link to the new annex on Monte-Carlo simulation guidelines (see 6.2.2.6).

6.2.1.8 Chapter 10 “Pointing error index contribution: AST-3”

The table in “Overview” chapter has been extended to account for the variance equations of the additional metrics (e.g. WPD or location-dependent metrics, see 6.2.1.1) for both time- and frequency domain.

As a consequence, also the explicit expressions for the metrics are listed in the tabular overview in the “Frequency-domain” chapter (excerpt in Table 6-4). Rational approximations for these exact weighting functions were derived (where possible with low order) and improved rational approximations for the already existing metrics are provided where considered necessary (e.g. to provide conservative upper bound envelopes). Further, some typos in PEEH Table 10.3 were fixed (e.g. consistent naming of stability time in plots and equations, naming of WM filter in WMS expression).

All metrics present in the currently released version of the PEEH are defined on ‘power-level’ which makes them directly applicable to PSDs. As these metrics do not account for the phase information which is required for a more detailed processing of periodic signals, equivalent metrics on signal level have been derived as well and were included in tabular form in a similar way (excerpt in Table 6-5).

This also enables a description and evaluation of selected ‘transient’ signals, e.g. exponentially decay or exponentially decaying sinusoids modelled as Fourier series approximation (see Table 6-3).

A respective publication of the derived frequency domain metrics is intended after the end of the study.

Table 6-4: Additional power level metrics

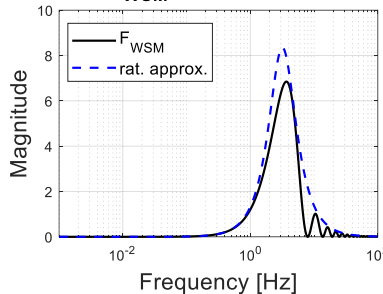
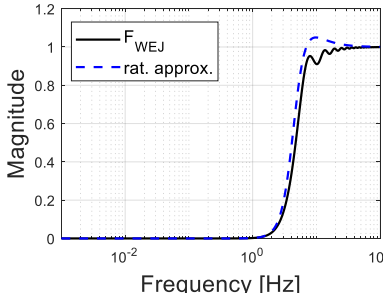
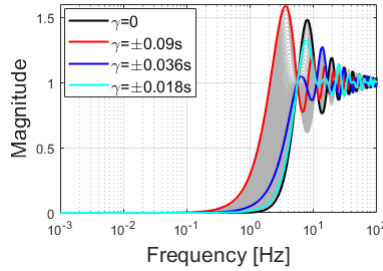
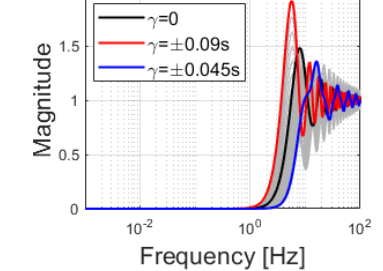
Pointing Error Metric Weighting Functions F_{metric}	
Windows Smear (WSM)	F_{WSM} with $\Delta t=0.18s$
$F_{WSM}(\omega, \Delta t) =$ $\left(\frac{12}{\omega \Delta t} \left[\cos\left(\frac{\omega \Delta t}{2}\right) - \text{sinc}\left(\frac{\omega \Delta t}{2}\right) \right] \right)^2$	
$\tilde{F}_{WSM}(s, \Delta t) = \left \frac{13s\Delta t}{(s\Delta t)^2 + 4.5s\Delta t + 13} \right ^2$	
Windowed Expected Jitter (WEJ)	F_{WEJ} with $\Delta t=0.18s$
$F_{WEJ}(\omega, \Delta t) = 1 - F_{WM}(\omega, \Delta t) - \frac{1}{12} F_{WSM}(\omega, \Delta t)$ $= 1 - \text{sinc}^2\left(\frac{\omega \Delta t}{2}\right) - \frac{1}{12} \left(\frac{12}{\omega \Delta t} \left[\cos\left(\frac{\omega \Delta t}{2}\right) - \text{sinc}\left(\frac{\omega \Delta t}{2}\right) \right] \right)^2$	
$\tilde{F}_j(s, \Delta t) = \frac{(s\Delta t)^2}{(s\Delta t)^2 + 6.5(s\Delta t) + 27}$	
Windowed Relative Stability (WRS)	$F_{WRS}(\gamma)$ with $\Delta t=0.18s$
$F_{WRS}(\omega, \Delta t, \gamma) = 1 - 2 \cos(\omega \gamma) \text{sinc}\left(\frac{\omega \Delta t}{2}\right) + \text{sinc}^2\left(\frac{\omega \Delta t}{2}\right)$	
Windowed Relative Jitter (WRJ)	$F_{WRJ}(\gamma)$ with $\Delta t=0.18s$
$F_{WRJ}(\omega, \Delta t, \gamma)$ $= \left 1 - e^{-j\omega \gamma} \text{sinc}\left(\frac{\omega \Delta t}{2}\right) - e^{-j\omega \gamma} \frac{12\gamma}{j\omega \Delta t^2} \left[\cos\left(\frac{\omega \Delta t}{2}\right) - \text{sinc}\left(\frac{\omega \Delta t}{2}\right) \right] \right ^2$	



Table 6-5: Exemplary signal level metrics

Pointing Error Metric Weighting Functions W_{metric}	
Windowed Mean (WM)	$W_{\text{WM}} \text{ with } \Delta t = 0.18\text{s}$
$W_{\text{WM}}(\omega, \Delta t, \gamma) = e^{-j\omega\gamma} \text{sinc}\left(\frac{\omega\Delta t}{2}\right)$	
Windowed Mean Stability (WMS)	$W_{\text{STA}} \text{ with } \Delta t = 0.18\text{s} \text{ and } \Delta t_s = 60\text{s}$
$W_{\text{WMS}}(\omega, \Delta t, \Delta t_s, \gamma) = e^{-j\omega\gamma} (1 - e^{j\omega\Delta t_s}) \text{sinc}\left(\frac{\omega\Delta t}{2}\right)$	
Windowed Smear (WSM)	$W_{\text{WSM}} \text{ with } \Delta t = 0.18\text{s}$
$W_{\text{WSM}}(j\omega, \Delta t, \gamma) = e^{-j\omega\gamma} \frac{12}{j\omega\Delta t} \left[\cos\left(\frac{\omega\Delta t}{2}\right) - \text{sinc}\left(\frac{\omega\Delta t}{2}\right) \right]$	
Windowed Relative Stability (WRS)	$W_{\text{WRS}}(\gamma) \text{ with } \Delta t = 0.18\text{s}$
$W_{\text{WRS}}(j\omega, \Delta t, \gamma) = 1 - e^{-j\omega\gamma} \text{sinc}\left(\frac{\omega\Delta t}{2}\right)$	



6.2.1.9 Chapter 11 “Pointing error evaluation: AST-4”

Chapter “Evaluation methods”

This subchapter was updated to account for the generalized statistical interpretation concept using ensemble domains (see chapter 5.3.1.3). The different evaluation options (common and individual) were introduced, discussed and illustrated and the existing workflow schemes were adapted accordingly.

Chapter “Simplified Method”

- The summation rules for the total error compilation with the SSM in the current handbook version is recalled in Table 6-6. Only for APE/AKE and MPE/MKE indices, also time-constant contributions (B) are relevant and summed linearly to the time-random contributions (ε_{index}).

Table 6-6: Current rule for total error compilation from time-constant and time-random contributions

Total Pointing Error per Index	
<i>index</i>	<i>compilation</i>
<i>APE</i> (Δt_D)/ <i>AKE</i> (Δt_D)	$e_{index} = B + \varepsilon_{index}(\Delta t_D)$
<i>MPE</i> ($\Delta t, \Delta t_D$)/ <i>MKE</i> ($\Delta t, \Delta t_D$)	$e_{index} = B + \varepsilon_{index}(\Delta t, \Delta t_D)$
<i>RPE</i> ($\Delta t, \Delta t_D$)/ <i>RKE</i> ($\Delta t, \Delta t_D$)	$e_{index} = \varepsilon_{index}(\Delta t, \Delta t_D)$
<i>PDE</i> ($\Delta t, \Delta t_s, \Delta t_D$)/ <i>KDE</i> ($\Delta t, \Delta t_s, \Delta t_D$)	$e_{index} = \varepsilon_{index}(\Delta t, \Delta t_s, \Delta t_D)$
<i>PRE</i> ($\Delta t, \Delta t_s$)/ <i>KRE</i> ($\Delta t, \Delta t_s$)	$e_{index} = \varepsilon_{index}(\Delta t, \Delta t_s)$
e_{index}	<i>max. error per index complying with P_c</i>
Δt_s	<i>stability time</i>
Δt	<i>window time</i>
Δt_D	<i>drift re-set time</i>

Here, each contributor is already evaluated individually with respect to the level of confidence (confidence factor n_p for the SSM) of the associated requirement, i.e. according to “ $|\mu_{sum}| + n_p \cdot \sigma_{sum}$ ”.



This leads to a more conservative result compared to statistically adding both contributions first and then applying the confidence factor to the common result. While having intermediate evaluated results for B and ε_{index} is considered useful e.g. for budget driver identification, there is no obvious need for maintaining this conservatism in the overall error compilation. As further the statistical interpretation ensures that both time-constant and time-random contributions are expressed in the same domain (i.e. temporal or ensemble behaviour) and thus a statistical summation is “physically” correct, the summation rule in Table 6-7 is proposed for the PEEH update:

Table 6-7: Proposed rule for total error compilation

Total Pointing Error per Index	
<i>index</i>	<i>compilation</i>
<i>APE</i> / <i>AKE</i>	$e_{index} = \mu_B + \mu_{index} + n_p \sigma_{B+index,sum}$
<i>MPE</i> (Δt)/ <i>MKE</i> (Δt)	$e_{index} = \mu_B + \mu_{index}(\Delta t) + n_p \sigma_{B+index,sum}(\Delta t)$
<i>RPE</i> (Δt)/ <i>RKE</i> (Δt)	$e_{index} = \varepsilon_{index}(\Delta t, \Delta t_D)$
<i>PDE</i> ($\Delta t, \Delta t_s$)/ <i>KDE</i> ($\Delta t, \Delta t_s$)	$e_{index} = \varepsilon_{index}(\Delta t, \Delta t_s, \Delta t_D)$
<i>PRE</i> ($\Delta t, \Delta t_s$)/ <i>KRE</i> ($\Delta t, \Delta t_s$)	$e_{index} = \varepsilon_{index}(\Delta t, \Delta t_s)$

The overall standard deviation $\sigma_{B+index,sum}$ is then computed according to the equation below, i.e. summing all uncorrelated standard deviation quadratically and all correlated ones linearly – no matter if they refer to time-constant or time-random contributions:

$$\sigma_{B+index,sum}^2 = \sum_{i=1}^{N_{B,nc}} \sigma_{B,nc,i}^2 + \sum_{i=1}^{N_{index,nc}} \sigma_{index,nc,i}^2 + \left[\sum_{i=1}^{N_{B,c}} \sigma_{B,c,i} + \sum_{i=1}^{N_{index,c}} \sigma_{index,c,i} \right]^2$$

Correlation between these contributors can exist in case of ensemble or mixed interpretation, while for temporal interpretation the time-constant contributions always reduce to discrete values.

The reason why the absolute value of the time-constant mean $|\mu_B|$ and the absolute value of the time-random mean $|\mu_{index}|$ are summed in Table 6-7 – rather than the absolute value of the sum $|\mu_B + \mu_{index}|$ is the following: in the ECSS tables for approximate ([AD1], Appendix B) which are usually applied to extract the relevant statistical moments for a given error index, all time-random contributors (periodic, drift and



uniform/Gaussian random errors) already consider the “positive” direction of the error in the mean values while the bias errors can result in a signed contribution.

- Having two different rules for computing the standard deviation of the sum of correlated error contributions with the simplified method is expected to be more confusing than helpful. Consequently, the alternative second upper bound summation rule (Eq. (*2) in Table 11-2 of [AD2] with derivation in E.2) is removed from the tables of time-constant and time-random contributions and only the expression which is also used in the ECSS standard is kept.
- This expression is further in line with those provided in the extended and new chapters for statistical properties and the derivation based on correlation coefficients (see bullets in 6.2.1.3).
- Notes on the application of the generalized domain for all steps (time-constant, time-random and total error compilation) were added – which follows the same summation rules, but to repeated individually for each domain.

Chapter “Advanced Method”

This subchapter was complemented by providing the basic computation rules for the level of confidence evaluation on PDF level for completeness. Further, the relevant equations for the combination of errors from different domains using the generalized domain concept (see chapter 5.3.1.3.2) are introduced.

In addition, the chapter introduces the procedure and additional step to be applied for temporal statistical interpretation based on simulation results concerning the determination of the worst-case temporal realization – which is determined by applying the associated confidence level over time first to each temporal realization and then selecting the worst-case (rather than applying the level of confidence to the realization with the overall worst-case value only).

Chapter “Comparison of methods”

This new chapter was introduced to give a general overview about the benefits and drawbacks of the simplified and advanced statistical method. Further, specific limitations and situations where special care needs to be taken when applying the simplified method are highlighted and illustrated (e.g. cases of dominant non-Gaussian contributions, LoS error determination).

6.2.2 Annexes

6.2.2.1 Annex A “Pointing scene”

This annex was removed as the relevant information has been introduced in chapter 4 in a more general form.

6.2.2.2 Annex “Approximate inputs to an error budget”

This annex was introduced to mainly recall the respective Annex B of the ECSS-E-ST-60-10C on approximate inputs to an error budget. It explicates the general tables in sections for time-constant and time-random error description for specific error source classes and extends them to account for both the statistical interpretation and the pointing error index



associated to a requirement – including necessary assumptions in that respect. Further it includes a clear decomposition of time-random variables in their time-constant and time-random contributions and additional clarifications to the information provided in ECCS-ST-60-10C.

Table 6-8: Complemented budget contributions for uniform random errors

Index	S.I.	Distribution			Notes
		p(e)	μ(e)	σ(e)	
APE	E	p(C)	μ _C	σ _C	For p(C), μ _C and σ _C see Table 6.1
	T	U(0,C _{WC})	$\frac{1}{2} C_{WC}$	$\frac{1}{\sqrt{12}} C_{WC}$	U(e _{min} ,e _{max})=uniform in range e _{min} to e _{max} . C _{WC} =worst case C
	M	$\int U(0,C)p(C)dC$	$\frac{1}{2} \mu_C$	see A.7	For p(C), μ _C see Table 6.1. For derivation see A.7
MPE	E	p($\frac{1}{2}C$)=2p(C)	$\frac{1}{2} \mu_C$	$\frac{1}{2} \sigma_C$	For p(C), μ _C and σ _C see Table 6.1
	T	$\delta(\frac{1}{2} C_{WC})$	$\frac{1}{2} C_{WC}$	0	C _{WC} =worst case C
	M	p($\frac{1}{2}C$) = 2p(C)	$\frac{1}{2} \mu_C$	$\frac{1}{2} \sigma_C$	For p(C), μ _C and σ see Table 6.1. For derivation see A.7
RPE	E	p($\frac{1}{2}C$)=2p(C)	$\frac{1}{2} \mu_C$	$\frac{1}{2} \sigma_C$	For p(C), μ _C and σ _C see Table 6.1
	T	U(- $\frac{1}{2}C_{WC}$, $\frac{1}{2}C_{WC}$)	0	$\frac{1}{\sqrt{12}} C_{WC}$	U(x _{min} ,x _{max})=uniform in range x _{min} to x _{max} . C _{WC} =worst case C
	M	$\int U(-\frac{1}{2}C,\frac{1}{2}C)p(C)dC$	0	$\frac{1}{\sqrt{12}} \psi_C$	For p(C), μ _C see B.6. For derivation and ψ _C see B.7
PDE	All	No contribution			Short timescale, and assume mean value does not change over time
PRE	All				
WPD	All	No contribution			Short timescale and assume no linear slope over time
WPR	All	As for RPE			Short timescale; mean value does not change over time

Table 6-9: Separation of uniform random errors into time-constant/-random contributions

Index	S.I.	U(a, p(b))*		U(-p(c),p(c))	
		p(e) of CRV	p(e) of RV	p(e) of CRV	p(e) of RV
APE	E	$\frac{a + p(b)}{2}$	$\frac{p(b) - a}{2}$	δ(0)	p(c)
	T	$\frac{a + \delta(b_{WC})}{2}$	$U\left(-\frac{b_{WC} - a}{2}, \frac{b_{WC} - a}{2}\right)$	δ(0)	U(-c,c)



	M	$\frac{a+p(b)}{2}$	$\int U(-x,x)p(x)dx$ $x = \frac{b-a}{2}$	$\delta(0)$	$\int U(-c,c)p(c)dc$
MPE	E	$\frac{a+p(b)}{2}$	$\delta(0)$	$\delta(0)$	$\delta(0)$
	T	$\frac{a+\delta(b_{wc})}{2}$	$\delta(0)$	$\delta(0)$	$\delta(0)$
	M	$\frac{a+p(b)}{2}$	$\delta(0)$	$\delta(0)$	$\delta(0)$
RPE	E	$\delta(0)$	$\frac{p(b)-a}{2}$	$\delta(0)$	$p(c)$
	T	$\delta(0)$	$U\left(-\frac{b_{wc}-a}{2}, \frac{b_{wc}-a}{2}\right)$	$\delta(0)$	$U(-c,c)$
	M	$\delta(0)$	$\int U(-x,x)p(x)dx$ $x = \frac{b-a}{2}$	$\delta(0)$	$\int U(-c,c)p(c)dc$
WPD	All	No contribution			
WPR	All	As for RPE			

6.2.2.3 Annex B “Pointing error description using different statistical interpretation”

The simplified satellite pointing example is maintained and complemented with notes on the generalized concept. Further a link to the more detailed “PointingSat” application example on the ESA PEET website is provided.

6.2.2.4 Annex D “Notes on pointing error metrics”

This annex is mainly kept as it is, apart from a introducing in addition the relation between Allan variance and of the windowed mean stability variance (including the derivation of this relation). Further a missing factor in the WMS weighting filter expression is corrected.

6.2.2.5 Annex E “Notes on summation rules”

This annex is considered obsolete as it includes the derivation of alternative upper bound expression for standard deviation the sum of correlated random variable which was removed from the AST-4 tables (see chapter 6.2.1.9).

6.2.2.6 Annex “Monte Carlo – Application Guidelines”

This new annex provides guidelines to justify that the data generated by a Monte Carlo simulation campaign is meaningful. These guidelines address the following questions:

- How to sample the parameter space of a simulation model?



- How to obtain representative pointing error data in a single simulation run?
- How many simulation runs are required in a Monte Carlo simulation campaign to obtain representative statistics of the pointing error, or in general terms the performance quantity of interest?



7 Study Cases

One of the main objectives of the study was to improve PEET not only from a general perspective, but with a specific focus of its application to telecommunication missions.

For that purpose, at least 3 missions from at least 2 ESA telecommunications primes shall be selected with at least one “typical” and at least one “high accuracy” mission type.

Further, such candidates shall be missions with high interest to ESA and industry in terms of pointing requirements, pointing challenges and pointing error engineering process as well as computations. All telecommunication mission primes in Europe (Airbus Defence and Space, OHB Systems AG and Thales Alenia Space) were asked to propose reference case candidates and the study team provided document templates with guidelines for requested information.

It is highly appreciated by the study team that in the end all 3 primes agreed to support the study as consultants although only marginal budget could be provided. 4 different missions could be selected as reference case studies which are summarized in the following subsections.

Two main goals were targeted by the case studies, namely to:

- Identify application specific pointing error engineering needs for telecommunication missions which were not yet covered by the existing version of PEET and also by the PEEH
- Compare budget results and methods from heritage approaches to those following the PEEH methodology and using the (updated) PEET version as analysis tool.

The first topic led to several additional features available in the tool update. Apart from general needs and suggestions for improvement, specific needs for telecommunication applications were mainly addressed by the newly introduced analysis features which are described in section 5.2.2.3.

The results of the second topic are presented and summarized in the respective subchapter individually for each case study, complemented by a comparison of results to in-flight data where available.

Note: Actual numerical results could not be disclosed to anyone but ESA in all cases. Consequently, in the following subsections of the study case analysis, not all values might be displayed or those displayed may represent ‘normalized’ or artificial values only - however in a reasonable order of magnitude in the latter case.

7.1 SmallGEO (OHB)

The SmallGEO platform development has been started end of the last decade targeting a niche in the telecommunication satellite market for a payload mass of up to 300kg and a payload power of up to 3kW. A first mission realization was signed in 2009 with Hispasat s.a. which led after an intense design, development and finally a tedious protoflight verification phase to the satellite Hispasat 36W1 being launched on January 27th 2017 into geostationary transfer orbit (GTO). The satellite was in the following days successfully transferred to its in-orbit test slot on the geostationary (GEO) arc.

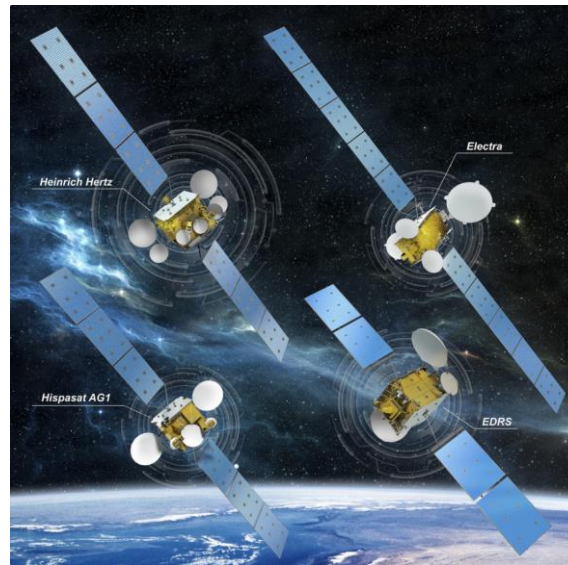


Figure 7-1: Small GEO Product Line Overview [RD18]

The platform is designed to serve various telecom mission needs mainly of the broadcast type, but can also accommodate spot beam applications or even laser links (e.g. EDRS-C satellite). The SmallGEO platform has also been adapted for scientific weather forecast measurements as part of the Meteosat Third Generation satellites, but these needed a high end AOCS system and are not discussed in this document as they are not telecom satellites. The telecom SmallGEO product line is depicted in Figure 7-1.

The design goal of the SmallGEO platform in terms of pointing is to suffice standard telecom applications and to allow various types of transfers to geostationary orbit (GTO, SSTO with electric or chemical propulsion). Pointing requirements are thus important throughout the mission, starting from standard robust sun pointing requirements for sun acquisition and safe modes through more stringent pointing requirements during transfer orbit (depending also on the type of propulsion system used) and ending up with the most stringent on-station pointing requirements ensuring full payload capability. Most of the requirements are to be fulfilled permanently during the respective mission phase, but transients can also be of relevance such as after ignition of the main engine for chemical propulsion transfers.

The typical AOCS architecture used to fulfil the above-described pointing requirements is the following:

Table 7-1: Typical AOCS architecture for Telecom Missions

Mode:	Sun Pointing	Transfer	On-station
Sensors:			
Sun Sensors	X		
Star Trackers		X	X
Gyros	X	X	(X)
GNSS Receiver		(X)	(X)
Actuators:			



Reaction Wheels	(X)	X	X
Thrusters (EP, CP, Cold Gas)	(X)	X	X

As can be seen in the table above, a variety of sensors and actuators is used on the SmallGEO platform. It is however to be said that depending on the mission (chemical transfer, electrical transfer, high pointing knowledge stability for laser communication terminal,...), the actual embarked set of AOCS sensors and actuators differs and is usually a subset of the above.

The pointing reference is given either by a specific orientation of the satellite body with respect to the sun in safe mode, by time-varying attitude profiles in transfer mode or by an earth pointing estimation based on on-board orbit propagation or GNSS receiver data.

The mission proposed for this study is a typical telecom mission with one or more broadcast antennas. The mission phase of prime interest regarding pointing requirements is the on-station phase, meaning the operational phase on the geostationary arc including regular station keeping manoeuvres.

7.1.1 Motivation

OHB System AG is one of the 3 major telecom platform providers and has been working on pointing error engineering in the frame of several telecom missions mainly under ESA contracts (SmallGEO platform under Artes 11, Electra platform under Artes 33, as well as the EDRS-C satellite for which ESA is the end customer). The first mission Hispasat 36W-1 is fully operational since more than one year and OHB has been able to gather a large amount of in-orbit data from both LEOP and on-station operation.

OHB is currently using a pointing error engineering based on the PEEH as described in the previous chapters and is currently also employing PEET on some non-telecom satellites requiring more demanding pointing capabilities. Therefore, a good knowledge of the tool is available at OHB, also because OHB has iterated strongly with Astos on the available PEET functionalities and needed bug-fixing.

OHB has thus both experience in the engineering and design of telecom satellites as well as knowledge of the PEET tool. Paired with the available in-orbit experience from the first flying SmallGEO platform, it is deemed that the OHB platform is an ideal candidate for selection.

7.1.2 Pointing Requirements

The pointing requirements for the SmallGEO platforms employed for the telecom missions are usually expressed as APE for the RF boresight in satellite frame. They are depending on the development or mission contract either directly specified to the satellite or are derived by OHB in order to fulfil a certain coverage area on the earth with a certain RF power density.

The APE error index is used as only requirement for the platform/antenna design, as it is the goal to ensure a continuous signal broadcasting with the same quality over the whole mission duration, which includes the regular station keeping manoeuvres.

The APE (half-cone) requirement has been exemplarily set to 0,12 deg (3σ) in this study and mixed statistical interpretation is applied. The same value also applies to the yaw component



The mission requirements further asked for computation of the RPE over 24h and over 12 months, but there was no explicit requirement set forth for it. OHB in turn however specified a RPE over 24h (0.06 deg half-cone, 3σ , mixed SI), 12 months (0.08 deg half-cone, 3σ) and lifetime to the payload supplier, which in turn also indirectly applied to the satellite. The daily/yearly RPE budgets are also included.

For some specific applications, such as the laser communication terminal on EDRS, it is of course necessary to look at further pointing performance indices besides the APE, as the operation of the terminal requires different accuracies, especially in terms of attitude knowledge over the timespan of laser link establishment.

The main challenges regarding the pointing requirements is the breakdown from system level to the different subsystems in order to ensure a well balanced satellite design. Therefore, a profound understanding of the payload operation is necessary and a good knowledge of heritage or reference missions is mandatory in order not to overdesign but also to identify design weaknesses in different subsystems.

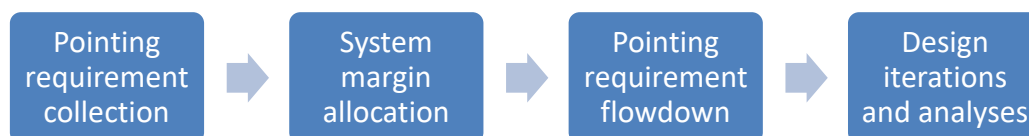
It is also important to understand whether the system pointing requirement is expressed per axis or as cone deviation from the nominal RF boresight together with a yaw error requirement. The latter is normally the case in OHB's heritage pointing requirements.

7.1.3 Heritage Approach

The pointing error engineering approach for the OHB telecom satellites is consisting of the following steps:

- 1) Collection of relevant pointing requirements from customer specifications or internal design goals (for instance in platform development phases where no specific customer payload is selected)
- 2) Selection of system margin depending on the development phase (usually between 5 and 20%)
- 3) Flow-down of pointing requirements to the different subsystems or disciplines. These typically include AOCS, Structure/Thermoelastic, Payload, OBDH, AIT/Alignment. The pointing requirements. The attribution of the allowed pointing errors is based on a preliminary satellite architecture and preliminary analyses if available. OHB heritage also plays an important role in this step, as in early phases typically analyses from telecom satellite heritage or similar satellites are taken into account or even flight results if available for the corresponding contributors.
- 4) A re-iteration of the pointing budget allocation can take place in the later design phases (PDR/CDR) in case some problems to fulfil the requirements without substantial re-design are identified in one contributor whereas sufficient margin exists in another contributor or the system margin may be reduced due to the advanced project phase.
- 5) Finally, along the course of the project, the pointing error document is maintained including the results from the analyses or tests.

The approach is visually shown below:





The pointing error sources are obtained mainly by analyses at different levels: AOCS pointing analyses, satellite thermoelastic distortion analyses, payload internal analyses. These parts are usually final at system CDR and not modified thereafter as they are not subject to any further verification by test. But for some parts, such as the clock drift, the GNSS receiver accuracy or the alignment, further knowledge is gathered via specific testing or measurements and is then included in the final pointing analysis document.

The pointing budget for the telecom satellites is computed at OHB using Excel as main tool for gathering and combining the different pointing error sources. The sources are different analyses or test reports or sometimes similarity assessments. If further computation is needed to translate a unit or subsystem error (e.g. from thermoelastic distortion) into a system error, this can be done in the available Excel tables or by the use of specific tools (e.g. translating a structural distortion into a RF-boresight pointing error).

7.1.4 Pointing Budgets

The OHB pointing budgets contain typically 20 to 30 different lines of contributors. This includes however less PES, as for instance the thermoelastic effects or payload contributions appear in the bias, seasonal and daily frequency categories.

It is also to be noted that this system level pointing budget includes some PECs, which are actually already a combination of a variety of lower-level PECs. For instance, the AOCS short-term effects include star tracker noise equivalent angle, friction jumps, thruster transients, etc.

7.1.4.1 Heritage PES Tables

In the following, the pointing error sources are presented as defined and categorized in the SmallGEO pointing budget.

Table 7-2: Heritage Budget Error Sources

Pointing Budget: Broadcast Antenna		
		Time scale
	PES	
Group A (Bias)		
Structure	TED structure	Bias
Structure	TED payload interconnecting structure	Bias
Structure	Desorption	Bias
Structure	Gravity Release	Bias
Payload	Payload internal bias	Bias
AOCS	STS internal bias	Bias
AOCS	STS BRF-ARF	Bias
AIT	Alignment Accuracy payload	Bias
AIT	Alignment measurement accuracy payload	Bias
AIT	Alignment measurement accuracy STS	Bias
Group B (Seasonal & Long-term)		



Structure	TED structure	Periodic
Structure	TED payload interconnecting structure	Periodic
Payload	TED payload internal	Periodic
Group C (Daily)		
Structure	TED structure	Periodic
Structure	TED payload interconnecting structure	Periodic
Payload	TED payload internal	Periodic
AOCS	STS LSFE	Periodic
AOCS	Orbit Propagator	Periodic
Group D (Fast)		
AOCS	Attitude Performance	Noise
Total per axis		
Total Half Cone		
APE Requirement (Half Cone / Yaw)		

7.1.4.2 Heritage Budget

The pointing error sources are classified in 4 groups describing their temporal behaviour: the first (A) contains the time constant error sources and the remaining 3 contain time random error sources with different characteristic durations (seasonal and long-term (B), periodic over a day (C), short term (D)).

The deviation of each group is the square root of the sum of the squared individual deviations. The total deviation is the linear sum of the deviations of each group. This is as laid out in the general description chapter 6.

$$\Delta_{tot} = \sqrt{\sum_{i_A} \Delta_{i_A}^2} + \sqrt{\sum_{i_B} \Delta_{i_B}^2} + \sqrt{\sum_{i_C} \Delta_{i_C}^2} + \sqrt{\sum_{i_D} \Delta_{i_D}^2}$$

Based on the PEEH, the summation above can be interpreted as (considering the APE index):

- Such summation of deviations is valid under the assumption of the central limit theorem, (i.e. all error sources are approximated with Gaussian distributions).
- In the PEEH, the total error is the sum of the time-constant error and the time-random error. Similarly, the OHB-heritage approach extends the time random errors in three groups that are linearly added with the time constant error. This is generally more conservative as it corresponds to an 'individual' level of confidence evaluation for each of the time-random error classes (B,C,D) while the current PEEH applies a 'common' level of confidence value to all time-random contributors.
- The quadratic summation of the variances within each group is justified under the assumption that the error sources are uncorrelated. In general, a certain degree of (temporal) correlation can be expected for certain contributors such as TED effects (at same frequency), but even in this case, the same maxima do not necessarily show up at the same time over the day/year, etc. which is why in the heritage approach an uncorrelated summation was chosen rather than a fully correlated linear summation.



7.1.4.3 PES Characterization

Table 7-4 to Table 7-3 show the justification, classification and properties of the PES used for the SmallGEO platform – in line with the PEEH and PEET input specifications:

Table 7-3: Justification of Pointing Error Sources

Definition of PES				Justification of PES
Subsystem	Unit	PES	Name	Origin
AOCs	Star trackers	STS ARF to BRf alignment knowledge	AOCs_STs_ALIG	STS alignment frame to STS measurement frame transfer matrix uncertainty
		STS internal bias	AOCs_STs_BIAS	ARF to BRf bias due to on-ground handling, launch loads, gravity release, temperature shift between calibration temperature and on-orbit operating temperature
		STS LSFE	AOCs_STs_LSFE	STS LSFE
	OOP	Propagation	AOCs_OOP_PROP	On-board Orbit Propagator induced attitude error
		Time Error	AOCs_OOP_TIME	Clock drift
	Attitude Performance	AOCs Slow contributions	AOCs_AP_SLOW	Typical slow AOCs errors including e.g. thruster plumes and torques
AOCs Fast contributions		AOCs_AP_FAST	Typical AOCs closed-loop errors including STS HSFE and TE, RW friction jumps etc	
Payload	Broadcast Antenna	Constant	PL_ANT_BIAS	Payload Biases (TED, gravity release, desorption, ...)
		Orbital	PL_ANT_ORB	Payload Orbital effects (mainly TED)
		Seasonal	PL_ANT_SEAS	Payload Seasonal effects (mainly TED)
AIT	Alignments	Payload alignment wrt platform ref.cube	AIT_ALA_PL	PL-PF alignment performance
		Payload alignment knowledge wrt ref. cube	AIT_ALM_PL	PL-PF alignment knowledge
		STS alignment knowledge wrt ref. cube	AIT_ALM_STS	STS-PF alignment knowledge
STRUCTURE	Others	Desorption	STR_OTH_DES	Orbital desorption
		Gravity release	STR_OTH_0G	Gravity release
	Thermo-elastic	Constant	STR_TED_BIAS	Mean value variation
		Orbital	STR_TED_ORB	Orbital variation
		Seasonal	STR_TED_SEAS	Seasonal variation

Table 7-4: Classification of Pointing Error Sources

Definition of PES				Description of PES					
Subsystem	Unit	PES	Name	Time-random	Ensemble-random (= time-constant)	Class	On interface	Type	
AOCs	Star trackers	STS ARF to BRf alignment knowledge	AOCs_STs_ALIG		X	bias	no	variable	
		STS internal bias	AOCs_STs_BIAS		X	bias	no	variable	
		STS LSFE	AOCs_STs_LSFE	X		random	no	process	
	OOP	Propagation	AOCs_OOP_PROP	X		drift	no	variable	
		Time Error	AOCs_OOP_TIME	X		drift	no	variable	
	Attitude Performance	AOCs Slow contributions	AOCs_AP_SLOW	X		random	no	variable	
AOCs Fast contributions		AOCs_AP_FAST	X		random	no	process		
Payload	Broadcast Antenna	Constant	PL_ANT_BIAS		X	bias	no	variable	
		Orbital	PL_ANT_ORB	X		periodic	no	process	
		Seasonal	PL_ANT_SEAS	X		periodic	no	process	
AIT	Alignments	Payload alignment wrt platform ref.cube	AIT_ALA_PL		X	bias	no	variable	
		Payload alignment knowledge wrt ref. cube	AIT_ALM_PL		X	bias	no	variable	
		STS alignment knowledge wrt ref. cube	AIT_ALM_STS		X	bias	no	variable	
STRUCTURE	Others	Desorption	STR_OTH_DES		X	bias	no	variable	
		Gravity release	STR_OTH_0G		X	bias	no	variable	
	Thermo-elastic	Constant	STR_TED_BIAS			X	bias	no	variable
		Orbital	STR_TED_ORB	X		periodic	no	process	
		Seasonal	STR_TED_SEAS	X		periodic	no	process	



Table 7-5: Properties of Pointing Error Sources

Definition of PES				Description of PES						
Subsystem	Unit	PES	Name	Distribution	Time-Random			Ensemble-Random		
					Frequency [rad/s] with $f = 1/T$ or f_{nyqu} or Time [s]				Origin	random process data type
					x	y	z			
AOCS	Star trackers	STS ARF to BRF alignment knowledge	AOCS_STS_ALIG						Gaussian	
		STS internal bias	AOCS_STS_BIAS						uniform	
		STS LSFE	AOCS_STS_LSFE							
	OOP	Propagation	AOCS_OOP_PROP	drift specific PDF					T= 7 days	discrete
		Time Error	AOCS_OOP_TIME	drift specific PDF					T= 7 days	discrete
	Attitude Performance	AOCS Slow contributions	AOCS_AP_SLOW	Gaussian (discrete std)						
AOCS Fast contributions		AOCS_AP_FAST							BLWN	
Payload	Broadcast Antenna	Constant	PL_ANT_BIAS							uniform
		Orbital	PL_ANT_ORB	bimodal (discrete amplitude)					T = 1 day	
		Seasonal	PL_ANT_SEAS	bimodal (discrete amplitude)					T = 1 year	
AIT	Alignments	Payload alignment wrt platform ref.cube	AIT_ALA_PL							uniform
		Payload alignment knowledge wrt ref.cu	AIT_ALM_PL							truncated Gaussian
STRUCTURE	Others	STS alignment knowledge wrt ref.cube	AIT_ALM_STS							truncated Gaussian
		Description	STR_OTH_DES							uniform
		Gravity release	STR_OTH_DG							uniform
		Constant	STR_TED_BIAS							uniform
		Orbital	STR_TED_ORB	bimodal (discrete amplitude)					T = 1 day	
Thermo-elastic	Seasonal		STR_TED_SEAS	bimodal (discrete amplitude)					T = 1 year	

7.1.4.4 PEET Model and Budget

As a first step, the SmallGEO budget was implemented in PEET using the PES definitions from the characterization performed during the workshop.

The deviations provided in the heritage budget are specified as 3-sigma, and in the case of uniform distributions, understood as min/max boundaries. Therefore, the min/max values of the uniform distributions implemented in the PEET model are chosen to be the 3σ deviations in the original budget.

An APE scenario was defined with both temporal and ensemble domains as statistical (advanced method) with a level of confidence of 99.7%.

RPE was analysed in normal mode for both 1 day and 1 year window times. The RPE over lifetime does not differ from the 1 year RPE, since there are no contributors in this example that act over a time window longer than one year (OOP drifts have a reset time of 1 week and seasonal effects are defined with a 1-year period).

For comparison, a similar APE scenario was defined with the simplified method (which is similar to the OHB heritage approach).

The PES models in PEET are parameterized based on the values in the heritage budget as follows (as all values are already 3-Sigma values for the different contributors, the aim is to achieve corresponding 3-Sigma results for each individual source):

- Time-constant uniform distributions directly use the respective tables values as (symmetric) bound
- Time-constant Gaussian distributions use the table values divided by 3 as standard deviation and zero mean
- PSD (BLWN) models are realized such that the standard deviation also corresponds to the table value divided by 3 (plus an equivalent scaling according to the modelled bandwidth)
- Periodic signal amplitudes are derived from the relation $\sigma^2=A^2/2$ (again using one third of the table values as standard deviation)

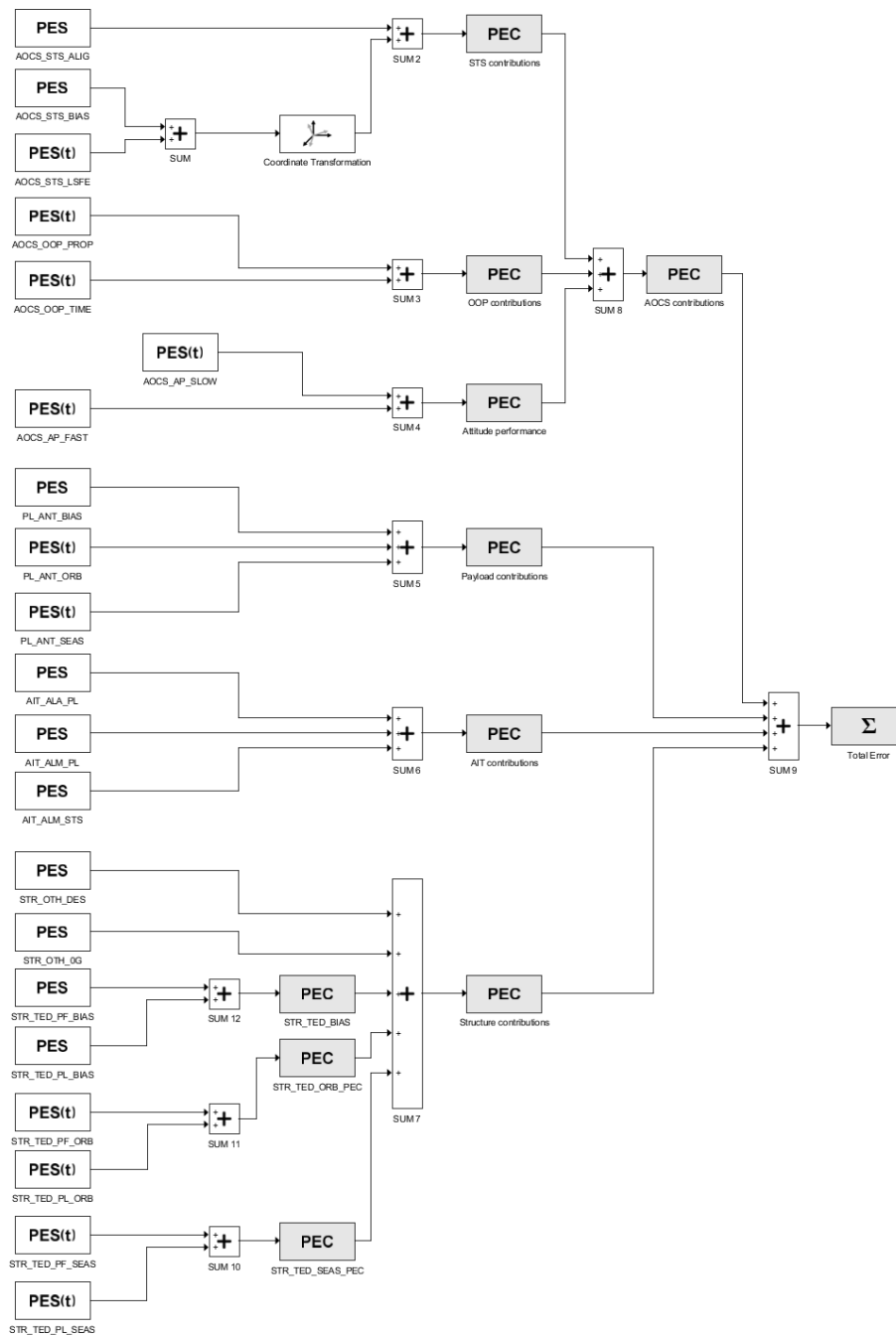


Figure 7-2: PEET implementation of the original SmallGEO budget

The PEET results for normal mode RPE (daily, yearly) and APE and SK mode APE are listed below. No specific ensemble domains are introduced in the PEET model to reflect the frequency classes of the heritage budget. This generally leads to a less conservative summation of the contributions from the different classes ('statistical' summation rather



than linear summation over the different classes. To assess the impact of a more detailed modelling with PEET alone (i.e. using non-Gaussian distributions and frequency-domain models) and the additional step of PDF-based evaluation, results have been computed using both the advanced and simplified statistical method.

Table 7-6: Normal mode APE advanced method

PEC Name	Level	Output Unit	Domain	Value Type	Time Constant Error				Time Random Error				Total Error			
					x	y	z	LOS	x	y	z	LOS	x	y	z	LOS
Total Error	0	°	overall	Budget	0.05527	0.0556	0.05553	0.06531	0.04721	0.04757	0.04731	0.06586	0.07945	0.0796	0.0793	0.1018
				Requirement ID												0.12
AIT contributions	1	°	overall	Budget	0.01617	0.01618	0.0162	0.02099					0.01617	0.01618	0.0162	0.02099
				Requirement ID												
AOCS contributions	1	°	overall	Budget	0.01765	0.01801	0.01765	0.02419	0.02132	0.02177	0.02138	0.028	0.03524	0.03597	0.03526	0.04782
				Requirement ID												
Payload contributions	1	°	overall	Budget	0.01994	0.01994	0.01994	0.02719	0.01642	0.01642	0.01642	0.02322	0.03401	0.03408	0.03401	0.04378
				Requirement ID												
Structure contributions	1	°	overall	Budget	0.01984	0.01982	0.01979	0.02305	0.01642	0.01642	0.01642	0.02322	0.03033	0.03035	0.03032	0.03734
				Requirement ID												
Attitude performance	2	°	overall	Budget					0.009895	0.009881	0.009924	0.01136	0.009895	0.009881	0.009924	0.01136
				Requirement ID												
OOP contributions	2	°	overall	Budget	0.01452	0.01488	0.01452	0.02079	0.01653	0.01694	0.01653	0.02367	0.03098	0.03175	0.03098	0.04436
				Requirement ID												
STR_TED_BIAS	2	°	overall	Budget	0.01422	0.01421	0.01422	0.01762					0.01422	0.01421	0.01422	0.01762
				Requirement ID												
STR_TED_ORB_PEC	2	°	overall	Budget	0	0	0	0	0.007069	0.007069	0.007069	0.009998	0.007069	0.007069	0.007069	0.009998
				Requirement ID												
STR_TED_SEAS_PEC	2	°	overall	Budget	0	0	0	0	0.009429	0.009429	0.009429	0.01333	0.009429	0.009429	0.009429	0.01333
				Requirement ID												
STS contributions	2	°	overall	Budget	0.003317	0.003318	0.003313	0.003905	0.002972	0.002968	0.002966	0.003418	0.004631	0.004641	0.00465	0.005362
				Requirement ID												

Table 7-7 Normal mode RPE advanced method (daily)

PEC Name	Level	Output Unit	Domain	Value Type	Time Constant Error				Time Random Error				Total Error			
					x	y	z	LOS	x	y	z	LOS	x	y	z	LOS
Total Error	0	°	overall	Budget	0	0	0	0	0.0314	0.03172	0.03148	0.04345	0.0314	0.03172	0.03148	0.04345
				Requirement ID												
AIT contributions	1	°	overall	Budget	0	0	0	0					0	0	0	0
				Requirement ID												
AOCS contributions	1	°	overall	Budget	0	0	0	0	0.01858	0.019	0.0186	0.02477	0.01858	0.019	0.0186	0.02477
				Requirement ID												
Payload contributions	1	°	overall	Budget	0	0	0	0	0.009459	0.009459	0.009459	0.01338	0.009459	0.009459	0.009459	0.01338
				Requirement ID												
Structure contributions	1	°	overall	Budget	0	0	0	0	0.007111	0.007111	0.007111	0.01006	0.007111	0.007111	0.007111	0.01006
				Requirement ID												
Attitude performance	2	°	overall	Budget					0.009895	0.009881	0.009924	0.01136	0.009895	0.009881	0.009924	0.01136
				Requirement ID												
OOP contributions	2	°	overall	Budget	0	0	0	0	0.01452	0.01488	0.01452	0.0208	0.01452	0.01488	0.01452	0.0208
				Requirement ID												
STR_TED_BIAS	2	°	overall	Budget	0	0	0	0					0	0	0	0
				Requirement ID												
STR_TED_ORB_PEC	2	°	overall	Budget	0	0	0	0	0.007069	0.007069	0.007069	0.009998	0.007069	0.007069	0.007069	0.009998
				Requirement ID												
STR_TED_SEAS_PEC	2	°	overall	Budget	0	0	0	0	0.00004684	0.00004684	0.00004684	0.00006624	0.00004684	0.00004684	0.00004684	0.00006624
				Requirement ID												
STS contributions	2	°	overall	Budget	0	0	0	0	0.002972	0.002968	0.002966	0.003418	0.002972	0.002966	0.002966	0.003418
				Requirement ID												



Table 7-8 Normal mode RPE advanced method (yearly)

PEC Name	Level	Output Unit	Domain	Value Type	Time Constant Error				Time Random Error				Total Error			
					x	y	z	LOS	x	y	z	LOS	x	y	z	LOS
Total Error	0	°	overall	Budget	0	0	0	0	0.04721	0.04757	0.04731	0.06586	0.04721	0.04757	0.04731	0.06586
				Requirement ID												
AIT contributions	1	°	overall	Budget	0	0	0	0					0	0	0	0
				Requirement ID												
AOCS contributions	1	°	overall	Budget	0	0	0	0	0.02132	0.02177	0.02138	0.028	0.02132	0.02177	0.02138	0.028
				Requirement ID												
Payload contributions	1	°	overall	Budget	0	0	0	0	0.01642	0.01642	0.01642	0.02322	0.01642	0.01642	0.01642	0.02322
				Requirement ID												
Structure contributions	1	°	overall	Budget	0	0	0	0	0.01642	0.01642	0.01642	0.02322	0.01642	0.01642	0.01642	0.02322
				Requirement ID												
Attitude performance	2	°	overall	Budget					0.009895	0.009881	0.009924	0.01136	0.009895	0.009881	0.009924	0.01136
				Requirement ID												
OOP contributions	2	°	overall	Budget	0	0	0	0	0.01653	0.01694	0.01653	0.02367	0.01653	0.01694	0.01653	0.02367
				Requirement ID												
STR_TED_BIAS	2	°	overall	Budget	0	0	0	0					0	0	0	0
				Requirement ID												
STR_TED_ORB_PEC	2	°	overall	Budget	0	0	0	0	0.007069	0.007069	0.007069	0.009998	0.007069	0.007069	0.007069	0.009998
				Requirement ID												
STR_TED_SEAS_PEC	2	°	overall	Budget	0	0	0	0	0.009429	0.009429	0.009429	0.01333	0.009429	0.009429	0.009429	0.01333
				Requirement ID												
STS contributions	2	°	overall	Budget	0	0	0	0	0.002972	0.002968	0.002966	0.003418	0.002972	0.002968	0.002966	0.003418
				Requirement ID												

Table 7-9: Normal mode APE simplified method

PEC Name	Level	Output Unit	Domain	Value Type	Time Constant Error				Time Random Error				Total Error			
					x	y	z	LOS	x	y	z	LOS	x	y	z	LOS
Total Error	0	°	overall	Budget	0.04916	0.04916	0.04933	0.06964	0.07099	0.0715	0.07099	0.1008	0.08938	0.08986	0.0895	0.1288
				Requirement ID												0.12
AIT contributions	1	°	overall	Budget	0.02613	0.02613	0.02613	0.03695					0.02613	0.02613	0.02613	0.03695
				Requirement ID												
AOCS contributions	1	°	overall	Budget	0.003988	0.004005	0.004005	0.005664	0.04152	0.04239	0.04152	0.05934	0.04181	0.04268	0.04182	0.05975
				Requirement ID												
Payload contributions	1	°	overall	Budget	0.03455	0.03455	0.03472	0.04898	0.02492	0.02492	0.02492	0.03525	0.0426	0.0426	0.04274	0.06035
				Requirement ID												
Structure contributions	1	°	overall	Budget	0.02293	0.0229	0.02291	0.03239	0.02492	0.02492	0.02492	0.03525	0.03387	0.03384	0.03386	0.04787
				Requirement ID												
Attitude performance	2	°	overall	Budget					0.01	0.01002	0.01	0.01416	0.01	0.01002	0.01	0.01416
				Requirement ID												
OOP contributions	2	°	overall	Budget					0.03942	0.04034	0.03942	0.0564	0.03942	0.04034	0.03942	0.0564
				Requirement ID												
STR_TED_BIAS	2	°	overall	Budget	0.01937	0.01935	0.01935	0.02737					0.01937	0.01935	0.01935	0.02737
				Requirement ID												
STR_TED_ORB_PEC	2	°	overall	Budget					0.01501	0.01501	0.01501	0.02122	0.01501	0.01501	0.01501	0.02122
				Requirement ID												
STR_TED_SEAS_PEC	2	°	overall	Budget					0.02001	0.02001	0.02001	0.0283	0.02001	0.02001	0.02001	0.0283
				Requirement ID												
STS contributions	2	°	overall	Budget	0.003988	0.004005	0.004005	0.005664	0.003008	0.003008	0.003008	0.004254	0.004995	0.005009	0.005009	0.007084
				Requirement ID												



Table 7-10 SK mode APE advanced method

PEC Name	Level	Output Unit	Domain	Value Type	Time Constant Error				Time Random Error				Total Error				
					x	y	z	LOS	x	y	z	LOS	x	y	z	LOS	
Total Error	0	*	overall	Budget	0.05527	0.0556	0.05553	0.06531	0.05428	0.05459	0.05439	0.0721	0.08293	0.08345	0.08286	0.1052	
				Requirement													
				Requirement ID													
AIT contributions	1	*	overall	Budget	0.01617	0.01618	0.0162	0.02099					0.01617	0.01618	0.0162	0.02099	
				Requirement													
				Requirement ID													
AOCS contributions	1	*	overall	Budget	0.01765	0.01801	0.01765	0.02419	0.0328	0.03315	0.03274	0.03944	0.04536	0.0461	0.04543	0.05759	
				Requirement													
				Requirement ID													
Payload contributions	1	*	overall	Budget	0.01994	0.01994	0.01994	0.02719	0.01642	0.01642	0.01642	0.02322	0.03401	0.03408	0.03401	0.04378	
				Requirement													
				Requirement ID													
Structure contributions	1	*	overall	Budget	0.01984	0.01982	0.01979	0.02305	0.01642	0.01642	0.01642	0.02322	0.03033	0.03035	0.03032	0.03734	
				Requirement													
				Requirement ID													
Attitude performance	2	*	overall	Budget					0.02475	0.02472	0.02482	0.02842	0.02475	0.02472	0.02482	0.02842	
				Requirement													
				Requirement ID													
OOP contributions	2	*	overall	Budget	0.01452	0.01488	0.01452	0.02079	0.01653	0.01694	0.01653	0.02367	0.03098	0.03175	0.03098	0.04436	
				Requirement													
				Requirement ID													
STR_TED_BIAS	2	*	overall	Budget	0.01422	0.01421	0.01422	0.01762					0.01422	0.01421	0.01422	0.01762	
				Requirement													
				Requirement ID													
STR_TED_ORB_PEC	2	*	overall	Budget	0	0	0	0	0.007069	0.007069	0.007069	0.009998	0.007069	0.007069	0.007069	0.009998	
				Requirement													
				Requirement ID													
STR_TED_SEAS_PEC	2	*	overall	Budget	0	0	0	0	0.009429	0.009429	0.009429	0.01333	0.009429	0.009429	0.01333		
				Requirement													
				Requirement ID													
STS contributions	2	*	overall	Budget	0.003317	0.003318	0.003313	0.003905	0.002972	0.002968	0.002966	0.003418	0.004631	0.004641	0.00465	0.005362	
				Requirement													
				Requirement ID													

Table 7-11 SK mode APE simplified method

PEC Name	Level	Output Unit	Domain	Value Type	Time Constant Error				Time Random Error				Total Error			
					x	y	z	LOS	x	y	z	LOS	x	y	z	LOS
Total Error	0	*	overall	Budget	0.04916	0.04916	0.04933	0.06964	0.07549	0.076	0.07549	0.1071	0.09284	0.0933	0.09295	0.1317
				Requirement												
				Requirement ID												
AIT contributions	1	*	overall	Budget	0.02613	0.02613	0.02613	0.03695					0.02613	0.02613	0.02613	0.03695
				Requirement												
				Requirement ID												
AOCS contributions	1	*	overall	Budget	0.003988	0.004005	0.004005	0.005664	0.04986	0.05063	0.04999	0.07115	0.05009	0.05086	0.05021	0.07147
				Requirement												
				Requirement ID												
Payload contributions	1	*	overall	Budget	0.03455	0.03455	0.03472	0.04898	0.02492	0.02492	0.02492	0.03525	0.0426	0.0426	0.04274	0.06035
				Requirement												
				Requirement ID												
Structure contributions	1	*	overall	Budget	0.02293	0.0229	0.02291	0.03239	0.02492	0.02492	0.02492	0.03525	0.03387	0.03384	0.03386	0.04787
				Requirement												
				Requirement ID												
Attitude performance	2	*	overall	Budget					0.0251	0.0251	0.0251	0.03549	0.0251	0.0251	0.0251	0.03549
				Requirement												
				Requirement ID												
OOP contributions	2	*	overall	Budget					0.03942	0.04034	0.03942	0.0564	0.03942	0.04034	0.03942	0.0564
				Requirement												
				Requirement ID												
STR_TED_BIAS	2	*	overall	Budget	0.01937	0.01935	0.01935	0.02737					0.01937	0.01935	0.01935	0.02737
				Requirement												
				Requirement ID												
STR_TED_ORB_PEC	2	*	overall	Budget					0.01501	0.01501	0.01501	0.02122	0.01501	0.01501	0.01501	0.02122
				Requirement												
				Requirement ID												
STR_TED_SEAS_PEC	2	*	overall	Budget					0.02001	0.02001	0.02001	0.0283	0.02001	0.02001	0.02001	0.0283
				Requirement												
				Requirement ID												
STS contributions	2	*	overall	Budget	0.003988	0.004005	0.004005	0.005664	0.003008	0.003008	0.003008	0.004254	0.004995	0.005009	0.005009	0.007084
				Requirement												
				Requirement ID												

In a second step, further investigations were conducted by replacing the AOCS attitude performance error source with a feedback system (PID-Plant) with STS LSF as estimation noise (angular) and RW friction noise (torque) as actuator noise. Representative values for PID, Plant and RW friction were taken and very similar results were obtained.



Note that the guidance errors and environmental disturbances are currently empty and are only represented for the example.

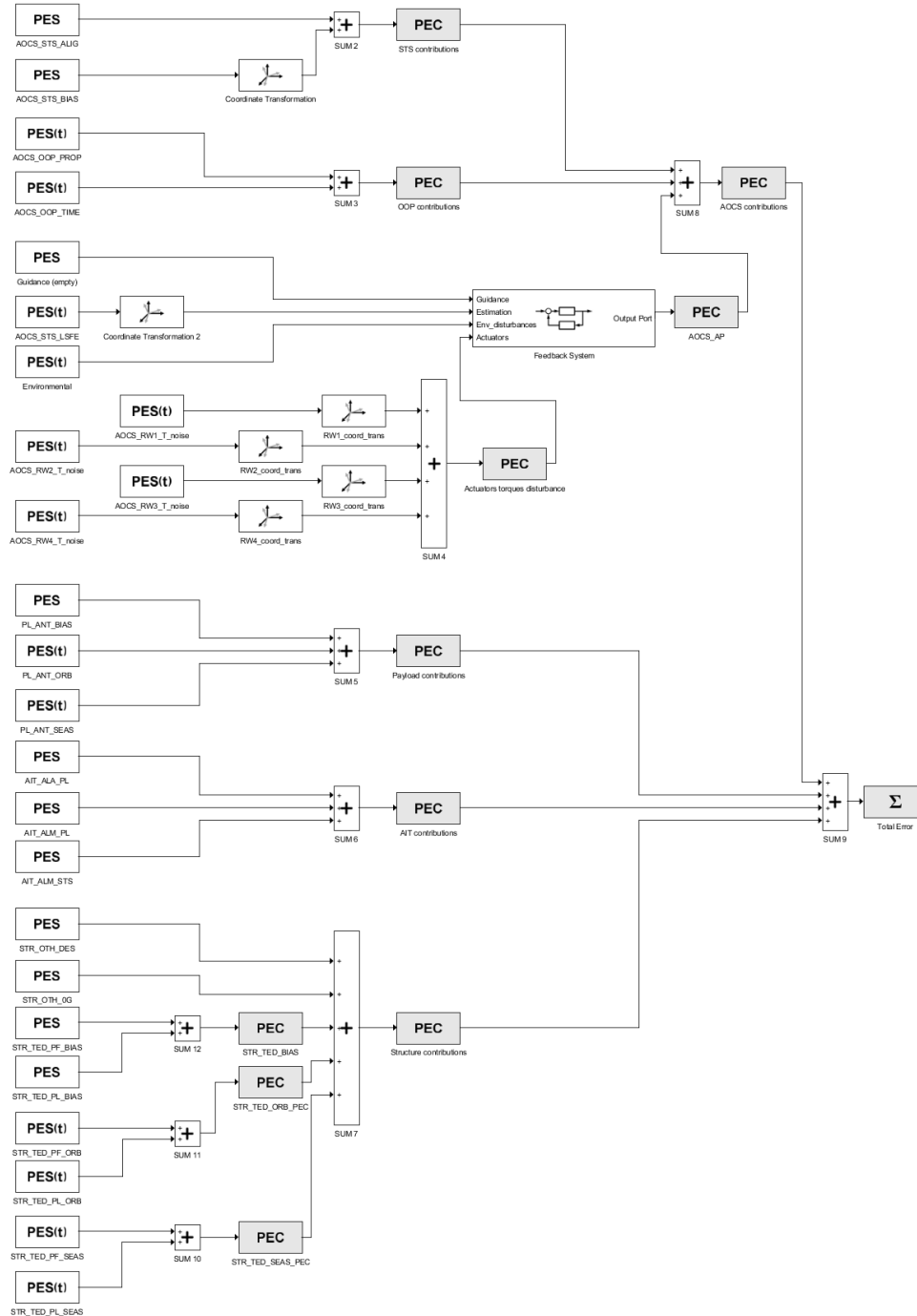


Figure 7-3: PEET implementation with feedback system replacing attitude pointing errors



7.1.5 Budget Comparison

7.1.5.1 PEET Budget vs Heritage Approach

The heritage method is compared in this chapter to the PEET advanced method and also to the PEET simplified method as further comparison means. Time constant, time random and total errors are compared for each axis and finally about the line of sight.

7.1.5.1.1 APE Budgets

7.1.5.1.1.1 Normal Mode

The assessment has been first been performed for the APE error index and normal mode. Results are summarized below:

Table 7-12 Normal mode pointing budget comparison*

[°] 3 σ		x	y	z	LOS	LOS (OHB)
PEET (APE simpl.)	Time constant	0.0492 (+72%)	0.0492 (+72%)	0.0493 (+72%)	0.0696	
	Time random	0.0710 (+25%)	0.0715 (+25%)	0.0710 (+25%)	0.1008	
	Total	0.0894 (+5%)	0.0899 (+5%)	0.0895 (+5%)	0.1268 (+28%)	0.1255
PEET	Time constant	0.0553 (+93%)	0.0556 (+93%)	0.0556 (+93%)	0.0653	
	Time random	0.0472 (-17%)	0.0476 (-17%)	0.0473 (-17%)	0.0659	
	Total	0.0795 (-12%)	0.0796 (-12%)	0.0793 (-12%)	0.1018 (+3%)	0.0921
Heritage	Group A	0.0286	0.0286	0.0286		
	Group B-D	0.0570	0.0570	0.0570		
	Total	0.0855	0.0855	0.0855		0.0990

* Percentages are given w.r.t. heritage budget of Group A for time-constant results and for the totals

LoS computation

The LOS errors are processed differently¹ and therefore not directly comparable, but it can be seen that some overconservatism is thereby removed from the heritage computation w.r.t. the instantaneous LoS equation, which was the intention. For better comparison, a column has been added to display all (total) LOS errors using the OHB methodology. The impact of approximate LOS mapping is further discussed in section 7.5.

$$^1 \text{ OHB: } e_{LoS} = \sqrt{0.67 \cdot (e_x^2 + e_y^2)}$$

$$\text{PEET simplified: } e_{LoS} = \sqrt{e_x^2 + e_y^2}$$

Time-constant budget (Class A errors)

First, due to the fact that most of the time-constant sources are uniformly distributed, the discrepancies between the different methods are in line with the approximations made in each approach:

- The heritage budget underestimates the resulting deviation by approximating any uniform distributions with Gaussian distributions whose 3σ deviation corresponds to the boundaries of the uniform distributions and applying the central limit theorem (i.e. the standard deviation of each source is $B/3$ where B is the budget value in the reference budget table).
- The PEET simplified method (compared to its advanced method) generally overestimates the resulting deviation from an actual non-Gaussian distribution at a PEC by converting it to a Gaussian distribution with equivalent variance (i.e. applying the central limit theorem). For each single uniform distribution, this would relate to an equivalent standard deviation of $\sigma_U = \frac{e_{max} - e_{min}}{\sqrt{12}}$ (see Figure 7-4).

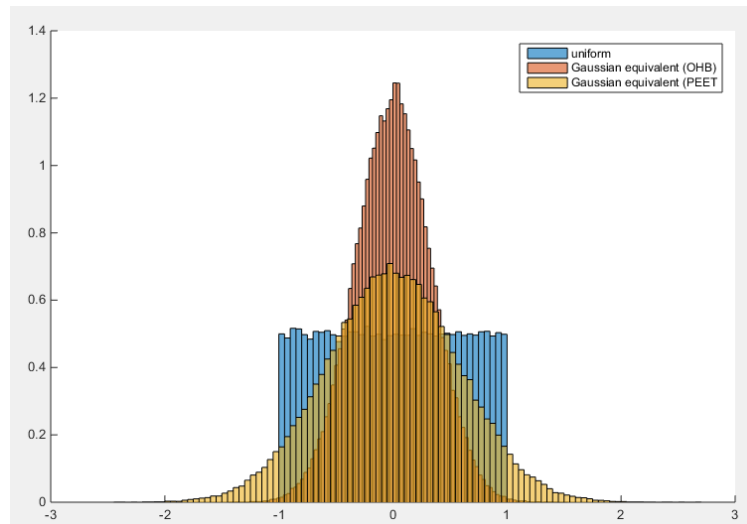


Figure 7-4: Equivalent Gaussian distribution for a uniform distribution approximated in OHB heritage method and PEET (simplified method) approach

With respect to the heritage approach, this relates to an assumed standard deviation of $B/\sqrt{3}$ for each source. Consequently, also the difference for the overall budget for Group A (i.e. time-constant) errors is expected to be larger by about a factor of $\sqrt{3}$ (i.e. 73%) with mainly uncorrelated uniform distributions present – which is in line with the difference identified in Table 7-13.

- Concerning the even larger difference between heritage budget and the PEET advanced method, it has to be noted that PEET formally also maps DC contributions from drift signals to the time-constant error budget (which is not applied to the simplified method to be more aligned with the approximate summation rules in the PEEH). Thus, this contribution does not only contain Group A contributions. For comparison, a scenario has been evaluated where the drift errors (from OOP) are not present.



Table 7-13 Normal mode PEET budget – no OOP drift

[°] 3 σ		x	y	z	LOS	LOS (OHB)
PEET (APE simpl.)	Time constant	0.0492	0.0492	0.0493	0.0696	
	Time random	0.0506	0.0506	0.0506	0.0716	
	Total	0.0706	0.0705	0.0707		0.0999
PEET	Time constant	0.0431	0.0431	0.0431	0.0501	
	Time random	0.0376	0.0377	0.0377	0.0508	
	Total	0.0643	0.0644	0.0644	0.0786	0.0742

The results in Table 7-13 show that the time-constant contributions are comparable in this case and the time-random contributions are decreased accordingly (more on the simplified method which contains the entire drift contribution). Further, as expected, the advanced method leads to less conservative results ($\approx 15\%$) for the axis budgets as it processes the underlying distribution according to its actual shape – which is close to Gaussian, but not entirely Gaussian due to some larger uniform contributions present (PL_ANT_BIAS and AIT_ALA_PL).

- It has to be noted however, that the large discrepancy between the group A budget and the time-constant PEET results does not relate to a weakness of the heritage approach itself, but to an (intentional) difference of how the heritage budget values are interpreted to form the uniform PES models.

To obtain a setup which allows a more direct comparison between PEET budgets and heritage approach, two additional scenarios were analysed where:

- All uniform bias contributions were replaced by Gaussian PES with a standard deviation of $B/3$
- All uniform distributions were modelled such that they have a standard deviation $B/3$ matching to the one derived from the heritage budget tables. Consequently, rather than having B as symmetric bound value, $B/\sqrt{3}$ is used as bound instead.

In both scenarios, the OOP drift contribution is disabled again to have only group A contributions present. The results are shown in Table 7-14 and Table 7-15.

In the entirely Gaussian case, the results of both PEET methods and the heritage budget match (up to the numerical accuracy) as expected as the central limit theorem fully applies.

In the case with 'matched' uniform distributions differ slightly, but corresponding to the expected behaviour. The advanced method is slightly less conservative than conservative than the heritage approach axis values - taking into account the close to, but not entirely Gaussian overall distribution present. The simplified method slightly overestimates the impact of this distribution by taking into account only its mean value and standard deviation for the evaluation. For the LoS contribution, the simplified method overestimates the contribution while the advanced method leads to a slightly reduced contribution. The latter



is considered exact while both the heritage and the simplified method use approximate expressions which may tend to either overestimating or underestimating results (see discussion in section 7.5).

Table 7-14 Normal mode PEET TC budget with Gaussian PES – no OOP drift

[°] 3σ		x	y	z	LOS	LOS (OHB)
PEET (APE simpl.)	Time constant	0.0287	0.0287	0.0287	0.0406	
PEET	Time constant	0.0284	0.0283	0.0283	0.0325	
Heritage	Group A	0.0286	0.0286	0.0286		0.033

Table 7-15 Normal mode PEET TC budget with 'matched' uniform PES Std – no OOP drift

[°] 3σ		x	y	z	LOS	LOS (OHB)
PEET (APE simpl.)	Time constant	0.02939 (+3%)	0.02939 (+3%)	0.02939 (+3%)	0.04157 (+26%)	
PEET	Time constant	0.02618 (-9%)	0.02614 (-9%)	0.02621 (-9%)	0.03037 (-8%)	
Heritage	Group A	0.0286	0.0286	0.0286		0.033

Time-random budget (Group B,C,D errors)

The main difference between the heritage budget approach and the PEET methods is in the modelling of the and treatment of the time-random error sources. PEET describes PSD, drift and periodic error in the frequency domain. This especially allows drift and periodic error sources to be summed accurate according to their frequency relation and to take into account the resulting non-Gaussian distribution in the evaluation.

Thus, the PEET results are expected to be less conservative compared to the heritage approach for the advanced method which is also the case (~17%) in the budget values in Table 7-12. For the simplified method a much more conservative result is expected and present (~25%), as the budget value is based on the mean and standard deviation of the overall time-random contribution – which is considerably non-Gaussian distribution (and thus leads to a similar effect as for the 3σ value derived from the standard deviation of a uniform distribution in Figure 7-4).

Total error budget

Even with the different modelling assumptions made on the uniform bias bounds, the OHB heritage method is more conservative than the PEET advanced method (about 10%) for the axis contributions and leads to about the same error on the LoS (see Table 7-12). The simplified method is more conservative in this case, but with about 5% less than would first be expected from the larger differences of the time-constant and time-random contributions. The reason is the common evaluation of these two contributions while the heritage approach follows a more conservative 'individual' evaluation of the different groups (cf. chapter 7.1.4.2), i.e. a linear summation of the contribution from each group.



Again, for a better comparability, another scenario has been evaluated using the ‘matched’ standard deviations for the uniform distribution PES in group A. The total contributions are shown in the table below.

Table 7-16 Normal mode PEET TC budget with ‘matched’ uniform PES Std

[°] 3σ		x	y	z	LOS	LOS (OHB)
PEET (APE simpl.)	Total	0.07818 (-9%)	0.07867 (-9%)	0.07818 (-9%)	0.1109 (+12%)	
PEET	Total	0.06823 (-20%)	0.6877 (-20%)	0.06817 (-20%)	0.09104 (-8%)	
Heritage	Total	0.0855	0.0855	0.0855		0.0990

Under these more comparable modelling assumptions, the OHB heritage method is more conservative than both the PEET simplified (~10% less conservative than heritage for the axis contributions) and advanced method (10% to 20% less conservative than heritage for LoS and axis budgets). The reason is a combination of the different evaluation of the combined contribution from different groups (common vs individual evaluation) and the more precise modelling of the time-random contributions.

An additional comparison with the actual mission values retrieved from the SmallGEO pointing budget document shows that the heritage approach is roughly 10% more conservative than the PEET advanced method.

7.1.5.1.1.2 Station Keeping

The SK budget differs from the normal mode only by a larger AOCS errors (attitude performance) which lead to an increased time-random contribution.

Table 7-17 SK pointing budget comparison

[°] 3σ		x	y	z	LOS	LOS (OHB)
PEET (APE simpl.)	Time constant	0.04916	0.04916	0.04933	0.06964	
	Time random	0.07549	0.07600	0.07549	0.1071	
	Total	0.9284	0.9330	0.9295	0.1317	0.1285
PEET	Time constant	0.05527	0.0556	0.05553	0.06531	
	Time random	0.05428	0.05459	0.05439	0.0721	
	Total	0.08293	0.08345	0.08286	0.1052	0.0958
Heritage	Group A	0.0286	0.0286	0.0286		
	Total	0.1005	0.1005	0.1005		0.1164



7.1.5.1.2 RPE Budgets

For RPE comparison, RPEs were approximated in the heritage method by removing the group A (Bias) for the 1-year RPE and the groups A and B (Bias and Long-term) for the 1-day RPE. This can be justified by the fact that the impact of the seasonal effects are negligible over one day.

Time-constant errors (i.e. group A) do not contribute, thus only the total contributions (corresponding to the time-random ones) are presented in the table below. PEET results are computed using the advanced statistical method.

The resulting differences are in line with the assumptions made. PEET provides more accurate frequency domain methods for the time-random models used (PSD, periodic and drift errors) and thus can be more precise in the summation of such contributors. Further, applying the frequency domain RPE filter decreases the impacts of such sources (w.r.t. to the APE budget, compare daily values) which fully appear in the heritage budget of the considered groups. This is in line with the decrease of the axis budget values present in the table. Again for the LOS, the PDF-based evaluation of the advanced method is considered to provide the most accurate results. The approximate expression used for the heritage budget can result in both larger or smaller values as further discussed in section 7.5 – in the range of 6% for this specific case.

Table 7-18 Normal mode RPE comparison (daily and yearly)

[°] 3σ		x	y	z	LOS	LOS (OHB)
PEET (1 day)	Total	0.0314 (-11%)	0.0372 (-11%)	0.0315 (-11%)	0.0435 (+6%)	(0.0363)
Heritage (1 Day)	Total	0.0352	0.0352	0.0352		0.0407
PEET (1 year)	Total	0.0472 (-17%)	0.0476 (-17%)	0.0473 (-17%)	0.0659 (<1%)	(0.0549)
Heritage (1 year)	Total	0.0570	0.0570	0.0570		0.0660

7.1.5.2 Comparison with In-Flight Data

In the frame of the present study, it was not deemed practicable to evaluate in-flight data for comparison with the obtained PEET results. This is due formally to the fact that the data is not available to OHB in an easy format that would be comparable to the PEET outputs and that it would be a cumbersome process to get the consent from the commercial end customer to distribute the data in the frame of this study. From a technical perspective, a straight forward comparison of the flight data would be only feasible for the part related to the control error and not for the total pointing error since in contrary to science or earth observation satellites, there is no direct measurement of it.

What could be done in a follow-up activity would be to compare the control error from the flight data directly with a PEET model which would only concentrate on the control error (e.g. taking only the feedback system part of the above mentioned model).



Further, one could envisage to post process data from the in-orbit calibration, where the satellite performs “cuts” of the antenna patterns measuring the received power on the ground station. The difficulty is that this is performed using a continuous slewing profile and no steady state pointing. On top, it would need to be evaluated what parts of the errors would be associated to the RF chain and what parts to the actual pointing error. It needs to be noted that this evaluation would only be feasible in normal mode and not in station keeping mode, as the calibration is performed in absence of station keeping manoeuvres. It is expected that a close collaboration with the payload engineers would be needed. The effort for this assessment is hard to estimate and it would be proposed to perform a feasibility assessment first needing a couple of weeks and in case of positive outcome to engage into a processing of the calibration data, which could take from 4 to 12 weeks.

7.1.6 Conclusions and Lessons Learnt

From the perspective of the OHB consultants, the conclusion from the pointing budget comparison exercise is that the PEET advanced method, which is deemed as being the physically most accurate one, allows to remove some conservatism from the heritage computations. This can be especially interesting for future telecom applications where pointing requirements are also getting more and more demanding.

In general, PEET was applied by OHB the first time for a telecom project, while its use has already been started in navigation, earth observation and reconnaissance missions previously. The tool has proven to be quite user friendly. It has been also acknowledged that for a meaningful use of the tool, the PES need to be very well understood and characterised and it has to be ensured that also their statistical properties are available for each source. This has to be thought of from the start of the project.

OHB intends to further intensify the use of PEET. OHB personnel has also been trained on PEET during a couple of sessions over the past years.

7.2 E3000 (Airbus DS Toulouse)

This case study describes a generic telecommunication mission which provides broadcast services with a geostationary satellite. The main payload is composed of a Ku/Ka band repeater, three shaping deployable antennas and two steerable top-floor antennas which allow to provide the uplink and downlink connections between the satellite and Earth to specified geographical regions and levels of gain across required frequency band and polarization, avoiding interfering with other coverages (whether on the same spacecraft or in neighbouring systems).

Mission AOCS is based on standard Plasmic configuration of the E3000 ADCS Mk1.5 design. It uses a star-tracker for attitude and rate determination. A set of chemical thrusters and SPT (Stationary Plasma Thruster) are used for the precision pointing attitude manoeuvres.

The mission scenario and the S/C are schematically illustrated in Figure 7-5. In the context of this study, the pointing of broadcast mission of East side deployable Gregorian antenna was analysed, including the worst-case station keeping manoeuvre performance.

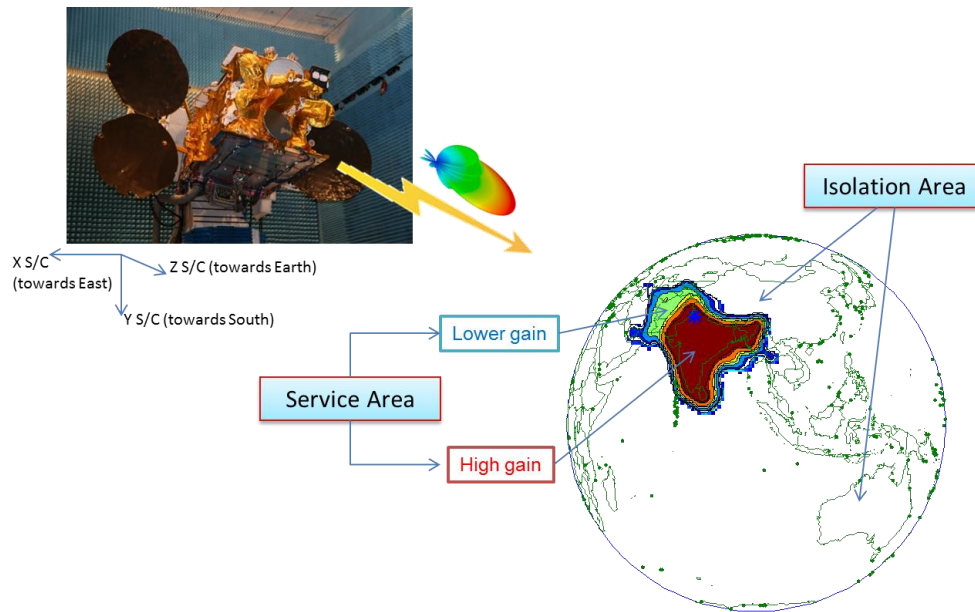


Figure 7-5: ComSat Mission Scenario [RD19]

Through the System Performance Specification, the customer provides a limited set of requirements, as far as the system pointing budget is concerned:

- coverage polygons: directly impacted by the absolute performance error (APE) of the computed S/C pointing error. The specified coverage polygons will be enlarged in all directions by the instantaneous half-cone angle.
- minimum G/T and EIRP inside the polygons: directly impacted by the absolute performance error (APE). Payload G/T and EIRP performance will be computed using the enlarged polygons from first point, so degraded because of the pointing error that shall cover the worst-case value over all the satellite lifetime.
- EIRP and G/T stability inside the polygons: directly impacted by the relative performance error (RPE) over a time window of 24h for the daily stability and satellite lifetime for lifetime stability. Payload G/T and EIRP stability will be computed using the daily 24h and lifetime pointing errors (excluding constant terms errors). The interest of this EIRP and G/T stability requirement for customer is to have an idea of how much the power could vary over the defined coverage along a day or during all satellite lifetime, to anticipate if any gain adjustment is needed to keep the good link budget performance (i.e not saturate and loss linearity).

Figure 7-6 show a schematic of how the total BPE (APE) and BPE stabilities (RPE) are applied on antenna coverage to compute the associated antenna minimum gain and gain stability variations.

Note: The schematic is done with numeric values for an example of BPE of 0.12° and daily stability of 0.07° and lifetime stability of 0.09° to 0.11° .

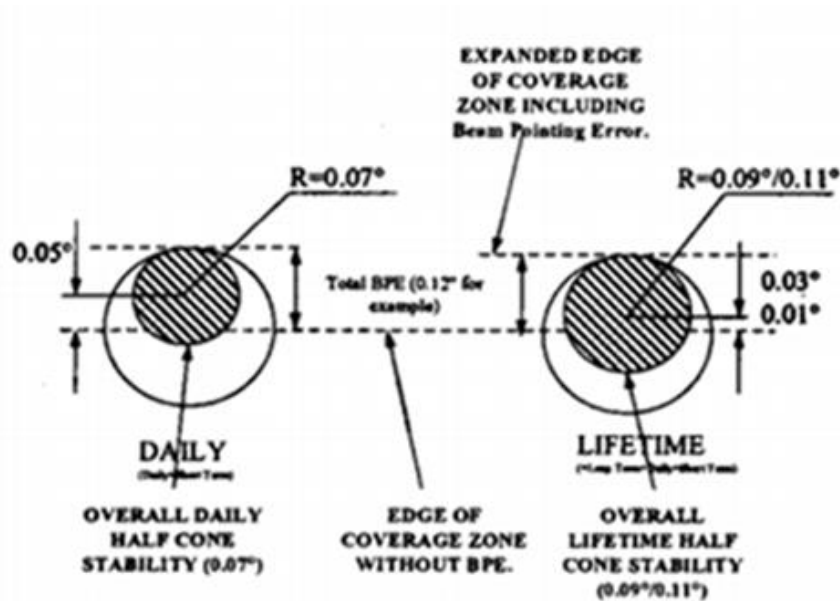


Figure 7-6 BPE and BPE stability applied on antenna coverage [RD19]

Satellite orbit control window: East/West and North/South: this will impact on some constraints to be considered for the AOCs design and the associated FDS error contribution to be considered in the pointing budget.

Satellite lifetime: this will impact on the definition of lifetime error sources contribution to be considered in the pointing budget.

As the BPE is usually not included in the customer specification, an allocation is determined at the beginning of the project, based upon preliminary system budget or past company heritage. Payload RF performance will be computed over the specified polygons enlarged by the spacecraft BPE to guarantee the compliance to customer requirements over satellite lifetime even for worst case satellite pointing.

The mission success is hence ensured if:

- The system pointing budget remains below the BPE specified to antenna supplier
- The Payload performance computed on the basis of this BPE and of the stability performance is compliant with the customer specification

7.2.1 Motivation

Broadcast missions represent a huge percentage of the Telecommunication market. Most part of Eurostar satellites have integrated this type of mission, hence several missions which are well documented in terms of pointing error engineering that could easily be used as reference case.

Further, in-orbit antenna mapping test data are available. This antenna mapping is aimed to verify the good RF health and pointing of the antennas and to validate the thermo-elastic daily variation allocated on the beam pointing error budget. Specific de-pointing biases of each deployable antenna detected during IOT mapping can be compensated using the



ADTM steering capacity (if needed) up to a compensation residual considered in the later budget.

The application of the previous PEET release (V1.0) seemed not directly possible for this mission due to some error sources specificity (thermo-elastic profiles) and particular reporting needs. Hence choosing this mission as reference case could result in PEET extensions that enable the application to such kind of extended missions in the future.

PEET/PEEH developments using this mission as reference are expected to remain appropriate also for other kind of telecommunication missions (e.g interactive broadband with multi-beam Ka-band satellites), since the general basis of error contributors and their modelling are applicable.

7.2.2 Pointing Requirements

The purpose of the pointing requirement in a Telecommunication satellite is mostly related to the need of guarantee a minimum antenna gain (signal level) within the specified coverage during the different mission phases (normal mode equinox, normal mode eclipse, station keeping manoeuvres) and considering the thermal environment over lifetime.

Typical pointing requirement is related to the absolute performance error (APE):

- The instantaneous half cone angle between the actual and desired payload boresight direction shall be less than 0.1deg for 99.7% of the time (including manoeuvres).

Additionally, in most of the missions the daily and over life stability of antenna gain shall be evaluated. It is related to the antenna pattern gain slope and pointing variation during a 24h period or over lifetime. For that, two additional pointing requirements in terms of relative performance error (RPE) need to be flow-down:

- A daily pointing stability absolute value (half cone angle) counting for error terms which evolve on a daily period (daily and short-term errors) in normal mode operation. Typical pointing requirement is 0.05deg.
- An over life pointing stability absolute value (half cone angle) counting for error terms which evolve during spacecraft lifetime (seasonal terms, long term drifts, daily and short-term errors) in normal mode operation. Typical pointing requirement is 0.07deg.

For most of the customers the pointing performances shall be provided with the detailed budget spreadsheets of the driving mission phases, showing:

- The Roll, Pitch and Yaw errors in satellite axis. The spacecraft reference coordinate system is illustrated in Figure 7-7.
 - The X-axis (roll) is parallel to the satellite velocity vector. A rotation around the roll axis induces a North (positive roll) or South (negative roll) de-pointing.
 - The Y-axis (pitch) is pointing south. A rotation around the pitch axis induces an East (positive pitch) or West (negative pitch) de-pointing.
 - The Z-axis (yaw) is pointing towards the sub-satellite point.
- The North/South and East/West errors, accounting for previous roll, pitch and yaw errors and the antenna boresight direction.
- The total half-cone error, estimated from the North/South and East/West pointing and corresponding to a 0.9974 probability.

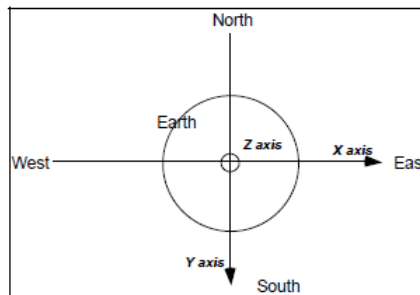


Figure 7-7: Spacecraft axes relate to coordinates on an Earth map [RD19]

Typical approach for coverage pointing performance declension process (top-down specification flow) in a Telecommunication satellite project, given a vision of the documentation involved in the process, is illustrated hereafter in Figure 7-8.

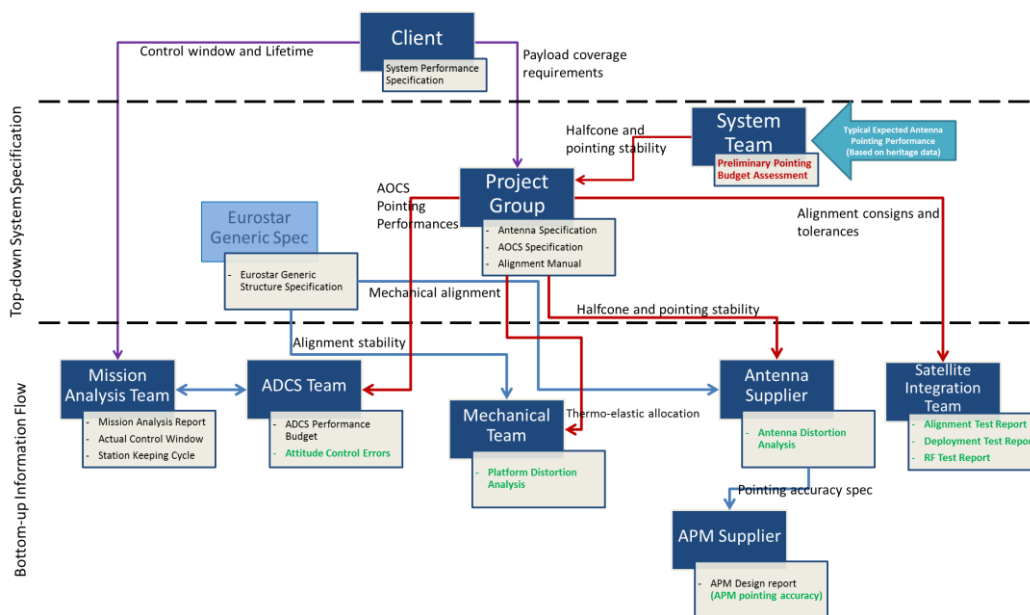


Figure 7-8: Pointing Performance Top-down specification allocation process [RD19]

The main contributor to pointing performance is both the antenna and spacecraft thermo-elastic distortions. In order to avoid counting twice any error contributor, it is fundamental to unambiguously define the antenna/spacecraft interfaces, to specify which equipment/contributors shall be considered as part of the spacecraft rather than of the antenna.

Note that the statistical interpretation is not defined in the requirement of the study case. This is not necessary because the summation rules in the heritage approach are E3000 specific and not derived from the PEEH. For P4COM it is assumed that the proper statistical interpretation is temporal, but in terms of the APE also the mixed interpretation will be applied to the budget computation to get the respective budget for comparison. The pointing requirements are summarized in Table 7-19.



Table 7-19: Pointing Error Requirements in line the PEEH

Pointing Error Requirement (PER)	APE					
Evaluation Period	At any time during satellite life time					
Error Index	APE					
Window-Time [s]	-					
Stability-Time [s]	-					
Unit	deg				%	
Required Error Value	x	y	z	LOS	Pc	n _p
	0,100	0,100	0,150	-	99,7	-
Statistical Interpretation	temporal with joint level of confidence evaluation					
Error reference frame	Earth Map Coordinate System, see TN-005.					
Purpose	Ensure that S/C pointing error 3sigma half-cone stays within defined range for RF performance computation.					

Pointing Error Requirement (PER)	daily RPE					
Evaluation Period	At any time during satellite life time					
Error Index	dailyRPE					
Window-Time [s]	86400					
Stability-Time [s]	-					
Unit	deg				%	
Required Error Value	x	y	z	LOS	Pc	n _p
	0,050	0,050	0,055	-	99,7	-
Statistical Interpretation	temporal with joint level of confidence evaluation					
Error reference frame	Earth Map Coordinate System, see TN-005.					
Purpose	EIRP and G/T stability inside the polygons: directly impacted by the relative performance error (RPE) over a time window of 24h for the daily stability.					

Pointing Error Requirement (PER)	lifetime RPE					
Evaluation Period	At any time during satellite life time					
Error Index	lifetimeRPE					
Window-Time [s]	3,15E+07					
Stability-Time [s]	-					
Unit	deg				%	
Required Error Value	x	y	z	LOS	Pc	n _p
	0,070	0,070	0,075	-	99,7	-
Statistical Interpretation	temporal with joint level of confidence evaluation					
Error reference frame	Earth Map Coordinate System, see TN-005.					
Purpose	EIRP and G/T stability inside the polygons: directly impacted by the relative performance error (RPE) over a time window representing the satellite lifetime.					

7.2.3 Heritage Approach

This paragraph describes the currently applied approach for the system pointing budget assembly method (bottom-up information flow). As illustrated in Figure 7-8, this information comes from:

- Heritage data at the very initial phase of the project, based on similar spacecraft configuration

- Analysis report of each subsystem defined in the top-down specification for the different project phases (PDR, CDR...).

The high-level pointing error engineering approach structure is illustrated hereafter:

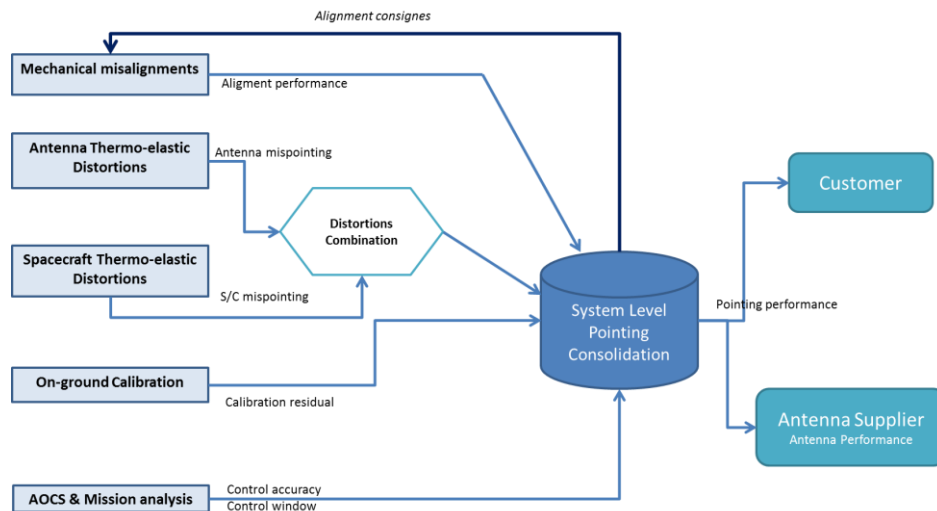


Figure 7-9: Pointing error engineering high level schematic [RD19]

As observed in Figure 7-9, the overall pointing error of a Eurostar Telecommunication mission is the result of four error main types:

- Mechanical misalignments and stabilities
- Thermo-elastic distortions
- Attitude control errors and orbital drifts
- Calibration residual errors

Apart from the mechanical misalignments and residual errors, the other error contributors will vary in function of the season (summer and winter solstice, equinox in or out of eclipse) and/or the mission phase (Normal mode, EW and NS orbit control manoeuvre).

As a consequence, the error terms contributing to the pointing budget within each category type will be classified depending on their time scale variation as describe hereafter, and differentiating between spacecraft operating modes/mission phase:

- Class A, constant error:
 - Bias or average value not varying with time.
 - Bias issued from phenomena taking place at beginning of life and rapidly settled.
- Class B, lifetime or long-term variation error:
 - Error term caused by effects occurring all along lifetime but not constant, such as thermal properties degradation with time.
 - Seasonal varying error, mainly caused by the changing solar incidence upon satellite behaviour.
- Class C, daily variation error: caused by daily phenomenon such as the rotation of the solar incidence around the spacecraft each day

- Class D, short term variation error:
 - Error term cause by spurious/unpredictable event or
 - Error observed over a 1 to 2 hours period

The system pointing budget analysis is organised around input Excel files.

- ADCS performance (including orbital effects), where it is defined the data common to all antenna budgets for the satellite modes of interest. These data are classified by Roll, Pitch and Yaw errors and per error Class A, B, C and D.
- Mechanical alignment and stability errors. These data is classified by Roll, Pitch and Yaw errors. All these errors are Class A.
- Thermo-elastic distortions. Excel file with the Roll, Pitch and Yaw translations and rotations of each antenna interface with platform evolution over three different seasons (summer and winter solstice, equinox including eclipse) and for beginning and end of life. From these six profiles data Class A, B and C errors due to thermo-elastic distortions is derived for each antenna on the spacecraft using an Excel macro.

The inputs coming from these three principal Excel files (ADCS, mechanical and thermo-elastic) are exported to a master Excel file, built to compute the total pointing error (Roll, Pitch, Yaw and Half-cone) per antenna and satellite operating case. This is illustrated in Figure 7-10.

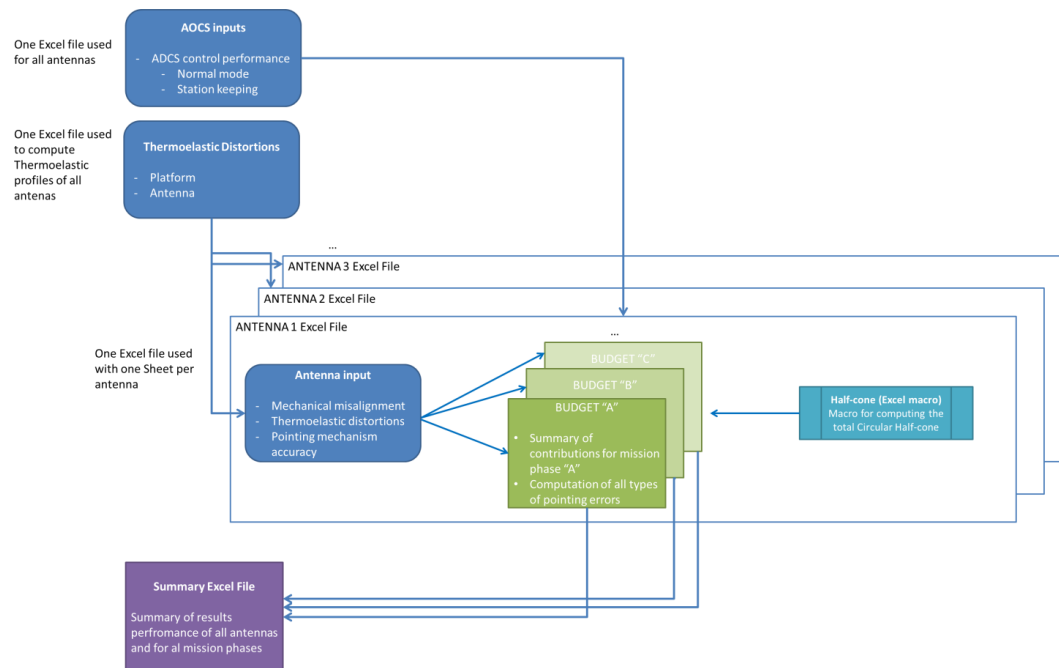


Figure 7-10: Pointing error computation files organisation [RD19]

For each antenna and satellite operating case a pointing budget is computed, by applying an error summation procedure described hereafter. This pointing error computation obeys conventions used for the entire Eurostar satellites family, which follows error combination rules agreed by the space community (agencies, industrials and customers) and based on ECSS-E-ST-60-10C standard and following a simplified method (uncorrelated errors are added using a root square sum approach, whereas correlated errors are added linearly).



This error combination procedure is illustrated in rough outlines in Figure 7-11.

The pointing errors are first combined by axis in the satellite reference frame (roll, pitch, yaw), then processed to obtain North-South and East-West pointing errors. An envelope of the pointing error is further derived from a combination of the North-South and East-West pointing errors. This envelope, called half cone error, is a circular cone covering the worst-case de-pointing with respect to the reference pointing direction.

The method followed to combine the various types of error is defined hereafter.

For each error class and each axis, the individual errors are identified as R_{ai} , P_{ai} , Y_{ai} :

- R, P, Y stand for Roll, Pitch and Yaw
- i represents the type of error, i.e alignment stability or short term AOCs control error
- α stands for A, B, C or D error variation class

Within each error class and along each axis, a root square summation of the errors is performed. Afterwards, following a conservative approach the overall pointing error along a given axis is computed as the arithmetic sum of the errors of different classes along this axis.

The North/South and the East/West pointing error of the antenna boresight are derived from the Roll, Pitch and Yaw total errors. They account for the reference beam pointing direction via the antenna specific coupling coefficients of the Yaw movement to N/S and E/W directions, KNS and KEW:

$$NS = \sqrt{R^2 + (KNS \times Y)^2} \quad EW = \sqrt{P^2 + (KEW \times Y)^2}$$

with:

$$KNS^2 = \frac{(\cos l \sin L)^2}{\left(\frac{Ro}{Re}\right)^2 + 2(1 - \cos l \cos L)\left(1 + \frac{Ro}{Re}\right)}$$
$$KEW^2 = \frac{(\sin l)^2}{\left(\frac{Ro}{Re}\right)^2 + 2(1 - \cos l \cos L)\left(1 + \frac{Ro}{Re}\right)}$$

Being:

- $L = L_c - L_s$, where L_c is the longitude of the reference pointing direction sub-point and L_s is the satellite longitude.
- l is the latitude of the reference pointing direction sub-point
- R_e is the equatorial radius
- R_o (35786Km) is the distance from the satellite to the sub-satellite point

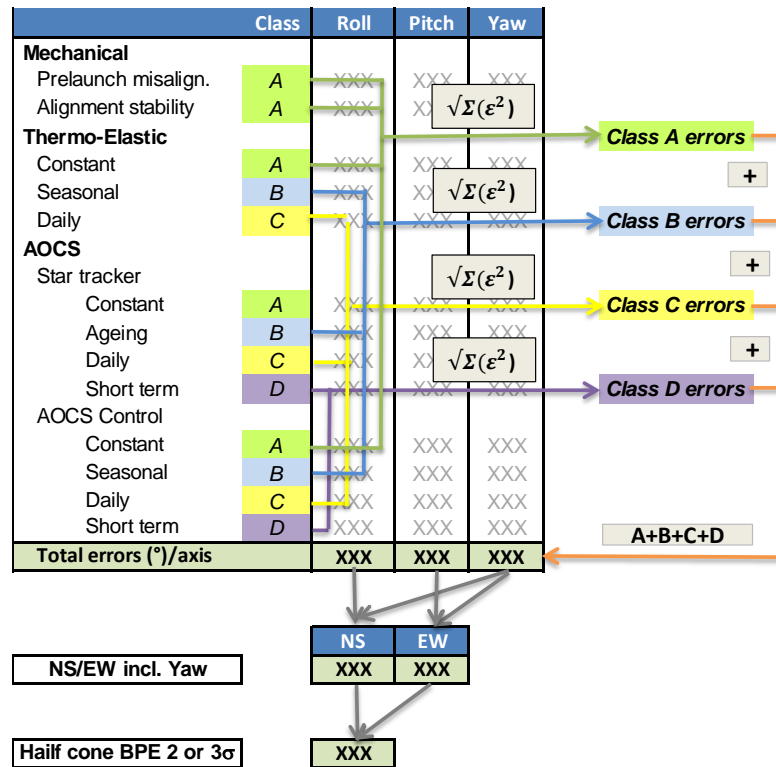


Figure 7-11: Pointing error budget computation

To obtain a worst-case pointing error, the yaw coupling effect should be computed for the point of the antenna coverage leading to the largest coupling coefficients. Intuitively, this point is on the pattern boundary, the furthest away from the sub-satellite point. Standard approach is to take into account a KNS and KEW factor that covers all visible Earth from Geostationary orbit.

For small angles, the circular half-cone pointing error can be expressed as follows, in function of the NS and EW pointing errors:

$$\theta_{1/2} = \sqrt{e_{NS}^2 + e_{EW}^2}$$

The half cone error is defined as the value for which the probability that $\theta_{1/2} \leq \theta_{1/2,MAX}$ is equal to the requested probability of 3σ . Assuming that the N/S and E/W errors are zero-mean independent Gaussian random variables, the half-cone error is computed on the basis of the circular error probability theory (numerically using an Excel sheet with the ratio of approximated standard deviations from the N/S and E/W errors ($\sigma_x = \max(e_{NS}, e_{EW})/n_p$ and, $\sigma_y = \min(e_{NS}, e_{EW})/n_p$ as input).

The Daily and Lifetime RPE are computed on the same basis of pointing error computation detailed in this section but excluding from the budget:

- The Class A and Class B errors for Daily RPE (only Class C and D errors are taken into account).

- The Class A errors for Lifetime RPE (only Class B, C and D errors are taken into account).

7.2.4 Pointing Budgets

7.2.4.1 Reference Budget

There are different pointing budgets for each antenna and principal satellite operating mode, since the AOCS Control error depends on the mission phase (normal mode or station keeping, in and out of transient).

In the reference pointing budget, a simplified statistical approach is followed for the characterization of each PES. For each one of them a maximum value ϵ_{max} is considered such that at least 99.7% of all magnitude values (analysed or heritage) are smaller than that value, which corresponds to consider each source is represented by a Gaussian PDF characterised by its 3σ value.

In the case particular case of thermo-elastic periodic signals, in the reference pointing budget the maximum amplitude of these PES obtained by specific platform analysis is considered and not a 3-sigma value.

The only transformation needed is to assembly the thermo-elastic distortions of each platform interface related to the antenna considering the antenna geometry optic to translate them into pointing error in each satellite axis. Then, as explained in section 7.2.3, the different seasonal profiles are used to derive the error contributor per class (A, B and C) and per axis with the definition illustrated hereafter in Figure 7-12.

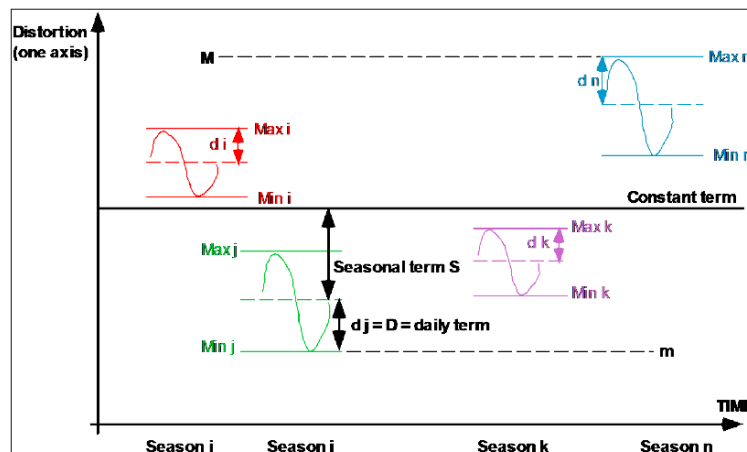


Figure 7-12: TED in Pointing error budget computation

The beam pointing error analysis for study reference is shown below. As explained and illustrated in Figure 7-11, the pointing error sources are grouped into three main categories: mechanical, thermo-elastic and AOCS errors. Within each one of these categories the error sources are grouped into four different error classes depending on their variation over spacecraft lifetime.

The BPE computation is performed according to the methodology explained in section 7.2.3.



Broadcast East Deployable Antenna		Normal mode			ISK (inc. Transient)		
		Class	Roll (°)	Pitch (°)	Yaw (°)	Roll (°)	Pitch (°)
Pre-launch Mechanical misalignments							
	Antenna alignment	A					
	AOCS sensor alignment	A					
	CATR measurement accuracy	A					
	ADTM step accuracy	A					
Alignment stabilities (after launch)							
	Launch vibration Feed chain	A					
	Launch vibration reflector	A					
	Launch vibration AOCS sensor	A					
	ADTM deployment repeatability	A					
	TED bias compensation residual	A					
	"0g" residual	A					
Thermo-Elastic							
	Constant term platform	A					
	Seasonal term platform	B					
	Daily term platform	C					
	Daily term allocation antenna	C					
AOCS							
	Star tracker						
	Bias error	A					
	Long term Bias stability	B					
	Relativist aberration	C					
	Short Term stability	D					
	FoV error	D					
	Pixel noise error	D					
	FDS						
	Orbit knowledge Semi axis	B					
	Orbit knowledge Initial Longitude	B					
	On-board manoeuvre PPS EW efficiency	B					
	On-board manoeuvre PPS triaxiality	B					
	On-board latitude determination SCU drift	B					
	OD initial inclination	C					
	OD excentricity	C					
	On-board latitude determination OBOC perfo	C					
	AOCS Control						
	Bias	A					
	Wheel Friction step	D					
	Transient ISK manoeuver	D					
Class A errors (°) per axis							
Class B errors (°) per axis							
Class C errors (°) per axis							
Class D errors (°) per axis							
TOTAL errors (°) per axis (A+B+C+D)							
Beam Pointing Error (3 σ) °RF				0.103		0.108	
Life time stability BPE (3 σ) °RF				0.070			
Daily stability BPE (3 σ) °RF				0.053			

(explicit contributors are not presented due to confidentiality)

Table 7-20: Reference pointing error budget for P4COM study case broadcast mission²

7.2.4.2 PES Characterization

The parameter values of Table 7-20 are converted in parameter values for PEET based on the following relations:

- For periodic signals the above values are taken as amplitude of a periodic random process.

² Note that the 'AOCS sensor alignment' contributions refer to the alignment accuracy/precision, thus to the alignment knowledge



- For Gaussian PDFs the above values are taken as 3-sigma values.
- For uniform distributions the above values are taken as 3-sigma values and converted into upper and lower bound of a uniform PDF.
- Drifts are modelled as general periodic signals and thus more accurately than assuming a Gaussian or Uniform distribution. The values in the reference budget are considered to be 3-sigma values and converted as such.
- Exponential decaying transients are modelled as such instead of 3-sigma values of a Gaussian distribution as considered in the reference budget. The values in the reference budget are considered to be 3-sigma values of a Gaussian distribution and converted as such.
- Spikes are modelled as triangular general periodic signal. The values in the reference budget are considered to be 3-sigma values of a Gaussian distribution and converted as such.

SADM disturbances are negligible and thus are not included as PES in the budget. The thermo-elastic deformation PES are given as time series that are converted into PSDs for the model in PEET. As there are several time series due to the season and BOL/EOL, the PSD with the largest power is considered for the model in PEET as a conservative approach but resulting in a more accurate modelling compared to the approach in Table 7-20.

All errors sources defined for the PEET scenario including their properties, justification and classification according to the PEEH are shown in Table 7-23. They are already expressed in the satellite coordinate system (Roll, Pitch and Yaw) which avoids the necessity of further coordinate system transformations in the PEET model.

The different pointing error source classes from the heritage budget in Table 7-20 are represented in PEET as different ensemble domains.



Table 7-21: Classification of Pointing Error Sources

Definition of PES				Description of PES					
Subsystem	Unit	PES	Name	Time-random	Ensemble-random (= time-constant)	Class	On interface	Type	
MECHANICAL	Alignments	Antenna alignment wrt platform ref.cube	MEC_AL_ANT		X	bias	no	variable	
		STR alignment wrt platform ref. cube	MEC_AL_STR		X	bias	no	variable	
		CATR RF boresight measurement accuracy	MEC_AL_CATR		X	bias	no	variable	
		ADTM step accuracy	MEC_AL_ADTM		X	bias	no	variable	
	Stability	Launch vibration Feed chain	MEC_ST_FCA			X	bias	no	variable
		Launch vibration reflector	MEC_ST_REF			X	bias	no	variable
		Launch vibration STR	MEC_ST_STR			X	bias	no	variable
		ADTM deployment repeatability	MEC_ST_ADTM			X	bias	no	variable
		TED bias compensation residual	MEC_ST_TED			X	bias	no	variable
		"0g" release residual	MEC_ST_0G			X	bias	no	variable
THERMOELASTIC	Platform TED	Constant	TED_A_SC		X	bias	no	variable	
		Seasonal	TED_SC_seasonal		X	periodic	no	process	
		Daily	TED_SC_daily	X		random	no	process	
		Antenna allocation	TED_ANT_daily	X		periodic	no	process	
AOCS	Star tracker	Individual STR internal bias error	AOCS_ST_IAB		X	bias	no	variable	
		Individual STR internal short term stability	AOCS_ST_STS	X		periodic	no	process	
		Individual STR internal long term bias stability	AOCS_ST_LTS	X		random	no	variable	
		Relativist aberration	AOCS_ST_RA		X	bias	no	variable	
		Field of View error	AOCS_ST_FOV	X		random	no	process	
		Pixel noise error	AOCS_ST_PNE	X		random	no	process	
	Orbit Knowledge	OD Semi axis	AOCS_AK_LT_saxis	X		random	no	variable	
		OD Initial longitude	AOCS_AK_LT_long	X		random	no	variable	
		On-board manoeuvre management PPS EW efficiency	AOCS_AK_LT_Eweff	X		random	no	variable	
		On-board manoeuvre management PPS triaxiality	AOCS_AK_LT_triax	X		random	no	variable	
		On-board Latitude determination SCU drift	AOCS_AK_LT_SCU	X		random	no	variable	
		OD initial inclination	AOCS_AK_DT_incl	X		random	no	variable	
		OD excentricity	AOCS_AK_DT_excen	X		random	no	variable	
		On-board latitude determination OBOC perfo	AOCS_AK_DT_OBOC	X		random	no	variable	
	Control Performance	Bias	AOCS_CP_Bias			X	bias	no	variable
		Wheel Friction step	AOCS_CP_wheel	X		periodic	no	process	
		Transient ISK manoeuvre	AOCS_CP_ISK	X		periodic	no	process	



Table 7-22: Justification of Pointing Error Sources

Definition of PES				Justification of PES		
Subsystem	Unit	PES	Name	Origin	Reference	
MECHANICAL	Alignments	Antenna alignment wrt platform ref.cube	MEC_AL_ANT	Antenna alignment performance	Based on heritage of E3000 satellite alignment measurements	
		STR alignment wrt platform ref. cube	MEC_AL_STR	STR alignment performance		
		CATR RF boresight measurement accuracy	MEC_AL_CATR	INS-STR alignment knowledge		
		ADTM step accuracy	MEC_AL_ADTM	APM angular step size. APM is used to compensate Antenna alignment and TED bias in x-axis and y-axis of reference frame.		
	Stability	Launch vibration Feed chain	MEC_ST_FCA	Alignment error induce by launch vibrations	Based on heritage of E3000 satellite stability measurements after mechanical tests.	
		Launch vibration reflector	MEC_ST_REF	Alignment error induce by launch vibrations		
		Launch vibration STR	MEC_ST_STR	Alignment error induce by launch vibrations		
		ADTM deployment repeatability	MEC_ST_ADTM	Accuracy of deployment, stability of the end of deployment stop		
		TED bias compensation residual	MEC_ST_TED	Residual error from TED constant term compensation in x-axis and y-axis of reference frame, based on thermal prediction accuracy of S/C thermal model.		
		'0g' release residual	MEC_ST_0G	Gravity release effects		
THERMOELASTIC	Platform TED	Constant	TED_A_SC	Mean value, pointing error induced by difference between on-ground conditions for antenna alignment and mean temperature distribution encountered by the spacecraft over the orbital life	Based on dedicated satellite thermo-elastic analysis including STR, reflector and Feed Chain Interfaces TED.	
		Seasonal	TED_SC_seasonal	Seasonal mean value variation wrt overlife mean value (including BOL-EOL variation)		
		Daily	TED_SC_daily	Maximum variation during a day wrt seasonal mean value		
		Antenna allocation	TED_ANT_daily	Allocation for antenna depointing due to intrinsic thermo-elastic distortions of reflector and Feed Chain.		
AOCS	Star tracker	Individual STR internal bias error	AOCS_ST_IAB	Bias error due to on-ground handling, launch loads, gravity release, temperature shift between calibration temperature and on-orbit operating temperature range, etc.	From E3000 STR Optical Head unit characterization and measurement performance. As assuming a STR measure using a single optical head.	
		Individual STR internal short term stability	AOCS_ST_STS	Variation of the thermal and mechanical environment throughout 1 orbit		
		Individual STR internal long term bias stability	AOCS_ST_LTS	Aging, long term drift of operational temperature		
		Relativist aberration	AOCS_ST_RA	Durnal error due to relativistic aberration of light		
		Field of View error	AOCS_ST_FOV	Field of view noise		
		Pixel noise error	AOCS_ST_PNE	Pixel noise. But, in fact it is filtered by AOCS bandwidth for maneuver case.		
		OD Semi axis	AOCS_AK_LT_saxis	Ground and on-board orbit knowledge long term errors (tri-axiality, efficiency manoeuvre management, orbit determination semi-axis, initial longitude, SCU drift...)		
	OD Initial longitude	AOCS_AK_LT_long				
	On-board manoeuvre management PPS EW efficiency	AOCS_AK_LT_eweff				
	On-board manoeuvre management PPS tri-axiality	AOCS_AK_LT_triax				
	On-board Latitude determination SCU drift	AOCS_AK_LT_SCU				
	OD initial inclination	AOCS_AK_DT_incl	Ground and on-board orbit knowledge daily errors (orbit eccentricity, initial inclination, OBOC perfo...)			
	OD eccentricity	AOCS_AK_DT_excen				
	Orbit Knowledge	On-board latitude determination OBOC perfo	AOCS_AK_DT_OBOC			
		Control Performance	Bias	AOCS_CP_Bias	Constant off-pointing	Based on E3000 AOCS perfo analysis and measurements
			Wheel Friction step	AOCS_CP_wheel	Exceptional event due to wheel zero-crossing	
	Transient ISK manoeuvre		AOCS_CP_ISK	Exponentially decaying transient depointing during the thrust phase		

Table 7-23 Properties of Pointing Error Sources

Definition of PES				Description of PES							
Subsystem	Unit	PES	Name	Time-Random				Ensemble-Random			
				Distribution	Frequency [rad/s] with f = 1/T or f _{typ} or Time [s]				Origin		
					x	y	z				
MECHANICAL	Alignments	Antenna alignment wrt platform ref.cube	MEC_AL_ANT						uniform		
		STR alignment wrt platform ref. cube	MEC_AL_STR						uniform		
		CATR RF boresight measurement accuracy	MEC_AL_CATR						uniform		
		ADTM step accuracy	MEC_AL_ADTM						uniform		
	Stability	Launch vibration Feed chain	MEC_ST_FCA						uniform		
		Launch vibration reflector	MEC_ST_REF						uniform		
		Launch vibration STR	MEC_ST_STR						uniform		
		ADTM deployment repeatability	MEC_ST_ADTM						uniform		
		TED bias compensation residual	MEC_ST_TED						uniform		
		'0g' release residual	MEC_ST_0G						uniform		
THERMOELASTIC	Platform TED	Constant	TED_A_SC						-		
		Seasonal	TED_SC_seasonal	arcsine	1/T	1/T	1/T	T = 365d	Based on S/C seasonal and EOL/BOL data.	-	
		Daily	TED_SC_daily	Gaussian					PSD Specific profile of depointing over 24h (UCT time, each hour) available	-	
		Antenna allocation	TED_ANT_daily	arcsine	1,16E-05	1,16E-05	1,16E-05	T = 24h		delta	
AOCS	Star tracker	Individual STR internal bias error	AOCS_ST_IAB	-						Gaussian	
		Individual STR internal short term stability	AOCS_ST_STS	arcsine	1,16E-05	1,16E-05	1,16E-05	T = 24h			
		Individual STR internal long term bias stability	AOCS_ST_LTS	Gaussian							
		Relativist aberration	AOCS_ST_RA	-							delta
		Field of View error	AOCS_ST_FOV	Gaussian	4,00E+00	4,00E+00	4,00E+00		BLWN		
		Pixel noise error	AOCS_ST_PNE	Gaussian					BLWN		
		OD Semi axis	AOCS_AK_LT_saxis	Gaussian							
	Orbit Knowledge	OD Initial longitude	AOCS_AK_LT_long	Gaussian							
		On-board manoeuvre management PPS EW efficiency	AOCS_AK_LT_eweff	drift	6,0E+05	6,0E+05	6,0E+05	T=7days			
		On-board manoeuvre management PPS tri-axiality	AOCS_AK_LT_triax	drift	6,0E+05	6,0E+05	6,0E+05	T=7days			
		On-board Latitude determination SCU drift	AOCS_AK_LT_SCU	drift	6,0E+05	6,0E+05	6,0E+05	T=7days			
		OD initial inclination	AOCS_AK_DT_incl	Gaussian							
		OD eccentricity	AOCS_AK_DT_excen	Gaussian							
	Control Performance	On-board latitude determination OBOC perfo	AOCS_AK_DT_OBOC	Gaussian							
		Bias	AOCS_CP_Bias	-							delta
		Wheel Friction step	AOCS_CP_wheel	-	2,78E-04	2,78E-04	2,78E-04	T=1min	General Periodic Signal		
	Transient ISK manoeuvre	AOCS_CP_ISK	-						General Periodic Signal		



7.2.4.3 PEET Model and Budget

The PEET model of the entire pointing system is set up by grouping all errors sources according to the subsystem and unit they affect using container blocks. This is exemplarily illustrated for the control performance contributors of the AOCs in Figure 7-13.

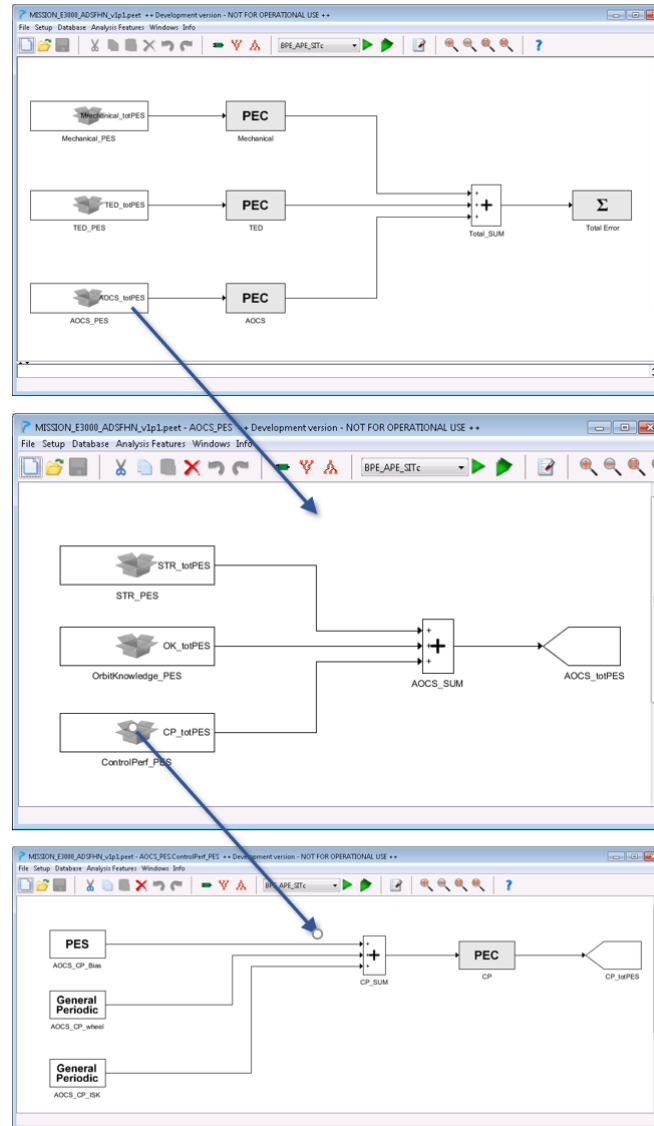


Figure 7-13: PEET pointing system model

In PEET the following different Beam Pointing Error budgets are computed:

- BPE_APE_SITc: is the pointing APE budget leading to the beam pointing error budget. It takes into account the APE requirement as specified in Table 7-19 with the temporal statistical interpretation. The level of confidence evaluation for the different ensemble domains (which correspond as mentioned to the different frequency classes A,B,C,D in the heritage budget) is common. This is computationally equivalent of having only one ensemble domain, but it structures the budget computation and according report by the



ensemble domains. Requiring the temporal statistical interpretation is equivalent with identifying the worst-case S/C in terms of time-constant PES for 99.7% of the time in orbit. This mainly concerns mechanical and alignment PES.

- REF_BPE_APE_SIMi: is the pointing APE budget leading to the beam pointing error budget. It takes into account another APE requirement as specified in Table 7-19. The difference is in the statistical interpretation and the level of confidence evaluation. The statistical interpretation is mixed and the level of confidence evaluation is done separately for each ensemble domain. This represents closest possible the heritage approach in Figure 7-11, i.e. a statistical summation of contributions within each frequency class (RSS for heritage) and linear summation over the different classes. There are some deviations remaining in terms of PES models as explained in the previous chapter mainly due to the use of frequency domain models or PES with non-Gaussian distributions.

The approach using an individual evaluation of the ensemble domain is flexible as it would allow specifying different level of confidence values to the different domains. However, in the reference budget the level of confidence is 99.7% for all the ensemble domains and thus kept for comparability. For the time-random behaviour the APE is ensured for 99.7% of the time in orbit. Note that this setup is implemented in PEET such that the budget computations are closest possible to the computation rules used in the reference budget.

- mSC_BPE_APE_SIMc: is the pointing APE budget leading to the beam pointing error budget. It takes into account another APE requirement as specified in Table 7-19. The difference is in the statistical interpretation. The statistical interpretation is mixed, but the level of confidence evaluation is done commonly. This approach corresponds to a purely statistical budget that treats all PES with its statistical nature and then evaluates it w.r.t. the level of confidence. The interpretation of such an approach is that all possible random combinations of S/C are considered and it is ensured that the S/C built will have a pointing APE that is smaller than the requirement value for 99.7% of all potentially built S/C and over 99.7% of the time in orbit.
- BPE_dailyRPE_SITc: is the pointing RPE budget leading to the beam pointing stability error budget over 24h. It takes into account the RPE requirement as specified in Table 7-19 with the temporal statistical interpretation. The level of confidence evaluation for the different ensemble domains is common. This is computationally equivalent of having only one ensemble domain, but it structures the budget computation and according report by the ensemble domains. Requiring the temporal statistical interpretation is equivalent with identifying the worst-case S/C in terms of time-constant PES for 99.7% of the time in orbit. This mainly concerns mechanical and alignment PES. Note that time-constant PES do not contribute to the RPE and thus the temporal statistical interpretation is equivalent to the mixed interpretation in this case.
- BPE_lifetimeRPE_SITc: is the pointing RPE budget leading to the beam pointing stability error budget over 365d. It takes into account the RPE requirement as specified in Table 7-19 with the temporal statistical interpretation. The level of confidence evaluation for the different ensemble domains is common. This is computationally equivalent of having only one ensemble domain, but it structures the budget computation and according report by the ensemble domains. Requiring the temporal statistical interpretation is equivalent with identifying the worst-case S/C in terms of time-constant PES for 99.7% of the time in orbit. This mainly concerns mechanical and alignment PES. Note the time-constant PES do not contribute to the RPE and thus the temporal statistical interpretation is equivalent to the mixed interpretation in this case.



Note that the budgets are computed with the transient ISK manoeuvre, i.e. the right side of Table 7-20. A summary of the results computed with PEET are shown in Table 7-24 and Table 7-25.

All APE budget values are normalized (per axis) with respect to the overall contribution of REF_BPE_APE_SIMi (marked in grey in Table 7-24). Similarly, all RPE budgets in Table 7-25 are normalized with respect to the overall contribution per axis for each requirement.

Table 7-24: Pointing APE budgets (normalized)

PEC Name	Level	Output Unit	Domain	Value Type	BPE_APE_SITc			Ref_BPE_APE_SIMi			mSC_BPE_APE_SIMc		
					Total Error			Total Error			Total Error		
					x	y	z	x	y	z	x	y	z
Total Error	0	°	Class A	Budget	0.579	0.513	0.616	0.314	0.275	0.489	0.314	0.275	0.489
			Class B	Budget	0.212	0.261	0.153	0.205	0.239	0.144	0.205	0.239	0.144
			Class C	Budget	0.321	0.341	0.128	0.321	0.341	0.128	0.321	0.341	0.128
			Class D	Budget	0.161	0.144	0.239	0.161	0.144	0.239	0.161	0.144	0.239
			overall	Budget	1.110	1.022	1.002	1.000	1.000	1.000	1.000	1.000	1.000
			Requirement		0.1	0.1	0.15	0.1	0.1	0.15	0.1	0.1	0.15
			Requirement ID		rAPEx_tot	rAPEy_tot	rAPEz_tot	rAPEx_tot	rAPEy_tot	rAPEz_tot	rAPEx_tot	rAPEy_tot	rAPEz_tot
AOCS	1	°	Class A	Budget	0.049	0.040	0.084	0.049	0.040	0.084	0.049	0.040	0.084
			Class B	Budget	0.005	0.219	0.008	0.005	0.219	0.008	0.005	0.219	0.008
			Class C	Budget	0.063	0.032	0.108	0.063	0.032	0.108	0.063	0.032	0.108
			Class D	Budget	0.161	0.143	0.239	0.161	0.144	0.239	0.161	0.143	0.239
			overall	Budget	0.223	0.327	0.361	0.277	0.436	0.439	0.223	0.327	0.361
Mechanical	1	°	Class A	Budget	0.530	0.473	0.532	0.284	0.251	0.421	0.284	0.251	0.421
			overall	Budget	0.530	0.473	0.532	0.284	0.251	0.421	0.284	0.251	0.421
TED	1	°	Class B	Budget	0.210	0.068	0.149	0.204	0.066	0.144	0.204	0.066	0.144
			Class C	Budget	0.309	0.339	0.068	0.309	0.340	0.068	0.309	0.339	0.068
			overall	Budget	0.480	0.372	0.198	0.514	0.405	0.212	0.427	0.354	0.169

Table 7-25: Pointing RPE budgets (normalized)

PEC Name	Level	Output Unit	Domain	Value Type	BPE_dailyRPE_SITc			BPE_lifetimeRPE_SITc		
					Total Error			Total Error		
					x	y	z	x	y	z
Total Error	0	°	Class A	Budget	0.000	0.000	0.000	0.000	0.000	0.000
			Class B	Budget	0.015	0.334	0.036	0.410	0.449	0.459
			Class C	Budget	0.888	0.869	0.528	0.619	0.781	0.370
			Class D	Budget	0.372	0.313	0.841	0.260	0.281	0.590
			overall	Budget	1.000	1.000	1.000	1.000	1.000	1.000
			Requirement		0.05	0.05	0.055	0.07	0.07	0.075
			Requirement ID		rdailyRPEx_tot	rdailyRPEy_tot	rdailyRPEz_tot	rlifetimeRPEx_tot	rlifetimeRPEy_tot	rlifetimeRPEz_tot
AOCS	1	°	Class A	Budget	0.000	0.000	0.000	0.000	0.000	0.000
			Class B	Budget	0.014	0.335	0.035	0.010	0.350	0.025
			Class C	Budget	0.173	0.082	0.443	0.121	0.074	0.311
			Class D	Budget	0.372	0.312	0.842	0.259	0.281	0.591
			overall	Budget	0.410	0.443	0.959	0.286	0.447	0.673
Mechanical	1	°	Class A	Budget	0.000	0.000	0.000	0.000	0.000	0.000
			overall	Budget	0.000	0.000	0.000	0.000	0.000	0.000
TED	1	°	Class B	Budget	0.003	0.001	0.003	0.406	0.156	0.444
			Class C	Budget	0.855	0.864	0.290	0.596	0.776	0.203
			overall	Budget	0.857	0.864	0.291	0.926	0.852	0.592

It can be observed from Table 7-24 that the statistical interpretation and the level of confidence evaluation (common or separately for the different ensemble domains) has a considerable impact on the overall value.

The RPE budgets in Table 7-25 are computed based on the same model in PEET. I.e., in PEET there is only one model that represents the S/C behaviour in terms of pointing and the daily and lifetime RPE are computed by PEET based on the nature of the PES in the frequency domain. This is one of the major advantages of PEET. It allows to compute several requirements with one model.

The probability density function (PDF) and corresponding cumulative distribution function of the pointing APE are shown in Figure 7-14. It can be seen that the overall pointing errors are not Gaussian distributed, especially for x- and z-axis. This non-Gaussian behaviour is



mainly caused by the thermoelastic deformation (TED) PES. However, PEET computes the level of confidence (LoC) based on the CDF in the figure and thus ensures precise evaluation.

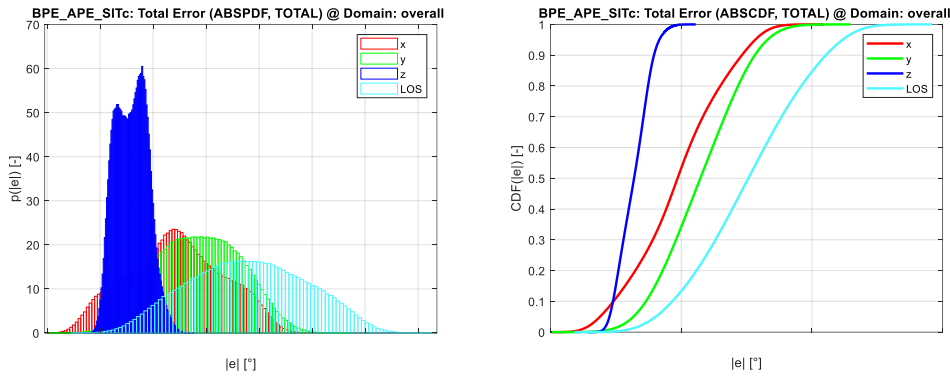


Figure 7-14: Overall Pointing Error PDF and CDF

The probability density function (PDF) of the North-South and East-West pointing errors are shown in Figure 7-15. The BPE is computed via a post-processing script in PEET that uses directly the accurately modelled pointing behaviour with its underlying PDFs and maps it to the half-cone BPE. Note that PEET does not use any assumption to compute the PDF at LoS and BPE. It uses the PDF on the single axes and combines them mathematically accurate in the sample-based approach implemented in PEET

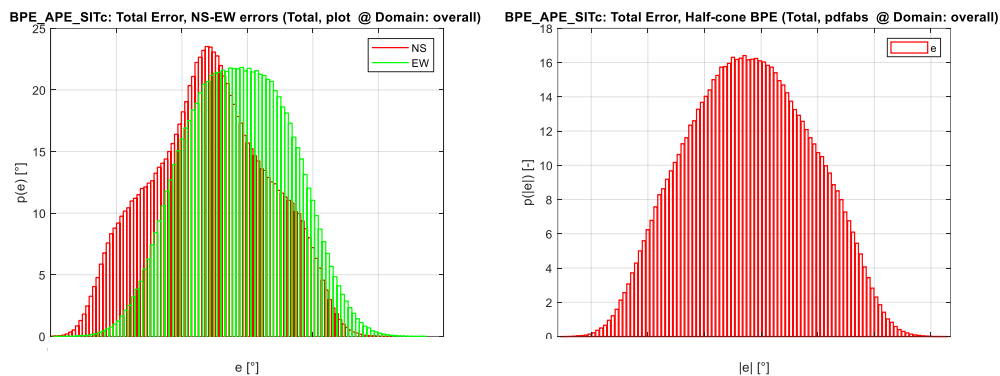


Figure 7-15: Overall PDF for NS/EW errors and half-cone BPE error

7.2.5 Budget Comparison

7.2.5.1 PEET Budget vs Heritage Approach

In this section the reference pointing error budgets of section 7.2.4.1 are compared to the pointing error budgets computed with PEET in section 7.2.4.3. The budgets are compared for the transient ISK manoeuvre, i.e. the left side of Table 7-20. The (normalized) results are shown in Table 7-26.

Table 7-26: Reference budget versus PEET budget (normalized)



Requirement		Reference budgets (section 7.2.4.1) in [°]	PEET budgets (section 7.2.4.3) in [°]
BPE_APE_SITc	x	1	1.13
	y	1	0.94
	z	1	0.83
	BPE	1	1.17
REF_BPE_APE_SIMi	x	1	1.03
	y	1	0.92
	z	1	0.83
	BPE	1	1.15
mSC_BPE_APE_SIMc	x	1	0.62
	y	1	0.57
	z	1	0.53
	BPE	1	0.60
BPE_dailyRPE_SITc	x	1	0.83
	y	1	0.67
	z	1	0.65
	BPE	1	0.75
BPE_lifetimeRPE_SITc	x	1	0.86
	y	1	0.57
	z	1	0.80
	BPE	1	0.77

The main differences are summarized in the following:

- The classification of PES in class A to D is introduced in the E3000 reference budget in Table 7-20 to evaluate pointing performance requirements w.r.t. seasonal or daily time-windows, i.e. the RPE requirements stated in section 7.2.2. This classification is not necessary when using PEET because the software determines automatically the contribution to a time-window by selecting the power/error in the corresponding frequency range. This leads to the following changes in the PES models used in PEET:
 - The six PES, TED_PF_seasonal_[...], modelled as delta distribution, and describing the TED seasonal worst case value of different seasons (summer solstice, winter solstice, equinox) and BOL/EOL, are substituted by a single PES.



This PES is modelled as a periodic signal with a uniform distributed amplitude that ranges from the minimum amplitude of all seasons as well as BOL/EOL to the max amplitude of all seasons as well as BOL/EOL.

- The six PES, TED_PF_daily_[...], are modelled as PSD as described in section 7.2.4.2. Using this modelling approach, the corresponding PEC is considerably smaller on the y-axis compared to the reference budget.
 - The wheel friction steps/spikes are modelled as general periodic signal in PEET instead of a Gaussian distributed PES. This increases accuracy as the PDF of a step/spike is not Gaussian by far. Note that it is assumed that the steps/spikes always occur in the same direction. Thus, such models capture also well the thereby introduced mean value.
 - The class A errors are modelled where suitable as uniform distribution instead of equivalent Gaussian. This reduces the conservatism compared to the reference method because 3-sigma LoC of a uniform distribution is >>100%.
- The semi-analytical and sample-based computation approach in PEET has the following essential differences compared to the approach of the reference in Figure 7-11:
- Daily TED in class C, i.e. TED_PF_daily and TED_ANT_daily, are not summed correlated although they have the same frequency, PEET does this automatically if the same frequency is detected and the phase is not changed by the user input.
 - In the reference method, biases are modelled as delta distribution, but they are summed quadratic instead of linearly. In PEET and the PEEH, delta distribution values are summed linearly as they are expected to be known exactly without distribution.
 - Drifts signals in class B have mean values which are summed linearly in PEET as they are not randomly distributed, see AOCs_OK_xx PES. In the reference method they are summed quadratic as part of the full drift contribution.
 - The accurate sample-based transformation from pointing APE per axis to half-cone BPE shows that the approach taken in the reference method is more optimistic for the given scenario.

Note that the REF_BPE_APE_SIMi budget is evaluated with the advanced statistical method and the simplified statistical method to demonstrate the gain in accuracy of using the advanced statistical method. In the majority of the cases one can say that the advanced statistical method is less conservative. However, that strongly depends on the definition of the statistical domains with their evaluation (separate or common; here: separate), the probability distributions of the PES and the resulting final distribution. In case of the E3000 case study the simplified method results in a budget that is 10-25% more conservative as can be seen in Table 7-27 (all results are normalized per axis w.r.t. the overall contribution obtained with the advanced method). This would be different with a common level of confidence evaluation, as in this case the time-constant contributions to a statistical domain could be of opposite sign and compensate each other.

PEC Name	Level	Output Unit	Domain	Value Type	Ref_BPE_APE_SIMi			Ref_BPE_APE_SIMi_SM		
					Total Error			Total Error		
					x	y	z	x	y	z
Total Error	0	°	Class A	Budget	0.314	0.275	0.489	0.343	0.302	0.646
			Class B	Budget	0.205	0.239	0.144	0.253	0.380	0.179
			Class C	Budget	0.321	0.341	0.128	0.472	0.438	0.136
			Class D	Budget	0.161	0.144	0.239	0.143	0.129	0.211
			overall	Budget	1.000	1.000	1.000	1.211	1.248	1.172
			Requirement	0.1	0.1	0.15	0.1	0.1	0.15	
Requirement ID					rAPEx_tot	rAPEy_tot	rAPEz_tot	rAPEx_tot	rAPEy_tot	rAPEz_tot



Table 7-27: REF_BPE_APE_SIMi budget with advanced statistical method (left) and with simplified statistical method (right)

Further, it is interesting to compare the PEET results from BPE_APE_SITc, REF_BPE_APE_SIMi and mSC_BPE_APE_SIMc which in fact all represent different requirements. As expected, the first leads to the most conservative result as the temporal interpretation accounts for the respective worst-case ensemble realizations of the different sources. Using the mixed interpretation instead (REF_BPE_APE_SIMi and mSC_BPE_APE_SIMc) leads to smaller budget values as the entire space of ensemble realizations is accounted for in the statistics rather than only worst-case temporal behaviour.

The different results for these mixed SI requirement sets are due to the fact that the ensemble domains are evaluated once commonly and once individually (although the same level of confidence is applied to each domain). As expected, the individual evaluation is more conservative as the level of confidence evaluation is applied to each domain contribution first before the resulting (scalar absolute) values from the different domains are summed linearly to compile the overall error. The common evaluation in mSC_BPE_APE_SIMc considers the entire statistical behaviour of all contributors together for the total error compilation leading to a less conservative result.

This comparison leads to the following conclusions:

- It is important to clearly specify the statistical interpretation applicable to a requirement according to the needs of mission as the results can differ significantly. This is also true for the two different evaluation methods (common/individual) when the domain concept is used.
- Further, it is helpful to be able to allocate contributors from similar origin (AIT, after-launch effects, seasonal & daily effects, etc) to dedicated domains and – although not used in the considered scenario - to assign even a different statistical treatment and level of confidence to each to tailor a requirement more precisely to the actual mission needs.

7.2.5.2 Comparison with In-Flight Data

In this section the reference pointing error budgets of section 7.2.4.1 are compared to the in-flight de-pointing measured during IOT campaign.

The main objective of the IOT antenna de-pointing measurement is to validate both that the daily excursion is within the allocation on the budget (mainly driven by the TED) and that the global bias de-pointing is within the expected value (mainly driven by TED bias term and mechanical alignment/stabilities). A comparison both in Roll and Pitch angles was performed between:

- The predicted TED profiles from platform interfaces with the antenna (no reflector TED contribution included in the S/C thermo-elastic FEM model) for the six seasons along lifetime: EQBOL, EQEOL, SSBOL, SSEOL, WSBOL and WSEOL.
- The in-flight measured de-pointing at the moment of IOT. The IOT measurement of the reference mission took place during Summer Solstice period, so the closest reference of the prediction is SSBOL data.

When making a comparison of the de-pointing profiles, the following conclusions are drawn:



- Consistency of the time series (in shape and order of magnitude) in terms of daily de-pointing excursion between the allocation in the (SSBOL) reference pointing error budgets of section 7.2.4.1 (based on worst-case platform prediction and an allocation for the reflector antenna) and the IOT measurement which furthermore includes both platform and reflector antenna TED effects.
- Consistency in order of magnitude in terms of de-pointing bias when comparing the IOT profile to the expected constant term of platform TED profile at the season of IOT (SSBOL) and the allocation in the reference pointing error budgets for mechanical alignment and launch stability errors.

7.2.6 Conclusions and Lessons Learnt

The following conclusions and lessons learnt can be drawn from this case study from the perspective of the consultants from Airbus (Toulouse).

Generally, the pointing budget approach of the reference study case (heritage) is sufficiently accurate, but a bit more conservative than the PEET approach. However, the approach is very specific as certain assumptions are taken that result in specific summation rules. This leads to correct pointing budgets in the end, but the computation approach likely differs for different companies and even projects. Having different approaches introduces unnecessary overhead in the projects in terms of achieving a common understanding and coherent approach.

The following PEET-related conclusions are drawn:

- The tool enables fast and accurate computations without going into the details of the actual summation. It is sufficient to understand and define well the PES models and requirements specification. The computation is then done by PEET. This is e.g. different for the reference budgeting approach in in Figure 7-11. The contribution to time-windowed errors is determined by PEET automatically. This reduces the budgeting effort and ensures consistency.
- The possibility of determining accurately the PDF of the overall performance error increases accuracy. The overall pointing errors in this study case are not Gaussian distributed.
- The tool eases the compartmentalization and exchange of the different PES coming from diverse subsystems.
- The new post-processing features in PEET enable to analyse several performance quantities that are linked to telecom-relevant pointing performance. In this way the advantage of PEET can be used also for computing these quantities.

As an outlook it is suggested to group the pointing error sources in ensemble domains representing activities on ground and operations in orbit. In this way specific level of confidence values can be assigned individually to represent better the actual needs. For instance, one might want to ensure that the worst-case S/C is built (i.e. time-constant PES) within the requirement, but a bias (time-constant in one observation) changing from one to another observation is considered acceptable.

7.3 Spacebus NEO (Thales Alenia Space)

SPACEBUS NEO is Thales Alenia Space's new telecommunication satellite product line. The AOCS concept based on a 3-axis measured and stabilized attitude control without on-board angular momentum is proposed to cover all the product line.



Figure 7-16: Spacebus NEO Thales Alenia Space spacecraft

NEOSAT AOCS is partially inherited from Alphabus and IRN AOCS, but has been improved to cope with new design drivers. NEOSAT AOCS design drivers have the following origins:

- Competitiveness improvement
- Specific concepts associated to full electrical configuration

It is proposed in several propulsion versions for Orbit Raising and Station Keeping, such as all chemical, all electric version and hybrid propulsion. The spacecraft is able to carry till 2 tons of payload with a power till 20 kW.

Some of the current developments of the Spacebus NEO are:

- SES 17: Ordered by SES, it is an all-electric version of SB NEO, providing 15kW of power, with 6.6 Tons of weight. It will have 200Ka band spots providing internet connections to North-Central America and Atlantic ocean. It will be launched in 2021.
- Konnect Africa: Commanded by Eutelsat, it is an all-electric configuration, with chemical thrusters for attitude control, it provides 7 kW of power to the payload and offers with 65 spot beam with a total capacity of 75 GBPS of data transmission. It will be launched in 2019.
- Konnect VHTS: Commanded by Eutelsat, it is an all-electric version to provide broadband connections to European countries. Capacity of 500Bbps in Ka band, 6.3 Tons and will start its mission in 2021.

The mission objectives in terms of pointing accuracy are to guarantee the coverage of a certain geographical area within the desired accuracy. The AOCS is composed by 4 modes:

- Station keeping mode (SKM)
- Safe Hold mode (SHM)
- Orbit Raising mode (ORM)

■ Nominal mode (NOM)

The main driver of the pointing system is to provide the desired accuracy for the whole mission duration (18 years) during nominal and station keeping modes. Only these two modes will be considered in the P4COM reference case.

The spacecraft as introduced is designed for geostationary orbit, and the AOCS is based on RW, XPS/CPS (Xenon or Chemical Power System) and Star trackers. The gyroscope utilization is limited for cost reductions. The overall AOCS architecture is made up of:

- 4 reaction wheels Honeywell HR16 with 100Nms capacity used for pointing stabilization and slew manoeuvres
- Two star trackers used in hot redundancy: a primary STR, tracking 10 stars with the back-up of a secondary one, tracking 5 stars, that is promoted in the case of primary STR occlusion.
- A GNSS is used to improve absolute pointing knowledge errors due to orbit determination
- A coarse gyroscope is used for Safe mode, while nominal mode is gyroless

The presented AOCS configuration provides an absolute pointing error with respect to the attitude guidance required to guarantee geographical zone coverage. The attitude pointing accuracy is a main driver for the antenna power and sizing. Indeed, if the attitude pointing error is high, the antenna must compensate this error with a higher transmission power, to ensure the required SNR on the whole zone.

The main performance indexes observed are the total APE of the line of sight for each antenna/spot, as well as its daily and seasonal stability. The proposed spacecraft configuration is the Spacebus Neo one for geostationary orbit presented below.

The telecommunication payloads can embark either classical RF antenna systems with Multi-spots or Single coverage, either Optical links. The following figure presents an example of the coverage zones:

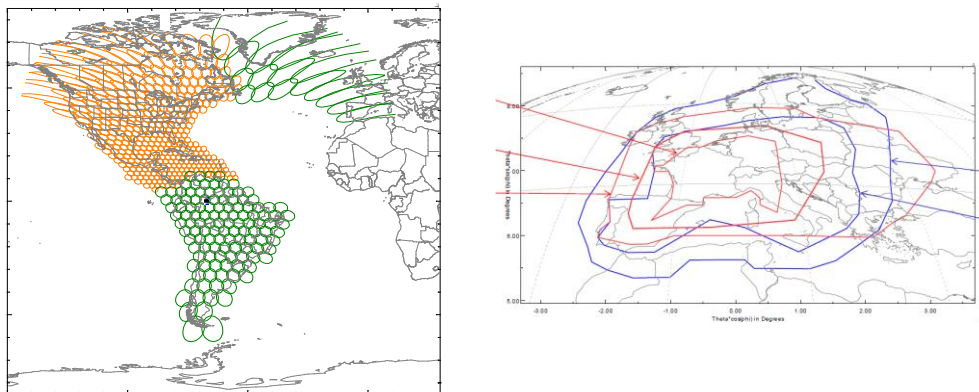


Figure 7-17: Reference mission coverage examples (American continent, West Europe) [RD20]



7.3.1 Motivation

The Thales Alenia Space Spacebus NEO has been an interesting scenario, because it consists in a high pointing performance GEO telecom spacecraft with a multispot antenna. Some of the interesting points to justify this selection are:

- The current version of PEET is quite adapted for the current spacecraft pointing budget at high level. However, to complete the Spacebus NEO platform system pointing budget the following features could be added:
 - The possibility of merging the performance of different modes during the same simulation could allow computing directly the overall pointing performance during different pointing modes for the whole lifetime, with a certain level of confidence.
 - The antenna coverage capability, which is common for a telecommunication spacecraft, could allow computing the overall pointing performance over the whole antenna coverage or over each spot (for multi-spots antennas). This performance can then be directly used by antenna team for the design.
- The spacecraft design is relatively advanced and consolidated, allowing a valid comparison between the PEET results and robustness analysis performance.

7.3.2 Pointing Requirements

With the ECSS approach, the pointing requirement for SBNEO is formulated as:

- *The Spacebus NEO platform shall provide an absolute steady state pointing error during the whole mission in nominal and station keeping mode, at antenna Line of Sight level (half cone) of R_z with 99.7% confidence level, using mixed interpretation*

Another performance index useful for the spacecraft design, not considered as a pointing requirement, is the Beam Pointing Error. This is a Relative Performance Error (RPE) computed on a large time window, such as a day or the whole spacecraft lifetime (daily and seasonal stability). With ECSS formalism the requirement can be formulated as:

- *The Spacebus NEO platform shall provide relative performance pointing error, over 1 day time window, during the whole mission in nominal and station keeping mode, at antenna Line of Sight level (half cone) of RPE_1 with 99.7% confidence level, using mixed interpretation*
- *The Spacebus NEO platform shall provide relative performance pointing error, over the spacecraft lifetime, in nominal and station keeping mode, at antenna Line of Sight level (half cone) of RPE_2 with 99.7% confidence level, using mixed interpretation*

In practice, the BPE daily is the APE of the line of sight without taking into account constant biases, aging and seasonal errors of the budget. In the same way, the BPE lifetime is the APE without the biases, including seasonal and aging terms.

In the same way, a performance index needed during the antenna design is the antenna coverage pointing performance. This means to integrate spatially the pointing error distribution over whole antenna solid angle, not only considering the boresight. This is useful to increase the width of the coverage, providing additional power to the antenna, to compensate the pointing error. An analytical approach seems quite complex, but a discrete approach could be evaluated:

- Subdivide the ground coverage zone in N samples.
- Compute the line of sights error probability density of each sample

- Combine the obtained probability density to obtain an overall distribution inside the zone.

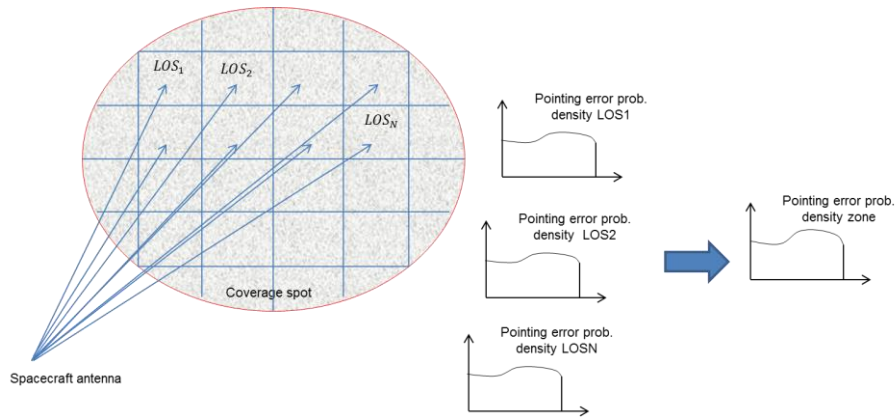


Figure 7-18: Illustration of the ground coverage zone pointing error possible computation [RD17]

7.3.3 Heritage approach

The pointing engineering approach used for Telecommunication Platform design in Thales Alenia Space is based on a classical V-cycle approach, coordinated by the system engineer who makes the interface between the different subsystem experts.

The first step is the definition of the mission pointing error needs at system or instrument level, derived directly from the payloads and the mission objectives.

The next phase is the allocation of the system pointing error at each subsystem and subsystem components, through a first iteration with all experts of the satellite design chain. The values are derived, if possible, from flight data and heritage, or preliminary analysis if no previous experience on the component is available.

Afterward, while the design process advances and the subsystem details are available, the pointing error is re-evaluated and the budget is refined or adapted to eventual design constraints.

The standards used for telecommunication satellites come from Thales Alenia Space internal heritage, or specific client needs. The main tools used for the interface of the process are interface documents including the results and the justification of the performed analysis. Excel spread sheets are widely used to summarize these results, annexing 3D models, mechanical and thermal models or Matlab files if necessary. The current system pointing budget is compiled in Microsoft Excel.

For the computation of the pointing budget, the different error sources are classified according to their time scale category:

- C : Constant errors
- D : Daily variation disturbances
- L : Long term disturbances, longer than daily.
- S : Short terms disturbances such as AOCS errors

All disturbances are considered with 99.73% confidence level, with a Gaussian probability distribution hypothesis. For each category different kinds of summation rules are used, such as:

- Uncorrelated errors in the same category are summed in an RSS (Root Sum Square) way.
- The total contribution of all categories, for each axis (roll, pitch, yaw), is calculated through a direct sum of all the terms, obtaining a total pointing error for each axis.
- Then, the yaw contribution error is included to the Roll and Pitch terms
- Finally, the half cone error is computed.

Yaw coupling error

To compute the half cone error, the yaw errors need to be taken into account into the roll and pitch errors. Indeed, for each antenna:

- The effect of the yaw error on the ground coverage is computed, the worst case on the coverage polygon is considered
- The ground error is projected on roll and pitch effect axes on ground.
- The corresponding angular error in roll and pitch is obtained

Figure 7-19 gives a representation of the effect of the yaw on the coverage zone, decomposed in roll and pitch. Once the Yaw contribution on roll and pitch is obtained, the half cone error can be computed.

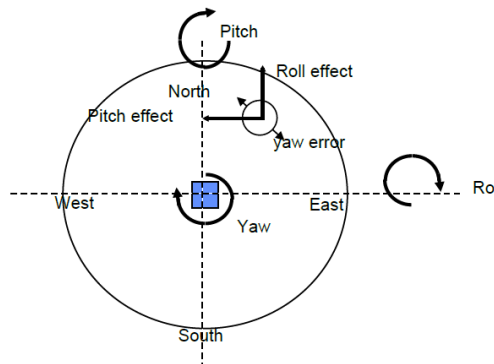


Figure 7-19: Yaw coupling effect [RD20]

Half cone computation

The half cone error, as introduced in previous section, given Roll (North/South) and Pitch (East/West) error angles E_x and E_y , is defined as the value of R_z , for which the probability of having $E_x + E_y \leq R_z$ is lower than the chosen confidence interval c (0.9973 in the budget). This quantity is computed as the integral of the product between the probability density functions of Roll and Pitch errors, over the area defined by $E_x + E_y < R_z$.

$$P_{confidence\ level} = \iint_{E_x + E_y < R_z} P(E_x)P(E_y) dE_x dE_y$$



The hypothesis of a Gaussian probability density function for each component $P(E_x)$ and $P(E_y)$ is made in the current version of the budget. Note that the hypothesis is valid if the number of contributors is large enough and no dominant non-Gaussian contributor is present, otherwise a more appropriate probability density function shall be used. Solving the integral in a numerical way, allows computing the function Φ , for which:

$$R_z = \Phi(E_x/E_y, c)$$

7.3.4 Pointing Budgets

7.3.4.1 Pointing Error Sources

The pointing budget is composed by several pointing error sources, between 15 and 20 according to implementation details, regrouped in the following families:

- Antenna internal errors:
This includes the characterization, behaviour and thermal distortion of the antenna
- Structure behaviour:
It consists in the alignment knowledge error between reflector and source, the stability during tests on ground and after launch, the structure distortion due to gravity, and all other sources related to assembly and measurements.
- Thermo-elastic distortions:
It comprehends star tracker distortion, platform thermo-elastic distortion, antenna pointing mechanism (ADPM) distortion.
- AOCS pointing error:
It consists in star tracker attitude estimation error, control pointing errors and disturbances due to orbit correction manoeuvres and SADM error.
- Orbit prediction errors:
- Errors due to orbit estimation (by GNSS) and propagation of on-board software.

7.3.4.2 PES Characterization

All errors sources defined for the PEET scenario including their properties, justification and classification according to the PEEH are shown in Table 7-28 to Table 7-30.



Table 7-28: SPACEBUS NEO - Properties of Pointing Error Sources

Subsystem	Unit	Definition of PES		Description of PES					Ensemble-Random		
		PES	Name	Distribution	Time-Random			Origin		random process data type	
					1/T or f_{freq} or Time [s]	x	y				z
AOCS	STR	Individual STR internal bias	AOCS_STR_BIAS	-	-	-	-	-	-	uniform	
		Individual STR support structure stability	AOCS_STR_STS	bimodal	1.16E-05	1.16E-05	1.16E-05	T = 24h	Amp. Spec.	-	
		Relative low frequency thermoelastic	AOCS_STR_LFTE	bimodal	1.16E-05	1.16E-05	1.16E-05	T = 24h	Amp. Spec.	-	
	On orbit propagator	OBT bias (+/- 1s)	AOCS_OBT_BIAS	Uniform	-	-	-	-	-	-	-
		OBT stability	AOCS_OBT_STAB	drift specific PDF	9.26E-05	9.26E-05	9.26E-05	T=3h	Drift	-	
	GNSS	ESK manoeuvre uncertainty	AOCS_ESK	Triangular periodic signal	7.72E-06	7.72E-06	7.72E-06	T=36h	Drift	-	
		Orbit window N/S	AOCS_GNSS_NS	drift specific PDF	9.26E-05	9.26E-05	9.26E-05	T=3h	Drift	-	
Attitude control	Orbit window E/W	AOCS_GNSS_EW	drift specific PDF	9.26E-05	9.26E-05	9.26E-05	T=3h	Drift	-		
	Attitude control errors ESK	AOCS_CTRL_ESK	Decaying cosine periodic sig	7.72E-06	7.72E-06	7.72E-06	T=36h	Amp. Spec.	Gaussian		
	Attitude control errors nominal	AOCS_CTRL	Gaussian	1.0E+01	1.0E+01	1.0E+01	T=0.1s	BLWN	-		
ANTENNA	Antenna characterization & distortions	Antenna RF boresight characterization	ANT_RF_BRSG	-	-	-	-	-	-	Gaussian	
		Thermo-elastic Deployable Antenna - Feed	ANT_THRM_FEED	bimodal (discrete amplitude)	1.2E-05	1.2E-05	1.2E-05	T = 24h	Amp. Spec.	-	
		Thermo-elastic Deployable Antenna - Reflector	ANT_THRM_REFL	bimodal (discrete amplitude)	1.2E-05	1.2E-05	1.2E-05	T = 24h	Amp. Spec.	-	
	Antenna & Sensors Integration	Antenna Angular alignment	ANT_ALIGN_ACC	-	-	-	-	-	-	Uniform	
		Gravity compensation error during alignment	ANT_ALIGN_GRAV	-	-	-	-	-	-	Uniform	
		Alignment measurement	ANT_ALIGN_MEAS	-	-	-	-	-	-	Gaussian truncated	
		ADPM resolution (Roll&Pitch)	ANT_ADPM_RES	-	-	-	-	-	-	Uniform	
Alignments	Structure hysteresis due to launch loads	ST_HYST	-	-	-	-	-	-	Gaussian		
	Gravity residual effect	ST_GRAV	-	-	-	-	-	-	uniform		
	Hygroscopic effect	ST_HYGR	-	-	-	-	-	-	uniform		
Thermo-elastic	Structure thermo-elastic bias	ST_THRM_BIAS	-	-	-	-	-	-	Uniform		
	Seasonal structure thermo-elastic distortion	ST_THRM_DIST	bimodal (discrete amplitude)	3.2E-08	3.2E-08	3.2E-08	T=1 year	Amp. Spec.	-		
	STR Support thermo-elastic distortion	ST_STR_DIST	bimodal (discrete amplitude)	1.2E-05	1.2E-05	1.2E-05	T = 24h	Amp. Spec.	-		
	ADPM thermo-elastic distortion	ST_ADPM_DIST	bimodal (discrete amplitude)	1.2E-05	1.2E-05	1.2E-05	T = 24h	Amp. Spec.	-		

Table 7-29: SPACEBUS NEO - Classification of Pointing Error Sources

Subsystem	Unit	PES	Name	Time-random	Ensemble-random (= time-constant)	Class	On interface	Type	
AOCS	STR	Individual STR internal bias	AOCS_STR_BIAS		X	bias	no	variable	
		Individual STR support structure stability	AOCS_STR_STS	X		periodic	no	process	
		Relative low frequency thermoelastic	AOCS_STR_LFTE	X		periodic	no	process	
	On orbit propagator	OBT bias (+/- 1s)	AOCS_OBT_BIAS		X		random	no	variable
		OBT stability	AOCS_OBT_STAB		X		drift	no	Process
	GNSS	ESK manoeuvre uncertainty	AOCS_ESK		X		Periodic	no	Process
		Orbit window N/S	AOCS_GNSS_NS				drift	no	Process
Attitude control	Orbit window E/W	AOCS_GNSS_EW				drift	no	Process	
	Attitude control errors ESK	AOCS_CTRL_ESK		X		Periodic	no	Process	
	Attitude control errors nominal	AOCS_CTRL		X		random	no	process	
ANTENNA	Antenna characterization & distortions	Antenna RF boresight characterization	ANT_RF_BRSG	X	X	Bias	no	variable	
		Thermo-elastic Deployable Antenna - Feed	ANT_THRM_FEED	X		Periodic	no	process	
		Thermo-elastic Deployable Antenna - Reflector	ANT_THRM_REFL	X		Periodic	no	process	
	Antenna & Sensors Integration	Antenna Angular alignment	ANT_ALIGN_ACC			X	Bias	no	variable
		Gravity compensation error during alignment	ANT_ALIGN_GRAV			X	Bias	no	variable
		Alignment measurement	ANT_ALIGN_MEAS			X	Bias	no	variable
	ADPM resolution (Roll&Pitch)	ANT_ADPM_RES			X	Bias	no	variable	
Alignments	Structure hysteresis due to launch loads	ST_HYST			X	bias	yes	variable	
	Gravity residual effect	ST_GRAV			X	bias	no	variable	
	Hygroscopic effect	ST_HYGR			X	bias	no	variable	
Thermo-elastic	Structure thermo-elastic bias	ST_THRM_BIAS		X		bias	no	variable	
	Seasonal structure thermo-elastic distortion	ST_THRM_DIST			X	Periodic-1year	no	process	
	STR Support thermo-elastic distortion	ST_STR_DIST			X	Periodic 1 day	no	process	
	ADPM thermo-elastic distortion	ST_ADPM_DIST			X	Periodic 1 day	no	process	



Table 7-30: SPACEBUS NEO - Justification of Pointing Error Sources

Definition of PES				Justification of PES
Subsystem	Unit	PES	Name	Origin
AOCS	STR	Individual STR internal bias	AOCS_STR_BIAS	ARF to BRF bias due to on-ground handling, launch loads, gravity release, temperature shift between calibration temperature and on-orbit operating temperature range, etc.
		Individual STR support structure stability	AOCS_STR_STS	Thermo-elastic stability of the star tracker support structure throughout 1 orbit
		Relative low frequency thermoelastic	AOCS_STR_LFTE	Thermo-elastic stability (STR internal) causing a periodic variation of the relative alignment of the two BRFS throughout 1 orbit
	On orbit propagator	OBT bias (+/- 1s)	AOCS_OBT_BIAS	On board time accuracy
		OBT stability	AOCS_OBT_STAB	On board time stability
	GNSS	ESK maneuver uncertainty	AOCS_ESK	Maneuver uncertainty introduced in on board propagator, general periodic triangular signal with 36h period and 8.3% of activation time
		Orbit window N/S	AOCS_GNSS_NS	Pointing error due to orbit uncertainties in N/S direction
Attitude control	Orbit window E/W	AOCS_GNSS_EW	Pointing error due to orbit uncertainties in E/W direction	
	Altitude control errors ESK	AOCS_CTRL_ESK	Disturbance on AOCS due to station keeping maneuvers	
ANTENNA	Antenna characterization & distortions	Altitude control errors nominal	AOCS_CTRL	Typical AOCS closed-loop filtered errors
		Antenna RF boresight characterization	ANT_RF_BRSG	Accuracy of the characterization of the antenna boresight on ground
		Thermo-elastic Deployable Antenna - Feed	ANT_THRM_FEED	Thermo-elastic deformation of the feed during 1 orbit
	Antenna & Sensors Integration	Thermo-elastic Deployable Antenna - Reflector	ANT_THRM_REFL	Thermo-elastic deformation of the reflector during 1 orbit
		Antenna Angular alignment	ANT_ALIGN_ACC	Residual misalignment of the antenna with respect to the structure
		Gravity compensation error during alignment	ANT_ALIGN_GRAV	Gravity compensation error during the alignment
STRUCTURE	Alignments	Alignment measurement	ANT_ALIGN_MEAS	Accuracy of the alignment
		ADPM resolution (Roll&Pitch)	ANT_ADPM_RES	Resolution of the antenna pointing mechanism
		Structure hysteresis due to launch loads	ST_HYST	Payload-structure misalignment deformation due to launch loads
	Thermo-elastic	Gravity residual effect	ST_GRAV	Payload-structure misalignment deformation due to gravity
		Hygroscopic effect	ST_HYGR	Antenna misalignments after outgassing of the residual moisture absorbed
		Structure thermo-elastic bias	ST_THRM_BIAS	Structure thermo-elastic distortion bias
		Seasonal structure thermo-elastic distortion	ST_THRM_DIST	Structure seasonal thermo-elastic distortion
STR Support thermo-elastic distortion	ST_STR_DIST	Star tracker support daily thermoelastic distortion		
ADPM thermo-elastic distortion	ST_ADPM_DIST	Antenna pointing mechanism daily thermo-elastic distortion		

7.3.4.3 PEET Model and Budget

Figure 7-20 shows the top-level PEET model used with the PES as defined in the previous section. The only system transfer models used are frame transformation blocks, especially to compute attitude errors and distortions from star tracker error spacecraft body axes and from body axes to antenna reference frame.

Further, different ensemble domains were introduced to group the PES according to their 'physical nature' of the ensemble-randomness:

- Thermo-elastic
- AIT
- Onboard orbit propagator
- Spacecraft body pointing (sensing and AOCS)
- Structure behaviour
- Station-Keeping

These domains are evaluated commonly with a level of confidence of 99.73% and using mixed statistical interpretation (with the only exception of the station-keeping sources which are evaluated in a worst-case sense, i.e. with temporal interpretation). Thus, the ensemble domains do not directly reflect the frequency classes from the heritage approach. They generally contain sources from different heritage frequency classes are also entirely summed statistically – within each domain and over the various domains.

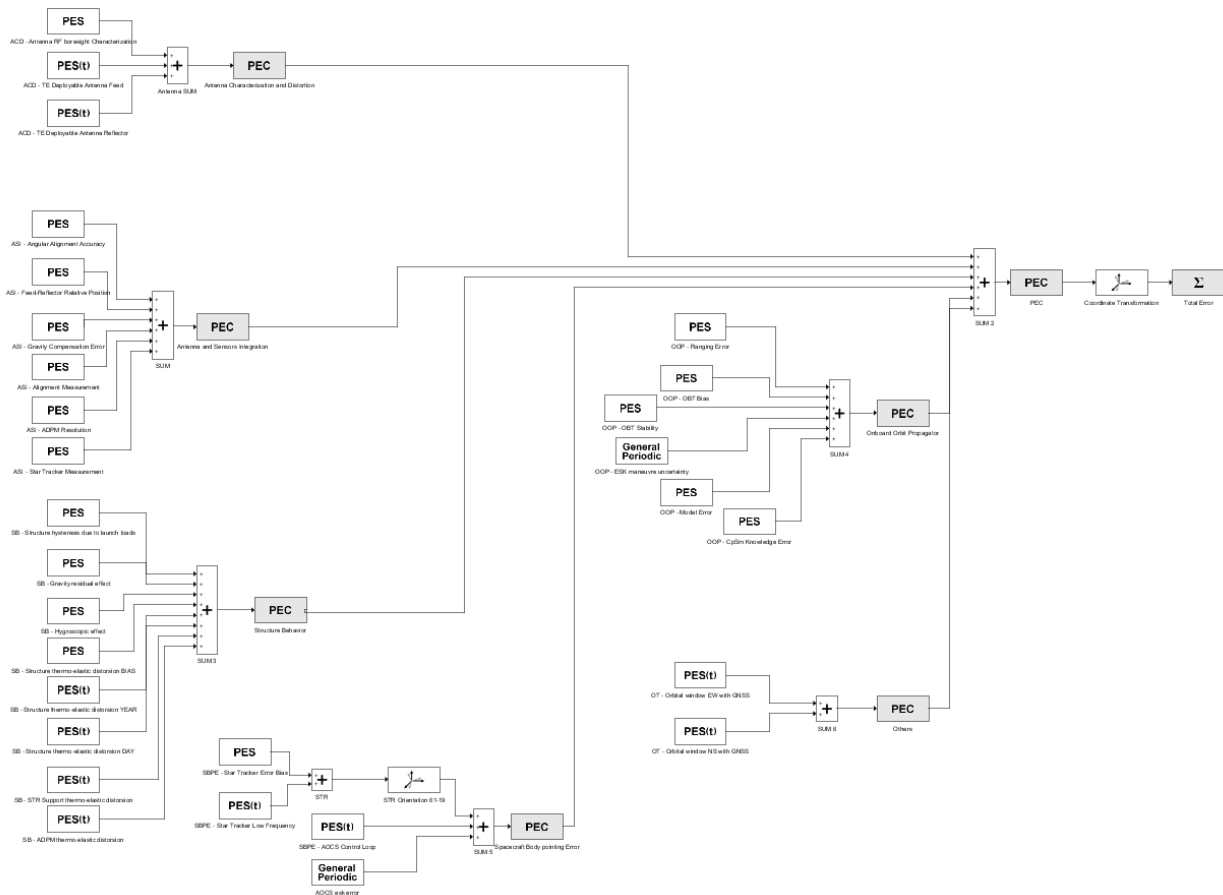


Figure 7-20: Overview of the SBNEO PEET model

The following figures gives a qualitative overview of the probability density functions for the APE, RPE daily and RPE lifetime performance indices over all the antenna spots obtained with the PEET model.

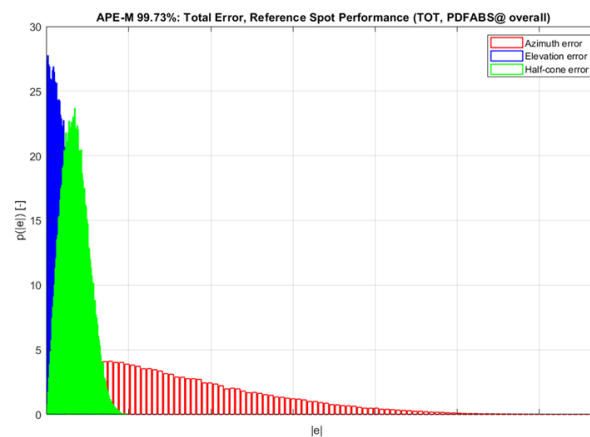


Figure 7-21: APE SBNEO model multi spot performance (ref. spot)

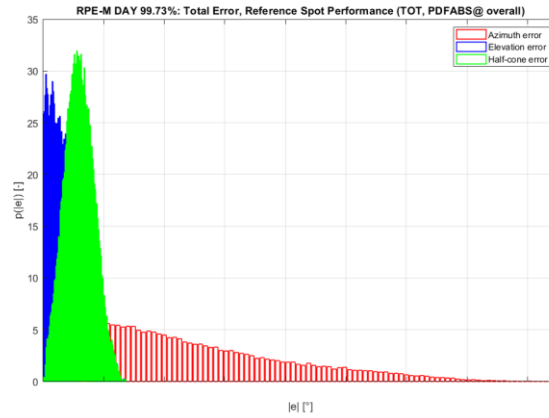


Figure 7-22: RPE daily SBNEO model multi spot performance (ref. spot)

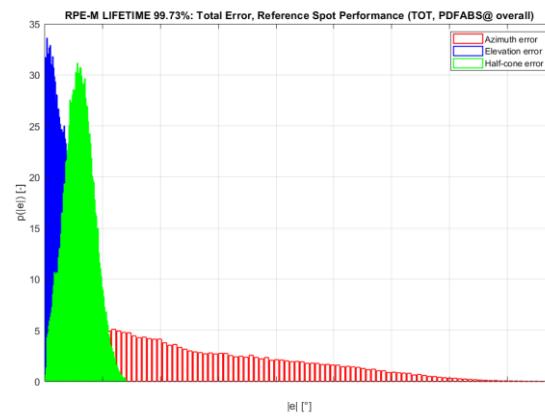
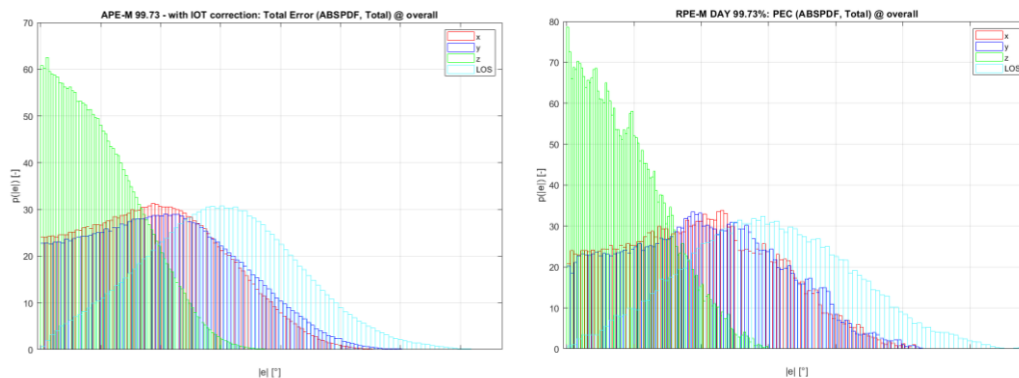


Figure 7-23: RPE lifetime SBNEO model multi spot performance (ref. spot)



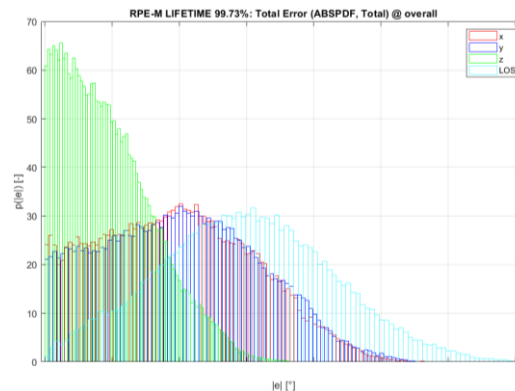


Figure 7-24: Overview of the overall SBNEO APE, RPE day and lifetime PDFs per axis

7.3.5 Budget Comparison

The following table summarizes the relative error between the pointing error budgets with the heritage tool and with PEET:

Table 7-31 Comparison between PEET budget and Thales Alenia Space heritage budget

Differences between PEET budgets and SBNEO Heritage Budget				
	Roll	Pitch	Yaw	LOS
APE	11%	1%	-28%	7%
RPE Daily	2%	-13%	-32%	3%
RPE Lifetime	2%	-9%	-31%	5%

One can note that the PEET budget shows similar results in the LOS direction on all performance indexes, and an improvement in the yaw component of about 30%. The difference on the axes budgets comes from the less conservative way to compute the error contributions with PEET: on the one hand due to a more accurate modelling taking into account the actual PDF and frequency domain models of the error signals (which results in generally smaller contributions compared to the results based on the assumption of Gaussian distributions, especially for high confidence levels); on the other hand due to less conservative statistical summation over different frequency classes compared to the linear summation in the heritage approach. LOS errors obtained by taking into account PDF information are slightly more conservative for the specific scenarios considered, but this is not generally predictable (see also section 7.5).

7.3.6 Conclusions and Lessons Learnt

In conclusion, from the consultants' perspective, the SBNEO scenario allowed implementing a consolidated spacecraft telecommunication pointing budget using the PEET tool, increasing the confidence on the tool thanks to the similar results with the heritage budget. Moreover, the functionalities developed in the study facilitated the implementation of some specific aspects, in particular for the multispot pointing performance, and the "General Periodic" pointing error sources.

Thales Alenia Space has already used PEET V1.1 in the frame of the SBNEO mission design and development and it envisages to use it for future telecom missions.

7.4 EDRS Global (Airbus DS Ottobrunn)

The Space Data Highway is a service offering provided by Airbus Defence and Space making use of the current infrastructure established within the framework of the EDRS (European Data Relay System) programme. The EDRS programme consists currently of two space segments and the appropriate Ground Segment. The space segment called EDRS-A is in operation since 2016. The space Segment EDRS-C was launched in 2019. The EDRS system is designed to improve the data download challenges of presently designed and future LEO Earth Observation (EO) satellites and to obtain a rapid imaging capability. Because the LEO orbit is generally polar sun-synchronous, the only common locations to directly download the data from the LEOs on every orbit are EO satellite downlink stations located as close as possible to the earth's poles. From these locations, one can receive LEO data from every satellite pass.

The future generation of EO satellites has a download requirement per orbit that may go beyond the performance of the X-band polar stations: While the Copernicus Sentinels will produce in the order of 400 Gigabit (Gb) of data per orbit with an average session duration of 10 minutes and a data rate of up to 600 Mbps, future reconnaissance satellites may surpass the Sentinel data capacity requirements by a factor of three or more.

The EDRS system overcomes these problems by providing considerably enhanced orbital access from the LEO to ground via GEO satellites. The GEO satellites act as relay nodes. The communication from the EO satellite to GEO takes place at optical wavelengths, using laser communication terminals (LCTs) on the LEO and GEO platforms. The communication from the GEO to ground uses a Ka-band feeder link.

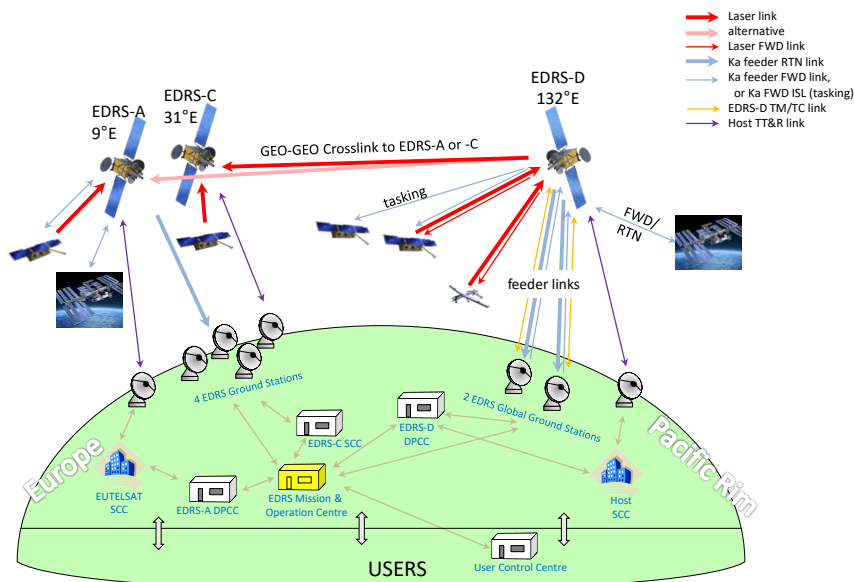


Figure 7-25: Overall Space Data Highway Configuration [RD21]

EDRS Global is used in the context of this study to represent a future Space Data Highway GEO satellite which will supplement the EDRS mission by providing additional coverage

(i.e. satellite located at 132° East orbital position), extended link capability by use of additional LCTs and enhanced security features taking into account airborne needs for commercial and military applications. The overall future system configuration, taking the current EDRS infrastructure and the EDRS-Global extension into account, is depicted in Figure 7-25.

The laser beam of a LCT has a half-cone beam divergence of $7.2 \mu\text{rad}$ at the $1/e^2$ level. In order for the optical link budget to have sufficient margin, the pointing error between the

LCT on the GEO spacecraft and the true pointing direction to the LEO needs to be in the order of $1\text{-}2 \mu\text{rad}$. Furthermore, due to the large distance (up to $45'000 \text{ km}$) between the LCTs, a point-ahead angle must be kept to cater for the relative motion between the LEO and GEO spacecraft.

Since such a low pointing error cannot be achieved open loop, a pointing, acquisition and tracking (PAT) algorithm is applied to bring the respective boresights of the LEO and GEO LCTs onto each other to the accuracy required for communication (cf. Figure 7-26). During coarse acquisition phase 1, the "master" LCT - usually the LCT mounted on the LEO satellite - uses its laser to scan across the area where the "slave" LCT is expected. The initial pointing error for this scan can be up to 0.2° . During this scan, the slave detects the short flashes of light coming from the master whenever its beam crosses the slave's aperture and uses the detections to reduce its pointing error. In coarse acquisition phase 2, the slave scans across the area where the master is expected, while the master reduces its pointing error. During fine acquisition, both LCTs are active and iteratively reduce their respective pointing errors until it is sufficiently low for tracking and the next acquisition step (where the frequencies of the respective lasers are locked onto each other to achieve homodyne communications).

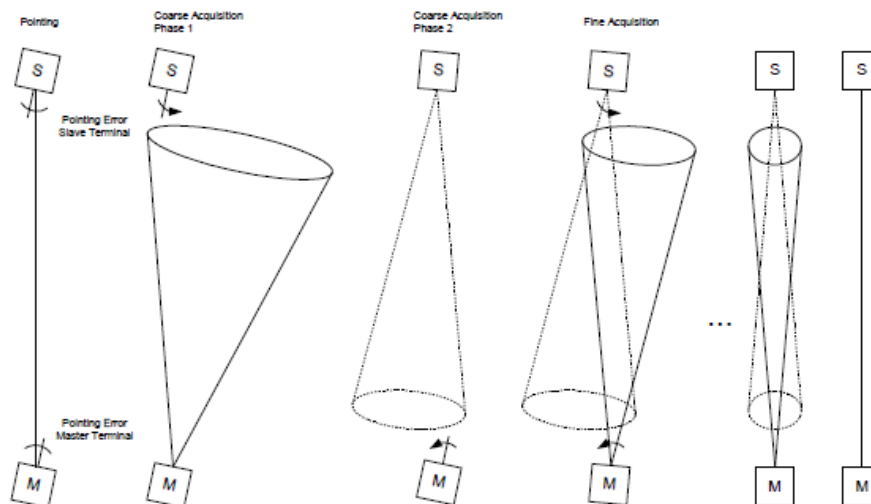


Figure 7-26: Spatial acquisition. "M" stands for the master LCT, "S" for the slave LCT. [RD21]

To achieve this, an open-loop pointing error that is sufficiently low for the PAT sequence to be successful, the GEO spacecraft is equipped with star sensors in addition to the attitude sensors that are usually found on GEO satellites. Spacecraft attitude is controlled via



reaction wheels. In addition, the LCT is equipped with a coarse pointing assembly (CPA), a fine pointing mirror assembly (FPA) and a point-ahead mirror assembly (PAA). While the CPA follows the nominal pointing vector to the LEO spacecraft - defined by the LEO and GEO orbit knowledge - the duo of FPA and PAA does the fine pointing and tracking.

Due to the pointing requirements stated above, EDRS is considered to be a *high-accuracy* mission.

For the purpose of the P4COM study, it would be valuable to study an existing mission scenario, for instance with one of the existing EDRS nodes, e.g. EDRS-C and one of the Sentinel 1/2 LEO satellites. Although the emphasis of the SpaceDataHighway is on the next mission (EDRS Global), the availability of in-orbit data from the operational EDRS-C and Sentinel satellites makes comparing PEET results with actual measurements more valuable. It is therefore proposed to study the case of EDRS-C performing links with Sentinel LEO satellites. In addition, the future needs for optical links between aircraft and GEO satellites may be investigated and identified in a next step.

7.4.1 Motivation

Selecting EDRS Global for the P4COM study means taking into account the needs of the emerging market of laser communications for the further development of PEET. While EDRS is the first operational system offering space-based telecommunications services with lasers, it is not the only one. Other GEO relay systems are under development, such as the Japanese Data Relay System (JDRS) and NASA's Laser Communications Relay Demonstration (LCRD). Furthermore, future LEO/MEO satellite constellations are likely to be equipped with laser communication systems to form orbital data networks.

With the available experience in EDRS, the consultants saw a great opportunity in using EDRS Global as one of the reference missions to further develop PEET and consolidate the European head-start into this new market.

Under the circumstances of telecommunications missions, EDRS Global certainly classifies as a "high-precision" pointing mission. In-orbit data is available from EDRS-A, which has (up to July 2018) performed more than 10'000 successful links for the four Sentinel 1 & 2 spacecraft. This data allows a valid comparison of current EDRS budgets and PEET models with actual measurements.

7.4.2 Pointing Requirements

Figure 7-27 illustrates the data download from a LEO satellite to the ground station via the LCT link with EDRS-C.

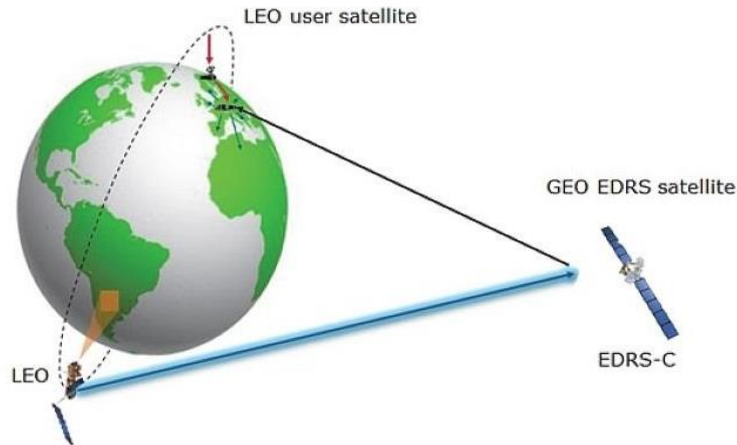


Figure 7-27: Data communication from LEO satellite via EDRS to ground station (ESA)

Throughout this analysis the scenario of GEO and LEO satellite lying in one line with the earth center, shall be considered, which leads to smallest distance between LEO and GEO and thus to the worst-case contribution of the LEO position knowledge error to the GEO LCT Uncertainty Cone. For this scenario, the Uncertainty Cone (UC) can be computed as the LoS error around the z_{LCT} -axis of the EDRS-SAT-LCT-REF frame as defined in RD01.

Pointing towards a target and following its trajectory is performed by combining Coarse Pointing Assembly (CPA) rotations around azimuth and elevation axes. The link acquisition process is performed in open loop and requires both high pointing accuracy of the beam towards the counter-part as well as high pointing stability of the beam. Figure 7-28 illustrates the LCT with the CPA.

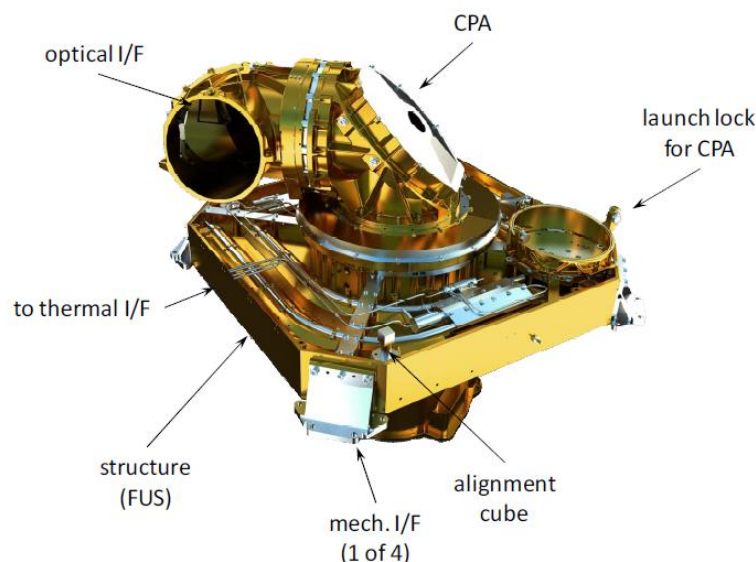


Figure 7-28: LCT in pointing position, showing the coarse pointing assembly (CPA), which is built in the form of a periscope.



7.4.2.1 Total Uncertainty Cone (AKE)

During the acquisition process both terminals contribute to the uncertainty cone with the dominating part being the uncertainty of the counter-terminal's position. In order to distinguish between the different uncertainty cones, the term Total Uncertainty Cone (TUC) was introduced in the EDRS project. Within the terminology of the ESA PEEH, the EDRS TUC corresponds to the Absolute Knowledge Error (AKE) of the LCT's pointing vector. In the following sections of this chapter the TUC definition and its geometrical meaning are described.

The satellite carrying the LCT for which the uncertainty cone shall be analysed is called the host satellite, while the satellite carrying the counter LCT is called the counter satellite.

The terms Host Uncertainty Cone (HUC) and Total Uncertainty Cone (TUC) will be used in the following. The HUC is defined as the sum of all own pointing error sources of the host satellite, i.e. position and attitude knowledge errors as well as LCT internal pointing errors. In contrast to that, the TUC is defined as the sum over all contributors and thus also includes the position knowledge error of the counter terminal. The TUC is the value which has to be looked at when analysing the performance of the LCT acquisition process. Table 7-32 summarizes the different contributors to HUC and TUC.

Table 7-32: HUC and TUC contributors

		LCT Pointing Uncertainty Contributors
TUC	HUC	1. Position knowledge accuracy of host S/C
		2. Attitude knowledge accuracy of the LCT on the host S/C. This attitude knowledge accuracy is considered at mechanical LCT interface, which forms the LCT reference frame, and it includes <ol style="list-style-type: none">Accuracy of attitude knowledge at attitude reference frame (AOCS)Accuracy of alignment knowledge between LCT reference frame and attitude reference frameThermal distortion between attitude reference frame and LCT
		3. LCT internal pointing accuracy
		4. Accuracy of counter terminal's position estimation

The items (1) and (2) reflect the knowledge accuracy in space. This information is delivered from the S/C to the LCT in real time and does not depend on the link planning interval. However, the position accuracy of a GEO-S/C on board may depend on the upload interval of orbital data from ground to S/C.

The item (3) is a given number which is also independent from the link planning interval. Whereas the item (4) describes the accuracy of the orbit forecast reflecting the position knowledge on ground used during command file generation. This value does clearly depend on the link planning interval.

The time accuracy w.r.t. a global time (e.g. UTC, GPS) will also result in a pointing error, as the position information of the counter S/C relies on the time base.

During the acquisition phase both communication terminals play different roles (master and slave) which makes the contribution of the uncertainty cones of both LCTs asymmetrical. It is beneficial to choose the terminal with the smaller Total Uncertainty Cone (TUC) as master in order to decrease the total duration of the acquisition phase.

Since the TUCs of LEO LCTs are frequently smaller than the ones of the GEO LCTs in the following description it is assumed that the LEO LCT starts as Master and GEO LCT as



Slave. But this is not a fixed definition and the description can be easily transformed to the opposite case of GEO being the Master and LEO being the Slave.

In more detail, the spatial acquisition process is sub-divided into following 3 steps:

1. Coarse acquisition phase 1 (master-slave): The LEO LCT performs spiral scanning (Master) whereas the GEO LCT watches for the hits on its sensors (CAS/FAS) and corrects the orientation if any hits are detected (Slave). The duration of this phase is a programmable parameter which is fixed for each acquisition. At the end of this phase the Slave LCT is best aligned towards the Master, i.e. its error cone is very small consisting of remaining error after the last adjustment step whereas the Master LCT has still no information about the counter terminal and thus its error cone is unchanged.
2. Coarse acquisition phase 2 (slave-master): The roles of both terminals swap and now LEO acts as slave and watches for the hits coming from GEO master. Thus, during this phase the orientation of the LEO LCT is improved whereas the orientation of the GEO LCT is drifting away (attitude knowledge instability). Because in the previous phase GEO LCT has been well oriented towards LEO LCT, the radius of the search spiral can be reduced to cover only the drift-away of the GEO LCT. The successful completion of this phase is declared when a fixed number of hits has been detected at the FAS of the slave LCT in LEO. At the end of this phase the LEO LCT is best aligned towards GEO LCT with the remaining error after the last adjustment step whereas the GEO LCT has drifted away from the best orientation it had after the coarse acquisition phase 1 (master-slave).
3. Fine acquisition phase (master-master): In this phase LEO LCT switches to the Master mode and so both terminals are working in the same mode sending signals to the counter terminal and receiving hits from it. Both terminals keep on correcting their orientation trying to bring all hits on the Tracking Sensor (TS) which is also responsible for data decoding. As soon as a stable signal reception on the TS of both terminals is established the acquisition is considered as complete and the LCT is considered to be in tracking mode. The transition from acquisition to tracking mode takes a few seconds.

As mentioned above, the main requirement for the whole acquisition process is that during its first Master-Slave phase the slave LCT is within the cone of the search spiral sent by the master LCT or with other words: The spiral has to cover the uncertainty cone of the slave LCT as seen from the master LCT.

7.4.2.1.1 LEO LCT

Figure 7-29 visualizes the geometry of the acquisition uncertainty cone during the first acquisition phase when the LEO satellite is working in Master and GEO satellite in Slave mode with the abbreviation L for the LEO and G for the GEO LCT. The superscript letter L means that the value is as estimated by the LEO LCT. In this figure the blue coloured real positions of the Master and Slave LCTs determine the optimal LoS direction (rf. blue vector) for the communication. To that optimal line the following error contributors are added:

- posErrG: LEO knowledge error of the GEO LCT position,
- posErrL: LEO knowledge error of its own position,
- timeErrG: Time error between GEO and a general time basis (e.g. GPS time),
- timeErrL: Time error between LEO and a general time basis (e.g. GPS time),

- attErrL: Attitude knowledge error of the LEO LCT.

The main rationale behind the geometrical relations presented in Figure 7-29 is the fact that the pointing of the Master LCT (LEO) is based on the estimated values of its own position/orientation and of the position of the counter terminal (GEO) as depicted by the green solid line in the drawing. Since the time synchronization of both terminals w.r.t. to a general basis (GPS) is different for both terminals, the estimated positions of each satellite also differ, i.e. the estimation of the own position (GEO) is different from the (GEO) position estimated by the counter terminal (LEO) and vice versa. For that reason, the superscript letters L and G are introduced to clarify at which LCT the estimation is performed.

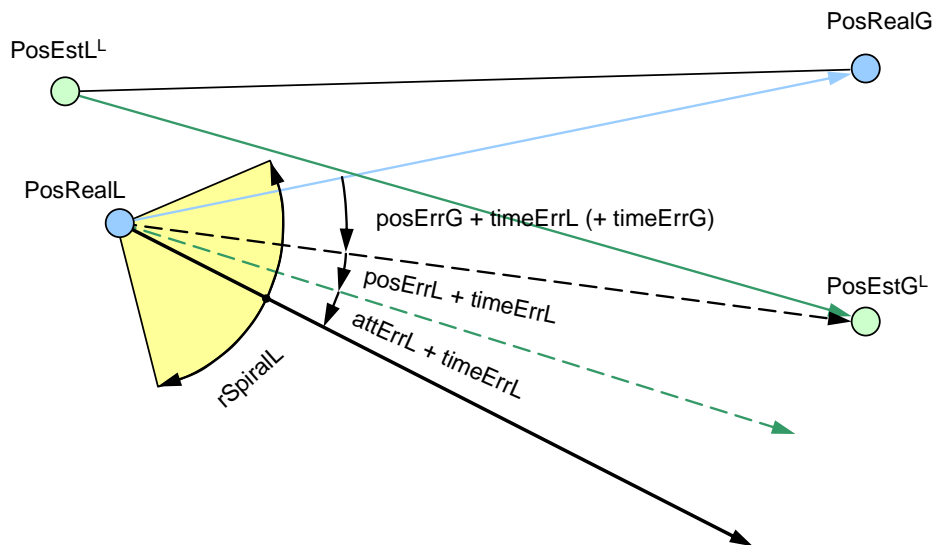


Figure 7-29: Geometry of the Total Uncertainty Cone as seen by LEO LCT (Master) during coarse acquisition phase 1 (L=LEO, G=GEO, superscript letter L="Estimated by LEO")

The difference between the real and LEO-estimated position of the GEO LCT is considered as the GEO position knowledge error increased by the time synchronization error of the LEO platform (timeErrL). In case the GEO position knowledge comes from the GEO S/C itself, the time synchronization error of the GEO platform has to be added to this contributor as well. Otherwise, if the GEO position is a result of a Ground measurement and estimation process which is well synchronized to the GPS time, the term timeErrG does not contribute to the error cone.

The green dashed line in the drawing is simply a parallel shift of the green solid line to the real LEO position and the angle between it and the black dashed line is the position knowledge error of the LEO LCT followed by the attitude knowledge error which is the last contributor to the total error cone. From the geometrical view presented in Figure 7-29, the aforementioned knock-out criteria for the acquisition process means that the blue vector which connects the real positions of LEO and GEO satellites must be inside the yellow zone of the search spiral which is performed by the LEO master LCT about the real LEO attitude (rf. black-bold vector in Figure 7-29).

During the Master-Slave phase the LEO LCT receives its own position and orientation as well as the position of the counter terminal from the satellite platform and thus a possible time synchronization error of the LEO platform (timeErrL) has an impact on all this data. The total synchronization error seen by the LCT algorithm can be split in two components



- platform clock error w.r.t. GPS time (timeErrL_P) and the I/F error between platform and LCT (timeErrL_IF):

$$\text{timeErrL} = \text{timeErrL_P} + \text{timeErrL_IF}.$$

Usually, the attitude and position knowledge errors of the LEO satellite do already contain the contribution from the platform clock timeErrL_P inaccuracy hence in this case the term attErrL should only cover the remaining part of the I/F error. In contrast to that the GEO position knowledge error does not contain any of those errors and thus the total acquisition uncertainty cone is obtained as the angle between the blue and the black-bold vectors in Figure 7-29 to

$$\text{TUC_L} = \text{posErrG} + \text{posErrL} + \text{attErrL} + \text{timeErrL_P} + \text{timeErrL_IFtotal},$$

assuming that the GEO position is determined by Ground w.r.t. GPS and that the LEO clock inaccuracy is included into the LEO's position and attitude knowledge errors, posErrL and attErrL. The term timeErrL_IFtotal contains contributions of the I/F synchronization error between platform and LCT on estimated positions of LEO and GEO as well as on LEO attitude, i.e. the time error weighted by LEO and GEO velocity as well as by LEO rotation rate. Finally, the above expression can be simplified to

$$\text{TUC_L} = \text{posErrG} + \text{HUC_LEO}$$

with HUC_LEO being the so-called Host Uncertainty Cone of the corresponding LEO satellite, because this term includes the position and attitude errors for the given satellite. For a successful acquisition process the Total Uncertainty Cone must be smaller than the radius of the search spiral and of thus smaller than the maximum possible spiral radius, i.e.

$$\text{TUC_L} < r_{\text{SpiralL}} < \text{maxR} = 2000^3 \mu\text{rad}.$$

7.4.2.1.2 GEO LCT

Considering the first phase of the acquisition process from the perspective of the GEO (Slave) LCT a drawing similar to Figure 7-29 can be envisaged, where the abbreviations L and G are swapped. With considerations similar to ones in section 7.4.2.1.1 the following equation can be derived for the acquisition uncertainty cone as seen from a GEO Slave LCT

$$\text{TUC_G} = \text{posErrL} + \text{posErrG} + \text{attErrG} + \text{timeErrG_P} + \text{timeErrG_IFtotal},$$

assuming GEO clock inaccuracy is included into the GEO's position and attitude knowledge errors, posErrG and attErrG. The term timeErrG_IFtotal contains contributions of the I/F synchronization error between platform and LCT on estimated positions of LEO and GEO as well as on GEO attitude, i.e. the time error weighted by LEO and GEO velocity as well as by GEO rotation rate. Finally, the above expression can be simplified to

³ Value altered due to confidentiality



$$TUC_G = posErrL + HUC_GEO$$

with HUC_GEO being the Host Uncertainty Cone of the corresponding GEO satellite, because this term includes the position and attitude errors for the given satellite. For a successful acquisition process the acquisition uncertainty cone must be smaller than the CAS FoV, i.e.

$$TUC_G < FoV_CAS = 2000^4 \mu rad.$$

For EDRS Global, it is a goal to achieve a TUC of less than $500^4 \mu rad$ in order to allow for faster acquisition that already starts with the fine acquisition sensor.

7.4.2.2 Attitude Knowledge Stability (KDE)

The LCT requirements regarding attitude knowledge stability of the platform are split in two parts: The low-frequency disturbances with frequencies below 1Hz are specified through Attitude Knowledge Error Stability (AKES) whereas all residual disturbances with frequencies between 1Hz and 1kHz are specified through the micro-vibration requirements at mechanical I/F between the satellite platform and the LCT. Thus, together the entire frequency range from 0Hz to 1kHz is covered. However, all micro-vibration related topics are summarized and handled through the micro-vibration control plan and are not part of this case-study.

During nominal operation (i.e. in acquisition and communication modes) the LCT receives information about its own platform's position and attitude as well as the position of the counter terminal. This data is provided by the S/C platform with a frequency of 2Hz and is used by the LCT internal SW algorithms running at rate of some kHz to calculate the reference pointing direction which is then used as trajectory for the CPA control. Because the attitude data is provided with 2Hz frequency to LCT (with internal interpolation to 1kHz), the CPA can only observe/correct frequencies below 1Hz. Therefore, the AKES is applicable for low frequencies only, i.e. below 1Hz. All higher frequencies (1Hz to 1kHz) are considered as micro-vibrations and handled by the corresponding requirements as mentioned before.

According to [RD22], the mathematical definition of the Attitude AKE Stability as needed for LCT has been agreed to:

$$AKES(t, \Delta t_s) := LPF_{1Hz} \{ e_t - e_{t-\Delta t_s} \} \frac{1}{\Delta t_s}$$

with e_t representing the absolute attitude knowledge error (attitude AKE), LPF_{1Hz} being a Low Pass Filter with the cut-off frequency of 1Hz and Δt_s being the stability time, which is the sample time at which the attitude data is provided to the LCT which is usually 0.5s. Figure 7-30 illustrates the AKES definition as defined above.

⁴ Values altered due to confidentiality

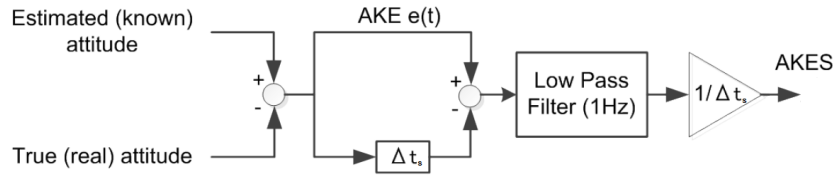


Figure 7-30: Attitude knowledge error (AKES) definition

The definition of the AKES is similar to the Knowledge Drift Error (KDE) definition in AD04:

$$KDE(t, \Delta t_s, \Delta t) = \langle e_t \rangle_{\Delta t} - \langle e_{t+\Delta t_s} \rangle_{\Delta t}$$

with e_t representing the absolute attitude knowledge error (attitude AKE), $\langle e_t \rangle_{\Delta t}$ being the mean value of e_t over time window Δt and Δt_s being the stability time, which is the sample time at which the attitude data is provided to the LCT which is usually 0.5sec.

While AKES is defined as the low-pass filtered knowledge stability error over one second, KDE is defined as time-window-averaged knowledge stability error over stability time Δt_s and thus needs to be divided by Δt_s . Neglecting the subsequent low-pass filter of the AKES and setting time-window $\Delta t = 0$ for the KDE it is:

$$\begin{aligned} AKES'(t, \Delta t_s) &= -KDE((t - \Delta t_s), \Delta t_s, 0) \frac{1}{\Delta t_s} \\ (e_t - e_{t-\Delta t_s}) \frac{1}{\Delta t_s} &= -(e_{(t-\Delta t_s)} - e_{(t-\Delta t_s)+\Delta t_s}) \frac{1}{\Delta t_s} \\ (e_t - e_{t-\Delta t_s}) \frac{1}{\Delta t_s} &= (e_t - e_{t-\Delta t_s}) \frac{1}{\Delta t_s} \end{aligned}$$

According to the PEEH, averaging over the time-window Δt is equivalent to low-pass filtering and thus the AKES requirement can be verified by calculating the KDE with $\Delta t_s = 0.5sec$ and $\Delta t = 0.5sec$, which is equivalent to a low-pass filter with cut-off frequency of 1Hz. According to [RD22] the AKES requirement r_{AKES} shall be verified by taking the maximum value over time of $AKES(t, \Delta t_s)$:

$$\max[|AKES(t, \Delta t_s)|] \leq r_{AKES}$$

Here, the KDE shall be used for a level of confidence evaluation such that:

$$Prob\left(KDE(t, \Delta t_s, \Delta t) \frac{1}{\Delta t_s} \leq r_{AKES}\right) \geq P_c$$

with $Prob(\dots)$ denoting probability and a level of confidence $P_c = 99.7\%$.

7.4.2.3 Requirement Definition

In this case study the TUC and AKES for the EDRS-C LCT shall be analysed. The corresponding requirements are defined as follows:



Table 7-33: EDRS-C LCT Total Uncertainty Cone Requirement

Pointing Error Requirement (PER)	Total Uncertainty Cone (TUC)		Comments
Evaluation Period	At any time during LCT link for whole mission life time		
Error Index	AKE		
Window-Time [s]	-		
Stability-Time [s]	-		
Unit	μrad		
Required Error Value	x	y z	LoS
			2000
Ensemble Domains	Pc		
'OOP' Ensemble (OED)	99.7%		
'Assembly + Launch' Ensemble (AED)	99.7%		
'LCT Communication' Ensemble (LED)	99.7%		
'Attitude Propagation' Ensemble (APED)	99.7%		
Domain Treatment	Temporal Domain		
	Statistical	Worst-case	
Ensemble Domain	Statistical	OED, LED, APED	-
	Worst-case	AED	-
Error reference frame	LoS (z-axis) of the EDRS-SAT-LCT-REF frame		
Applied PES	All		
Purpose	The Total Uncertainty Cone around the LoS of the host LCT defines the area in which the counter LCT must be in order to be covered by the LCT scanning spiral during acquisition procedure.		



Table 7-34: EDRS-C LCT Attitude Knowledge Stability Requirement

Pointing Error Requirement (PER)	Attitude Knowledge Error Stability (AKES)				Comments
Evaluation Period	At any time during LCT link for whole mission life time				
Error Index	KDE				
Window-Time [s]	0.5				
Stability-Time [s]	0.5				
Unit	μrad				
Required Error Value	x	y	z	LoS	
				4.5	
Ensemble Domains	Pc				
'OOP' Ensemble (OED)	-				
'Assembly + Launch' Ensemble (AED)	-				
'LCT Communication' Ensemble (LED)	99.7%				
'Attitude Propagation' Ensemble (APED)	99.7%				
Domains Treatment	Temporal Domain		Statistical		Worst-Case
Ensemble Domain	Statistical		LED, APED		
	Worst-Case				
Error reference frame	LoS (z-axis) of the EDRS-SAT-LCT-REF frame				
Applied PES	PES1, PES3, PES13, PES14				
Purpose	<p>LCT receives information about its own position and attitude as well as the position of the counter terminal with 2Hz which is used to calculate the reference pointing direction of the CPA. Thus the stability of this knowledge is of importance for the coverage of the whole uncertainty cone during acquisition procedure and the link stability in general.</p> <p>All frequencies above 1Hz are considered as micro-vibrations and treated separately.</p> <p>All LCT internal errors do not contribute to the AKES.</p>				



7.4.3 Heritage Approach

The current PEE approach consists of two parts:

- In the first part, the total uncertainty cones (TUC) of the LEO and GEO terminals are estimated based on pointing budgets. As this approach does not yield a probability distribution function (PDF) of the APE, a uniform PDF is generally assumed. Alternatively and if available, APE time series from AOCS simulations are used.
- In the second part, the link acquisition process is dynamically simulated (in Matlab/Simulink) using generated APE time series. Up to 10'000 acquisitions are simulated in order to obtain a PDF of the acquisition probability versus the time required.

The entire approach is document based. Exchange of information is done ad-hoc in formats most suitable for the individual purpose. Efforts are being made to comply to the ESA PEEH.

7.4.4 Pointing Budgets

7.4.4.1 PES Characterization

Table 7-35 provides an overview of all pointing error sources defined for the PEET scenario including their classification and justification according to the PEEH. Table 7-36 and Table 7-37 show the models used for these sources separately for time-constant and time-random sources and the requirement sets they contribute to.

Further, different ensemble domains were introduced to be used also in the PEET model to group the PES according to their 'physical nature' of the ensemble-randomness (see requirement tables in 7.4.2.3):

- Onboard orbit propagator
- AIT & Launch
- LCT communication
- Attitude propagation

These domains are evaluated commonly with a level of confidence of 99.7% and using mixed statistical interpretation for all but the AIT & Launch effect which are considered as worst-case.

Table 7-35: Pointing error source list

Definition of PES				Description of PES										Justification of PES				
Subsystem	Unit	PES	Name	Time-random	Ensemble-random (= time-constant)	Class	On interface	Type	Time-Random				Ensemble-Random	Origin	Reference	Identification	Comments	
									Distribution	Frequency [rad/s] with $f = 1/T$ or fnyqu or Time [s]								Origin
AOCS	Star trackers	Measurement error	PES1	X		random	no	process	Gaussian				PSD		This error describes the measurement error of the star tracker due temporal noise, FoV, spatial errors and many more.			
		Mirror cube bias	PES2		X	bias	no	variable						Gaussian	This bias is the measure of how well the functional coordinate frame of an instrument is known with respect to its mirror cube.	[RD-04] Table 4-1; [RD-06] Chapter 12.3.2; chapter 12.4	see reference	
	Gyro	Measurement error	PES3	X		random	no	process	Gaussian					PSD	This error describes the measurement error of the gyroscope due angle random walk, bias instability, rate random walk and quantization.			
		Position initialization error	PES4		X	bias	no	variable						Gaussian	Error in orbit position uploaded from ground for reinitialization of OOP	[RD-07] Table 3-2: Dual site orbit determination performance 24h data window	see reference	
	On-Board Orbit Propagator	Velocity initialization error	PES5		X	bias	no	variable						Gaussian	Error in orbital velocity uploaded from ground for reinitialization of OOP	[RD-07] Table 3-2: Dual site orbit determination performance 24h data window	see reference	
		Propagation error	PES6	X		drift	no	variable	drift specific PDF	604800s	604800s	604800s	Reset time		The orbit propagator can only consider a limited number of effects (number of expansion terms of the geopotential, incorporation of perturbations by planets, relativistic effects). Furthermore, parameters are known only with a limited accuracy (geopotential expansion coefficients, sun and moon ephemeris, modelling of solar pressure, etc.)	[RD-04] Chapter 4.1.3: Errors inherent to orbit propagator	see reference	
		Clock drift	PES7	X		drift	no	variable	drift specific PDF	604800s	604800s	604800s	Reset time		The on-board clock drift error with respect to EDRS-C reference time leads to errors in GEO and LEO position knowledge. Time synchronization with EDRS-C reference time is done once per week during the upload of orbit parameters.	[RD-04] Chapter 4.1.4	see reference	
	Thruster	Thrust error in nominal direction	PES8		X	bias	no	variable						Gaussian	The OOP incorporates the commanded thrusts during the orbit maneuver between two uploads of orbital data. Thruster errors lead to errors in the resulting velocity and therefore also to errors in the propagated position.	[RD-04] Chapter 4.1.3: Errors caused by thrust uncertainties	see reference	
		Thrust error cross coupling	PES9		X	bias	no	variable						Gaussian	The OOP incorporates the commanded thrusts during the orbit maneuver between two uploads of orbital data. Thruster errors lead to errors in the resulting velocity and therefore also to errors in the propagated position.	[RD-04] Chapter 4.1.3: Errors caused by thrust uncertainties	see reference	
STRUCTURE	Alignments	STR to LCT: Settling, Og, moisture	PES10		X	bias	yes	variable						uniform	This PES represents the alignment error between the STR and LCT resulting from settling effects during launch and Og-release, moisture, etc. However, once in orbit, this error remains constant over time.	[RD-04] Table 4-1: Group A, S/C structure (settling, Og, moisture) - STR/LCT	see reference	
		STR to LCT: Alignment measurement error	PES11		X	bias	yes	variable						Gaussian	After integration of both, the relative attitude between the alignment mirror cubes of STR and LCT are optically measured.	[RD-04] Table 4-1: Group A, On-ground calibration STR/LCT	see reference	

	STR to LCT: Bias	PES12		X	bias	yes	variable					Uniform	Time-constant part of thermal distortion error between STR und LCT due to temperature gradient between ground and orbit.	[RD-04] Table 4-1: Group A, S/C structure (Thermoelastics STR/LCT)	see reference
	<i>Thermo-elastic</i> STR to LCT: Seasonal	PES13	X		periodic	yes	process	bimodal	3,17e-8Hz	3,17e-8Hz	3,17e-8Hz	Seasonal period	Periodic part of thermal distortion error between STR und LCT over one year.	[RD-04] Table 4-1: Group B, S/C structure (Thermoelastics STR/LCT)	see reference
	STR to LCT: Orbital	PES14	X		periodic	yes	process	bimodal	1,16e-5Hz	1,16e-5Hz	1,16e-5Hz	Orbital period	Periodic part of thermal distortion error between STR und LCT over one orbit.	[RD-04] Table 4-1: Group C, S/C structure (Thermoelastics STR/LCT)	see reference
LCT	<i>Alignments</i> CPA to LCT: Alignment measurement error	PES15		X	bias	no	variable					Gaussian	This PES represents alignment measurement during LCT AIT. This alignment measurement takes out all mechanic and integration biases within the LCT. The optical LoS will be measured relative to the AC.	[RD-05] Table 2-1: LCT: Meas. accuracy on ground: CPA-LOS to LCT AC	see reference
	<i>Internal errors without CPA</i> Orbital harmonics	PES16	X		periodic	no	process	bimodal	1,16e-5Hz	1,16e-5Hz	1,16e-5Hz	Orbital period	Periodic part of internal LCT error over one orbit.	[RD-05] Table 2-1: LCT internal, without CPA: Harmonic	see reference
	Low frequency noise	PES17	X		random	no	process	Gaussian					The LCT internal low frequency noise in the frequency range from 0.01-1 Hz	[RD-05] Table 2-1: LCT internal, without CPA: Random	see reference
	High-frequency noise (Jitter)	PES18	X		random	no	process	Gaussian					The LCT internal high frequency noise in the frequency range >1 Hz	[RD-05] Table 2-1: LCT internal, without CPA: Jitter	see reference
	<i>CPA</i> Thermal over one orbit	PES19	X		periodic	no	process	Gaussian	1,16e-5Hz	1,16e-5Hz	1,16e-5Hz	Orbital period	CPA Thermal distortion over one orbit. This PES is the harmonic error before calibration	[RD-05] Table 2-1: LCT: CPA, thermal; [RD-03] Table 3-1	see reference
	Harmonic trajectory error without thermal Jitter	PES20	X		random	no	variable	Gaussian					This error is caused by different harmonic trajectory errors of the CPA (e.g. bearing run out, non-orthogonality of mounting axes, etc).	[RD-05] Table 2-1: LCT: CPA, harmonic, trajectory error, without thermal; [RD-03] Table 3-1	see reference
		PES21	X		random	no	process	Gaussian					The CPA jitter noise in the frequency range >1 Hz	[RD-05] Table 2-1: LCT: CPA, jitter	see reference
Sentinel 2 (Counter-Terminal)	Position knowledge error (GPS)	PES22		X	bias	no	variable					Gaussian	The position uncertainty of Sentinel-2 from EDRS-C based on the GPS error and three days orbit propagation on ground	GNC_F.TCN-788541.AIRB_EDRS-S2-LCT	see reference

Table 7-36: Time-constant pointing error source models

PES Name	PES applicability		PEET inputs				
			Ensemble Randomness				
	Total Uncertainty Cone (TUC)	Attitude Knowledge Error Stability (AKES)	PDF	PDF parameters			
			x	y	z	[unit]	
PES2	x		$G(\mu_G, \sigma_G)$	μ_G	Explicit values not shown due to confidentiality	σ_G	[μ rad]
PES4	x		$G(\mu_G, \sigma_G)$	μ_G		σ_G	[m]
PES5	x		$G(\mu_G, \sigma_G)$	μ_G		σ_G	[m/s]
PES8	x		$G(\mu_G, \sigma_G)$	μ_G		σ_G	[%]
PES9	x		$G(\mu_G, \sigma_G)$	μ_G		σ_G	[%]
PES10	x		$J(\theta_{min}, \theta_{max})$	θ_{min}		θ_{max}	[μ rad]
PES11	x		$G(\mu_G, \sigma_G)$	μ_G		σ_G	[μ rad]
PES12	x		$J(\theta_{min}, \theta_{max})$	θ_{min}		θ_{max}	[μ rad]
PES15	x		$G(\mu_G, \sigma_G)$	μ_G		σ_G	[μ rad]
PES22	x		$G(\mu_G, \sigma_G)$	μ_G		σ_G	[μ m]

Table 7-37: Time-random pointing error source models

PES Name	PES applicability		PEET inputs												
			Time-Randomness							Ensemble-Randomness of time-random property					
	Total Uncertainty Cone (TUC)	Attitude Knowledge Error Stability (AKES)	PDF	PDF parameters				Frequency [Hz] or [rad/s] Reset Time [s]			PDF	PDF parameters			
			x	y	z	[unit]	type	x	y	z		x	y	z	
PES1	x	x		Explicit values not shown due to confidentiality							Explicit values not shown due to confidentiality				
PES3	x	x													
PES6	x		$J(\theta_{min}, \theta_{max})$		θ_{min}	θ_{max}	[m]	Reset time							
PES7	x		$J(\theta_{min}, \theta_{max})$		θ_{min}	θ_{max}	[s]	Reset time							
PES13	x	x	$BM(A)$		A		[μ rad]	Freq.							
PES14	x	x	$BM(A)$		A		[μ rad]	Freq.							
PES16	x		$BM(A)$		A		[μ rad]	Freq.							
PES17	x		$G(\mu_G, \sigma_G)$		μ_G	σ_G	[μ rad]	Freq.							
PES18	x		$G(\mu_G, \sigma_G)$		μ_G	σ_G	[μ rad]	Freq.							
PES19	x		$BM(A)$		A		[μ rad]	Freq.							
PES20	x		$G(\mu_G, \sigma_G)$		μ_G	σ_G	[μ rad]								
PES21	x		$G(\mu_G, \sigma_G)$		μ_G	σ_G	[μ rad]	Freq.							

7.4.4.2 PEET Model and Budget

Figure 7-31 shows the top-level PEET model used with all PES as defined in the previous section and all system transfer models used (mainly static system transfer matrices and coordinate transformations).

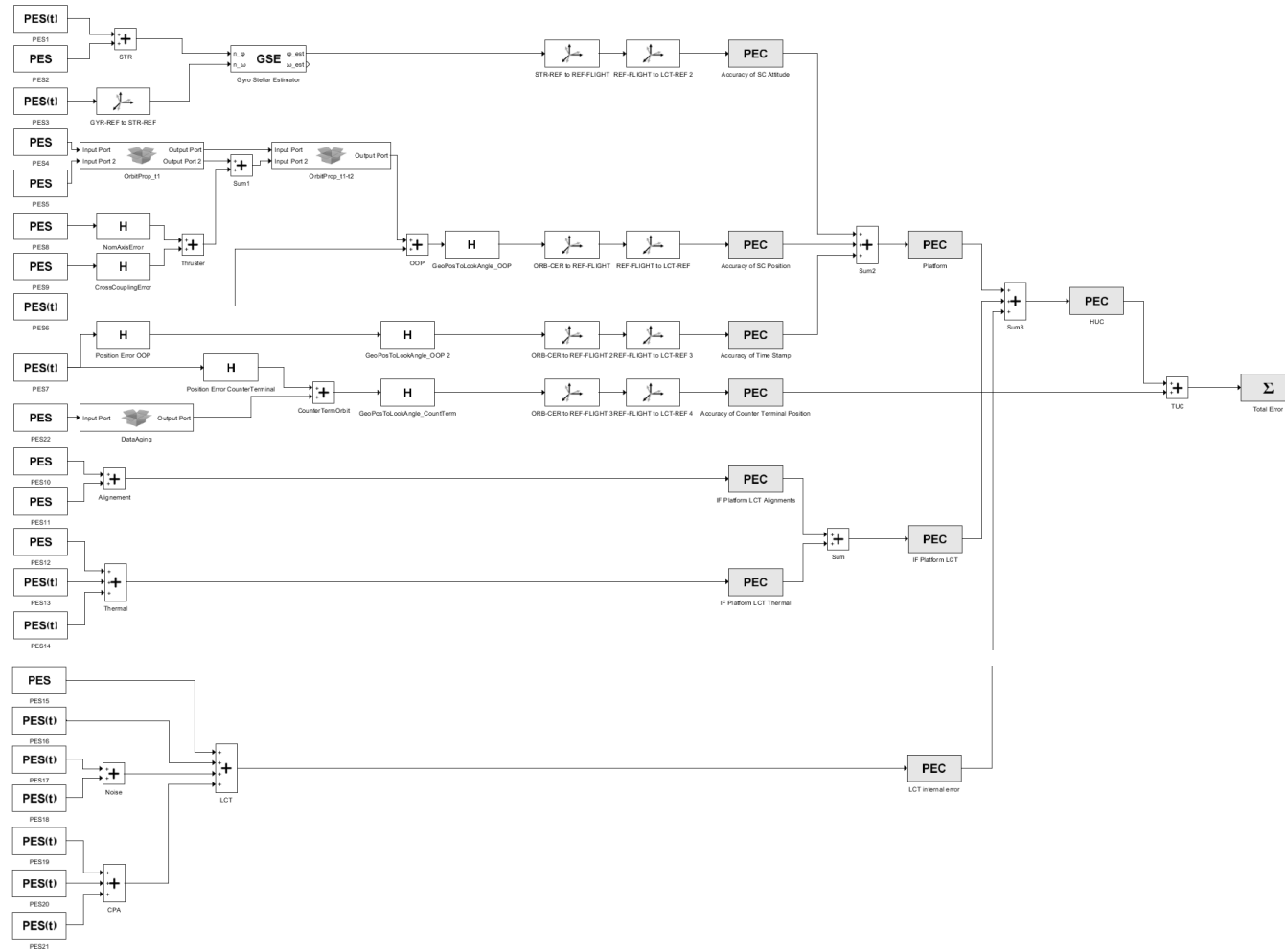


Figure 7-31: PEET pointing system model

A detailed description of the container blocks, especially the on-board propagation errors (OrbitProp_t1 and OrbitProp_t1-t2), is provided in [RD21] and too detailed for this report. Explicit values for the PEET budgets computed for the Total Uncertainty Cone budget, and the Attitude Knowledge Stability budget are not shown here due to confidentiality. However, a relative comparison of the results obtained with the simplified and advanced statistical method in comparison to the heritage approach is discussed in the next chapter.

7.4.5 Budget Comparison

7.4.5.1 PEET Budget vs Heritage Approach

Note that an Attitude Knowledge Stability (KDE) budget has not been computed yet in the old, document-based approach. Thus, only the Host Uncertainty Cone is compared here.

The HUC PEET budget has been computed with the simplified statistical method and the advanced statistical method. While the simplified statistical method represents the summation rules applied also in the previous document-based budget, the budgets still differ due to the different and more detailed modelling of the PES and pointing system as described in the remarks of Table 7-38. This comparison below also shows very well the conservatism of the simplified method, especial in the analysis of the pointing error contribution with dominant non-Gaussian components as in 'Accuracy of SV position', with dominant drift components, and 'Internal LCT error' with dominant periodic components. It also shows in the case of 'Accuracy of SV position', that after summation with other error sources to 'Satellite Platform', the PDF becomes more Gaussian, which decreases this effect. These observations further motivate the use of the advanced statistical method.

Table 7-38: Comparison Host Uncertainty Cone computed with document-based approach and PEET. All values 3D Angle (LoS error), 3-sigma – normalized w.r.t. heritage budget.

Spec Item		Req.	Document based Pointing Budget	PEET Pointing Budget Simplified Stat. Meth.	PEET Pointing Budget Advanced Stat. Meth.	Remarks
HUC		1.73	1.00	1.17	0.85	
HUC	Satellite Platform		0.52	0.25	0.25	
	I/F Platform-LCT		0.38	0.36	0.33	
	LCT		0.41	0.80	0.43	
Satellite Platform	Accuracy of SV Position		0.44	0.31	0.20	Advanced model in PEET: 7-day propagation of initial position and velocity errors (PES4&5), OOP error (PES6) and orbit maintenance maneuver after 6 days with additional thrust errors (PES8&9)
	Accuracy of SV Attitude		0.09	0.12	0.11	Advanced model in PEET including STR PSD (PES1), STR mirror cube calib. error (PES2) as well as Gyro PSD

						(PES3) and transfer through Gyro Stellar Estimator
		Absolute accuracy of time stamp	0.01	0.01	0.01	One error source for on-board clock error (PES7) for both, host platform position error here, and counter terminal position knowledge error (for TUC computation) in the same model.
I/F Platform - LCT		Alignment knowledge	0.21	0.24	0.24	STR cube and measurement error not included here in PEET budget, but 0g-settling added to budget.
		Max. alignment thermal distortion instability	0.10	0.12	0.09	Updated amplitude values and accurate sample-based level of confidence evaluation for periodic errors with PEET advanced statistical method.
LCT		Internal LCT error	0.41	0.80	0.43	Accurate sample-based level of confidence evaluation for periodic errors with PEET advanced statistical method.

7.4.5.2 Comparison with In-Flight Data

The EDRS-A LCT pointing error with measurements performed during 78 links on 2020-02-27 and 2020-02-28 has been provided by TESAT as follows:

- Pointing error during test (RMS): 20% of heritage budget value
- Pointing error during test (MAX): 45% of heritage budget value

In comparison to the pointing budget in Table 7-38, this still shows some conservatism. With the available in-flight measurements it is not possible to provide a more detailed assessment of the origin of this conservatism on pointing error source level. However, for the high confidence level applied for the requirement (99.73%), margin is expected to be present in the budget as the related extreme case may not occur during the actual operation.

Note that EDRS-C flight data is not available for a similar comparison for two reasons. First, EDRS-C has not been in orbit as long as EDRS-A. Second, analysis for EDRS-C is done by OHB.

7.4.6 Conclusions and Lessons Learnt

The following conclusions and lessons learnt can be drawn from this case study from the perspective of the consultants from Airbus (Ottobrunn).

- A document-based analysis is much more error-prone than a model-based approach with PEET (e.g. copy/paste errors, referencing wrong document version, etc.).
- The use of PEET ensures the correct application of the summation rules provided in the ESA PEEH and no discussions or assumptions are necessary in this respect.
- Tracking down analysis results und budgets through various documents using different formats, summation rules, "per axis"-values vs. LoS values is very untransparent and labour intensive. PEET can significantly improve the engineering process by simplifying information exchange and reducing corresponding sources of error. For

example, some sub-analyses (e.g. orbit propagator) have been directly included in PEET and could be easily exchanged with the help of PEET container blocks.

- A model-based engineering approach with PEET provides by far more flexibility especially in early phases with changing requirements and iterations between top-down allocation and bottom-up budgeting. For example, for this case study, a more detailed modelling of SC attitude knowledge (STR+gyro) allowed easy computation of the KDE budget (to which attitude knowledge is the main contributor) using the same PEET model.

7.5 Summary

This section summarizes the key aspects and results of the comparison of heritage approaches and the budgets computed with PEET.

In general, the intention of the study cases was to apply the systematic budgeting approach of the PEEH exploit by exploiting the possibilities for a more accurate modelling provided with PEET – in particular:

- PDF-based models for time-constant contributions and ensemble parameters
- Frequency-domain based models and error index contribution for time-random contributions
- Precise statistical summation including correlation without need of simplified summation rules
- PDF-based level of confidence evaluation and line-of-sight mapping without necessary assumptions on Gaussian contributions

To ensure a meaningful comparison to heritage budgets in the first place, a few restrictions were necessary. Obviously, the inputs to the heritage budgets need to have a corresponding magnitude when mapping to corresponding PEET models.

For all 'classical' telecommunication mission study cases (SmallGEO, SpacebusNEO and E3000), the contributors which are used as input for the heritage budgets represent worst-case values (on axis level) for the level of confidence given with the requirements (99.73% in all considered scenarios) or upper bounds of distributions or amplitudes.

For EDRS, all individual inputs to the budget also represent already worst-case values (for the level of confidence given with the requirement or upper bounds). But different to the other study cases, they are defined on LoS level and need to be broken down to axis level first based on best possible assumptions.

These 99.7% or worst-case values "X" were translated into PEET with the following guidelines:

- Discrete values directly correspond to X
- Gaussian distributions are modelled such that they result in the same standard deviation (e.g. $\mu = 0$, $\sigma = X/3$)
- Uniform or other bounded distributions are set up such that X represents the distribution bound

- An input which was initially assumed to represent a Gaussian distribution can be converted to another distribution by 'matching' the standard deviation (e.g. to a symmetric bound c of a uniform distribution with $c = X/\sqrt{3}$)
- Periodic signals are setup such that their amplitude corresponds to X
- PSDs are set up (if possible) with such that they have a matching standard deviation of $X/3$

In addition to the equivalence of PES input magnitudes, also the use of additional system transfer models in the PEET scenario was minimized as far as possible - to prevent differences due to effects which are not covered by the heritage budgets at least for the classical telecommunication scenarios. The use of coordinate transformations was considered acceptable. For the EDRS scenario, additional static transformations to account for specific effects were necessary.

The results obtained exemplary for the APE (AKE for EDRS) budgets of all study cases are summarized below – all normalized w.r.t. the respective results of the heritage budgets of each axis). Further, the results are considered in a reasonable range (~ -30% to +20% deviation) such that a systematic mismatch between the heritage methods and the tool implementation can be excluded. Due to the more precise modelling and evaluation methods, the PEET results are considered to provide the more accurate contribution based on the same closely equivalent inputs.

Table 7-39: PEET budget results with advanced method (normalized w.r.t. heritage budgets)

Study case	Roll	Pitch	Yaw	LoS
SmallGEO (APE) (Table 7-16)	0.80	0.80	0.80	0.92
E3000 (APE) (Table 7-26)	1.13	0.94	0.83	1.17
SpacebusNEO (APE) (Table 7-31)	1.11	1.01	0.72	1.07
EDRS (AKE) (Table 7-38)	N/A	N/A	N/A	0.85

A precise distinction and quantification of the impact of each modelling difference (as listed at the beginning of this section) between heritage and PEET implementation is hardly feasible for the complex overall budgets as they all act in parallel, but certain general aspects were assessed and are highlighted in the following subsections.

7.5.1 Summation Rules

Though using a different nomenclature, all heritage budgets for the 'classical' missions have a common categorization of all error sources into 4 different frequency classes:

- A: Biases
- B: Long term errors (seasonal or lifetime)
- C: Daily terms
- D: Short-term errors

All contributors within a class are summed up in an RSS sense with a subsequent linear summation of the overall results from each class.

The mapping from axes contributions to line-of-sight errors is performed under the assumption of Gaussian contributions on each axis or via an (adjusted) approximation using the instantaneous LoS equation.

Being an entirely different mission type, the heritage budget for EDRS follows a different approach without using similar frequency classes. However, also a separation between time-constant and time-random contributions is present. All time-constant contributions are summed linearly. Time-random contributions are summed either RSS (assuming they are uncorrelated) or linearly (assuming they are correlated). The total budget is then compiled by a linear sum of these three contributions.

But different to the other study cases, these inputs are already defined on LoS level, such that there is no final mapping step necessary. A direct comparison to the PEET results particularly difficult here as the LoS errors are broken down to axis level first before the LoS contribution is ultimately computed from the overall axis contributions.

Following the PEEH approach with PEET, no such artificial classification in frequency classes is necessary (nor recommended, as they are the result of assumptions necessary for the tabular heritage budget approaches only). All sources are summed and evaluated according to their relevant statistics and correlation for the given error index and statistical interpretation.

Unfortunately, using different summations rules together with different PES models in PEET (which are however matched to have a similar 3σ as in the heritage budget) further complicates the quantification of the individual benefits of more accurate modelling, summation and level of confidence evaluation – as they cannot be clearly separated.

This issue can be partially solved by introducing artificial ensemble domains which correspond to the heritage budget frequency classes. In this way, the summations rules within each 'class' and between the different 'classes' can be adjusted to some extent.

Having different domains specified, the level of confidence evaluation with PEET can be performed individually. As a consequence, also the summation over these domains is performed with a linear summation similar over the frequency classes in the heritage approaches - such that the impact of summation rules can be at least partially removed. This individual evaluation or linear summation in the heritage approaches generally represent a more conservative requirement formulation compared to a 'statistical' summation of the different contributions.

The summation within each class cannot be adapted in a similar manner, with the exception of time-constant error sources (corresponding to class A errors). Here, a mixed statistical interpretation can be (again artificially) chosen such that related errors from this class are

implicitly summed in an RSS sense – assuming they are uncorrelated. A temporal interpretation would correspond to a linear summation within class A as the individual worst-case values are summed above.

The assessment of the impact of such assessment was carried out for the E3000 case study with the results recalled in the table below for the axis budgets (LoS errors are treated separately in the next subchapter).

Table 7-40: E3000 APE budgets with different evaluations (normalized w.r.t. heritage budgets)

Requirement (Table 7-26)	Roll	Pitch	Yaw	Remarks on PEET setup
(1) BPE_APE_SITc	1.13	0.94	0.83	Temporal SI with common evaluation over artificial domains (corresponding to the frequency classes)
(2) REF_BPE_APE_SIMi	1.03	0.92	0.83	Mixed statistical interpretation with individual level of confidence evaluation for each domain
(3) mSC_BPE_APE_SIMc	0.62	0.57	0.53	Mixed statistical interpretation with common evaluation over artificial domains

(1) corresponds to the baseline requirement with temporal statistical interpretation and no artificial distinction between the frequency classes. (2) corresponds to the mentioned tailoring of the summation rules as far as possible. (3) considers an entirely mixed statistical interpretation without artificial distinction between the frequency classes.

Comparing the nearly identical results from (1) and (2), one might be tempted to conclude that the summation rules over the frequency classes only have a minor impact and are even slightly less conservative.

But in fact, considering the contributions from each individual class in Table 7-41, this is true only for the specific study case setup. In all different considered cases, the contributions of the individual non-bias classes (B-D) are basically identical (i.e. no driving variation over of an ensemble property is present which causes a significant different between mixed and temporal SI). What differs is contribution of the class A errors. For the intended temporal SI, scenario (2) - and thus the RSS summation within class A – underestimates the bias contribution with the heritage approaches. On the contrary, the individual evaluation of the different domains (and thus the linear summation over the frequency classes) overestimates the overall contribution – almost compensating the first effect in this specific case.

Table 7-41: Corresponding class contributions (normalized w.r.t. to total of (1))

Requirement (Table 7-26)	Angle	Class A	Class B	Class C	Class D
-----------------------------	-------	---------	---------	---------	---------

(1) BPE_APE_SITc	Roll	0.52	0.19	0.29	0.15
	Pitch	0.50	0.26	0.33	0.14
	Yaw	0.61	0.15	0.13	0.24
(2) REF_BPE_APE_SIMi	Roll	0.28	0.18	0.29	0.15
	Pitch	0.27	0.23	0.33	0.14
	Yaw	0.49	0.14	0.13	0.24
(3) mSC_BPE_APE_SIMc	Roll	0.28	0.18	0.29	0.15
	Pitch	0.27	0.23	0.33	0.14
	Yaw	0.49	0.14	0.13	0.24

A comparison of (2) and (3) reveals the general conservativeness of the linear summation over classes where all contributions from each class are basically identical and only the summation over classes differs (linear vs. statistical summation of contributions). In this specific case, the linear summation would significantly overestimate the overall error in the order of 40%. Again, this is not a 'globally' valid statement on the methods, but depends heavily the models used as input to a budget. The more a Gaussian distribution is present for the overall contributions of each class, the closer the results are expected which are obtained with the different methods and summation rules.

7.5.2 Impact of PDF-based LoC evaluation

Concerning the budgets on per-axis level, all heritage budget approaches assume implicitly Gaussian distributions for all contributions.

While the impact of the PDF-based evaluation alone between heritage approaches and PEET budgets is difficult to be quantified (mainly due to different simplified summation rules over the heritage frequency classes and specific, more accurate summations for different PES models in PEET), a relative comparison of the impact can be made in PEET by evaluating the same budget once based on statistical moments (simplified method) and using the PDF information (advanced method). This directly quantifies the gain in accuracy as the evaluated signals are identical at this point (though their contribution might differ already from the heritage budgets for the reasons mentioned).

Making this comparison, a reduction of the conservatism is expected whenever dominating non-Gaussian distributions are evaluated – especially for large confidence levels. The reason is that applying a confidence factor ('1/2/3 Sigma') to the signal's standard deviation for representing a 68%, 95.5% and 99.7% level of confidence is only exact for a Gaussian distribution. For other distributions (which are less tailed than a Gaussian in many cases), this assumption may be significantly overestimating the contribution. This is exemplary depicted in Figure 7-32 where already a 2σ bound applied to a uniform distribution would exceed its physically possible upper bound.

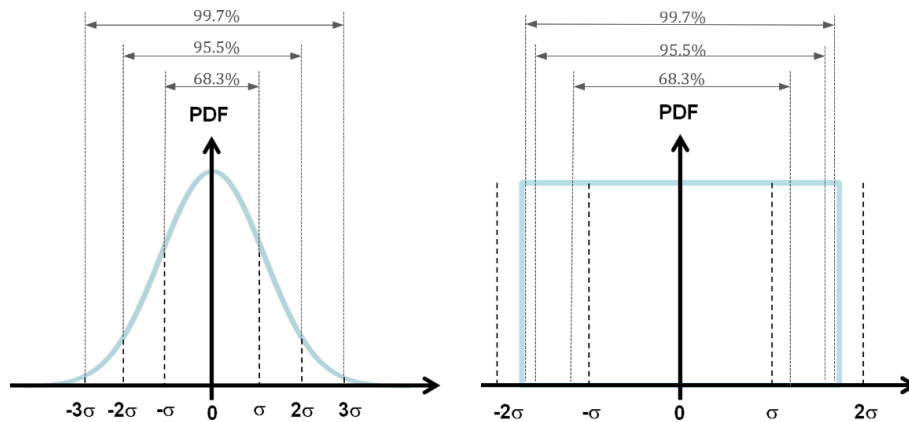


Figure 7-32: Error evaluation with confidence factor – applied to a Gaussian distribution (left) and to a uniform distribution (right)

The exercise of applying these two methods in comparison was conducted for several study cases with the results recalled below for the total errors:

Table 7-42: APE budgets with simplified/advanced method (normalized w.r.t. advanced method budgets)

Study case	Moment-based evaluation		PDF-based evaluation	
	Roll/Pitch/Yaw	LoS	Roll/Pitch/Yaw	LoS
SmallGEO (Table 7-16)	0.91 / 0.91 / 0.91	1.12	0.80 / 0.80 / 0.80	0.92
E3000 (Table 7-26, Table 7-27)	1.24 / 1.15 / 0.97	0.75	1.03 / 0.92 / 0.83	1.15
EDRS (Table 7-38)	N/A	1.17	N/A	0.85

As expected, the moment-based evaluation leads to more conservative results for the axes budgets – where in all cases non-Gaussian distributions were identified.

As mentioned, allows a direct comparison only between the two methods but not directly w.r.t. the heritage budgets (due to different summation rules over classes and within classes at this stage).

However, the results can be translated to a recommendation for the initial budget inputs for the heritage budgets – which already represent 99.73% LoC values for each source. In case these values are also derived from a given standard deviation only by applying a confidence factor (3σ), conservatism is already introduced from the beginning if the actual source is non-Gaussian. If any knowledge about the source distribution is available, it is advised to consider it already at the beginning (e.g. using the upper bound of a uniform

distribution directly rather than a 3σ value computed from its standard deviation). This recommendation especially holds when such large confidence levels are specified for the requirement and the presence of a dominating non-Gaussian source is expected.

A respective assessment has been carried out for time-constant error contributions of the SmallGEO study case by interpreting the heritage budget input values B in different ways in the mapping to PEET models (see discussion in section 7.1.5.1.1.1).

Regarding the LoS errors in Table 7-42, no similar reduction of conservatism (between heritage method and PEET or within the two PEET method) can be identified. This behaviour is also expected.

Table 7-43: Comparison of LoS error equations

PDF on axes	$e_{LoS} < x$ with P_c (and relative error)				LoS PDF (dashed: Rayleigh assumption)
	P_c [%]	Instant.	ECSS (Rayleigh)	exact (PDF)	
x: G(0,1) y: G(0,1)	68.3	1.414 (-7%)	1.516 (0%)	1.516	
	95.5	2.838 (14%)	2.490 (0%)	2.490	
	99.7	4.243 (24%)	3.409 (0%)	3.409	
x: G(1,1) y: G(1,1)	68.3	2.828 (29%)	1.516 (-30%)	2.190	
	95.5	4.246 (27%)	2.490 (-25%)	3.340	
	99.7	5.657 (30%)	3.409 (-22%)	4.357	
x: G(0,1) y: G(0,2)	68.3	2.236 (-3%)	3.032 (32%)	2.307	
	95.5	4.472 (8%)	4.981 (20%)	4.159	
	99.7	6.708 (11%)	6.817 (13%)	6.039	
* x: U(-√3, √3) y: G(0,1)	68.3	1.412 (-10%)	1.516 (-3%)	1.568	
	95.5	2.828 (23%)	2.490 (8%)	2.301	
	99.7	4.243 (34%)	3.409 (7%)	3.172	

* The uniform distribution bounds are chosen such that the same moments result as for the Gaussian.

Figure 7-33 Comparison of LoS error equations

The only conclusion which can be drawn is that the values significantly differ and that the PEET advance method evaluation is the most accurate by definition as it takes into account the actual distribution of the LoS errors, i.e. based on:

$$P_c = \int_0^{e_{index,LoS}} p_{LoS}(e) de \quad \text{with} \quad p_{LoS}(e) = p\left(\sqrt{e_x^2 + e_y^2}\right)$$

The PEET simplified method and the SmallGEO heritage approach take into account the equation for the instantaneous error (with a correction factor k applied in the SmallGEO case and k=1 for the PEET simplified method).

$$e_{LoS} = \sqrt{k(e_x^2 + e_y^2)}$$

The other study cases assume the special case of Gaussian distributions on axis level for a numerical evaluation similar to the approximation in the ECSS (i.e. resulting in a Rayleigh distribution on the LoS):

$$e_{LoS} = \max(\sigma_x, \sigma_y) \sqrt{-2 \log(1 - P_c)}$$

In presence of non-Gaussian distribution, the LoS errors can either over- or underestimate the actual contribution as illustrated in Table 7-43 – without having a simple measure available to predict the ‘direction’.

7.5.3 RPE Budgets

The impact of the evaluation of time-windowed error indices such as the RPE can be compared for the classical telecommunication mission study cases only as no RPE requirement is defined for EDRS.

For all heritage budgets, requirements exist for two different time-scales, namely daily and yearly (or lifetime) RPEs. The budgets are obtained for all cases using the same assumption:

- Yearly/lifetime RPE: only class B,C,D contributors are taken into account while biases (class A) are neglected
- Daily RPE: only contributions from classes C and D are taken into account while biases and long-term/seasonal effects are neglected

Concerning the biases, this is identical to the PEEH approach (and thus PEET) where time-constant contributions only contribute to APE and MPE indices. For all time-random contributions (i.e. classes B-D), the RPE contribution depends on the window-time and is ‘filtered’ by frequency domain metrics of approximate assumptions for random variables. Due to the relation $APE = RPE + MPE$, the RPE contribution is further generally smaller (at most equal) to the APE while in the heritage budgets, the full contribution of the considered classes is present.

Thus, having time-random PES described in the frequency domain (periodic signals or PSDs) modelled in PEET, a reduction of conservatism is expected as contributions of such sources can more precisely be evaluated. The normalized RPE budget results obtained with PEET and the advanced method are recalled in Table 7-44.

As expected, there is indeed a general reduction of conservatism compared to the heritage approaches, especially on the per-axis budgets (for the LoS errors, the same argumentation holds as in the previous section).

Table 7-44: RPE budgets (normalized w.r.t. heritage budgets)

Study case	Daily		Yearly/LifeTime	
	Roll/Pitch/Yaw	LoS	Roll/Pitch/Yaw	LoS
SmallGEO (Table 7-18)	0.89 / 0.89 / 0.89	1.06	0.83	0.99
E3000 (Table 7-26)	0.83 / 0.67 / 0.65	0.75	0.83 / 0.57 / 0.80	0.77
SpacebusNEO (Table 7-31)	1.02 / 0.87 / 0.68	1.03	1.02 / 0.91 / 0.69	1.05

It has to be noted again that such level of reduction is not 'guaranteed' by the more precise determination of the time-windowed error contribution, but strongly depend on the PES inputs and models (which is confirmed by the large range of relative improvements from about 57% up to even slightly more conservative values).

Further, the RPE budgets above are obviously also affected by the difference in summation rules and the PDF-based evaluation of the level of confidence. However, a comparison to the corresponding APE budgets in Table 7-39 (where the same differences apply) shows the clear tendency towards further relative reduction of the RPE cases.

8 Conclusion and Outlook

Within the P4COM study, PEET could be updated to account for identified main needs of the user community. The tool has been streamlined to cover requested 'comfort features' and to improve interfaces from and to the tool. In this respect, reporting functionalities have been extended for more flexible spreadsheet export and figure generation. Script-based execution and scenario data access have been improved for a smoother integration into toolchains and a generic interface has been created to integrate user-defined analyses. Coverage analyses algorithms - based on inputs from experts from all European telecommunication mission primes - were implemented to support the specific needs for applications in this sector.

The proposed draft for the PEEH update provides the necessary inputs to align the information with the extended concepts (e.g. the generalized domain concept) and models (e.g. Fourier series approximations) introduced in PEET in the predecessor and the current study. The mentioned concept allows a more flexible tailoring of requirements by allowing separate allocation of confidence levels and/or statistical interpretations for different sources of ensemble randomness (e.g. AIT, observations etc.). The Fourier series approximation can be used to model (periodically occurring) transients (e.g. damped sinusoids or spikes) or linear drift errors and accurately describe their dynamic system transfer behaviour and error index contribution via developed signal level metrics in the frequency domain.

The draft also includes extension and refinement of the existing frequency domain metrics for relative time-windowed errors - which resulted as a side product from the study – whose derivation and presentation is intended to be published in separate papers in the near future. These new metrics further detail the RPE contributions by breaking them down into drift and residual jitter contributions on the one hand and contributions for a fixed non-centred reference location in a time window on the other hand – thus also supporting a more flexible requirement definition and evaluation depending on application needs.

Further, recommendations for the application of Monte-Carlo campaigns were introduced which provide guidelines on the number of simulations runs to be performed – or on the margin to be applied to the results of a given number of simulation runs to achieve a sufficiently accurate estimation of the achievable performance. Guidelines are also provided for the application of the temporal statistical interpretation, i.e. the related steps for determination of the worst-case scenario - by evaluating first the level of confidence over time to each realization (rather than selecting the realization with the overall worst-case value only).

In addition, the update covers additional information and guidelines throughout all sections and additional appendices aiming to simplify the understanding and application of the PEET methodology, such that in overall, the provided draft is considered a valuable input and step towards a next release of the ESA handbook.

Four representative study cases for both “typical” and “high-accuracy” telecommunication missions were investigated in the study. First, scenarios were defined and documented following the error source classification/categorization and requirement formulation of the PEEH. In a second step, PEET scenarios were set up to compute the pointing budgets making use of the new features and analyses – all in close co-engineering with the telecommunication mission consultants. A comparison to heritage budgets revealed reasonable differences to the PEET results - which can be traced back to the more detailed modelling and more accurate summation of contributors based on PDF information –

showing that applying the PEEH process is indeed able to remove a certain degree of conservatism compared to heritage approaches.

From the consultants' perspective, implementing the PEEH process and realizing via PEET is considered to have an added value also for future telecommunication mission projects – as it provides potential to improve and simplify the pointing error engineering process. The model-based approach accounts for accurate summation of contributions by design and no assumptions on summation rules are necessary which allows setting the focus on a proper modelling of the pointing error sources. With the PDF- and frequency-domain based approach of the advanced statistical method, more accurate results can be achieved in particular for time-windowed errors and considering the combination of errors from different axes to the line of sight. The newly implemented analysis features allow a direct application for telecommunication mission specific performances such as beam pointing errors for single- or multi-spot antennas. Finally, the tool-based budgeting approach simplifies the exchange and tracking of modelling information and results compared to 'classical' spreadsheet budgets and improves the flexibility especially in early project phases.

The new PEET release (V1.1) is compatible with all current MATLAB versions starting from 2011b (as the previous releases) up to the latest version used for the test campaign (2020b). No immediate issues with newer MATLAB versions are expected in the near future, but for any future PEET releases, it might no longer be possible to maintain compatibility over such large range of MATLAB version.